Université de Montréal

Élaboration de réseaux poreux par la stratégie de la tectonique moléculaire

par

Jean-Hugues Fournier

Département de Chimie

Faculté des Arts et des Sciences

Thèse présentée à la Faculté des études supérieures

en vue de l'obtention du grade de

Philisophiae Doctor (Ph.D.)

en chimie

Janvier 2003

Université de Montréal
Faculté des études supérieures

Cette thèse intitulée :

Élaboration de réseaux poreux par la stratégie de la tectonique moléculaire

présentée par :

Jean-Hugues Fournier

a été évaluée par un jury composé des personnes suivantes :

Professeur William Lubell	président-rapporteur
Professeur James D. Wuest	directeur de recherche
Professeur Richard Giasson	membre du jury
Professeur Victor Snieckus	examinateur externe
Professeur William Lubell	représentant du doyen de la FES

Sommaire

Un des aspects fascinants de la chimie supramoléculaire est la possibilité de création de nouveaux matériaux ordonnés qu'elle laisse entrevoir. La stratégie de la *tectonique moléculaire* est une approche innovatrice basée dans ce sens. Elle repose sur l'utilisation de molécules, nommées tectons, sur lesquelles sont greffés des sites d'interactions intermoléculaires. Ces sites sont responsables de la capacité des tectons à s'auto-associer par le biais de forces intermoléculaires non-covalentes. Les matériaux générés par cette approche peuvent alors présenter d'intéressantes propriétés. Ainsi, en choisissant avec soin la forme moléculaire du tecton de même que la nature des sites d'interactions intermoléculaires, il est possible d'accomplir la création de nouveaux matériaux poreux organiques, analogues aux zéolites.

Les études menées dans le cadre de nos travaux se sont concentrées autour de deux axes principaux soit l'étude de nouveaux squelettes moléculaires pouvant servir de blocs de construction pour l'élaboration de tectons de même que l'exploration du potentiel de certaines fonctions comme sites d'interaction intermoléculaire.

De nombreux tectons étant basés sur l'utilisation du tétraphénylméthane ou du tétraphénylsilane, nous avons cherché dans un premier temps à élargir le nombre de dérivés existant dans ces familles de composés. L'approche retenue consiste à traiter les dérivés tétralithiés du tétraphénylméthane ou du tétraphénylsilane au moyen d'un électrophile approprié. Cette approche permet d'obtenir de nombreux dérivés inaccessibles jusqu'à présent dans d'excellents rendements en utilisant de simples processus de recristallisation comme méthodes de purification.

Parmi les dérivés synthétisés de la sorte, certains présentent en eux-même le potentiel d'agir comme tectons du fait de la présence de groupements pouvant établir des ponts hydrogène. Ainsi, le potentiel pour l'élaboration de réseaux surpramoléculaires poreux de trois tétraphénols dérivés du tétraphénylméthane ou du tétraphénylsilane a été examiné. Il ressort de cette étude que la fonction phénolique ne semble pas être

appropriée pour l'élaboration de réseaux poreux du fait du trop grand nombre de motifs d'association possibles.

Le potentiel des acides boroniques comme éléments d'association intermoléculaire a également été examiné. À la différence des phénols, ce mode d'association se révèle beaucoup plus fiable pour l'élaboration de réseaux supramoléculaires poreux. Ainsi, il a été possible d'utiliser les acides boroniques dérivés du tétraphénylméthane et tétraphénylsilane pour la construction de réseaux tridimensionnels poreux dans lesquels plus de 60% du volume est disponible pour l'inclusion et l'échange de molécules invitées.

Des études furent également entreprises afin d'examiner le potentiel comme squelette moléculaire des dérivés du 9,9'-spirobifluorène. Ces études ont permis le développement d'approches pour la synthèse de dérivés tétrasubstitués aux positions 3,3',7 et 7', dérivés inaccessibles jusque là. De plus, il a été également démontré que les dérivés du 9,9'-spirobifluorène peuvent être utilisés pour l'élaboration de réseaux supramoléculaires poreux dans lesquels près de 74% du volume est disponible pour l'inclusion de molécules invitées.

Mots clés : Chimie organique, supramoléculaire, pont hydrogène, tétraphénylméthane, tétraphénylsilane, phénol, boronique, 9,9'-spirobifluorène

Summary

Molecular tectonics is a strategy for the design of new ordered materials, which relies on the use of compounds with strong predispositions to associate in well-defined ways. Such molecules, called tectons, can be considered to have peripheral sticky sites directing molecular association, which are linked to a core holding the sticky sites in specific orientations. The directed intermolecular interactions disfavor close molecular packing, thus leading to the formation of open molecular networks with significant space for the inclusion of guests. The potential of molecular tectonics for the creation of new porous ordered materials is significant because both sticky sites and cores can be widely varied, allowing the creation of many different architectures.

Tetraphenylmethane and tetraphenylsilane derivatives are often used as subunits in molecular construction. A variety of new derivatives of tetraphenylmethane and tetraphenylsilane have been synthesized by efficient methods. In general, these compounds and the intermediates used in their syntheses can be purified by crystallization and chromatographic separations can be avoided. We expect these compounds to serve as useful precursors for the construction of complex molecules with tetrahedral geometries.

We have studied the potential of phenols as association sites in supramolecular chemistry. Three tetraphenols derived from tetraphenylmethane or silane were crystallized. X-ray diffraction studies show that the hydroxyl group of phenols is not highly effective as a director of supramolecular assembly.

The potential of boronic acids as recognition units in supramolecular chemistry has been studied. Our studies show that boronic acids derived from tetraphenylmethane and tetraphenylsilane associate by hydrogen bonding and form open three-dimensional, four-connected networks with significant internal volumes for the inclusion of guests.

We have studied the behavior of tectons incorporating the 9,9'-spirobifluorene in order to understand how enhanced rigidity of the core can influence the geometry of supramolecular networks. We have developed synthetic routes for *para*-substituted derivatives of 9,9'-spirobifluorene. In addition, our studies show that tectons derived from this more rigid analog of tetraphenylmethane can yield crystalline supramolecular networks in which up to 75% of the unit-cell volume is available for the inclusion of guests.

Keywords: Organic chemistry, supramolecular, hydrogen bond, tetraphenylmethane, tetraphenylsilane, phenol, boronic, 9,9'-spirobifluorene

Note

Afin d'éviter toute confusion quant à la nature exacte de ma contribution aux travaux présentés dans cette thèse, je tiens à apporter les précisions suivantes. L'article du deuxième chapitre décrivant la synthèse de dérivés du tétraphénylméthane et du tétraphénylsilane a été entièrement rédigé par moi-même, sous la supervision du professeur James D. Wuest. Il en va de même pour l'article du chapitre 5 relatant la synthèse et l'utilisation de dérivés du 9,9'-spirobifluorène. J'ai également participé à la rédaction des articles des chapitres 3 et 5 en collaboration avec le professeur Wuest. J'ai effectué l'entière rédaction des chapitres écrits en français.

J'ai accompli l'ensemble du travail expérimental décrit dans ces publications avec les exceptions suivantes : les études cristallographiques ont été réalisées par le docteur Thierry Maris et le docteur Michel Simard. La synthèse du tetrakis(4-bromophénylsilane) a été réalisée par le docteur Xin Wang. Nous avons également collaboré avec le professeur Elena Galopinni et Wenzhu Guo de Rutgers University dans le cadre des travaux portant sur la résolution des structures cristallographiques des acides boroniques.

Table des matières

Chapitre 3 : Utilisation des phénols en tectonique moléculaire

Chapitre 4 Utilisation des acides boroniques en tectonique moléculaire

Chapitre 5 Utilisation des dérives du 9,9'-spirobifluorène en tectonique moléculaire

Liste des figures

Chapitre 3

Article 2

Chapitre 4

Article 3

Liste des abréviations

Å	: Ångström
Ac	: acétyle
aq	: aqueux
Ar	: aryl
atm	: atmosphère
Bu	: butyle
br	: *broad*
°C	: degré Celsius
calcd	: *calculated*
cat	: catalytique
CCD	: diffractomètre par couplage de charges
cm	: centimètre
conc	: concentré
Δ	: reflux
δ	: déplacement chimique
d	: doublet (en RMN)
dd	:doublet de doublet (en RMN)
DMF	: N,N-diméthylformamide
DMSO	: diméthylsulfoxyde
dppf	: 1,1'-bis(diphénylphosphino)ferrocene
EI	: *electronic impact*
Et	: éthyle
FAB	: *fast atom bombardment*
g	: gramme
h	: heure
HRMS	: *high resolution mass spectrometry*
Hz	: hertz
IR	: infrarouge
J	: constante de couplage

kcal	: kilocalorie
L	: litre
M	: molaire
m	: mètre
m	: multiplet (en RMN)
Me	: méthyle
mg	: milligramme
MHz	: mégahertz
min	: minute
mL	: millilitre
mm	: millimètre
mmole	: millimole
mol	: mole
mp	: *melting point*
N	: normal
NBA	: alcool 3-nitrobenzylique
nm	: nanomètre
ORTEP	: *Oak Ridge Thermal Ellipsoid Program*
Ph	: phényle
ppm	: partie par million
RMN	: résonance magnétique nucléaire
s	: singulet (en RMN)
SM	: spectre de masse
Tf	: trifluorométhanesulfonyle
TFA	: acide trifluoroacétique
THF	: tétrahydrofurane
THIO	: thioglycérol
µL	: microlitre
UV	: ultraviolet

Remerciements

Je tiens tout d'abord à remercier mon directeur de recherche, le professeur James D. Wuest, pour m'avoir donné l'opportunité de travailler au sein de son groupe de recherche. La direction, les encouragements et les conseils qu'il m'a prodigué au cours des cinq dernières années ont été chaque fois appréciés infiniment. Son très grand professionnalisme de même que l'étendu de sa culture tant scientifique que générale constituent un modèle à imiter. Je garderai également toujours une immense admiration pour le respect qu'il a constamment démontré envers ses étudiants.

Je tiens également à remercier le docteur Thierry Maris pour tous les efforts et l'énergie déployés à résoudre les différentes structures cristallographiques présentées dans cette thèse. Je le remercie pour son aide de même que pour la patience dont il a su faire preuve constamment.

Je remercie tout le personnel du département de chimie de l'Université de Montréal et en particulier le docteur Michel Simard qui m'a enseigné mes premières notions de cristallographie. Il a également effectué la résolution de quelques structures cristallographiques et je lui suis reconnaissant de son aide.

Je tiens également à remercier le CRSGN, le FCAR de même que l'Université de Montréal pour le soutien financier tout au long de mes études graduées.

Les vieux routards maintenant : Erwan, Dominic, Fred et Gerson resteront les bons vieux compagnons du bac et des premières années d'études graduées, ceux avec qui j'ai gardé de si nombreux bons souvenirs. Un gros merci également à Éric pour l'agréable cohabitation dans le lab, j'aurais difficilement pu mieux tomber en terme de partenaire de paillasse. Je ne peux pas passer sous silence les copains du fumoir, ceux avec qui je grillais une cigarette en discutant de tout, de rien, du boulot, de la vie en général et du monde dans lequel nous vivons. Ces pauses ont été l'occasion de rencontrer

des gens que j'apprécie énormément : Luc, Alexandre et Catherine, merci pour ces instants de détente (et pour les rudiments de biochimie que vous avez tenté de m'enseigner).

Et finalement, toutes mes excuses à ceux dont j'ai cassé les oreilles avec ma musique durant toutes ces années. Votre patience a été infiniment appréciée…

Chapitre 1

Introduction

1.1 Préambule

Un des aspects les plus fascinant de la chimie de synthèse est certainement l'extraordinaire capacité de transformation de la matière qu'elle assure à celui qui la pratique. Au prix d'inlassables efforts, les chimistes ont développé une science qui permet de passer d'un substrat ayant une composition et des propriétés définies à un produit possédant une toute autre identité en effectuant une suite d'étapes de transformations logiques et rationnelles. C'est en suivant une telle démarche que l'on peut par exemple transformer des sucres en fibres textiles, créer des matériaux en partant d'extraits de pétrole ou encore générer de nouveaux antibiotiques en utilisant des produits n'ayant absolument aucune propriété médicinale. Ce ne sont là que quelques exemples qui illustrent toutefois très bien la versatilité de cette science.

Peu à peu, la recherche dans le domaine de la synthèse de molécules a permis d'étendre la gamme de transformations chimiques disponibles, élargissant ainsi les possibilités de transformation. Ces transformations chimiques, que le chimiste désigne familièrement sous le terme de réactions, peuvent être résumées comme étant en fait une recombinaison des atomes composant une ou plusieurs molécules, processus menant à la formation d'une nouvelle entité chimique. Cette définition volontairement simpliste peut faire sourire mais elle a le mérite de mener à la question suivante : deux molécules distinctes peuvent-elles interagir entre elles tout en conservant leur identité propre ? Peut-il y avoir interactions entre plusieurs molécules de façon à générer un assemblage qui ne serait toutefois pas le résultat de réactions chimiques ? C'est autour de cette problématique que s'est développé le domaine de recherche désigné sous l'appellation de chimie supramoléculaire.

1.2 La chimie supramoléculaire

Jean-Marie Lehn, co-récipiendaire avec Donald J. Cram et Charles J. Pedersen du prix Nobel de chimie en 1987, donna cette définition de la chimie supramoléculaire lors de son allocution :

"*Supramolecular chemistry is the chemistry of the intermolecular bond, covering the structures and functions of the entities formed by association of two or more chemical species.*"[1]

En des termes simples, Lehn définit la place de ce domaine de recherche par rapport à la synthèse moléculaire traditionnelle : la chimie dite moléculaire est basée sur l'étude et la manipulation du lien covalent entre atomes, sur la connectivité des atomes composant une molécule, tandis qu'à un niveau d'organisation supérieur, la chimie supramoléculaire s'occupe de l'étude et de la manipulation du lien intermoléculaire entre molécules, de la connectivité des molécules entre elles. Ce que la chimie moléculaire réussit à créer, la chimie supramoléculaire cherche à l'organiser.[2]

Ainsi, la chimie supramoléculaire vise en quelque sorte à étudier et ultimement à diriger le comportement d'une population de molécules identiques ou différentes : elle utilise certaines propriétés intrinsèques aux molécules telles que la polarisabilité, la présence de sites donneurs ou accepteurs de ponts hydrogène, les interactions électrostatiques ou encore la présence de sites de coordination métallique pour diriger la formation d'assemblages discrets ou infinis. Ces molécules deviennent ainsi les briques de construction d'une organisation plus complexe, soit l'assemblage supramoléculaire. Il est à noter que lors de ces processus d'assemblage supramoléculaire, chaque molécule garde son identité propre : elle reste distincte et n'est pas modifiée dans sa constitution chimique, soit les atomes qui la composent. Pour mieux comprendre ce concept, il est utile de considérer l'analogie suivante : lorsque plusieurs individus se donnent la main de façon à former une chaîne, nous obtenons un « assemblage » humain dans lequel chaque membre possède une place définie dans l'organisation. Même s'il interagit avec son

voisin par le biais d'une poigné de main, chaque individu conserve tout de même son identité propre dans l'assemblage. De la même façon, lorsque des molécules interagissent entre elles de façon à générer un assemblage supramoléculaire, elles conservent leurs identités propres tout en ayant une place précise dans l'organisation supramoléculaire.

La chimie supramoléculaire n'est pas un concept artificiellement inventé par l'humain; les phénomènes supramoléculaires sont à la base même d'un nombre important de processus biologiques. Que l'on pense au processus de liaison d'un substrat avec son enzyme, à la structure du code génétique enfermé dans la double hélice de l'ADN, à la formation des bicouches lipidiques des membranes cellulaires, au transport de molécules au travers des parois d'une cellule, à l'interaction anticorps-antigène : tous sont des phénomènes d'interactions supramoléculaires dans lesquels des entités chimiques distinctes interagissent les unes avec les autres par le biais d'interactions intermoléculaires non-covalentes.

C'est en puisant dans ces phénomènes biologiques mais également dans leurs imaginations que les chimistes trouvent l'inspiration pour créer de nouveaux assemblages supramoléculaires. Quelles sont les applications de tels systèmes ? Citons pour l'exemple la création de récepteurs artificiels pour la reconnaissance sélective de molécules, l'élaboration de dispositifs moléculaires électroniques ou optiques, le développement de nouveaux matériaux ordonnés. Ce dernier domaine de recherche en particulier suscite un intérêt grandissant tant au niveau académique qu'industriel; le design de nouveaux matériaux apparaît désormais comme une branche incontournable des nanotechnologies émergentes. Parmi les nombreuses approches développées à ce jour, la stratégie nommée sous le terme de *tectonique moléculaire* émerge comme une voie prometteuse pour la création de nouveaux matériaux ordonnés.

1.3 La tectonique moléculaire

Introduit au début des années 90 par le groupe de recherche du professeur James D. Wuest à l'Université de Montréal, la *tectonique moléculaire* se présente comme une nouvelle stratégie pour la conception de matériaux ordonnés par des processus d'auto-assemblage spontanés.[3] Cette approche repose sur l'utilisation de *tectons*, molécules de formes soigneusement choisies sur lesquelles des sites d'interaction intermoléculaire ont été greffés. Ces sites sont en fait des groupements de reconnaissance moléculaire ayant pour caractéristique de s'auto-associer à la fois fortement et de manière prévisible.

Lors du processus de cristallisation, ces groupes contrebalancent la tendance naturelle des molécules à former un empilement compact qui maximiserait les forces de van der Waals tout en minimisant la présence d'espaces vides, défavorisée énergétiquement (Figure 1.1). Dans le cas des tectons, les groupes de reconnaissance établissent des interactions avec ceux des tectons voisins, amorçant ainsi un processus d'auto-assemblage menant à la formation d'un réseau supramoléculaire. La géométrie du

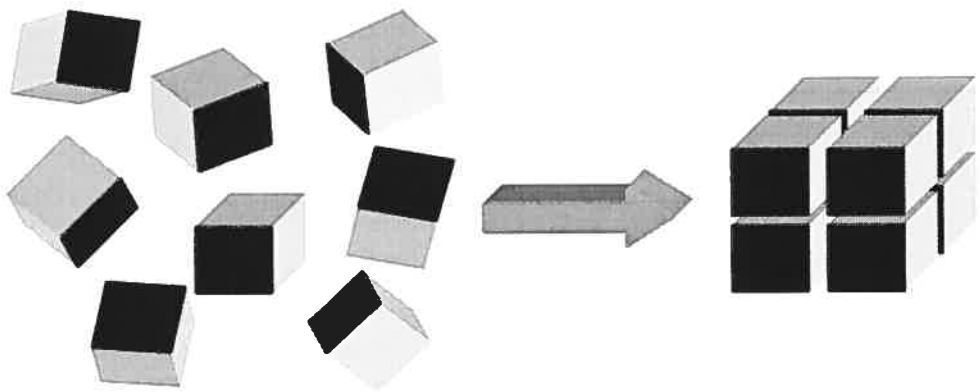

Figure 1.1 Représentation schématique de la tendance naturelle des molécules à former un empilement compact. Les molécules, symbolisées sous la forme de cubes, formeront préférentiellement un arrangement compact qui maximise les forces de van der Waals et minimise la présence d'espace vide, défavorisée énergétiquement.

réseau formé est dictée par l'orientation des groupes de reconnaissance dans l'espace. La forme de la molécule devient donc un facteur critique puisque, servant de support aux groupes de reconnaissance moléculaire, elle oriente ceux-ci dans certaines directions préférentielles. La structure de l'assemblage supramoléculaire résulte donc du processus d'association des sites de reconnaissance combiné avec l'influence de la forme moléculaire.

Une des possibilités les plus intéressantes de la tectonique moléculaire est qu'elle permet la création de nouveaux matériaux poreux par un processus d'assemblage spontané par cristallisation tel que montré à la Figure 1.2. Cet exemple hypothétique illustre le cas d'un tecton tétraédrique aux extrémités duquel sont greffés des groupes de

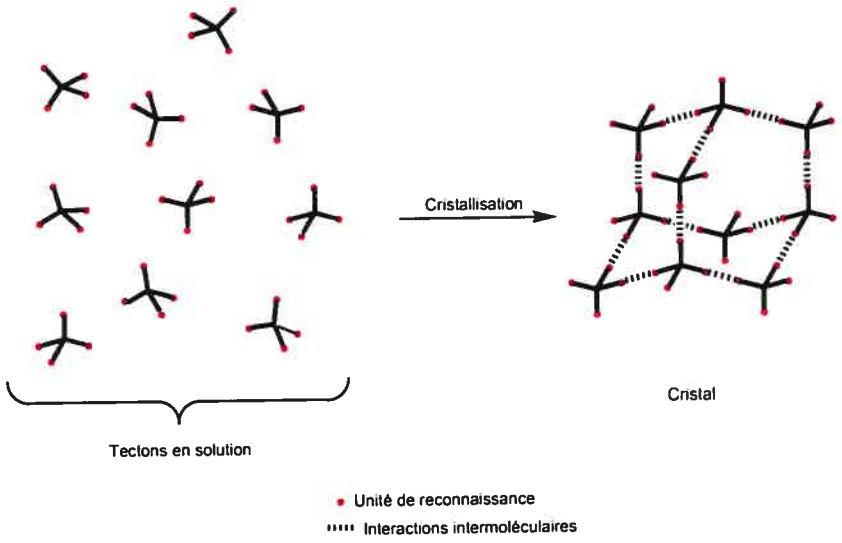

Figure 1.2 Formation d'un réseau supramoléculaire poreux par la stratégie de la tectonique moléculaire.

reconnaissance moléculaire. Lors du processus de cristallisation, les groupes de reconnaissance moléculaire des tectons s'associent fortement entre eux et deviennent la force directrice de l'assemblage. Du fait de l'orientation tétraédrique des groupes de reconnaissance, il y aura formation d'un réseau supramoléculaire différent de celui qui

résulterait d'un empilement compact. La géométrie du réseau formé peut être diamantoïde, tel qu'illustré à la Figure 1.2, mais peut également se présenter sous d'autres types de topologies. Mais quelle que soit l'architecture adoptée, il est à noter qu'un tel processus d'assemblage spontané laisse un espace libre pour l'inclusion de molécules invitées. Ces cavités ne sont pas vides et sont le plus souvent occupées par des molécules provenant des solvants utilisés lors de la cristallisation.

Ce type de matériau devient intéressant lorsque les espaces « libres » sont reliés entre eux de façon à former des canaux traversant le solide cristallin. Ces canaux, qui peuvent être parallèles ou interconnectés, amènent alors la possibilité d'échanger les molécules initialement présentes dans les cavités avec d'autres composés. Ainsi, lorsque le matériau tectonique est placé dans des conditions appropriées, les molécules incluses à l'intérieur du solide cristallin sont libres de diffuser vers le milieu extérieur tout en étant remplacées par d'autres molécules.

Cette possibilité d'échange devient particulièrement importante lorsque l'on considère les perspectives d'application des matériaux développés par la stratégie de la tectonique moléculaire. Ainsi, une application potentielle des matériaux tectoniques pourrait être leur utilisation dans des processus de séparation. En effet, du fait de la présence de canaux, les solides tectoniques peuvent laisser diffuser en leur sein des molécules. Cependant, les dimensions mêmes des canaux limitent la taille des substrats pouvant pénétrer à l'intérieur des cavités. Ainsi, pour des canaux cylindriques ayant un diamètre fixe tels que ceux représentés à la Figure 1.3, seul des molécules ayant une taille inférieure à ce diamètre pourront diffuser dans le solide. Les molécules de taille supérieure ne pourront pénétrer dans le matériau. Un processus de séparation en fonction de la taille prendra donc place et permettra de séparer les molécules en fonction de leurs dimensions. D'autres facteurs de séparation pourraient également intervenir. Ainsi, on peut imaginer un environnement intérieur ionique favorisant l'inclusion de molécules chargées, un milieu de type hydrophobe retenant préférentiellement les composés non-polaires ou encore un intérieur présentant des éléments d'asymétrie qui tendrait à retenir préférentiellement un énantiomère en particulier. Quel que soit le type d'environnement

choisi, les possibilités de séparations sont un des aspects prometteurs de la tectonique moléculaire. Il est possible d'imaginer des systèmes chromatographiques dans lesquels des matériaux tectoniques serviraient de phases mobiles ou encore l'utilisation de ceux-ci comme « éponges » sélectives qui absorberaient préférentiellement un produit et pourraient rendre celui-ci après un traitement approprié.

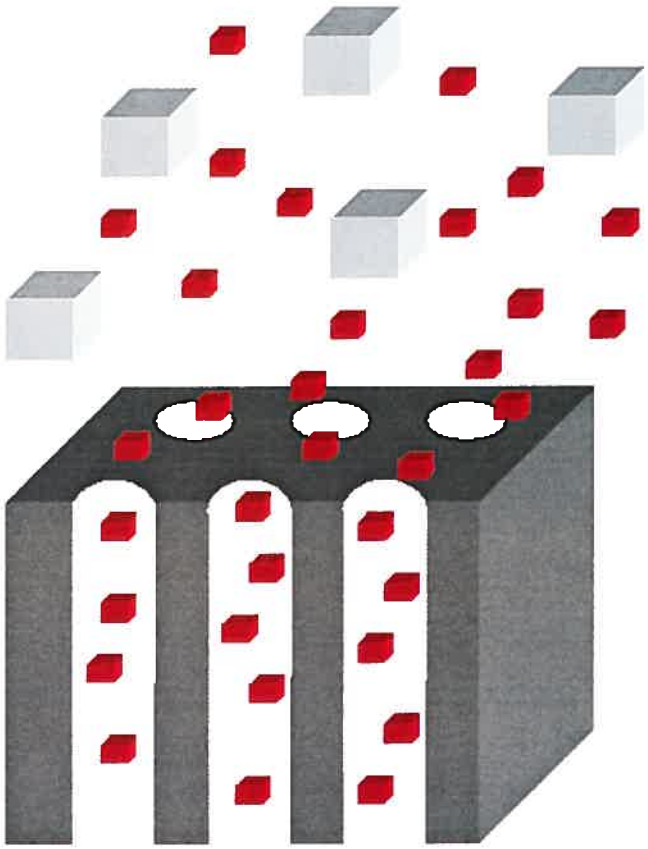

Figure 1.3. Diffusion sélective de molécules à l'intérieur d'un matériau tectonique. Seules les molécules ayant une taille inférieure aux dimensions des canaux pénètrent dans ceux-ci (cubes rouges). Les molécules de taille supérieure (cubes gris) sont confinées à l'extérieur du réseau.

Une autre application potentielle serait la catalyse de réactions chimiques. L'intérieur des canaux dans un solide tectonique est en général un milieu hautement

ordonné. La présence de sites de catalyse dans un tel type d'environnement pourrait amener à une classe de catalyseurs présentant d'intéressantes propriétés. Ainsi, un matériau tectonique pourrait être assemblé de telle façon à sélectionner certaines molécules de tailles précises pouvant pénétrer dans le réseau. Une fois à l'intérieur du réseau, ces molécules pourraient subir des réactions chimiques catalysées par la présence de sites fonctionnels précis intégrés à la structure même des tectons (Figure 1.4).

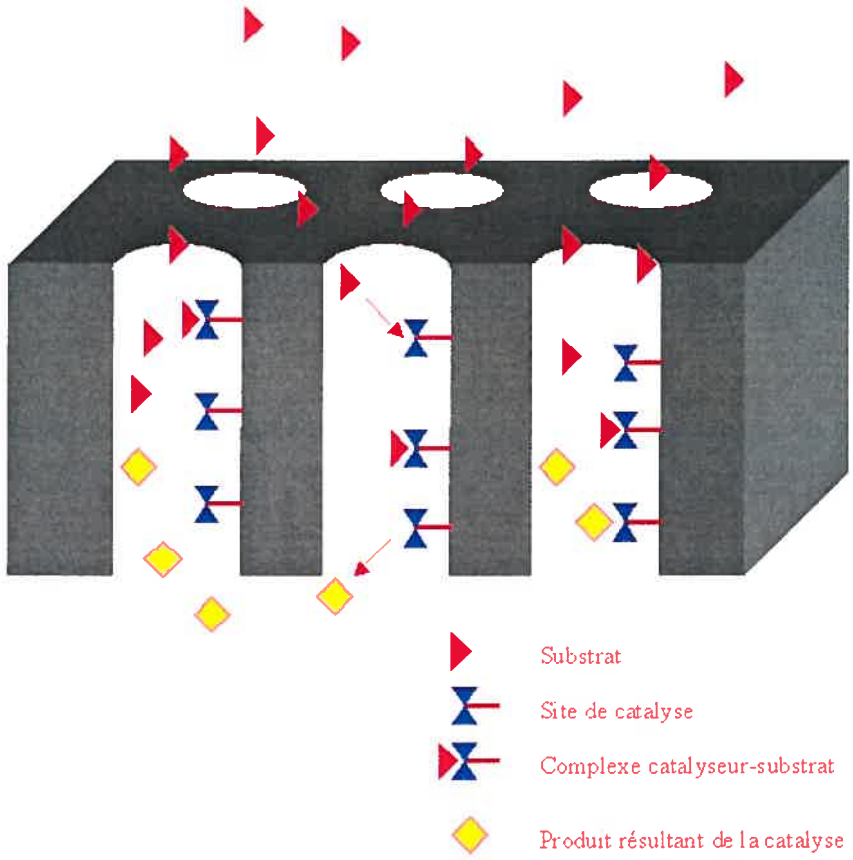

Figure 1.4. Utilisation des matériaux tectoniques en catalyse. Le substrat (triangle rouge) diffuse à l'intérieur des cavités, s'associe à un site de catalyse qui le transforme en un autre produit (losange jaune).

Ces processus de catalyse profiteraient d'un environnement hautement ordonné pouvant faciliter certains états de transition par des interactions stabilisantes, d'une façon un peu analogue aux processus catalysés par des enzymes. De plus, un des avantages des

matériaux tectoniques, non-mentionné jusqu'à présent, réside dans leur solubilité réduite dans la plupart des solvants organiques usuels. L'utilisation des matériaux tectoniques en catalyse hétérogène présenterait donc l'avantage de la récupération du catalyseur par simple filtration à la fin de la réaction.

À la lumière des précédents paragraphes, il est tentant de comparer les matériaux tectoniques aux zéolites, composés inorganiques à base d'aluminosilicates ou d'aluminophosphates. Les zéolites sont des matériaux poreux utilisés en industrie et en recherche académique notamment pour des processus de séparation et de catalyse. Régulièrement, les chimistes utilisent les capacités hygroscopiques que possèdent certains zéolites pour piéger sélectivement en leur sein des molécules d'eau. De plus, certains zéolites sont également employés comme catalyseurs : des molécules diffusent à l'intérieur de leurs cavités et subissent des transformations catalysées par la présence d'acides de Brønsted ou de Lewis tels que les atomes d'aluminium ou de bore contenus dans leurs structures. Les matériaux tectoniques sont donc en quelque sorte analogues aux zéolites. Étant donné que les tectons utilisés sont le plus souvent des molécules organiques, la robustesse du réseau tectonique est généralement moins grande que celle des zéolites, par exemple dans des conditions de haute température ou d'acidité élevée. Toutefois, ces inconvénients sont compensés par les avantages suivants :

- Le volume « libre » des zéolites dépasse rarement 50% alors qu'il dépasse couramment cette valeur dans le cas des solides tectoniques.

- La modulation des dimensions des cavités est beaucoup plus aisée dans le cas de la tectonique moléculaire puisqu'il suffit en principe de modifier les dimensions des tectons pour observer une modification conséquente à l'échelle du réseau. De plus, les tectons peuvent incorporer certains éléments de flexibilité conférant aux réseaux une capacité d'adaptation aux déformations mécaniques.

- L'incorporation de sites catalytiques est elle aussi en principe plus aisée puisqu'il suffit d'incorporer lors de la synthèse des tectons des groupements fonctionnels

pouvant servir de sites de catalyse ou de ligand à ceux-ci. De plus, la vaste gamme de catalyseurs existants en chimie organique ne limite pas le choix de sites catalytiques aux seuls atomes de bore ou d'aluminium des zéolites.

- Il est également possible d'incorporer par synthèse à la structure du tecton des composantes tels que des chromophores ou encore des éléments de chiralité selon l'usage souhaité.

1.3.1 Les groupes de reconnaissance moléculaire

Pour procéder à l'assemblage de structures supramoléculaires, la tectonique moléculaire utilise des motifs de reconnaissance. Ceux-ci sont en fait des groupements fonctionnels pouvant établir des interactions intermoléculaires fortes avec soit un second groupement identique ou encore avec un groupement de fonctions complémentaires. Pour pouvoir être utilisé de façon efficace dans l'élaboration de réseaux, un motif de reconnaissance doit notamment présenter les caractéristiques suivantes :

- Les interactions générées doivent être fortes afin de contrebalancer la tendance à l'empilement compact dirigée par les forces de van der Waals.

- Les interactions doivent être directionnelles pour orienter efficacement dans l'espace la formation du réseau supramoléculaire.

- Les interactions doivent présenter un certain caractère de prévisibilité, c'est à dire qu'elles favorisent la formation répétée de certains motifs plutôt que d'autres.

Les motifs de reconnaissance basés sur les ponts hydrogène répondent bien à ces critères et représentent la classe d'interactions intermoléculaires le plus souvent utilisées jusqu'à présent en tectonique moléculaire.

1.3.2 Le pont hydrogène

Le pont hydrogène se définit comme étant l'interaction entre un atome d'hydrogène, lié de façon covalente à un atome normalement électronégatif, D , avec un atome A possédant au moins une paire d'électrons libres (ou une molécule possédant des électrons p polarisables).[4-6] L'atome D est alors nommé *donneur de pont hydrogène* tandis que A est appelé *accepteur de pont hydrogène* (Figure 1.5). Le pont hydrogène se forme lorsque D est plus électronégatif que l'atome d'hydrogène, causant ainsi une polarisation partielle du lien D-H et laissant l'atome d'hydrogène partiellement positif. Les électrons libres de A viennent alors par interaction électrostatique se lier partiellement au proton. La présence de ponts hydrogène peut être détectée notamment par les études de diffraction des rayons X et ce même s'il est rare d'observer directement les atomes d'hydrogène dans de telles études.

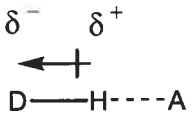

D = O, N, Halogène, C, S

A = O, N, Halogène, S, système π

Figure 1.5. Le pont hydrogène.

De façon générale, l'angle D-H-A adopte des valeurs comprises majoritairement entre 180° et 120°.[5] Quant à la force du pont hydrogène, elle se situe généralement entre 4 et 15 Kcal mol^{-1}.[6] L'ordre de grandeur de la force de ce lien dépend de plusieurs facteurs complexes pour lesquels la contribution exacte de chacun est encore matière à débat. Toutefois, il est possible de tirer quelques règles générales :[7]

- La force du pont hydrogène aura tendance de façon générale à diminuer avec la réduction de l'angle D-H-A par rapport à la linéarité.

- L'augmentation de la distance entre A et D tendra à affaiblir la force de l'interaction.

- La nature de D et A influencera également la force de l'interaction. Ainsi, plus l'atome D aura une électronégativité élevée, plus il sera à même d'agir comme donneur de ponts hydrogène. De façon parallèle, moins A sera électronégatif (et plus il sera polarisable), plus il sera en mesure d'interagir avec l'atome d'hydrogène. La Figure 1.5 identifie les atomes les plus fréquemment rencontrés pour D et A.

Le pont hydrogène représente donc une des interactions les plus utilisées en chimie supramoléculaire et ce pour plusieurs raisons :

- La force relativement élevée du pont hydrogène permet l'élaboration de réseaux supramoléculaires relativement robustes par effet additif.

- Le caractère directionnel du pont hydrogène permet un certain degré de prévisibilité dans le design d'association intermoléculaires.

1.3.3 Motif d'association utilisant le pont hydrogène

La tectonique moléculaire utilise donc principalement des motifs de reconnaissance basés sur le pont hydrogène notamment pour les raisons précédemment énoncées mais également pour la grande variété de motifs de reconnaissance par pont hydrogène existante. Un exemple de tel motif de reconnaissance est donné par la dimérisation des composés de la classe des 2-pyridones (Figure 1.6). L'interaction entre les donneurs amino et les accepteurs carbonyles favorisent la formation d'un dimère en solution[8] de même qu'à l'état cristallin.[9]

Figure 1.6. Dimérisation des 2-pyridones.

Un autre motif de reconnaissance fréquemment utilisé en chimie supramoléculaire est celui des acides carboxyliques. Les acides carboxyliques peuvent s'associent à l'état cristallin principalement selon deux motifs soit sous la forme de dimères ou encore de catémères (Figure 1.7).[10] Le motif de dimérisation est toutefois largement favorisé et la forme catémère n'est généralement caractéristique que des acides de petites tailles (acide formique, acétique).[7]

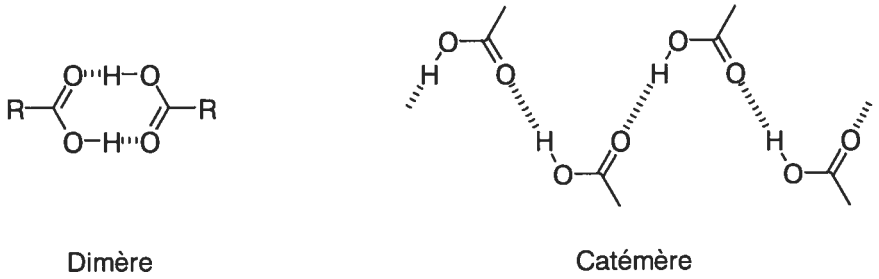

Figure 1.7. Motifs d'association des acides carboxyliques.

Un intéressant exemple de la dimérisation des acides carboxyliques se trouve dans la structure cristalline de l'acide trimésique.[11] Chaque groupement acide dimérise avec celui d'une autre molécule de façon à former l'arrangement supramoléculaire hexagonal représenté à la Figure 1.8. Ce processus d'association amène à la formation de feuillets d'hexamères avec des ouvertures périodiques dont le diamètre atteint 14 Å. Toutefois, les cavités ne sont pas ici reliées entre elles mais plutôt remplies par d'autres feuillets indépendants : c'est le phénomène d'interpénétration.[12] Ce phénomène se produit lorsque l'on peut définir dans une structure au moins deux réseaux qui sont totalement indépendants l'un de l'autre en terme de connections, mais qui sont imbriqués l'un dans l'autre. La Figure 1.9 illustre ce phénomène pour des réseaux de type diamantoïde. Ce

phénomène peut parfois empêcher, comme dans le cas de l'acide trimésique, la formation de cavités pour l'inclusion de molécules invitées.

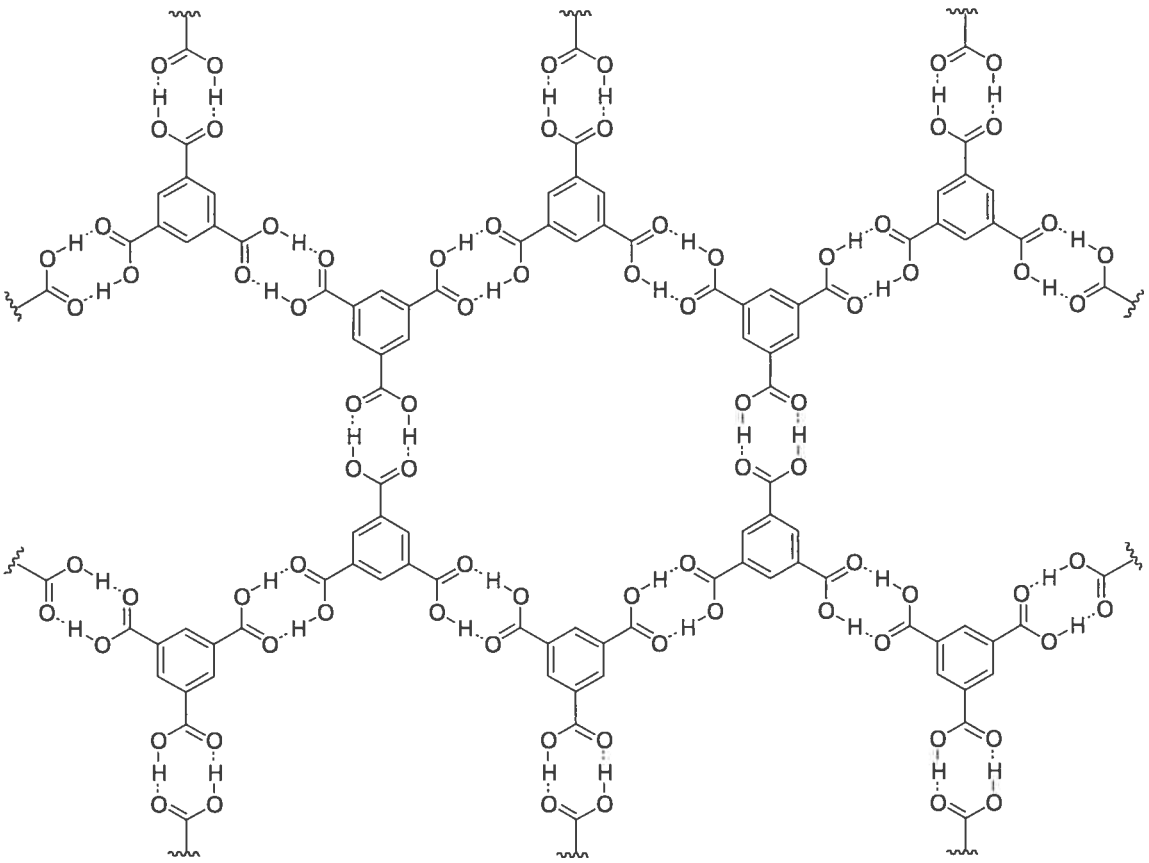

Figure 1.8 Représentation schématique d'une couche formée par ponts hydrogène dans la structure de l'acide trimésique.

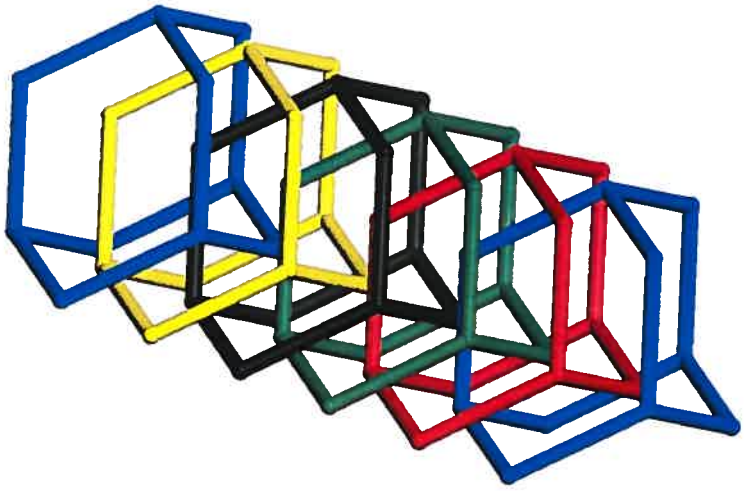

Figure 1.9 Interpénétration de 5 réseaux diamantoïdes. Le premier réseau (en bleu) est représenté 2 fois.

Différents dérivés des 2,4-diaminotriazines peuvent également être utilisés comme groupement de reconnaissance (Figure 1.10). L'utilisation de ce groupe de reconnaissance présente plusieurs avantages : présence de nombreux donneurs et accepteurs de ponts hydrogène, présence de groupements $-NH_2$ pouvant être ultérieurement fonctionnalisés et bonne résistance à différentes conditions réactionnelles. De plus, les diaminotriazines peuvent être rapidement synthétisées à partir de simples dérivés nitriles ou amino.[13] De nombreux réseaux supramoléculaires poreux ont pu ainsi être élaborés en utilisant des dérivés du type **1.1** ou encore **1.2**.[14-24] Des différents motifs d'association pour les 2,4-diaminotriazines présentés à la Figure 1.11, le mode **1.3** est habituellement prépondérant mais il est possible d'observer les motifs **1.4** ou encore **1.5** sous certaines conditions à l'état cristallin.[20]

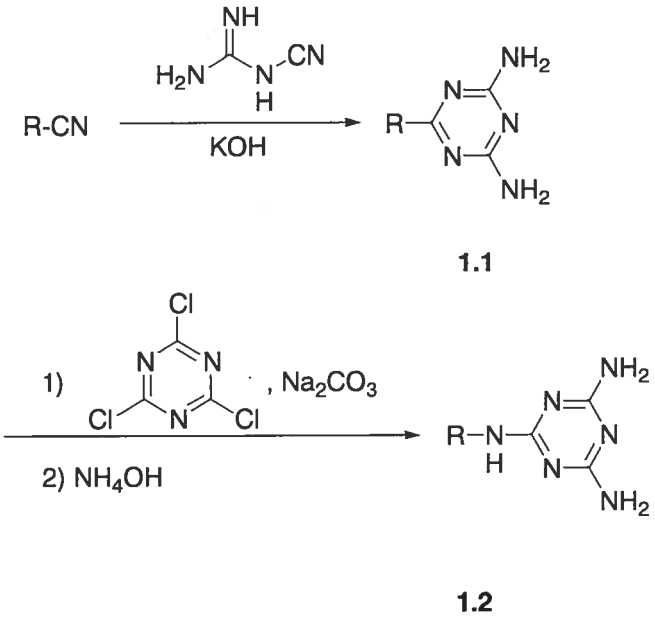

Figure 1.10 Synthèse des dérivés de la classe des 2,4-diaminotriazines.

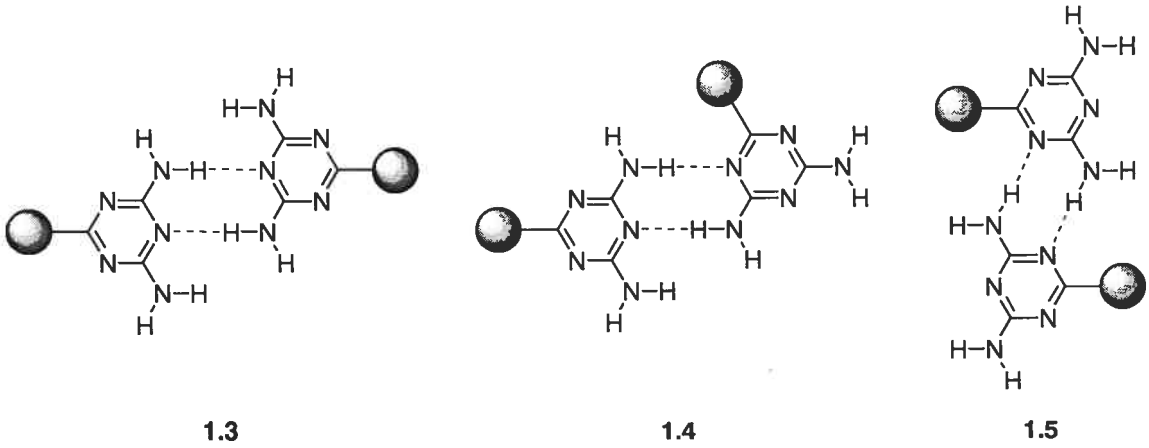

Figure 1.11 Motifs d'association des 2,4-diaminotriazines.

Les trois groupes de reconnaissance venant d'être présentés ne représentent qu'une infime portion des motifs de reconnaissance intermoléculaire disponibles. Des tentatives ont été faites afin de classer les groupes de reconnaissance entre eux en fonction de leur efficacité à établir des interactions intermoléculaires. Ainsi le groupe de Allen a développé un programme informatique d'analyse des structures cristallographiques archivées dans la *Cambridge Structural Database* (CSD) afin de repérer les motifs de reconnaissance les plus récurrents.[27] Les résultats d'une telle analyse doivent cependant être considérés soigneusement. En effet, l'analyse ne se base que sur les structures cristallographiques rapportées; il se peut qu'un motif de reconnaissance possible n'apparaisse pas simplement du fait qu'aucune étude cristallographique n'ait été effectuée. Toutefois, ce type d'analyse donne une certaine idée de la fiabilité à reproduire un certain patron de reconnaissance pour un groupe de fonctions données.

1.4 Les différents squelettes moléculaires.

La forme moléculaire du tecton est également un facteur à considérer lors de l'élaboration de réseaux supramoléculaires et ce pour deux raisons :

- Le squelette moléculaire est responsable de l'orientation des groupes de reconnaissance dans l'espace.

- La forme même de la molécule peut défavoriser l'empilement compact lors de la cristallisation. Elle semble également jouer un rôle dans la présence ou l'absence de réseaux interpénétrés pour des raisons toutefois encore mal comprises.

À la lumière de ces considérations, certaines formes seront privilégiées : les molécules présentant un certain caractère de rigidité permettront plus facilement la formation de réseaux poreux en maintenant de façon plus ou moins permanente les groupes de reconnaissance dans une direction donnée. La Figure 1.12 donnent quelques exemples de squelettes moléculaires utilisés avec succès pour l'assemblage de réseaux

tectoniques. Les dérivés **1.6-1.8** orientent les groupements de reconnaissance dans un même plan, favorisant ainsi la formation de réseaux en forme de couche.[14-18] Par contre, les squelettes **1.9**, **1.10** et **1.11** dirigent les groupes de reconnaissance de façon tétraédrique et prédisposent ainsi à la formation de réseaux supramoléculaires tridimensionnels.[3, 19-24] Il à noter que bien que tous ces dérivés présentent une certaine rigidité, quelques degrés de flexibilité peuvent être tolérés tel que dans le cas des composés **1.12** et **1.13**.[25,26]

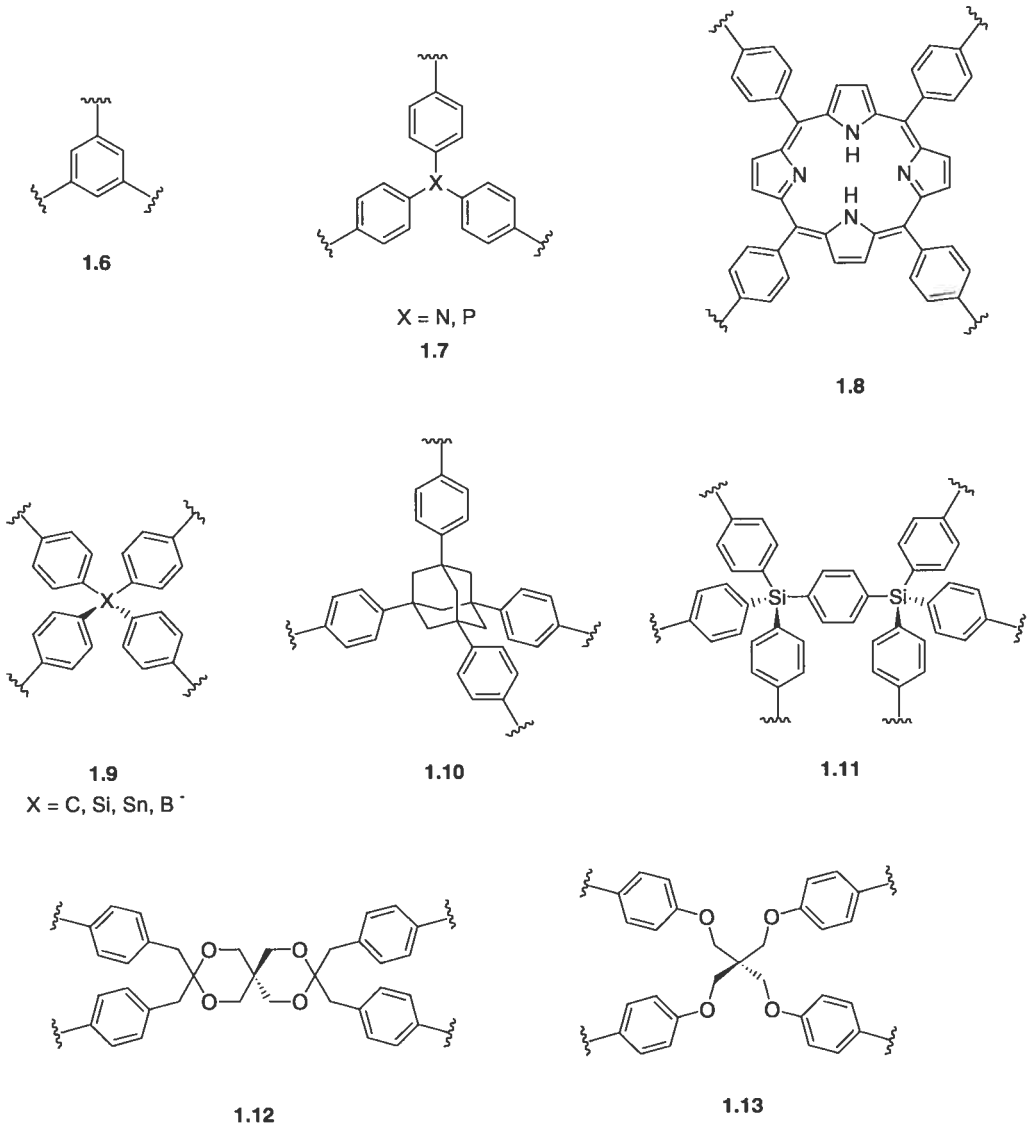

Figure 1.12 Différents squelettes utilisés en tectonique moléculaire.

1.5 Tecton présentant une grande intégralité structurale

Le tecton **1.14** est constitué de quatre groupements 2,4-diaminotriazine maintenus dans une orientation tétraédrique par le squelette du tétraphénylméthane.[19] La cristallisation de ce composé par diffusion de dioxane dans une solution d'acide formique permet d'obtenir des cristaux de qualité suffisante pour une étude cristallographique.

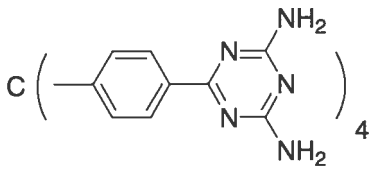

1.14

L'analyse cristallographique révèle que chaque tecton utilise les diaminotriazines pour établir des ponts hydrogène avec huit molécules voisines. Quatre de ces voisins sont alignés dans le plan des axes cristallographiques *a* et *b*, définissant ainsi une cavité, représentée à la Figure 1.13, dont le diamètre est de 11,8 Å selon la dimension la plus large. Le tecton établit en plus des liaisons hydrogène avec quatre autres voisins orientés suivant l'axe *c*. Cet arrangement tridimensionnel a pour effet d'aligner les cavités, les reliant ainsi entre elles suivant l'axe *c*, de façon à créer des canaux parallèles parcourant le réseau cristallin suivant cet axe. Au total, près de 45% du volume du cristal est disponible pour l'inclusion de molécules invitées. Ces cavités sont occupées par des molécules de dioxane et d'acide formique. Chaque tecton participe en tout à 16 ponts hydrogène et la somme de ces interactions permet la formation d'un réseau supramoléculaire résistant à une évacuation partielle du solvant. Ainsi, lorsque des cristaux du tecton **1.14** sont mis sous vide (0.1 Torr) pendant 66 heures, près de 63% des molécules de solvant peuvent être retirées tout en préservant l'intégralité de la structure. Cette dernière particularité est remarquable puisque généralement les réseaux supramoléculaires poreux basés sur l'utilisation de ponts hydrogène résistent parfois mal à l'évacuation des molécules incluses. De plus, les molécules de solvants incluses

initialement dans le cristal peuvent être librement échangées avec d'autres invités. Ainsi, lorsque des cristaux du tecton **1.14** sont immergés dans l'acétonitrile, toutes les molécules de dioxane et d'acide formique sont remplacées.

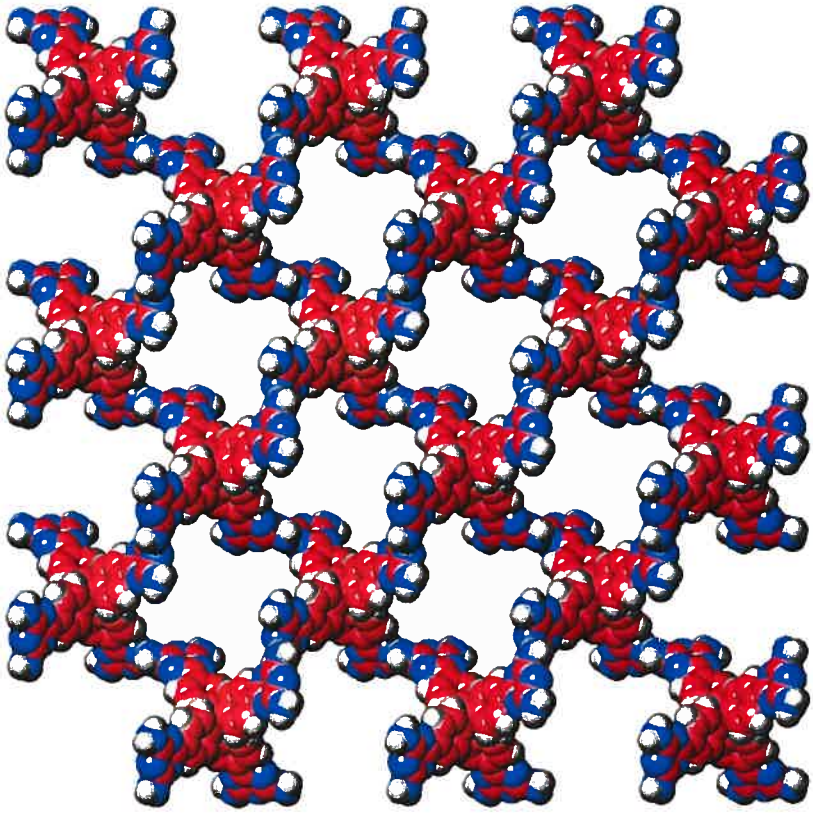

Figure 1.13 Vue selon l'axe *c* du réseau formé par la cristallisation du tecton **1.14**. Les cavités forment des canaux parallèles à l'axe *c*. Les molécules de solvant ont été omises pour plus de clarté. Sauf indications contraires, le code de couleur utilisé au tout au long du texte est le suivant : carbone (rouge), azote (bleu), hydrogène (gris), phosphore (jaune), brome (bleu azur).

1.6 Tecton anionique.

La tectonique moléculaire ne se limite pas aux molécules neutres; elle peut également servir à la création de réseaux dits « ioniques ». Dans de tels réseaux, le

squelette du tecton comporte un ou plusieurs atomes chargés (cation ou anions) modifiant les propriétés du réseau. Ainsi, la cristallisation par diffusion de toluène dans une solution du tecton **1.15** dans le DMSO génère le réseau tridimensionnel poreux représenté à la Figure 1.14.[24]

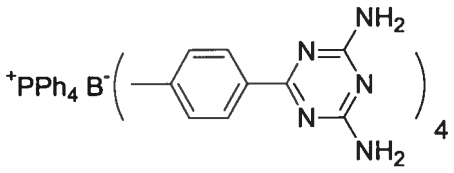

1.15

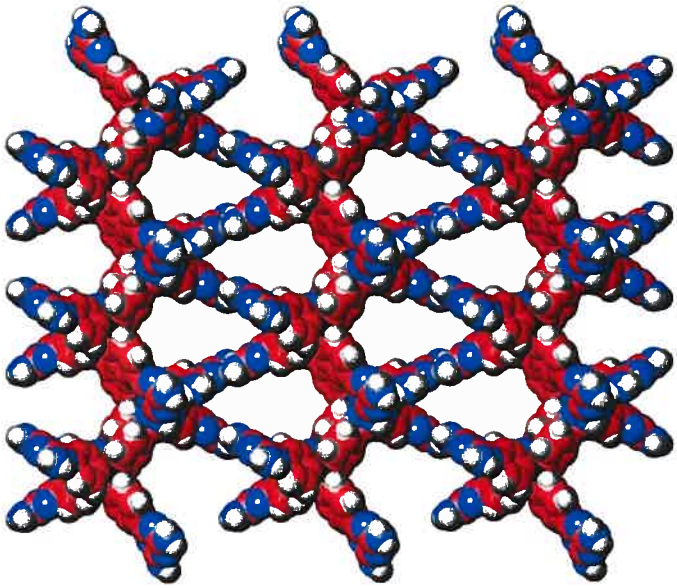

Figure 1.14 Vue selon l'axe *c* du réseau formé par la cristallisation du tecton **1.15** sans les molécules de solvant et les cations désordonnés. Les cavités forment des canaux parallèles à l'axe *c*.

Chaque tecton établit 16 ponts hydrogène mais avec six voisins seulement de façon à réduire les répulsions coulombiennes. Les canaux formés incluent des molécules de DMSO ainsi que le contre-ion nécessaire afin de maintenir l'équilibre des charges (ici

$^{+}PPh_4$). Au total, l'espace libre dans le réseau atteint près de 74%. Ce cristal constitue donc un réseau anionique immobile dans lequel des charges cationiques mobiles sont incluses. Ces cations peuvent être par la suite librement échangés avec d'autres types de molécules chargées positivement. De plus, les dimensions fixes des cavités du réseau (8 x 12 Å) ne laissent passer que les cations d'une taille inférieure à celles-ci. Ce type de réseau semble donc prometteur pour l'élaboration de matériaux chargés pouvant reconnaître et piéger sélectivement selon la taille des molécules de charge opposée. Il démontre également la compatibilité entre la présence de charges et la formation de ponts hydrogène.

1.7 Tecton trigonal.

Les deux exemples précédents se basaient sur des tectons de géométrie tétraédrique. Le composé **1.16** illustre cette-fois le cas d'un tecton de géométrie trigonale.[16] La cristallisation de ce composé génère le réseau poreux représenté à la Figure 1.15.

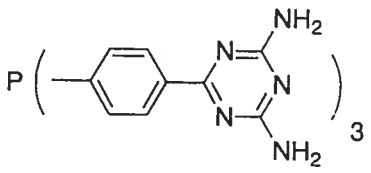

1.16

Chaque tecton s'associe avec trois voisins en formant au total 10 ponts hydrogène via les diaminotriazines de façon à générer un assemblage sous forme de couche en deux dimensions. Différentes couches se superposent et, contrairement au cas de l'acide trimésique présenté à la Figure 1.8, les espaces libres générés sont reliés entre eux de façon à former des canaux. Les dimensions de ceux-ci sont d'environs 15 x 5 Å et ils contiennent des molécules de DMSO et de toluène. Au total, environs 60% de l'espace du cristal est disponible pour l'inclusion de molécules invitées.

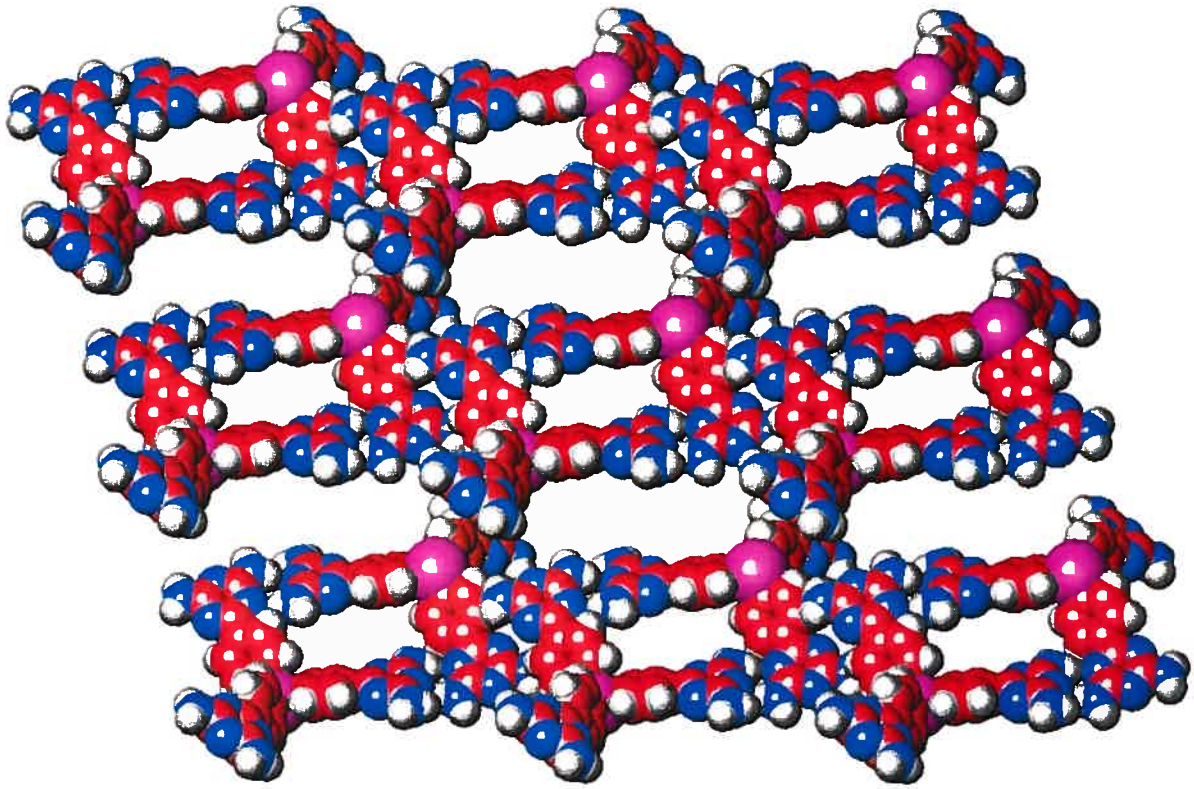

Figure 1.15. Vue selon l'axe *c* du réseau formé par la cristallisation du tecton **1.16**. Les cavités forment des canaux parallèles à l'axe *a*. Les molécules de solvant ont été omises pour plus de clarté.

Une des caractéristiques les plus intéressantes du tecton **1.16** réside dans le fait que l'atome de phosphore peut être utilisé comme nucléophile. Par exemple, en effectuant des réactions de type S_n2 sur des substrats halogénés, il est possible d'obtenir un tecton chargé pouvant être cristallisé à son tour (Figure 1.16).

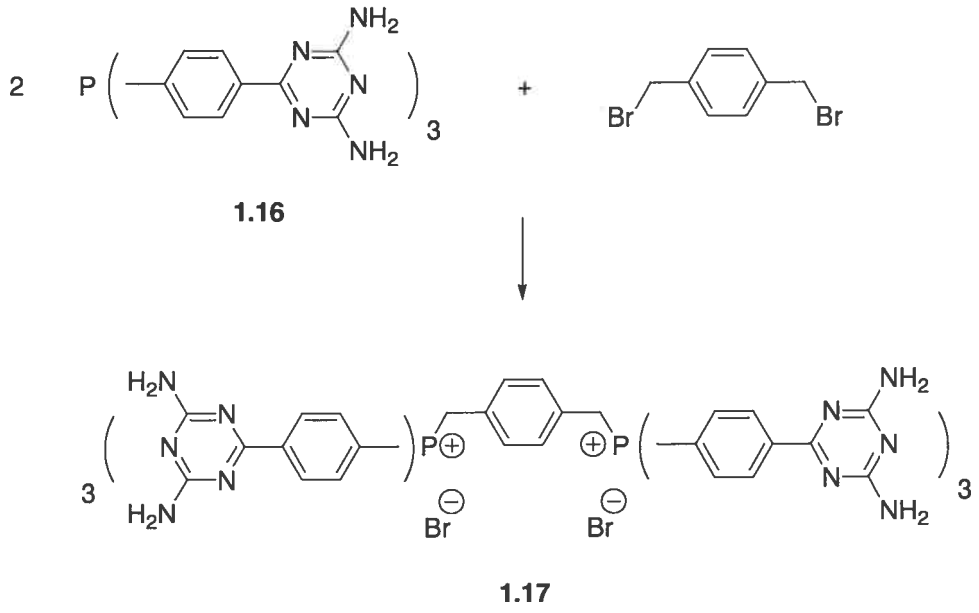

Figure 1.16 Exemple de synthèse de sels de phosphonium utilisant la nucléophilicité de l'atome de phosphore du tecton **1.16**. Les sels obtenus peuvent ensuite être cristallisés de façon à générer des réseaux cationiques.

Ainsi, le sel obtenu par la réaction de la Figure 1.16 donne après cristallisation un réseau poreux cationique dans lequel les anions peuvent être échangés librement. La présence de canaux est montrée à la Figure 1.17. Le tecton **1.16** devient donc une sorte d'élément modulaire servant à la construction de réseaux chargés; il suffit de changer la nature de la molécule portant l'halogénure pour obtenir un autre type de matériau.

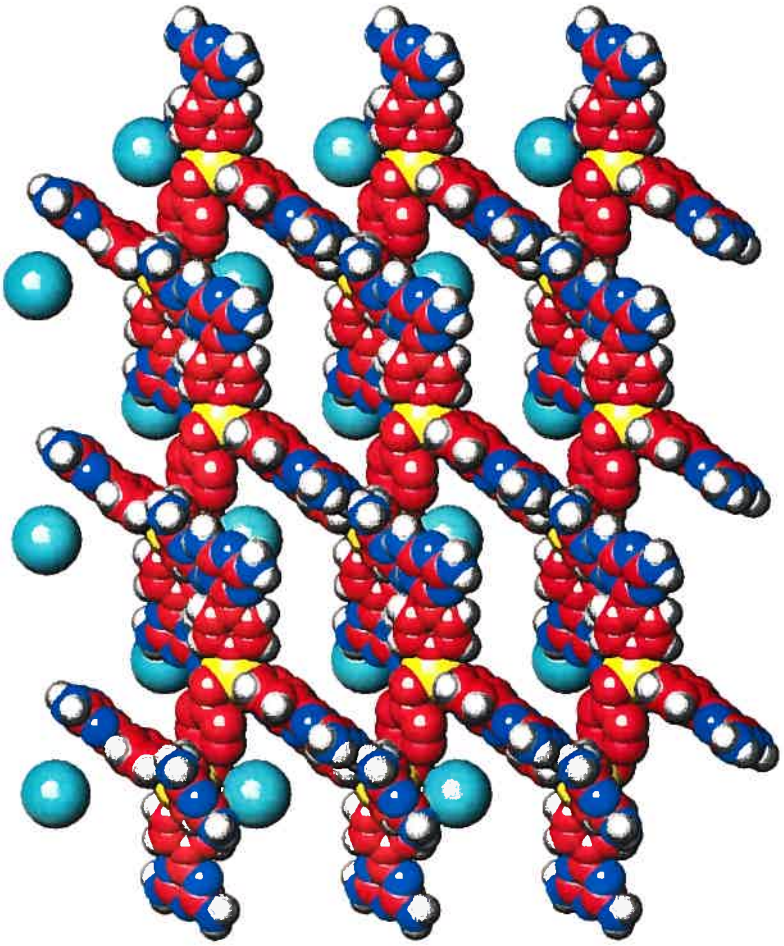

Figure 1.17 Vue selon l'axe *b* du réseau formé par la cristallisation du tecton **1.17**. Les cavités forment des canaux parallèles à l'axe *c*. Les molécules de solvant ont été omises pour plus de clarté.

Les chapitres suivants reprendront les thèmes précédemment développés pour développer d'avantages les connaissances en tectonique moléculaire. Plus précisément, la discussion sera orientée autour de deux thèmes majeurs, soit l'étude de nouveaux motifs de reconnaissance de même que l'utilisation de nouveaux squelettes moléculaires pour le design de tectons. Le Chapitre 2 sera consacré au développement de nouveaux blocs de construction moléculaires pour le design de tectons. L'utilisation des phénols comme unités de reconnaissance sera par la suite examinée de plus près au Chapitres 3.

Le potentiel des acides boroniques comme motif d'association sera également examiné dans le Chapitre 4. Finalement, l'utilisation des dérivés du 9,9'-spirobifluorene comme squelette moléculaire sera discutée au Chapitres 5.

1.8 Références

1. Lehn, J.-M. *Angew. Chem., Int. Ed. Engl.* **1988**, *27*, 89.
2. Pour une collection d'excellentes monographies sur la chimie supramoléculaire, le lecteur est invité à consulter : Lehn, J.-M. *Supramolecular Chemistry*; VCH Publishers : Weinheim, 1995. Schneider, H.-J.; Dürr, H. *Frontiers in Supramolecular Organic Chemistry and Photochemistry*; VCH Publishers : Weinheim, 1991. Dunitz, J. D.; Hafner, K.; Ito, S.; Lehn, J.-M.; Raymond, K. N.; Rees, C. W.; Thiem, J.; Vögtle *Topics in Current Chemistry* **1995**, *175*. Dewar, M. J. S. Dunitz, J. D.; Hafner, K.; Ito, S.; Lehn, J.-M.; Raymond, K. N.; Rees, C. W.; Thiem, J.; Vögtle *Topics in Current Chemistry* **1993**, *165*.
3. Simard, M.; Su, D.; Wuest, J. D. *J. Am. Chem. Soc.* **1991**, *113*, 4696.
4. Philp, D.; Stoddart, J. F. *Angew. Chem., Int. Ed. Engl.* **1996**, *35*, 1154.
5. Steiner, T. *Angew. Chem., Int. Ed. Engl.* **2002**, *41*, 48.
6. Jeffrey, G. A. *An Introduction to Hydrogen Bonding*, Oxford University Press, Oxford, 1997.
7. Weber, E. *Topics in Current Chemistry* **1998**, *198*.
8. Ducharme, Y.; Wuest, J. D. *J. Org. Chem.* **1988**, *24*, 5787.
9. Ohms, U.; Guth, H.; Hellner, E.; Dannoelh, H.; Schweig, A. *Z. Kristallogr.* **1984**, *169*, 185. Kvick, A.; Booles, S. S. *Acta Crystallogr., Sect. B.: Struct. Crystallogr. Chem.* **1972**, *B28*, 3405. Amlöf, J.; Kvick, A.; Olovson, I. *Acta Crystallogr., Sect. B.: Struct. Crystallogr. Chem.* **1971**, *B27*, 1201. Penfold, B. *Acta Crystallogr.* **1953**, *6*, 591.
10. Kolotuchin, S. V.; Fenlon, E. E.; Wilson, S. R.; Loweth, C. J.; Zimmerman, S. C. *Angew. Chem., Int. Ed. Engl.* **1995**, *34*, 2654.
11. Duchamp, D. J.; Marsh, R. E. *Acta Crystallogr., Sect. B.: Struct. Crystallogr. Chem.* **1969**, *B25*, 5.

12. Batten, S. R.; Robson, R. *Angew. Chem., Int. Ed. Engl.* **1998**, *37*, 1460.
13. Quirke, J. M. E. *Comprehensive Heterocyclic Chemistry*; Katritzky, A. R.; Rees, C. W. Eds.; Pergamon: Oxford, 1984; Vol. 3, p 457. Smolin, E. M.; Rapoport, L. *The Chemistry of Heterocyclic Compounds*; Weissberger, A., Ed.; Interscience: New York, 1959, Vol 13.
14. Desharnais, J. *Thèse de doctorat*, Université de Montréal, 2001.
15. Dumas, L. *Mémoire de maîtrise*, Université de Montréal, 2002.
16. Gonzalez Gonzalez, G.; *Mémoire de maîtrise*, Université de Montréal, 2002. Gonzalez Gonzalez, G.; Simard, M.; Maris, T.; Wuest, J. D., résultats non publiés.
17. Helzy, F.; Simard, M.; Maris, T.; Wuest, J. D., résultats non publiés.
18. Lautman, M.; Maris, T.; Wuest, J. D., résultats non publiés.
19. Brunet, P.; Simard, M.; Wuest, J. D. *J. Am. Chem. Soc.* **1997**, *119*, 2737.
20. Su, D.; Wang, X.; Simard, M.; Wuest, J. D. *Supramolecular Chem.* **1995**, *6*, 171. Wuest, J. D. *Mesomolecules: From Molecules to Materials*; Mendenhall, G. D., Greenberg, A., Liebman, J. F.; Chapman & Hall: New York, 1995; p 107.
21. Wang, X.; Simard, M.; Wuest, J. D. *J. Am. Chem. Soc.* **1994**, *116*, 12119.
22. Le Fur, E. *Mémoire de maîtrise*, Université de Montréal, 2000.
23. Demers, E. Simard, M.; Maris, T.; Wuest, J. D., résultats non publiés.
24. Malek, N. *Thèse de doctorat*, Université de Montréal, 2001.
25. Sauriat Dorizon, H.; Maris, T.; Wuest, J. D. *J. Org. Chem.*, accepté pour publication.
26. Laliberté, D. Maris, T.; Wuest, J. D., résultats non publiés.
27. Allen, F. H.; Motherwell, W. D. S.; Raithby, P. R.; Shields, G.; Taylor, R. *New J. Chem.* **1999**, 25.

Chapitre 2

Synthèse de dérivés du tétraphénylméthane et du tétraphénylsilane

2.1 Introduction

Les dérivés du tétraphénylméthane et du tétraphénylsilane ont été à de nombreuses reprises utilisées dans l'élaboration de réseaux tectoniques puisqu'ils dirigent efficacement dans une orientation tétraédrique les groupes d'association intermoléculaire. Le développement de nouveaux tectons basés sur ce type d'armature moléculaire passe notamment par la synthèse de nouveaux dérivés servant de précurseurs de blocs de construction pour l'élaboration de nouveaux réseaux poreux. Dans ce chapitre, nous résumons nos contributions à la synthèse de dérivés du tétraphénylméthane et du tétraphénylsilane.

La première isolation du tétraphénylméthane **2.1** remonte aussi loin que 1897.[1] Ce composé suscitait alors l'intérêt des scientifiques de l'époque tant du point de vue structural que de l'accomplissement synthétique pour l'époque. L'intérêt était notamment du à l'intrigante possibilité de lier quatre cycles aromatiques à un même atome central. Ce fut finalement Moses Gomberg qui réussit à préparer la cible convoitée tel qu'illustré à la Figure 2.1.[1]

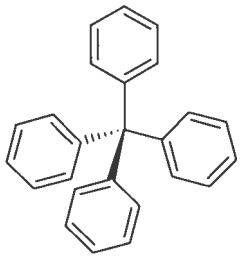

2.1

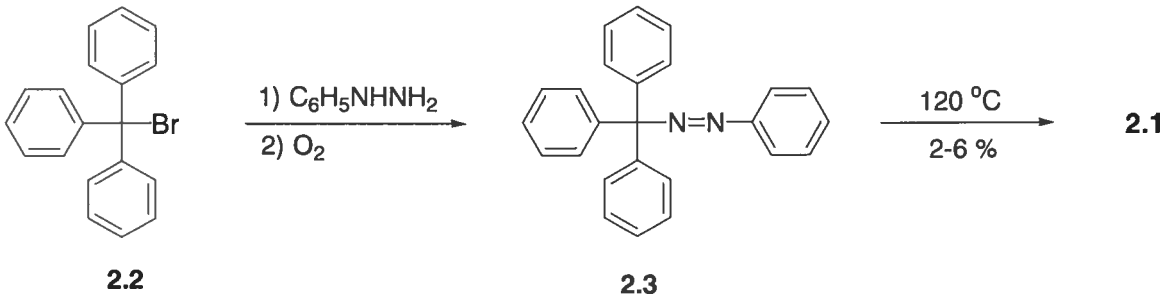

2.2 2.3

Figure 2.1 Première synthèse du tétraphénylméthane par Gomberg en 1897.[1]

Toutefois, les difficultés d'isolation de même que le rendement extrêmement bas de la dernière étape ne rendent pas ce processus viable à grande échelle. Un protocole plus moderne reposant sur une alkylation régiosélective de Friedel-Crafts sur l'aniline en présence de triphénylméthanol (Figure 2.2) permet d'obtenir le tétraphénylméthane sur une échelle de plusieurs dizaines de grammes en deux étapes.[2]

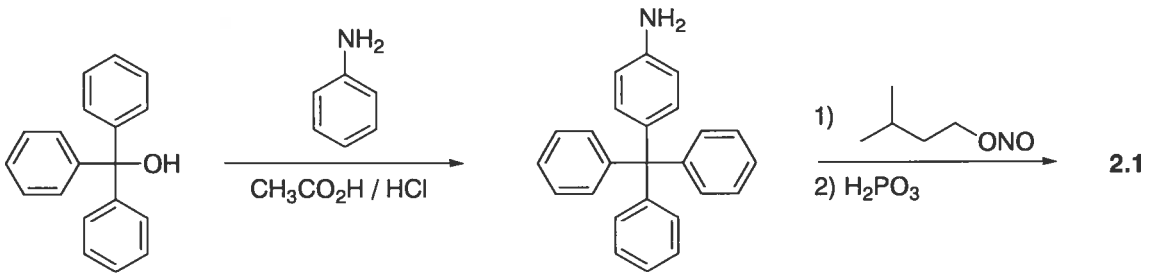

2.4 2.5

Figure 2.2 Synthèse moderne du tétraphénylméthane.[2]

La synthèse du tétraphénylméthane présente non-seulement un intérêt du point de vue scientifique mais également historique. En effet, Gomberg, suite à ces travaux sur la synthèse du tétraphénylméthane, s'intéressa à la synthèse de l'hexaphényléthane (**2.7**) et tenta de le préparer en traitant le chlorure de triphénylméthane en présence d'argent métallique. Bien que ses tentatives ne menèrent pas à la formation de l'hexaphényléthane

désiré, l'observation clé de Gomberg fut de remarquer la formation d'un intermédiaire fortement coloré en solution. Tentant de le caractériser, Gomberg en vint à la conclusion que les conditions réactionnelles provoquaient la formation du radical triphénylméthyle (**2.8**).[3] Il s'agissait de la première fois que l'existence d'espèces radicalaires était proposée en chimie organique. Cette hypothèse suscita un houleux débat à l'époque puisqu'une partie de la communauté scientifique était réfractaire à l'existence de radicaux organiques et il fallut attendre plusieurs années avant qu'il soit admis que Gomberg avait vu juste.

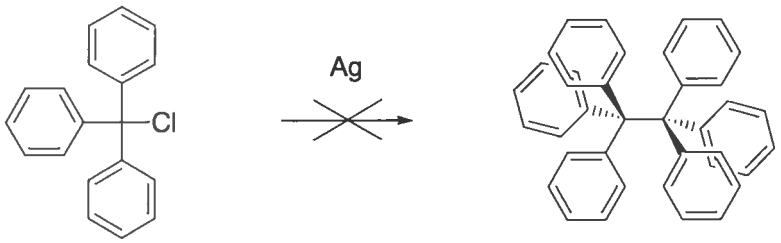

2.6 **2.7**

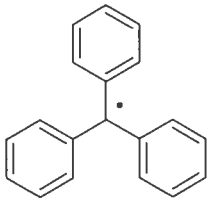

2.8

Intermédiaire proposé
par Gomberg

Figure 2.3 Tentative de Gomberg pour synthétiser l'hexaphényléthane et génération de la première espèce radicalaire en chimie organique.

2.2 Exemples d'utilisation du tétraphénylméthane

Les dérivés du tétraphénylméthane ont trouvé des applications non-seulement dans l'élaboration de réseaux supramoléculaires poreux mais également dans d'autres domaines. Ainsi, le groupe Stoddart utilise régulièrement ce type de dérivé dans

l'élaboration de « moteurs moléculaires » : les groupes tétraphénylméthane présents aux extrémités du rotaxane **2.9** empêchent la chaîne centrale de sortir hors de l'anneau constitué par les groupements éther-couronne.[4]

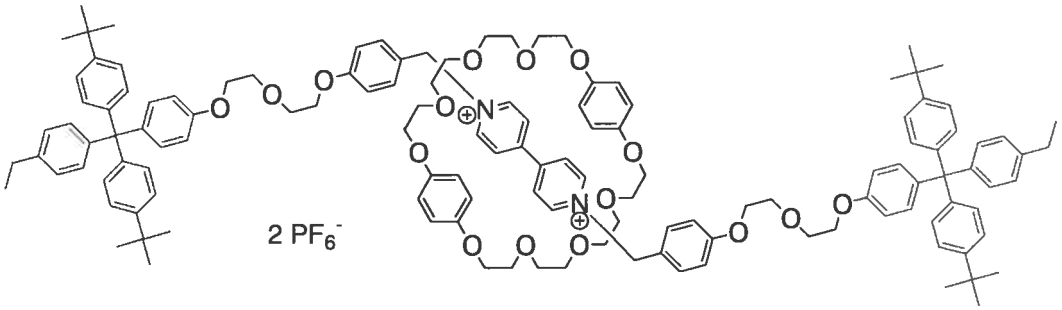

2.9

Figure 2.4 Utilisation de dérivés du tétraphénylméthane comme élément constitutif des rotaxanes.

Le tétraphénylméthane a également servi de support pour l'élaboration de sels radicalaires cationiques. Le groupe de Rathore a ainsi utilisé le tétraphénylméthane comme squelette de base pour le sel **2.10**.[5] Chaque branche de la molécule contient un sel radicalaire cationique pouvant servir de site rédox dans des réactions de transfert d'électrons. Étant donné que la structure du tétraphénylméthane ne permet pas la conjugaison électronique entre les différentes branches, chaque site devient indépendant les uns des autres.

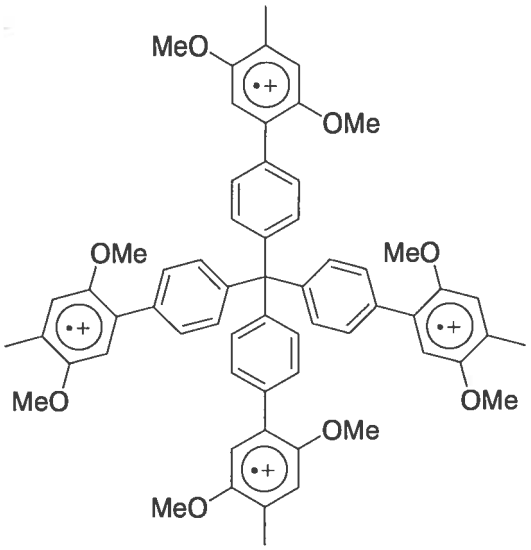

2.10

2.3 Élaboration de réseaux supramoléculaires poreux

La structure du tétraphénylméthane rend celle-ci attrayante pour l'élaboration de tectons. En effet, il est possible d'utiliser ce squelette pour orienter des sites d'association de façon tétraédrique : la structure rigide du tétraphénylméthane assure leur maintien dans cette orientation de façon permanente. Si les interactions présentent le caractère directionnel souhaité, il est possible alors d'élaborer des réseaux tridimensionnels tel que ceux discutés au Chapitre 1. Plusieurs réseaux tridimensionnels poreux ont ainsi pu être élaborés en utilisant des tectons basés sur le tétraphénylméthane tels qu'illustrés à la Figure 2.5.[6-8]

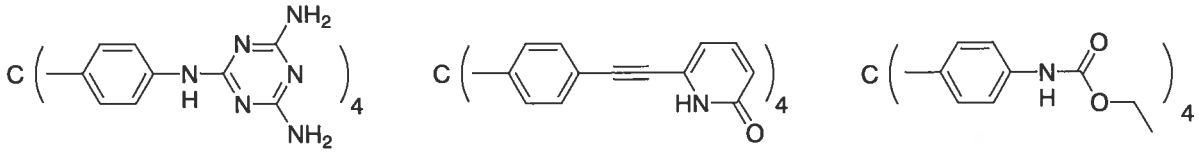

2.11 **2.12** **2.13**

Figure 2.5 Exemple de tectons utilisant le tétraphénylméthane comme squelette moléculaire.

Il est également possible d'utiliser des analogues du tétraphénylméthane afin de maintenir des sites d'association intermoléculaires dans une orientation spatiale tétraédrique. Les tectons **2.14** et **2.15** dérivés du tétraphénylsilane (Figure 2.6) ont ainsi pu être utilisés pour l'élaboration de réseaux tectoniques.[9]

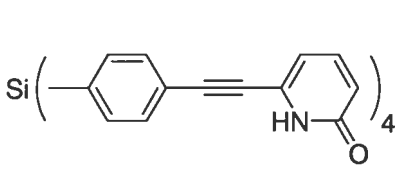

2.14

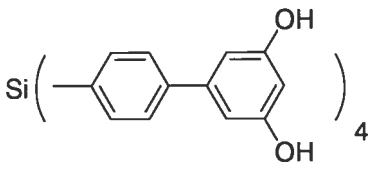

2.15

Figure 2.6 Exemples de tectons utilisant le tétraphénylsilane comme squelette moléculaire.

2.4 Fonctionalisation du tétraphénylméthane et du tétraphénylsilane

Les exemples précédents ont pour caractéristique de reposer sur l'utilisation de dérivés para-substitués. Ce patron de substitution assure l'orientation tétraédrique des groupes d'association. Afin de pouvoir générer un plus grand nombre de tectons, il est essentiel de disposer d'un vaste gamme de dérivés fonctionnalisés en position 4 (par rapport à l'atome central) du tétraphénylméthane ou du tétraphénylsilane. Dans le cas du tétraphénylméthane, la stratégie généralement employée pour la fonctionnalisation utilise des réactions de substitution électrophile aromatique. Ces substitutions prennent avantage de la régiosélectivité associée à cette molécule, préférence due non seulement au caractère électronique relativement plus riche de la position 4 mais également à l'inaccessibilité des positions 2 et 6 pour des raisons d'encombrement stérique (Figure 2.7).

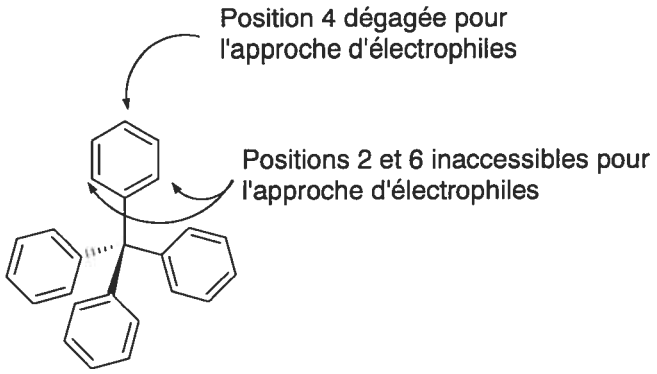

Figure 2.7 Réactivité du tétraphénylméthane envers les électrophiles.

Il est ainsi possible d'halogéner[2b] ou encore de nitrer[6] le tétraphénylméthane régiosélectivement sur chacun des sites aromatiques (Figure 2.8). Toutefois, les conditions expérimentales sont généralement sévères et limitent un peu les différentes fonctionnalisations possibles.

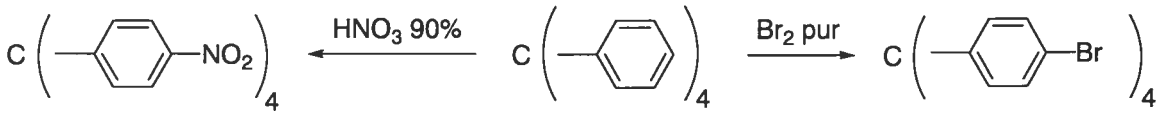

Figure 2.8 Réactions de substitution électrophile aromatique du tétraphénylméthane.

La situation du tétraphénylsilane est totalement différente puisque les tentatives de fonctionnalisation par des processus de substitution électrophile aromatique emploient des conditions provoquant généralement le bris de la liaison Si-C. Les fonctionnalités désirées doivent généralement être introduites au moment de la synthèse même du cœur silané. Les tétraphénylsilanes se synthétisent généralement en traitant le $SiCl_4$ ou un dérivé en présence d'un réactif organométallique de type Grignard ou aryllithium (Figure 2.9).

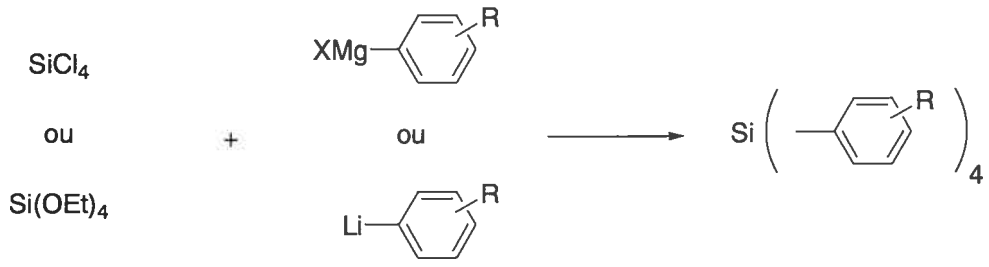

Figure 2.9 Synthèse des dérivés du tétraphénylsilane

Étant donné le potentiel important des dérivés du tétraphénylméthane et tétraphénylsilane pour l'élaboration de tectons, il est apparut nécessaire d'explorer différentes approches visant à générer un plus grand nombre de dérivés. L'approche retenue dans le présent travail consiste à traiter, au moyen de butyllithium, les dérivés tétrahalogénés du tétraphénylméthane ou tétraphénylsilane. L'espèce tétralithiée générée est par la suite traitée au moyen d'électrophiles appropriés (Figure 2.10). Une telle approche permet de générer un important nombre de dérivés à partir d'un seul précurseur. Les résultats obtenus sont présentés sous forme d'article dans les pages qui suivent.

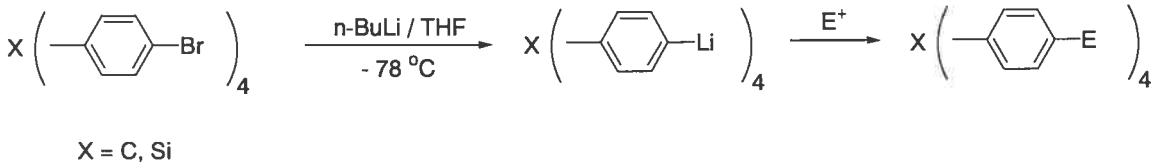

Figure 2.10 Approche vers la fonctionnalisation du tétraphénylméthane et tétraphénylsilane.

2.5 Références

1) Gomberg, M. *Ber. Dtsch. Chem. Ges.* **1897**, *30*, 2043. Gomberg, M. *J. Am. Chem. Soc.* **1898**, *20*, 773.
2) a) Ullmann, F.; Münzhuber, A. *Ber. Dtsch. Chem. Ges.* **1903** *36*, 404. b) Grimm, M.; Kirste, B.; Kurreck, H. *Angew. Chem., Int. Ed. Engl.* **1986**, *25*, 1097.
3) Gomberg, M. *J. Am. Chem. Soc.* **1900**, *22*, 757.
4) Asakawa, M.; Ashton, P. R.; Ballardini, R.; Balzani, V.; Belohradsky, M.; Gandolfi, M. T.; Kocian, O.; Prodi, L.; Raymo, F. M.; Stoddart, J. F.; Venturi, M. *J. Am. Chem. Soc.* **1997**, *119*, 302.
5) Rathore, R.; Burns, C. L.; Deselnicu, M. I. *Org. Lett.* **2001**, *3*, 2887.
6) Hetzel, S.; Simard, M.; Wuest, J. D., Résultats non-publiés.
7) Chapitre 1, référence 3.
8) Laliberté, D.; Simard, M.; Wuest, J. D., Résultats non-publiés.
9) Wang, X.; Simard, M.; Wuest, J. D., Résultats non-publiés.
10) Neugebauer, F. A.; Fischer, H.; Bernhardt, R. *Chem. Ber.* **1976**, *109*, 2389.

Article 1

Fournier, J.-H.; Wang, X.; Wuest, J. D. "Derivatives of Tetraphenylmethane and Tetraphenylsilane. Synthesis of New Tetrahedral Building Blocks for Molecular Construction" *Canadian Journal of Chemistry*, **2003**, *81*, 376.

Derivatives of Tetraphenylmethane and Tetraphenylsilane. Synthesis of New Tetrahedral Building Blocks for Molecular Construction

Jean-Hugues Fournier, Xin Wang and James D. Wuest

J.-H. Fournier,[1] X. Wang and J. D. Wuest.[1] Département de Chimie, Université de Montréal, Montréal, Québec H3C 3J7, Canada.

[1]Corresponding authors (telephone: (514) 343-6266; fax: (514) 343-6281; e-mail: [redacted]

Abstract: Useful derivatives of tetraphenylmethane and tetraphenylsilane have been synthesized by efficient methods that give crystalline products without chromatographic purification. New compounds include tetrakis(4-hydroxyphenyl)methane (**3**), tetrakis(4-formylphenyl)methane (**4**), tetrakis[(4-hydroxymethyl)phenyl]methane (**5**), tetrakis[(4-chloromethyl)phenyl]methane (**6**), tetrakis(4-bromophenyl)silane (**7**), tetrakis(4-iodophenyl)silane (**8**), tetrakis(4-hydroxyphenyl)silane (**10**), tetrakis[(4-hydroxymethyl)phenyl]silane (**12**) and tetrakis[(4-chloromethyl)phenyl]silane (**13**). These compounds are valuable precursors for the construction of complex molecules with tetrahedral geometries.

Key words: organic synthesis, molecular and supramolecular design and construction, tetraphenylmethane, tetraphenylsilane, tetrahedral building blocks.

Introduction

Recent publications have underscored the importance of derivatives of tetraphenylmethane and tetraphenylsilane as subunits in molecular construction (1-33). Such tetrahedral building blocks have been successfully incorporated in supramolecular networks (1-12) and have also found uses in many other applications (13-33). Unfortunately, few different functionalized derivatives of tetraphenylmethane and tetraphenylsilane have been reported. In order to make a wider range of tetrahedral building blocks readily available for molecular construction, we now report efficient syntheses of a variety of new and previously known derivatives of tetraphenylmethane and tetraphenylsilane. Our syntheses use simple reactions and yield crystalline products without chromatographic purification. Newly characterized derivatives include tetrakis(4-hydroxyphenyl)methane (**3**), tetrakis(4-formylphenyl)methane (**4**), tetrakis[(4-hydroxymethyl)phenyl]methane (**5**), tetrakis[(4-chloromethyl)phenyl]methane (**6**), tetrakis(4-bromophenyl)silane (**7**), tetrakis(4-iodophenyl)silane (**8**), tetrakis(4-hydroxyphenyl)silane (**10**), tetrakis[(4-hydroxymethyl)phenyl]silane (**12**) and tetrakis[(4-chloromethyl)phenyl]silane (**13**).

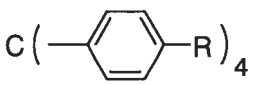

1 (R = Br)
2 (R = Me)
3 (R = OH)
4 (R = CHO)
5 (R = CH_2OH)
6 (R = CH_2Cl)

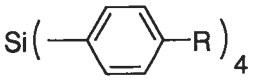

7 (R = Br)
8 (R = I)
9 (R = Me)
10 (R = OH)
11 (R = CO_2H)
12 (R = CH_2OH)
13 (R = CH_2Cl)

Results and Discussion

Our general approach to syntheses of derivatives of tetraphenylmethane and tetraphenylsilane is based on tetralithiation (34) of tetrakis(4-bromophenyl)methane (**1**) (11,33,35) or tetrakis(4-bromophenyl)silane (**7**) (3), followed by the addition of an appropriate electrophile. This approach has the advantage of providing a wide variety of derivatives simply by modifying the nature of the electrophile in a common experimental protocol. For example, treatment of tetrakis(4-bromophenyl)methane (**1**) with excess BuLi, followed by the addition of CH_3I, afforded tetrakis(4-methylphenyl)methane (**2**) (34) in 60% yield after purification by recrystallization. Analogous procedures using $B(OCH_3)_3/H_2O_2$ or *N*,*N*-dimethylformamide (DMF) provided the corresponding tetraphenol **3** and tetraaldehyde **4** in 62% and 46% yields, respectively, again after purification by recrystallization. The reduction of tetraaldehyde **4** with $NaBH_4$ gave tetrakis[(4-hydroxymethyl)phenyl]methane (**5**) in 90% yield, which was converted into tetrakis[(4-chloromethyl)phenyl]methane (**6**) in 94% yield by treatment with $SOCl_2$.

Compounds **3-6** are useful new tetrahedral building blocks that can obviously be subjected to further chemical modifications for use in molecular construction.

The corresponding tetraphenylsilanes were made in a similar way. Tetrakis(4-bromophenyl)silane (**7**) was prepared by the monolithiation of 1,4-dibromobenzene with BuLi, followed by the addition of $SiCl_4$ (3). This procedure provided target **7** in 45% yield after two recrystallizations. Alternatively, tetrakis(4-iodophenyl)silane (**8**) could be synthesized from 1,4-diiodobenzene by an analogous method in 56% yield (3). Tetrakis(4-methylphenyl)silane (**9**) (36) and tetrakis(4-hydroxyphenyl)silane (**10**) could be prepared from tetrakis(4-bromophenyl)silane (**7**) in 65% and 59% yields, respectively, by tetralithiation and addition of appropriate electrophiles, using methods analogous to those used to make the corresponding tetraphenylmethanes. However, attempts to synthesise the aldehyde corresponding to compound **4** by using DMF as electrophile resulted in complex mixtures that proved to be difficult to purify. Carboxylation of tetrakis(4-bromophenyl)silane (**7**) was achieved by adding excess BuLi in THF and bubbling CO_2 through the resulting solution, which gave tetraacid **11** (12) in 68% yield after purification by recrystallization. The acid was subsequently reduced with $LiAlH_4$ in THF to afford tetrakis[(4-hydroxymethyl)phenyl]silane (**12**) in 80% yield. The reaction of tetraol **12** with $SOCl_2$ then yielded tetrakis[(4-chloromethyl)phenyl]silane (**13**) in 76% yield.

Conclusions

The syntheses we describe provide convenient access to a wide variety of functionalized derivatives of tetraphenylmethane and tetraphenylsilane. The availability of these compounds creates many new opportunities for molecular and supramolecular construction using tetrahedral building blocks.

Experimental

Tetrahydrofuran (THF) and ether were dried by distillation from the sodium ketyl of benzophenone. *N*,*N*-Dimethylformamide (DMF) was purified by distillation under reduced pressure and dried over 4 Å molecular sieves. All other reagents were commercial products that were used without further purification.

Tetrakis(4-methylphenyl)methane (2) (34)

A solution of tetrakis(4-bromophenyl)methane (**1**; 635 mg, 0.998 mmol) (11,33,35) in THF (60 mL) was stirred at -78 °C under dry N_2 and treated dropwise with a solution of butyllithium (3.20 mL, 2.5 M in hexane, 8.0 mmol). The resulting mixture was kept at –78 °C for 30 min, and then CH_3I (1.00 mL, 16.1 mmol) was added dropwise. The mixture was stirred overnight while the temperature was allowed to rise to 25 °C. Saturated aqueous $Na_2S_2O_3$ was then added, and the resulting mixture was concentrated by partial evaporation under reduced pressure. The remaining aqueous concentrate was extracted with ethyl acetate, and the combined organic extracts were washed with brine and dried over $MgSO_4$. Volatiles were removed by evaporation under reduced pressure, and the residue was recrystallized from ethyl acetate to afford tetrakis(4-methylphenyl)methane

(34) (**2**; 226 mg, 0.600 mmol, 60%) as a colorless solid : mp 254-256 °C (lit. (34) mp 254.5-255.5 °C); ^{1}H NMR (300 MHz, $CDCl_3$) δ 7.12-7.03 (m, 16H), 2.31 (s, 12H); ^{13}C NMR (75 MHz, $CDCl_3$) δ 144.2, 135.0, 130.8, 128.0, 63.5, 20.8; MS (FAB, 3-nitrobenzyl alcohol) *m/e* 376; HRMS (FAB, 3-nitrobenzyl alcohol) calcd for $C_{29}H_{28}$ *m/e* 376.21912, found 376.22050. Anal. Calcd for $C_{29}H_{28}$: C, 92.50; H, 7.50. Found: C, 92.50; H, 7.71.

Tetrakis(4-hydroxyphenyl)methane (3)

A solution of tetrakis(4-bromophenyl)methane (**1**; 635 mg, 0.998 mmol) (11,33,35) in THF (60 mL) was stirred at -78 °C under dry N_2 and treated dropwise with a solution of butyllithium (3.20 mL, 2.5 M in hexane, 8.0 mmol). The resulting mixture was kept at –78 °C for 30 min, and then $B(OCH_3)_3$ (1.80 mL, 16.1 mmol) was added dropwise. The mixture was stirred overnight while the temperature was allowed to rise to 25 °C. To the solution was added 3 M aqueous NaOH (3 mL) followed by 30% aqueous H_2O_2 (2 mL), and then the mixture was heated at reflux for 1 h. The resulting mixture was acidified with 1 M aqueous HCl and concentrated by partial evaporation under reduced pressure. The aqueous concentrate was extracted with ethyl acetate, and the combined organic extracts were washed with water and brine, dried over $MgSO_4$ and filtered. Volatiles were removed by evaporation under reduced pressure, and the residue was recrystallized from ethyl acetate/hexane to afford tetrakis(4-hydroxyphenyl)methane (**3**; 238 mg, 0.619 mmol, 62%) as a colorless solid: IR (KBr) 3601, 3254 cm^{-1}; mp > 300 °C; ^{1}H NMR (400 MHz, DMSO-d_6) δ 9.30 (s, 4H), 6.82 (d, 8H, ^{3}J = 8.8 Hz), 6.61 (d, 8H, ^{3}J = 8.8 Hz); ^{13}C NMR (100 MHz, DMSO-d_6) δ 154.9, 138.1, 131.5, 114.0, 61.5; MS (FAB, 3-nitrobenzyl alcohol) *m/e* 384; HRMS (FAB, 3-nitrobenzyl alcohol) calcd for $C_{25}H_{20}O_4$ *m/e*

384.13617, found 384.13720. Anal. Calcd for $C_{25}H_{20}O_4 \cdot 0.5\ H_2O$: C, 76.32; H, 5.38. Found: C, 76.96; H, 5.08.

Tetrakis(4-formylphenyl)methane (4)

A solution of tetrakis(4-bromophenyl)methane (**1**; 1.12 g, 1.76 mmol) (11,33,35) in THF (150 mL) was stirred at -78 °C under dry N_2 and treated dropwise with a solution of butyllithium (6.4 mL, 2.5 M in hexane, 16 mmol). The resulting mixture was kept at -78 °C for 30 min, and then DMF (2.5 mL, 32 mmol) was added dropwise. The mixture was stirred overnight while the temperature was allowed to rise to 25 °C. To the solution was added 1 M aqueous HCl (20 mL), and volatiles were partially removed by evaporation under reduced pressure. The remaining aqueous concentrate was extracted with ethyl acetate, and the combined organic extracts were washed with water and brine, dried over $MgSO_4$ and filtered. Volatiles were removed by evaporation under reduced pressure, and the residue was recrystallized from ethyl acetate to provide tetrakis(4-formylphenyl)methane (**4**; 350 mg, 0.809 mmol, 46%) as a light yellow solid: IR (KBr) 1702 cm^{-1}; mp > 180 °C dec; ^1H NMR (400 MHz, $CDCl_3$) δ 10.01 (s, 4H), 7.84 (d, 8H, ^3J = 8.7 Hz), 7.44 (d, 8H, ^3J = 8.7 Hz); ^{13}C NMR (100 MHz, $CDCl_3$) δ 191.6, 151.2, 135.1, 131.4, 129.8, 66.4; MS (FAB, 3-nitrobenzyl alcohol) *m/e* 433; HRMS (FAB, 3-nitrobenzyl alcohol) calcd for $C_{29}H_{20}O_4$ + H *m/e* 433.14398, found 433.14540.

Tetrakis([(4-hydroxymethyl)phenyl]methane (5)

A suspension of tetrakis(4-formylphenyl)methane (**4**; 90.3 mg, 0.209 mmol) in CH_3OH (10 mL) was stirred at 0 °C and treated with $NaBH_4$ (200 mg, 5.29 mmol), added in small

portions. The resulting mixture was stirred at 0 °C for 30 min and then at 25 °C for 1 h. The mixture was poured into cold H_2O (150 mL), and the resulting precipitate was filtered, washed with water and dried under vacuum. Recrystallization from ethyl acetate/hexane gave tetrakis[(4-hydroxymethyl)phenyl]methane (**5**; 83.4 mg, 0.189 mmol, 90%) as a colorless solid: IR (KBr) 3305 cm^{-1}; mp > 300 °C; ^1H NMR (300 MHz, DMSO-d_6) δ 7.21 (d, 8H, ^3J = 8.5 Hz), 7.09 (d, 8H, ^3J = 8.5 Hz), 5.12 (t, 4H, ^3J = 5.6 Hz), 4.44 (d, 8H, ^3J = 5.6 Hz); ^{13}C NMR (100 MHz, DMSO-d_6) δ 145.2, 140.0, 130.2, 125.9, 63.7, 62.6; MS (FAB, 3-nitrobenzyl alcohol) *m/e* 440; HRMS (FAB, 3-nitrobenzyl alcohol) calcd for $C_{29}H_{28}O_4$ *m/e* 440.19876, found 440.20030.

Tetrakis[(4-chloromethyl)phenyl]methane (6)

A solution of tetrakis[(4-hydroxymethyl)phenyl]methane (**5**; 440 mg, 0.999 mmol) in dioxane (25 mL) was treated dropwise with $SOCl_2$ (600 μL, 8.2 mmol) under N_2, and the mixture was heated at reflux for 16 h. Volatiles were removed by evaporation under reduced pressure, and the residue was recrystallized from $CHCl_3$/hexane to give tetrakis[(4-chloromethyl)phenyl]methane (**6**; 483 mg, 0.939 mmol, 94%) as light yellow needles: mp > 300 °C; ^1H NMR (400 MHz, $CDCl_3$) δ 7.28 (d, 8H, ^3J = 8.6 Hz), 7.20 (d, 8H, ^3J = 8.6 Hz), 4.57 (s, 8H); ^{13}C NMR (100 MHz, DMSO-d_6) δ 147.2, 136.3, 131.5, 129.5, 65.0, 46.7. Anal. Calcd for $C_{29}H_{24}Cl_4$: C, 67.72; H, 4,70. Found: C, 67.31; H, 4.79.

Tetrakis(4-bromophenyl)silane (7)

A solution of 1,4-dibromobenzene (23.6 g, 100 mmol) in ether (250 mL) was stirred at -10 °C under dry N_2 and treated dropwise with a solution of butyllithium (40 mL, 2.5 M in

hexane, 100 mmol). The resulting mixture was kept at –10 °C for 15 min, and then $SiCl_4$ (2.85 mL, 24.9 mmol) was added dropwise. The mixture was stirred at -10 °C for 30 min and at 25 °C for 1 h. Then 1 M aqueous HCl was added, and the resulting mixture was extracted with ether. The combined extracts were washed with H_2O and brine, dried over $MgSO_4$ and filtered. Volatiles were removed by evaporation under reduced pressure, and the residue was recrystallized twice from $CHCl_3$/ethanol to afford tetrakis(4-bromophenyl)silane (**7**; 7.28 g, 11.2 mmol, 45%) as a colorless solid: mp 240-241 °C; ^{1}H NMR (300 MHz, $CDCl_3$) δ 7.55 (d, 8H, ^3J = 8.4 Hz), 7.35 (d, 8H, ^3J = 8.4 Hz); ^{13}C NMR (75 MHz, $CDCl_3$) δ 137.6, 131.4, 131.4, 125.4; MS (FAB, 3-nitrobenzyl alcohol) *m/e* 652. Anal. Calcd for $C_{29}H_{16}Br_4Si$: C, 44.21; H, 2.47. Found: C, 43.83; H, 2.45.

Tetrakis(4-iodophenyl)silane (8)

A solution of 1,4-diiodobenzene (13.2 g, 40.0 mmol) in THF (250 mL) was stirred at -78 °C under dry N_2 and treated dropwise with a solution of butyllithium (16 mL, 2.5 M in hexane, 40 mmol). The resulting mixture was kept at –78 °C for 20 min, and then $SiCl_4$ (1.15 mL, 10.0 mmol) was added dropwise. The mixture was stirred at –78 °C for 30 min and at 25 °C for 1 h. Then 1 M aqueous HCl (100 mL) was added, and the phases were separated. The organic phase was washed with saturated aqueous $Na_2S_2O_3$ (100 mL), H_2O (100 mL), and brine (100 mL), and then it was dried over $MgSO_4$ and filtered. Volatiles were removed by evaporation under reduced pressure, and the residue was recrystallized twice from $CHCl_3$/ethanol to afford tetrakis(4-iodophenyl)silane (**8**; 4.70 g, 5.59 mmol, 56%) as a colorless solid: mp > 310 °C; ^{1}H NMR (300 MHz, $CDCl_3$) δ 7.75 (d, 8H, ^3J =

7.9 Hz), 7.20 (d, 8H, ^3J = 7.9 Hz); ^{13}C NMR (75 MHz, $CDCl_3$) δ 137.5, 137.2, 131.7, 97.7. Anal. Calcd for $C_{29}H_{16}I_4Si$: C, 34.31; H, 1.92. Found: C, 34.17; H, 1.78.

Tetrakis(4-methylphenyl)silane (9) (36)

A solution of tetrakis(4-bromophenyl)silane (**7**; 1.31 g, 2.01 mmol) in THF (150 mL) was stirred at -78 °C under dry N_2 and treated dropwise with a solution of butyllithium (6.4 mL, 2.5 M in hexane, 16 mmol). The resulting mixture was kept at –78 °C for 30 min, and then CH_3I (2.00 mL, 32.1 mmol) was added dropwise. The mixture was stirred overnight while the temperature was allowed to rise to 25 °C. Saturated aqueous $Na_2S_2O_3$ was then added, and volatiles were partially removed from the resulting mixture by evaporation under reduced pressure. The aqueous concentrate was extracted with ethyl acetate, and the combined extracts were washed with brine, dried over $MgSO_4$ and filtered. Volatiles were removed by evaporation under reduced pressure, and the residue was recrystallized from toluene to afford tetrakis(4-methylphenyl)silane (**9**; 512 mg, 1.30 mmol, 65%) as a colorless solid. The spectroscopic data were identical to those reported in the literature (36).

Tetrakis(4-hydroxyphenyl)silane (10)

A solution of tetrakis(4-bromophenyl)silane (**7**; 652 mg, 1.00 mmol) in THF (60 mL) was stirred at -78 °C under dry N_2 and treated dropwise with a solution of butyllithium (3.20 mL, 2.5 M in hexane, 8.00 mmol). The resulting mixture was kept at –78 °C for 30 min, and then $B(OCH_3)_3$ (1.80 mL, 16.1 mmol) was added dropwise. The mixture was stirred overnight while the temperature was allowed to rise to 25 °C. To the solution was

added 3 M aqueous NaOH (3 mL) followed by 30% aqueous H_2O_2 (2 mL), and then the mixture was heated at reflux for 1 h. The resulting mixture was acidified with 1 M aqueous HCl and concentrated by partial evaporation of volatiles under reduced pressure. The aqueous concentrate was extracted with ethyl acetate, and the combined extracts were washed with water and brine, dried over $MgSO_4$ and filtered. Volatiles were removed by evaporation under reduced pressure, and the residue was recrystallized from ethyl acetate/hexane to afford tetrakis(4-hydroxyphenyl)silane (**10**; 238 mg, 0.594 mmol, 59%) as a colorless solid: IR (KBr) 3607, 3300 cm^{-1}; mp 274-278 °C; ^1H NMR (400 MHz, DMSO-d_6) δ 9.59 (s, 4H), 7.22 (d, 8H, ^3J = 8.4 Hz), 6.78 (d, 8H, ^3J = 8.4 Hz); ^{13}C NMR (75 MHz, DMSO-d_6) δ 158.8, 137.5, 124.3, 115.4; MS (FAB, 3-nitrobenzyl alcohol) *m/e* 400. Anal. Calcd for $C_{24}H_{20}O_4Si \cdot H_2O$: C, 68.88; H, 5.30. Found: C, 69.16; H, 5.12.

Tetrakis(4-carboxyphenyl)silane (11) (12)

A solution of tetrakis(4-bromophenyl)silane (**7**; 2.6 g, 4.0 mmol) in THF (250 mL) was stirred at -78 °C under dry N_2 and treated dropwise with a solution of butyllithium (8.0 mL, 2.5 M in hexane, 20 mmol). The resulting mixture was kept at –78 °C for 30 min, and then CO_2 was bubbled through it. The mixture was stirred at –78 °C for 3 h and was then acidified with 1 M aqueous HCl (125 mL). The organic phase was separated, washed with H_2O (100 mL) and brine (100 mL), dried over $MgSO_4$ and filtered. Volatiles were removed by evaporation under reduced pressure, and the residue was recrystallized from ethyl acetate/hexane to afford tetrakis(4-carboxyphenyl)silane (**11**; 1.40 g, 2.73 mmol, 68%) as a white solid. The spectroscopic data were identical to those reported in the literature (12).

Tetrakis[(4-hydroxymethyl)phenyl]silane (12)

A suspension of tetrakis(4-carboxyphenyl)silane (**11**; 123 mg, 0.240 mmol) in THF (10 mL) was stirred at 0 °C under N_2 and treated with $LiAlH_4$ (45 mg, 1.2 mmol), added in small portions. The resulting mixture was heated at reflux overnight. The mixture was then cooled, treated carefully with 6 M aqueous NaOH and diluted with H_2O. The resulting mixture was filtered, and volatiles were removed by evaporation under reduced pressure. The solid residue was washed with water and dried under vacuum. Recrystallization from ethanol/hexane gave tetrakis[(4-hydroxymethyl)phenyl]silane (**12**; 87.6 mg, 0.192 mmol, 80%) as a colorless solid: IR (KBr) 3339 cm^{-1}; mp 298-299 °C; ^1H NMR (400 MHz, DMSO-d_6) δ 7.42-7.36 (m, 16H), 5.24 (bs, 4H), 4.52 (s, 8H); ^{13}C NMR (75 MHz, DMSO-d_6) δ 144.4, 135.8, 132.1, 126.3, 63.0. Anal. Calcd for $C_{24}H_{20}O_4Si \cdot 0.5$ H_2O: C, 72.22; H, 6.28. Found: C, 72.45; H, 6.25.

Tetrakis[(4-chloromethyl)phenyl]silane (13)

A solution of tetrakis[(4-hydroxymethyl)phenyl]silane (**12**; 205 mg, 0.449 mmol) in dioxane (10 mL) was stirred at 25 °C under N_2 and treated dropwise with $SOCl_2$ (260 μL, 3.6 mmol). The resulting mixture was heated at reflux for 16 h. Volatiles were removed by evaporation under reduced pressure, and the residue was recrystallized from ethyl acetate to give tetrakis[(4-chloromethyl)phenyl]silane (**13**; 180 mg, 0.339 mmol, 76%) as a light yellow solid: mp 251-253 °C; ^1H NMR (300 MHz, $CDCl_3$) δ 7.55 (d, 8H, ^3J = 8.1

Hz), 7.42 (d, 8H, ^3J = 8.1 Hz), 4.61 (s, 8H); ^{13}C NMR (100 MHz, $CDCl_3$) δ 139.1, 136.7, 133.8, 128.1, 46.0.

Acknowledgments

We are grateful to the Natural Sciences and Engineering Research Council of Canada (NSERC), the Ministère de l'Éducation du Québec (MÉQ) and Merck Frosst for financial support. In addition, acknowledgment is made to the donors of the Petroleum Research Fund, administered by the American Chemical Society, for support of this research. Jean-Hugues Fournier gratefully acknowledges fellowships from MÉQ (2000-2002) and NSERC (1998-2000).

Supplemental Material

^{1}H and ^{13}C NMR spectra of tetrakis[(4-chloromethyl)phenyl]silane (**13**)

References

1. L. Vaillancourt, M. Simard, and J. D. Wuest, J. Org. Chem. **63**, 9746 (1998).
2. P. Brunet, M. Simard, and J. D. Wuest, J. Am. Chem. Soc. **119**, 2737 (1997).
3. D. Su, X. Wang, M. Simard, and J. D. Wuest, Supramolecular Chem. **6**, 171 (1995).
4. X. Wang, M. Simard, and J. D. Wuest, J. Am. Chem. Soc. **116**, 12119 (1994).
5. M. Simard, D. Su, and J. D. Wuest, J. Am. Chem. Soc. **113**, 4696 (1991).

6. R. Thaimattam, D. S. Reddy, F. Xue, T. C. W. Mak, A. Nangia, and G. R. Desiraju, New J. Chem. 143 (1998).

7. F.-Q. Liu and T. D. Tilley, J. Chem. Soc., Chem. Commun. 103 (1998).

8. E. Galoppini and R. Gilardi, J. Chem. Soc., Chem. Commun. 173 (1998).

9. G. P. Lorenzi, A. Manessis, N. C. Tirelli, and V. Gramlich, Struct. Chem. **8**, 435 (1997).

10. D. Venkataraman, S. Lee, J. S. Moore, P. Zhang, K. A. Hirsch, G. B. Gardner, A. C. Covey, and C. L. Prentice, Chem. Mater. **8**, 2030 (1996).

11. B. F. Hoskins and R. Robson, J. Am. Chem. Soc. **112**, 1546 (1990).

12. J. B. Lambert, Y. Zhao, and C. L. Stern, J. Phys. Org. Chem. **10**, 229 (1997).

13. S. Wang, W. J. Oldham, Jr., R. A. Hudack, Jr., and G. C. Bazan, J. Am. Chem. Soc. **122**, 5695 (2000).

14. J. P. Novak and D. L. Feldheim, J. Am. Chem. Soc. **122**, 3979 (2000).

15. T. J. Zimmermann, O. Freundel, R. Gompper, and T. J. J. Müller, Eur. J. Org. Chem. 3305 (2000).

16. G. M. Hübner, G. Nachtsheim, Q. Y. Li, C. Seel, C., and F. Vögtle, Angew. Chem., Int. Ed. Engl. **39**, 1269 (2000).

17. R. K. R. Jetti, F. Xue, T. C. W. Mak, and A. Nangia, J. Chem. Soc., Perkin Trans. 2 1223 (2000).

18. E. C. Constable, O. Eich, C. E. Housecroft, and D. C. Rees, Inorg. Chim. Acta ***300-302***, 158 (2000).

19. E. C. Constable, O. Eich, D. Fenske, C. E. Housecroft, and L. A. Johnston, Chem. Eur. J. **6**, 4364 (2000).

20. A. Pegenau, T. Hegmann, C. Tschierske, and S. Diele, Chem. Eur. J. **5**, 1643 (1999).

21. U.-M. Wiesler and K. Müllen, J. Chem. Soc., Chem. Commun. 2293 (1999).

22. N. Armaroli, V. Balzani, J.-P. Collin, P. Gaviña, J.-P. Sauvage, and B. Ventura, J. Am. Chem. Soc. **121**, 4397 (1999).

23. Y. Yao and J. M. Tour, J. Org. Chem. **64**, 1968 (1999).

24. H. W. Gibson, P. T. Engen, and S.-H. Lee, Polymer **40**, 1823 (1999).

25. R. J. Reid, H. Li, and M. J. Marsella, Polym. Prepr. **40**, 195 (1999).

26. S. Sengupta and S. K. Sadhukhan, Tetrahedron Lett. **40**, 9157 (1999).

27. F. M. Raymo, K. N. Houk, and J. F. Stoddart, J. Am. Chem. Soc. **120**, 9318 (1998).

28. O. Mongin and A. Gossauer, Tetrahedron **53**, 6835 (1997).

29. D. Su and F. M. Menger, Tetrahedron Lett. **38**, 1485 (1997).

30. C. Pugh, J.-Y Bae, J. R. Scott, and C. L. Wilkins, Macromolecules **30**, 8139 (1997).

31. A. M. W. Cargill Thompson, J. Hock, J. A. McCleverty, and M. D. Ward, Inorg. Chim. Acta **256,** 331 (1997).

32. I. Sava, M. Bruma, B. Schulz, F. Mercer, V. N. Reddy, and N. Belomoina, J. Appl. Polym. Sci. **65**, 1533 (1997).

33. L. M. Wilson and A. C. Griffin, J. Mater. Chem. **3**, 991 (1993).

34. B. Kirste, M. Grimm, and H. Kurreck, J. Am. Chem. Soc. **111**, 108 (1989).

35. M. Grimm, B. Kirste, and H. Kurreck, Angew. Chem., Int. Ed. Engl. **25**, 1097 (1986).

36. M. Charissé, S. Roller, S., and M. Dräger, J. Organomet. Chem.**427**, 23 (1992).

Chapitre 3

Utilisation des phénols en tectonique moléculaire

3.1 Introduction

Un des objectifs de la tectonique moléculaire est de réussir à identifier les motifs de reconnaissance qui peuvent être utilisés avec confiance dans l'élaboration de réseaux supramoléculaires prévisibles. Pour cela, il est essentiel que les motifs de reconnaissance possèdent une tendance à produire préférentiellement et de façon répétée un mode d'association en particulier. De plus, il est évidemment avantageux de réussir à identifier des motifs d'association moléculaires fiables qui auraient l'avantage d'être facilement accessibles d'un point de vue synthétique. C'est en ayant ces considérations en tête que les présents travaux sur l'utilisation des phénols en tectonique moléculaire ont été entrepris de façon à examiner le potentiel de cette fonction pour l'élaboration de réseaux supramoléculaires.

3.2 Utilisation des phénols en chimie supramoléculaire.

Des précédents existent quant à l'utilisation des phénols en chimie supramoléculaire. Ainsi, le groupe de recherche du professeur Aoyama a utilisé le résorcinol pour l'élaboration de réseaux supramoléculaires basés sur le composé **3.1**.[1] La cristallisation de ce composé génère un réseau en deux dimensions sous forme de couches. Chaque molécule établit quatre ponts hydrogène avec des molécules voisines, générant le réseau représenté à la Figure 3.1. Les cavités définies par cet assemblage ont un diamètre d'environs 10 Å selon la dimension la plus grande et sont normalement occupées par des molécules du solvant utilisé lors de la cristallisation. La superposition des couches ainsi formées relie entre elles les cavités et génère des canaux parallèles à l'axe *a*. Les donneurs et accepteurs de ponts hydrogène non-impliqués dans l'interassociation des groupements résorcinol forment des liaisons avec les molécules incluses lors de la cristallisation.

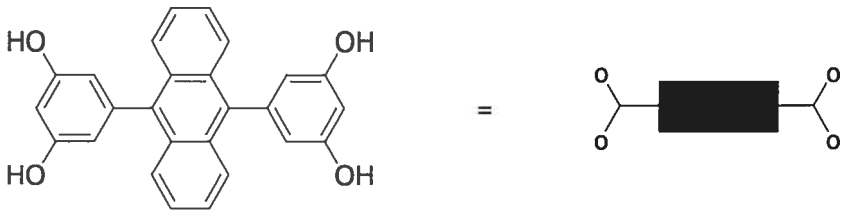

3.1

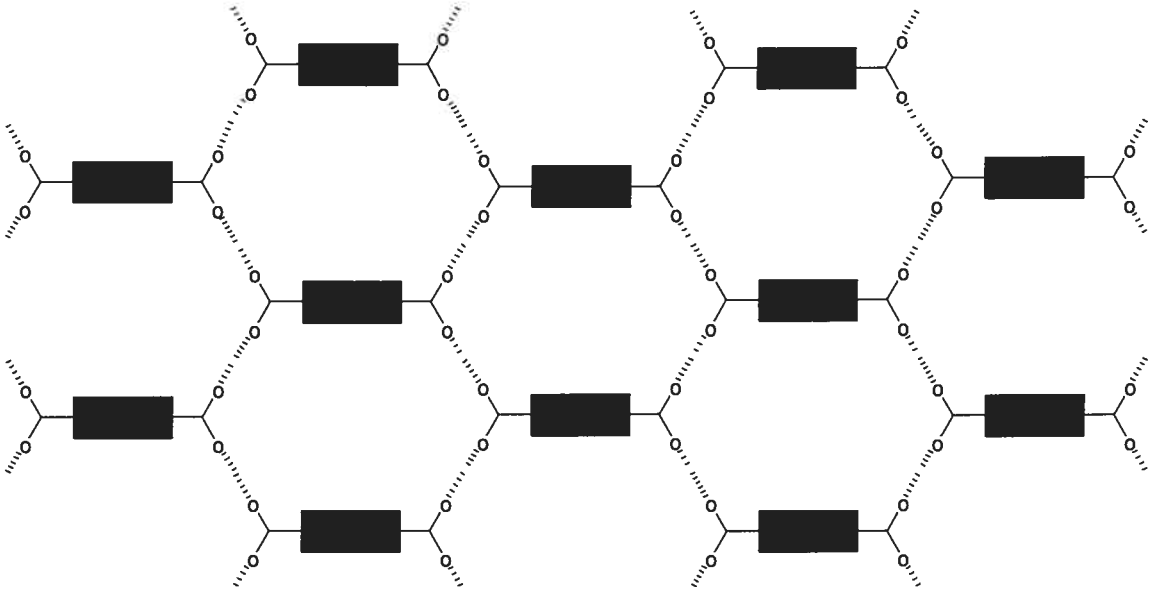

Figure 3.1 Utilisation de l'association des résorcinols pour l'assemblage de dérivés de l'anthracène par Aoyama.[1] Les atomes d'hydrogène impliqués dans les ponts hydrogène ne sont pas indiqués.

Les groupements phénoliques des dérivés résorcinol ont également été utilisés par le groupe de Suslick pour l'assemblage de porphyrines à l'état solide. Ainsi, la cristallisation du composé **3.2** par diffusion d'heptane dans une solution de benzonitrile donne un cristal de composition **3.2** • 7 PhCN.[2] La formation de ponts hydrogène entre les unités résorcinol tel que montrée à la Figure 3.2 dirige encore une fois l'assemblage supramoléculaire. Un peu à l'instar du composé **3.1**, une structure en deux dimensions sous forme de couches est obtenue. La structure tri-dimensionnelle résulte d'un empilement de couches successives qui génère des cavités dont les dimensions atteignent

5 x 6 Å. Celles-ci sont interconnectées de façon à former des canaux incluant des molécules de benzonitrile. Au total, près de 67 % du volume du cristal est disponible pour l'inclusion de molécules invitées.

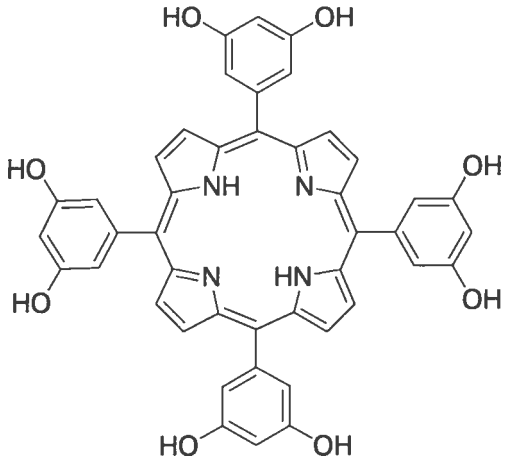

3.2

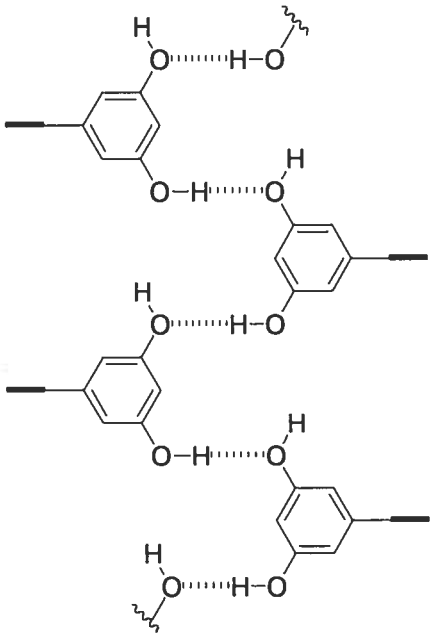

Figure 3.2 Formation de ponts hydrogène entre les unités résorcinol lors de la cristallisation de la porphyrine **3.2**.[2]

Les exemples précédents ont mis en cause des dérivés du résorcinol. La présence de deux groupes hydroxyles sur le cycle aromatique jouait un rôle déterminant dans la formation d'interactions intermoléculaires. De plus, les deux exemples précédents mettaient en jeu des composés planaires. Le groupe d'Aoyama a récemment publié un exemple intéressant dans lequel le tétraphénol **3.3** est co-cristallisé en présence de benzoquinone.[3] L'utilisation d'un squelette moléculaire dérivé du tétraphénylméthane assure une orientation tridimensionnelle aux groupements phénoliques. La formation de ponts hydrogène entre les sites donneurs présents sur les phénols et les sites accepteurs de la benzoquinone prend place tel que montré à la Figure 3.3. L'assemblage supramoléculaire adopte une topologie de type diamantoïde dans lequel les unités benzoquinone jouent le rôle d'espaceur entre les différents phénols tétraédriques. Une caractéristique remarquable de ce système consiste en l'utilisation de simples unités mono-phénol pour la construction d'un assemblage supramoléculaire tridimensionnel. Toutefois, l'utilisation d'espaceurs benzoquinone amène la formation d'un réseau interpénétré 11 fois, phénomène qui empêche la formation de cavités disponibles pour l'inclusion de molécules invitées.

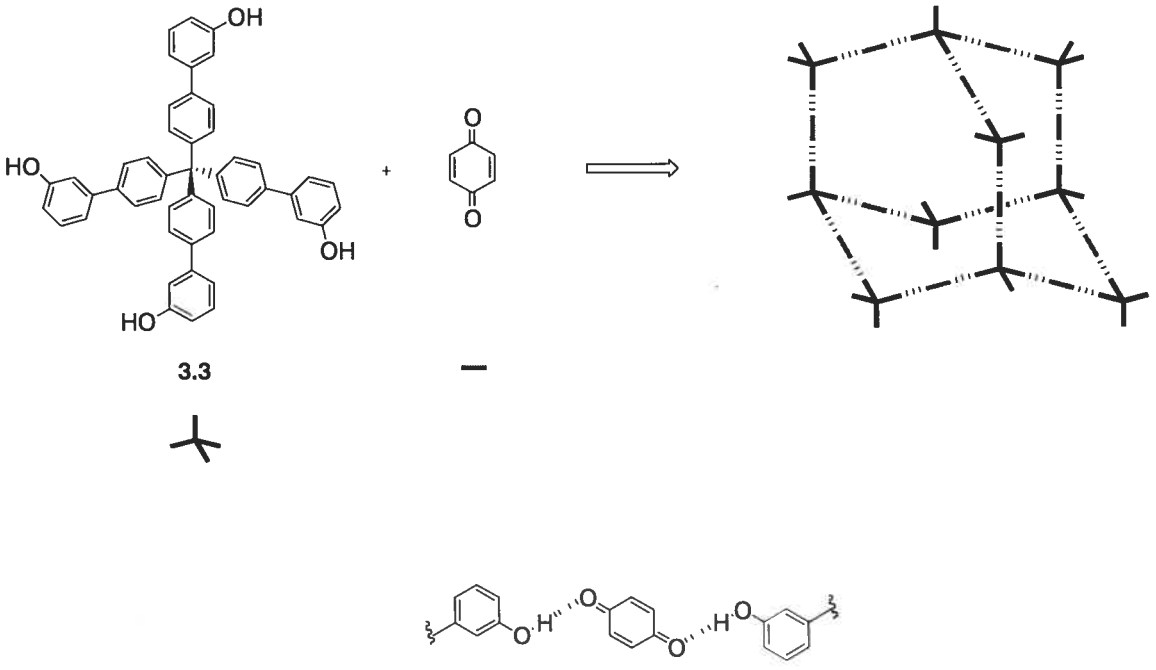

Figure 3.3 Co-cristallisation d'un tétraphénol tétraédrique en présence de benzoquinone.[3]

À la lumière des exemples précédents, la fonction phénolique semble présenter un intérêt comme unité de reconnaissance. Afin d'examiner le réel potentiel des phénols pour l'élaboration de réseaux supramoléculaires poreux, une étude cristallographique des composés de la Figure 3.4 fut entreprise. Cette étude, présentée dans les pages qui suivent sous la forme d'article, utilise donc les deux phénols précédemment synthétisés tout en y ajoutant un troisième composé.

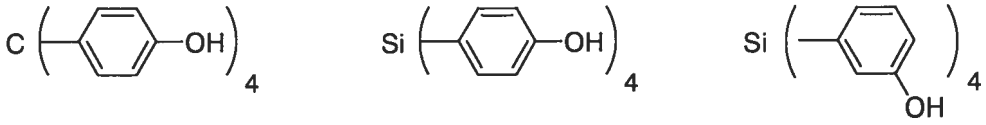

Figure 3.4 Phénols analysés en études cristallographiques.

3.3 Références

1) Endo, K.; Sawaki, T.; Koyanagi, M.; Kobayashi, K.; Masuda, H.; Aoyama, Y. *J. Am. Chem. Soc.* **1995**, *117*, 8341.
2) Bhyrappa, P.; Wilson, S. R.; Suslick, K. S. *J. Am. Chem. Soc.* **1997**, *117*, 8492.
3) Reddy, D. S.; Dewa, T.; Endo, K.; Aoyama, Y. *Angew. Chem., Int. Ed. Engl.* **2000**, *39*, 4266.

Article 2

Fournier, J.-H.; Maris, T.; Simard, M.; Wuest, J. D. "Molecular Tectonics. Hydrogen-Bonded Networks Built from Tetraphenols Derived from Tetraphenylmethane and Tetraphenylsilane" *Crystal Growth & Design*, **2003**, *3*, 535.

Molecular Tectonics. Hydrogen-Bonded Networks Built from Tetraphenols Derived from Tetraphenylmethane and Tetraphenylsilane

Jean-Hugues Fournier,[1] Thierry Maris, Michel Simard,[2] and James D. Wuest*

Département de Chimie, Université de Montréal
Montréal, Québec H3C 3J7 Canada

*Author to whom correspondence may be addressed: [redacted]

Abstract: Tetrakis(3-hydroxyphenyl)silane (**1**), tetrakis(4-hydroxyphenyl)methane (**2**), and tetrakis(4-hydroxyphenyl)silane (**3**), in which phenolic hydroxyl groups are attached to tetrahedral tetraphenylsilyl and tetraphenylmethyl cores, produce a series of hydrogen-bonded networks when crystallized from $CH_3COOC_2H_5$. Each hydroxyl group in meta-substituted tetraphenol **1** participates in two intermolecular hydrogen bonds as both donor and acceptor, producing helical chains of hydrogen bonds running along the *c* axis. Each molecule of tetraphenol **1** is linked to four symmetrically oriented neighbors by a total of eight hydrogen bonds, thereby creating a diamondoid network. No interpenetration is observed, and no significant volume remains for the inclusion of guests. The hydrogen-bonded networks derived from para-substituted analogues **2** and **3** are markedly different. Each molecule of tetraphenol **2** is hydrogen-bonded to six neighboring tetraphenols, and the resulting network defines zig-zag channels that run parallel to the *c* axis, measure about 3.3 x 4.4 Å at the narrowest point, and include $CH_3COOC_2H_5$ as guest. Approximately 28% of the volume of crystals of tetraphenol **2** is available for inclusion. Tetraphenol **3** crystallizes as a monohydrate, and H_2O is incorporated as a structural element in the resulting network. Each molecule of tetraphenol **3** forms hydrogen bonds with two molecules of H_2O and four unsymmetrically oriented neighboring molecules of tetraphenol **3**, producing a structure that is closely packed. The variety of structures obtained from compounds **1-3** under similar conditions confirms that the hydroxyl group of phenols is not a highly predictable director of supramolecular assembly.

Introduction

Molecular tectonics is a strategy for building predictably ordered structures from subunits called tectons, which are molecules that interact strongly with their neighbors in well-defined ways.[3-6] Useful subunits can be made by the conceptually simple process of grafting sites that promote intermolecular association onto geometrically suitable cores. The interactions of these sticky sites should be strong, specific, and directional, so that they play a dominant role in determining how neighboring molecules are oriented, despite the competing presence of many weaker interactions. Diverse sticky functional groups have proven useful as the principal sites of interaction in molecular tectonics,[7] but many others remain to be tested systematically.

An attractively simple candidate is the hydroxyl group of phenols, which are known to self-associate to form cyclic hydrogen-bonded oligomers (eq. 1), chains (eq. 2), and other

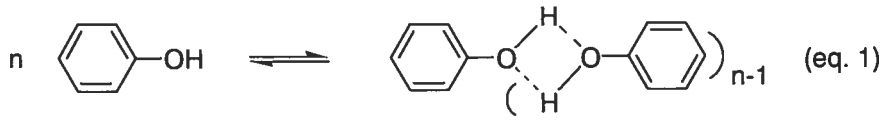

(eq. 1)

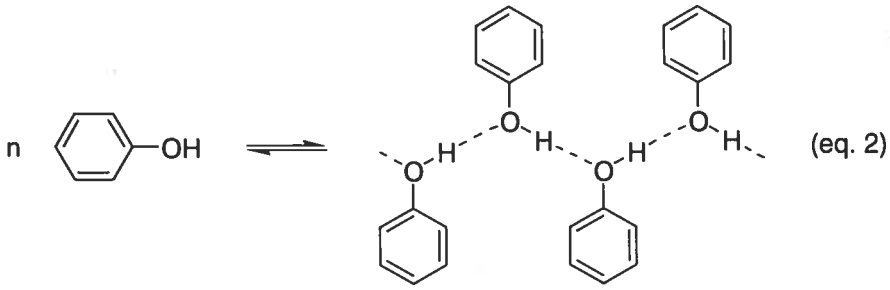

(eq. 2)

aggregates.[8] However, simple phenolic hydroxyl groups have not been used extensively to direct supramolecular construction.[6] In part, this is because 1) multiple hydrogen-bonding motifs are accessible to phenols, making the result of association difficult to foresee; and 2) the strength of phenolic association is modest compared with that of other groups available for use in supramolecular assembly.[9] To further examine the potential of the hydroxyl group of phenols in molecular tectonics, we decided to study the solid-state association of three structurally related tetraphenols **1-3** derived from tetraphenylmethane and tetraphenylsilane.

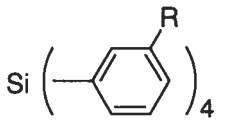

1 (R = OH)
4 (R = Br)

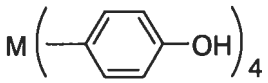

2 (M = C)
3 (M = Si)

Results and Discussion

Synthesis and Crystallization. Meta-substituted tetraphenol **1** was synthesized in 33% overall yield from 1,3-dibromobenzene by monolithiation (BuLi) and addition of $Si(OEt)_4$ to form tetrakis(3-bromophenyl)silane (**4**), followed by treatment of intermediate **4** with BuLi and $B(O\text{-}iPr)_3$, acidic hydrolysis, and oxidation with H_2O_2. Para-substituted analogues **2** and **3** were prepared by known methods.[10] Tetraphenols **1-3** were all crystallized from $CH_3COOC_2H_5$ under similar conditions, and their structures were determined by X-ray crystallography.

Hydrogen-Bonded Network Constructed from Tetraphenol 1. Tetraphenol **1** crystallizes in the tetragonal space group $I4_1/a$ to form an extensively hydrogen-bonded network. Each molecule forms hydrogen bonds with four symmetrically oriented neighbors, creating the characteristic motif represented in Figure 1. The central molecule forms two hydrogen bonds with each neighbor, one in which the central molecule acts as a donor and the other in which it acts as an acceptor; moreover, each hydroxyl group of the central molecule serves simultaneously as a donor and acceptor of hydrogen bonds involving two different neighbors. The resulting network can be considered to be held together by helical chains of hydrogen-bonded hydroxyl groups that run parallel to the *c* axis.

Each molecule of tetraphenol **1** participates in a total of eight hydrogen bonds and orients its neighbors tetrahedrally, thereby creating a three-dimensional, four-connected network with diamondoid geometry.[11] The intertectonic distance between the tetrahedral centers of hydrogen-bonded neighbors is only 8.772 Å, so the diamondoid network is not open enough to permit interpenetration by a second independent diamondoid network,[12-13] and no significant volume remains for the inclusion of guests. The characteristic tendency of tectons to form strong directional interactions disfavors efficient molecular packing and often leads to the assembly of structures in which substantial volume is occupied by guests. However, the behavior of meta-substituted tetraphenol **1** confirms that when the core of the tecton, the sticky sites, and their geometry of attachment to the core are suitably chosen, close molecular packing and effective hydrogen bonding can be achieved simultaneously.

Hydrogen-Bonded Network Constructed from Tetraphenol 2. Para-substituted tetraphenol **2** crystallizes in the monoclinic space group $P2_1/c$ as an inclusion compound with the composition **2** • 1 $CH_3COOC_2H_5$. Views of the structure are shown in Figures 2-5. Each molecule of tecton **2** forms hydrogen bonds with six unsymmetrically oriented neighboring tectons and one molecule of $CH_3COOC_2H_5$, producing the complex motif represented in Figure 2. In this view, 1) the central tecton (black) uses three of its hydroxyl groups simultaneously as a donor and acceptor of hydrogen bonds to interact with five neighboring tectons and one molecule of $CH_3COOC_2H_5$ (all shown in light gray); and 2) the remaining hydroxyl group of the central tecton serves as a simple hydrogen-bond donor to a sixth neighboring tecton (dark gray). As a result, the network can be considered to be held together by six hydrogen bonds per tecton, and a seventh hydrogen bond links the network to the guest. Together, the central tecton and the six hydrogen-bonded neighboring tectons define a simple cubic lattice analogous to that of α-Po, with two-fold interpenetration (Figure 3).[12-13]

Approximately 28% of the volume of crystals of tetraphenol **2** is available for the inclusion of guests.[14] In principle, the simple molecular shape of tetraphenol **2** would allow it to pack with ordinary efficiency to create a relatively compact periodic structure without guests; indeed, close analogues such as tetraphenylmethane, tetraphenylsilane, and simple substituted derivatives do not typically form inclusion compounds.[16] By failing to behave like these related compounds, tetraphenol **2** shows that participation in strong directional interactions normally disfavors efficient packing and leads to the

formation of open networks with significant space for the inclusion of guests. It is noteworthy that phenolic hydroxyl groups, which are sites of interaction with modest ability to direct intermolecular association, are sufficient to disrupt the pattern of close packing observed in analogues without such sites.

The available volume in the network constructed from tecton **2** defines zig-zag channels that run along the crystallographic *c* axis. Figure 4 shows that these channels have cross sections of approximately 3.3 x 4.4 Å at the narrowest points,[17] and Figure 5 portrays the channels themselves and shows that they have no significant interconnections.[18]

Hydrogen-Bonded Network Constructed from Tetraphenol 3. The analogous silane **3** crystallizes in the monoclinic space group C2/c as a monohydrate. Views of the structure appear in Figures 6-7. The included H_2O forms an integral part of a heterotectonic hydrogen-bonded network. Each molecule of tetraphenol **3** forms hydrogen bonds with two molecules of H_2O and four unsymmetrically oriented neighboring molecules of tetraphenol **3**, creating the unit represented in Figure 6. The four hydroxyl groups of the central molecule (dark gray) participate in a total of six hydrogen bonds in the following ways. One hydroxyl group donates a hydrogen bond to H_2O (black); a second donates a hydrogen bond to a neighboring molecule of tetraphenol **3** (light gray); a third simultaneously accepts a hydrogen bond from a neighbor and donates a hydrogen bond to a molecule of H_2O; and the fourth interacts as donor and acceptor with the remaining two neighbors. The central tecton and the four hydrogen-bonded neighboring tectons define a lattice with a distorted NbO topology and two-fold interpenetration (Figure 7).[19] The

resulting structure is closely packed, and no significant volume remains for the inclusion of guests.

Tetraphenylmethane **2** and tetraphenylsilane **3** have almost identical structures but crystallize under similar conditions to give very different networks. It is instructive to compare their behavior with that of boronic acids **5** and **6**, which crystallize to form isostructural diamondoid networks.[3] This difference underscores the importance in molecular tectonics of using sticky sites with strong preferences for particular patterns of association.

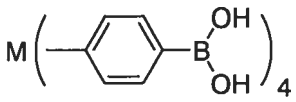

5 (M = C)
6 (M = Si)

Conclusions

Tetrakis(3-hydroxyphenyl)silane (**1**), tetrakis(4-hydroxyphenyl)methane (**2**), and tetrakis(4-hydroxyphenyl)silane (**3**) each contain four phenolic hydroxyl groups oriented by nominally tetrahedral tetraphenylsilyl and tetraphenylmethyl cores. As a result, the crystallization of compounds **1-3** is predisposed to produce extensively hydrogen-bonded networks in which each molecule interacts with multiple neighbors. Nevertheless, the specific architectures formed and the motifs of hydrogen bonding that hold them together

vary markedly among compounds **1-3**, demonstrating that phenolic hydroxyl groups are not highly effective directors of supramolecular assembly.

Experimental Section

Tetrahydrofuran (THF) was dried by distillation from the sodium ketyl of benzophenone. All other reagents were commercial products that were used without further purification.

Tetrakis(3-bromophenyl)silane (4). A solution of 1,3-dibromobenzene (23.6 g, 100 mmol) in THF (250 mL) was stirred at -78 °C under dry N_2 and treated dropwise with a solution of butyllithium (40 mL, 2.5 M in hexane, 100 mmol). The resulting mixture was kept at -78 °C for 15 min, and then $Si(OC_2H_5)_4$ (5.55 mL, 24.9 mmol) was added dropwise. The mixture was stirred at -78 °C for 2 h, H_2O (10 mL) was added, and the resulting mixture was stirred at 25 °C for 1 h. Volatiles were removed by evaporation under reduced pressure, and the residue was dissolved in ether. The solution was washed with H_2O and brine, dried over $MgSO_4$, and filtered. Evaporation of volatiles under reduced pressure left a residue of white solid, which was recrystallized twice from $CHCl_3/C_2H_5OH$ to afford tetrakis(3-bromophenyl)silane (**4**; 8.30 g, 12.7 mmol, 51%) as a colorless solid: mp 176-177 °C; ^{1}H NMR (400 MHz, $CDCl_3$) d 7.63 (d, 4H, ^3J = 7.4 Hz), 7.58 (s, 4H), 7.42 (d, 4H, ^3J = 7.4 Hz), 7.31 (t, 4H, ^3J = 7.4 Hz); ^{13}C NMR (100 MHz, $CDCl_3$) d 138.3, 135.0, 134.5, 133.4, 129.9, 123.2. Anal. Calcd for $C_{24}H_{16}Br_4Si$: C, 44.21; H, 2.47. Found: C, 44.18; H, 2.40.

Tetrakis(3-hydroxyphenyl)silane (1). A solution of tetrakis(3-bromophenyl)silane (**4**; 1.30 g, 1.99 mmol) in THF (125 mL) was stirred at -78 °C under dry N_2 and treated dropwise with a solution of butyllithium (6.4 mL, 2.5 M in hexane, 16 mmol). The resulting mixture was kept at -78 °C for 30 min, and then $B(O\text{-}iPr)_3$ (5.5 mL, 24 mmol) was added dropwise. The mixture was stirred at -78 °C for 20 min and at 25 °C for 1 h. Then 1 N aqueous HCl (25 mL) was added, and volatiles were partially removed by evaporation under reduced pressure. The residue was treated with aqueous 1 N NaOH, and the mixture was filtered and acidified with 1 N aqueous HCl. The resulting precipitate was separated by filtration and dried in air. The solid was dissolved in aqueous 1 N NaOH (20 mL), and the solution was treated with 30% aqueous H_2O_2 (5 mL) and stirred at 25 °C for 2 h. The resulting mixture was then acidified with 1 N aqueous HCl and concentrated by partial evaporation of volatiles under reduced pressure. The aqueous concentrate was extracted with $CH_3COOC_2H_5$, and the combined extracts were washed with water and brine, dried over $MgSO_4$, and filtered. Volatiles were removed by evaporation under reduced pressure, and the residue was recrystallized from $CH_3COOC_2H_5$/hexane to afford tetrakis(3-hydroxyphenyl)silane (**3**; 512 mg, 1.28 mmol, 64%) as a colorless solid: mp 272-273 °C; IR (KBr) 3262, 1584, 1435, 1242 cm^{-1}; ^1H NMR (400 MHz, acetone-d_6) d 8.38 (s, 4H), 7.29 (t, 4H, ^3J = 7.6 Hz), 7.07-7.03 (m, 8H), 6.96 (d, 4H, ^3J = 7.6 Hz); ^{13}C NMR (100 MHz, acetone-d_6) d 157.3, 136.2, 129.5, 127.8, 123.2, 117.1. Anal. Calcd for $C_{24}H_{20}O_4Si$: C, 71.97; H, 5.03. Found: C, 71.63; H, 5.17.

X-Ray Crystallographic Studies. The structures were solved by direct methods using SHELXS-97 and refined with SHELXL-97.[20] All non-hydrogen atoms were refined

anisotropically, whereas hydrogen atoms were placed in ideal positions (except for hydroxyl hydrogen localized by Fourier difference map) and refined as riding atoms.

Structure of Tetrakis(3-hydroxyphenyl)silane (1). Crystals of compound **1** were grown from $CH_3COOC_2H_5$. Data were collected using a Bruker SMART 2000 CCD diffractometer with Cu Kα radiation at 226 K. Crystals of compound **1** belong to the tetragonal space group I $4_1/a$ with $a = b = 17.1641(2)$ Å, $c = 7.2676(1)$ Å, $V = 2141.1(5)$ Å^3, $D_{calcd} = 1.242$ g cm^{-3}, and $Z = 4$. Full-matrix least-squares refinements on F^2 led to final residuals $R_f = 0.0444$ and $R_w = 0.1274$ for 1062 reflections with $I > 2\sigma(I)$.

Structure of Tetrakis(4-hydroxyphenyl)methane (2). Compound **2** was prepared by the published method and crystallized from $CH_3COOC_2H_5$.[10] Data were collected using an Enraf-Nonius CAD-4 diffractometer with Cu Kα radiation at 225 K. Crystals of compound **2** belong to the monoclinic space group P $2_1/c$ with $a = 10.243(4)$ Å, $b = 15.673(6)$ Å, $c = 15.412(8)$ Å, $\beta = 100.86(4)°$, $V = 2429.9(18)$ Å^3, $D_{calcd} = 1.292$ g cm^{-3}, and $Z = 4$. Full-matrix least-squares refinements on F^2 led to final residuals $R_f = 0.0579$ and $R_w = 0.1722$ for 4603 reflections with $I > 2\sigma(I)$.

Structure of Tetrakis(4-hydroxyphenyl)silane (3). Compound **3** was prepared by the published method and crystallized from $CH_3COOC_2H_5$.[10] Data were collected using an Enraf-Nonius CAD-4 diffractometer with Cu Kα radiation at 210 K. Crystals of compound **3** belong to the monoclinic space group C 2/c with $a = 14.962(9)$ Å, $b = 15.855(11)$ Å, $c = 19.697(13)$ Å, $\beta = 111.49(5)°$, $V = 4348(5)$ Å^3, $D_{calcd} = 1.279$ g cm^{-3},

and Z = 8. Full-matrix least-squares refinements on F^2 led to final residuals R_f = 0.0784 and R_w = 0.1879 for 4117 reflections with $I > 2\sigma(I)$.

Acknowledgment. We are grateful to the Natural Sciences and Engineering Research Council of Canada, the Ministère de l'Éducation du Québec, and Merck Frosst for financial support. In addition, acknowledgment is made to the donors of the Petroleum Research Fund, administered by the American Chemical Society, for support of this research.

Supplementary Material Available: ORTEP drawings and tables of crystallographic data, atomic coordinates, anisotropic thermal parameters, and bond lengths and angles for tetraphenols **1-3**. This material is available free of charge via the Internet at http://pubs.acs.org.

Notes and References

1. Fellow of the Ministère de l'Éducation du Québec, 2000-2002. Fellow of the Natural Sciences and Engineering Research Council of Canada, 1998-2000.
2. Laboratoire de Diffraction des Rayons-X, Département de Chimie, Université de Montréal.
3. Fournier, J.-H.; Maris, T.; Wuest, J. D.; Guo, W.; Galoppini, E. *J. Am. Chem. Soc.*, in press.
4. Vaillancourt, L.; Simard, M.; Wuest, J. D. *J. Org. Chem.* **1998**, *63*, 9746. Brunet, P.; Simard, M.; Wuest, J. D. *J. Am. Chem. Soc.* **1997**, *119*, 2737. Su, D.; Wang, X.;

Simard, M.; Wuest, J. D. *Supramolecular Chem.* **1995**, *6*, 171. Wuest, J. D. In *Mesomolecules: From Molecules to Materials*; Mendenhall, G. D., Greenberg, A., Liebman, J. F.; Chapman & Hall: New York, 1995; p 107. Wang, X.; Simard, M.; Wuest, J. D. *J. Am. Chem. Soc.* **1994**, *116*, 12119. Simard, M.; Su, D.; Wuest, J. D. *J. Am. Chem. Soc.* **1991**, *113*, 4696.

5. For recent studies of hydrogen-bonded supramolecular networks by other groups, see: Bhogala, B. R.; Vishweshwar, P.; Nangia, A. *Cryst. Growth Des.* **2002**, *2*, 325. Moorthy, J. N.; Natarajan, R.; Mal, P.; Venugopalan, P. *J. Am. Chem. Soc.* **2002**, *124*, 6531. Field, J. E.; Combariza, M. Y.; Vachet, R. W.; Venkataraman, D. *J. Chem. Soc., Chem. Commun.*, **2002**, 2260. Holman, K. T.; Pivovar, A. M.; Swift, J. A.; Ward, M. D. *Acc. Chem. Res.* **2001**, *34*, 107. Kuduva, S. S.; Bläser, D.; Boese, R.; Desiraju, G. R. *J. Org. Chem.* **2001**, *66*, 1621. Mak, T. C. W.; Xue, F. *J. Am. Chem. Soc.* **2000**, *122*, 9860. Sharma, C. V. K.; Clearfield, A. *J. Am. Chem. Soc.* **2000**, *122*, 4394. Corbin, P. S.; Zimmerman, S. C. *J. Am. Chem. Soc.* **2000**, *122*, 3779. Cantrill, S. J.; Pease, A. R.; Stoddart, J. F. *J. Chem. Soc., Dalton Trans.* **2000**, 3715. Batchelor, E.; Klinowski, J.; Jones, W. *J. Mater. Chem.* **2000**, *10*, 839. Videnova-Adrabinska, V.; Janeczko, E. *J. Mater. Chem.* **2000**, *10*, 555. Akazome, M.; Suzuki, S.; Shimizu, Y.; Henmi, K.; Ogura, K. *J. Org. Chem.* **2000**, *65*, 6917. Baumeister, B.; Matile, S. *J. Chem. Soc., Chem. Commun.* **2000**, 913. Chowdhry, M. M.; Mingos, D. M. P.; White, A. J. P.; Williams, D. J. *J. Chem. Soc., Perkin Trans. 1* **2000**, 3495. Gong, B.; Zheng, C.; Skrzypczak-Jankun, E.; Zhu, J. *Org. Lett.* **2000**, *2*, 3273. Krische, M. J.; Lehn, J.-M.; Kyritsakas, N.; Fischer, J.; Wegelius, E. K.; Rissanen, K. *Tetrahedron* **2000**, *56*, 6701. Aakeröy, C. B.; Beatty, A. M.;

Nieuwenhuyzen, M.; Zou, M. *Tetrahedron* **2000**, *56*, 6693. Kobayashi, K.; Shirasaka, T.; Horn, E.; Furukawa, N. *Tetrahedron Lett.* **2000**, *41*, 89. Dahal, S.; Goldberg, I. *J. Phys. Org. Chem.* **2000**, *13*, 382. Fuchs, K.; Bauer, T.; Thomann, R.; Wang, C.; Friedrich, C.; Mühlhaupt, R. *Macromolecules* **1999**, *32*, 8404. Holý, P.; Závada, J.; Císarová, I.; Podlaha, J. *Angew. Chem., Int. Ed. Engl.* **1999**, *38*, 381. Karle, I. L.; Ranganathan, D.; Kurur, S. *J. Am. Chem. Soc.* **1999**, *121*, 7156. Chin, D. N.; Palmore, G. T. R.; Whitesides, G. M. *J. Am. Chem. Soc.* **1999**, *121*, 2115. Hanessian, S.; Saladino, R.; Margarita, R.; Simard, M. *Chem. Eur. J.* **1999**, *5*, 2169. Biradha, K.; Dennis, D.; MacKinnon, V. A.; Sharma, C. V. K.; Zaworotko, M. J. *J. Am. Chem. Soc.* **1998**, *120*, 11894. Schauer, C. L.; Matwey, E.; Fowler, F. W.; Lauher, J. W. *J. Am. Chem. Soc.* **1997**, *119*, 10245. Lambert, J. B.; Zhao, Y.; Stern, C. L. *J. Phys. Org. Chem.* **1997**, *10*, 229. Félix, O.; Hosseini, M. W.; De Cian, A.; Fischer, J. *Angew. Chem., Int. Ed. Engl.* **1997**, *36*, 102. Adam, K. R.; Atkinson, I. M.; Davis, R. L.; Lindoy, L. F.; Mahinay, M. S.; McCool, B. J.; Skelton, B. W.; White, A. H. *J. Chem. Soc., Chem. Commun.* **1997**, 467. Schwiebert, K. E.; Chin, D. N.; MacDonald, J. C.; Whitesides, G. M. *J. Am. Chem. Soc.* **1996**, *118*, 4018. Kinbara, K.; Hashimoto, Y.; Sukegawa, M.; Nohira, H.; Saigo, K. *J. Am. Chem. Soc.* **1996**, *118*, 3441. Munakata, M.; Wu, L. P.; Yamamoto, M.; Kuroda-Sowa, T.; Maekawa, M. *J. Am. Chem. Soc.* **1996**, *118*, 3117. Hartgerink, J. D.; Granja, J. R.; Milligan, R. A.; Ghadiri, M. R. *J. Am. Chem. Soc.* **1996**, *118*, 43. Hollingsworth, M. D.; Brown, M. E.; Hillier, A. C.; Santarsiero, B. D.; Chaney, J. D. *Science* **1996**, *273*, 1355. Kolotuchin, S. V.; Fenlon, E. E.; Wilson, S. R.; Loweth, C. J.; Zimmerman, S.

C. *Angew. Chem., Int. Ed. Engl.* **1995**, *34*, 2654. Lawrence, D. S.; Jiang, T.; Levett, M. *Chem. Rev.* **1995**, *95*, 2229.

6. For recent studies of hydrogen-bonded supramolecular networks derived from phenols and related molecules, see: Tanaka, T.; Tasaki, T.; Aoyama, Y. *J. Am. Chem. Soc.* **2002**, *124*, 12453. Aitipamula, S.; Thallapally, P. K.; Thaimattam, R.; Jaskólski, M.; Desiraju, G. R. *Org. Lett.* **2002**, *4*, 921. Heinze, K.; Jacob, V. *J. Chem. Soc., Dalton Trans.* **2002**, 2379. Glidewell, C.; Ferguson, G.; Gregson, R. M.; Campana, C. F. *Acta Crystallogr.* **2000**, *B56*, 68. Kobayashi, K.; Shirasaka, T.; Sato, A.; Horn, E.; Furukawa, N. *Angew. Chem., Int. Ed. Engl.* **1999**, *38*, 3483. Bhyrappa, P.; Wilson, S. R.; Suslick, K. S. *J. Am. Chem. Soc.* **1997**, *119*, 8492. MacGillavray, L.; Atwood, J. *Nature* **1997**, *389*, 469. Ermer, O.; Eling, A. *J. Chem. Soc., Perkin Trans. 2* **1994**, 925. Ung, A. T.; Bishop, R.; Craig, D. C.; Dance, I. G.; Scudder, M. L. *Chem. Mater.* **1994**, *6*, 1269.
7. Nangia, A.; Desiraju, G. R. *Top. Curr. Chem.* **1998**, *198*, 57.
8. Brock, C. P.; Duncan, L. L. *Chem. Mater.* **1994**, *6*, 1307.
9. Steiner, T. *Angew. Chem., Int. Ed. Engl.* **2002**, *41*, 48.
10. Fournier, J.-H.; Wang, X.; Wuest, J. D., submitted for publication.
11. For a review of diamondoid hydrogen-bonded networks, see: Zaworotko, M. J. *Chem. Soc. Rev.* **1994**, *23*, 283.
12. For discussions of interpenetration in networks, see: Batten, S. R. *Cryst. Eng. Commun.* **2001**, *18*, 1. Batten, S. R.; Robson, R. *Angew. Chem., Int. Ed. Engl.* **1998**, *37*, 1460.

13. An updated list of examples of interpenetration is available on the web site of Dr. Stuart R. Batten at Monash University (www.chem.monash.edu.au).

14. The percentage of volume accessible to guests was estimated by the PLATON program.[15]

15. Spek, A. L. *PLATON, A Multipurpose Crystallographic Tool*; Utrecht University: Utrecht, The Netherlands, 2001. van der Sluis, P.; Spek, A. L. *Acta Crystallogr.* **1990**, *A46*, 194.

16. Galoppini, E.; Gilardi, R. *J. Chem. Soc., Chem. Commun.* **1999**, 173. Oldham, W. J., Jr.; Lachicotte, R.; Bazan, G. C. *J. Am. Chem. Soc.* **1998**, *120*, 2987. Thaimattam, R.; Reddy, D. S.; Xue, F.; Mak, T. C. W.; Nangia, A.; Desiraju, G. R. *New J. Chem.* **1998**, 143. Lloyd, M. A.; Brock, C. P. *Acta Crystallogr.* **1997**, *B53*, 780. Reddy, D. S.; Craig, D. C.; Desiraju, G. R. *J. Am. Chem. Soc.* **1996**, *118*, 4090. Charissé, M.; Gauthey, V.; Dräger, M. *J. Organomet. Chem.* **1993**, *448*, 47. Charissé, M.; Roller, S.; Dräger, M. *J. Organomet. Chem.* **1992**, *427*, 23. Gruhnert, V.; Kirfel, A.; Will, G.; Wallrafen, F.; Recker, K. *Z. Krist.* **1983**, *163*, 53. Robbins, A.; Jeffrey, G. A.; Chesick, J. P.; Donohue, J.; Cotton, F. A.; Frenz, B. A.; Murillo, C. A. *Acta Crystallogr.* **1975**, *B31*, 2395.

17. The dimensions of a channel in a particular direction correspond to the cross section of an imaginary uniform cylinder that could be passed through the network in the given direction in contact with the van der Waals surface. Such values are inherently conservative because 1) they measure the cross section at the most narrow constriction, and 2) they systematically underestimate the sizes of channels that are not uniform and linear.

18. Representations of channels were generated by the Cavities option in the program ATOMS Version 5.1 (Shape Software, 521 Hidden Valley Road, Kingsport, Tennessee 37663 USA; www.shapesoftware.com). We are grateful to Eric Dowty of Shape Software for integrating this capacity in ATOMS at our suggestion.

19. For other networks with the uncommon NbO topology, see: Carlucci, L.; Cozzi, N.; Ciani, G.; Moret, M.; Proserpio, D. M.; Rizzato, S. *Chem. Commun.* **2002**, 1354. Kuduva, S. S.; Craig, D. C.; Nangia, A.; Desiraju, G. R. *J. Am. Chem. Soc.* **1999**, *121*, 1936. Power, K. N.; Hennigar, T. L.; Zaworotko, M. J. *J. Chem. Soc., Chem. Commun.* **1998**, 595. Stainton, N. M.; Harris, K. D. M.; Howie, R. A. *J. Chem. Soc. Chem. Commun.* **1991**, 1781.

20. Sheldrick, G. M. *SHELXS-97, Program for the Solution of Crystal Structures* and *SHELXL-97, Program for the Refinement of Crystal Structures*; Universität Göttingen: Germany, 1997.

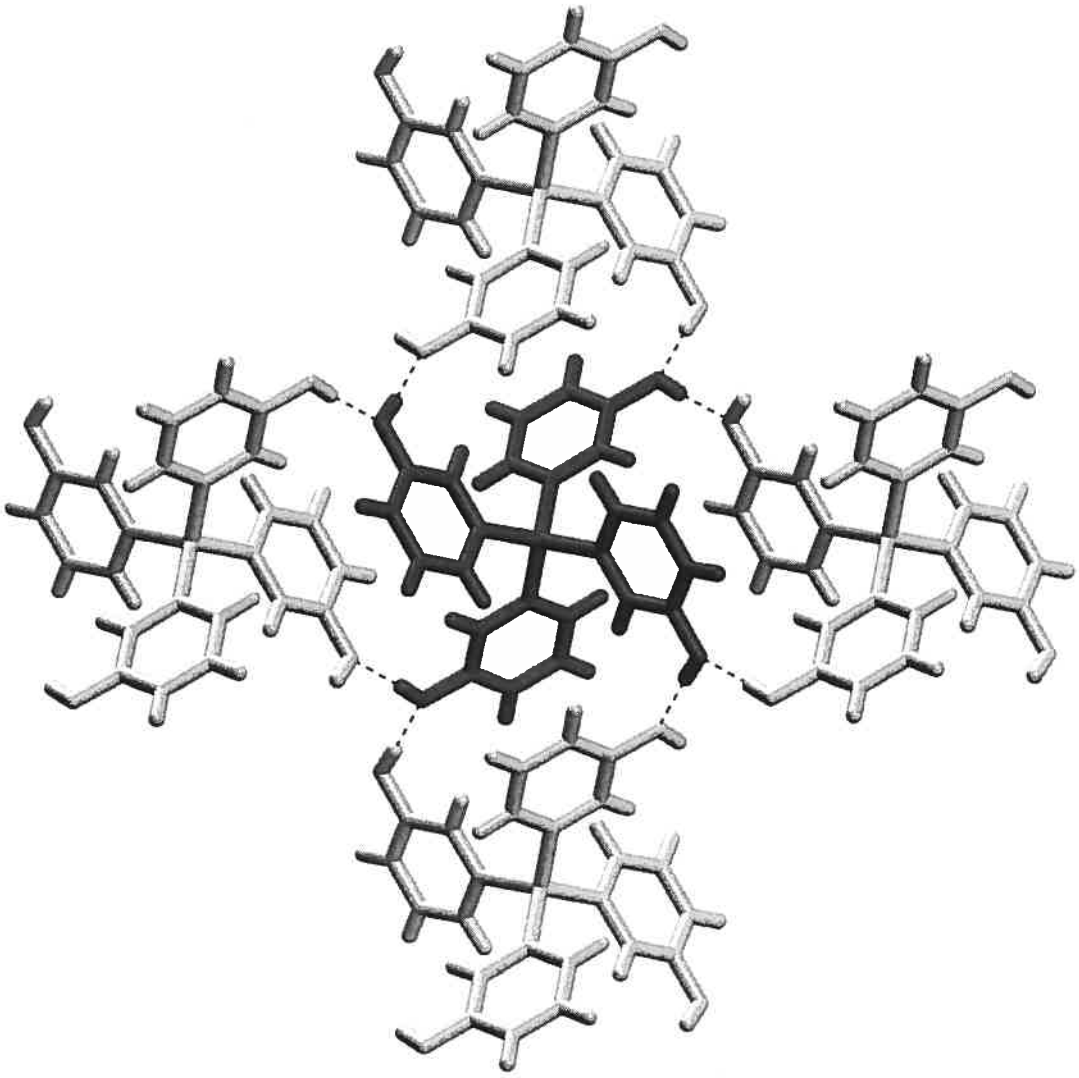

Figure 1. View of the structure of tetrakis(3-hydroxyphenyl)silane (**1**) along the *c* axis, showing a central molecule (black) and its four hydrogen-bonded neighbors (gray). Hydrogen bonds appear as broken lines.

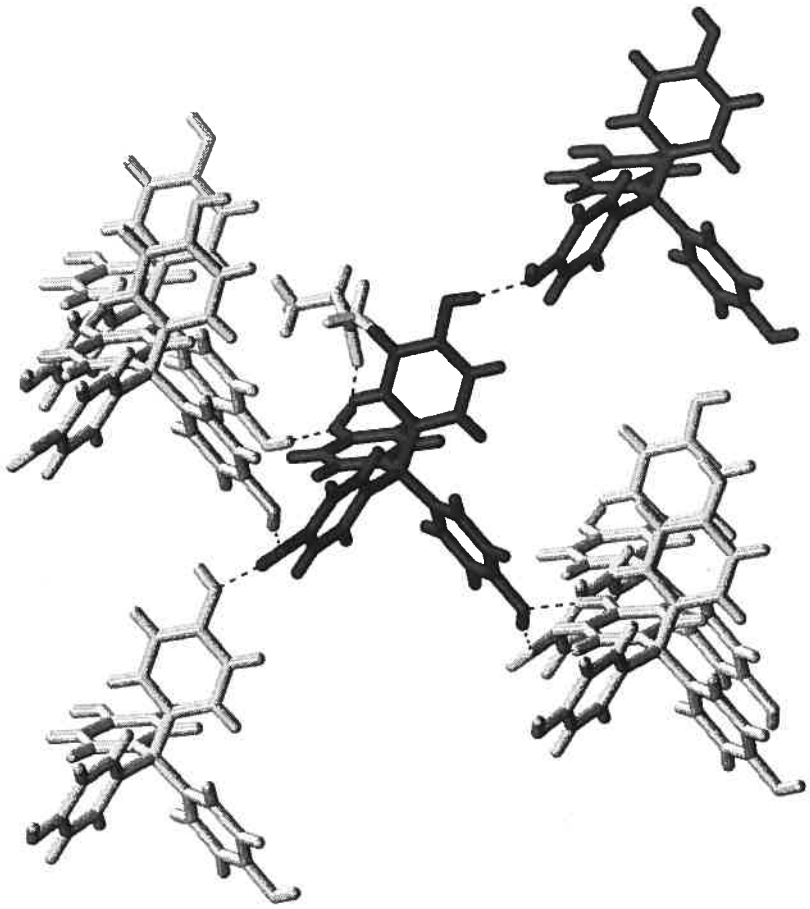

Figure 2. View of the structure of tetrakis(4-hydroxyphenyl)methane (**2**) and included $CH_3COOC_2H_5$, showing a central molecule (black) surrounded by its hydrogen-bonded neighbors. Hydrogen bonds appear as broken lines. The central tecton uses three of its hydroxyl groups simultaneously as a donor and acceptor of hydrogen bonds to interact with five neighboring tectons and one molecule of $CH_3COOC_2H_5$ (all shown in light gray); and 2) the remaining hydroxyl group of the central tecton serves as a simple hydrogen-bond donor to a sixth neighboring tecton (dark gray).

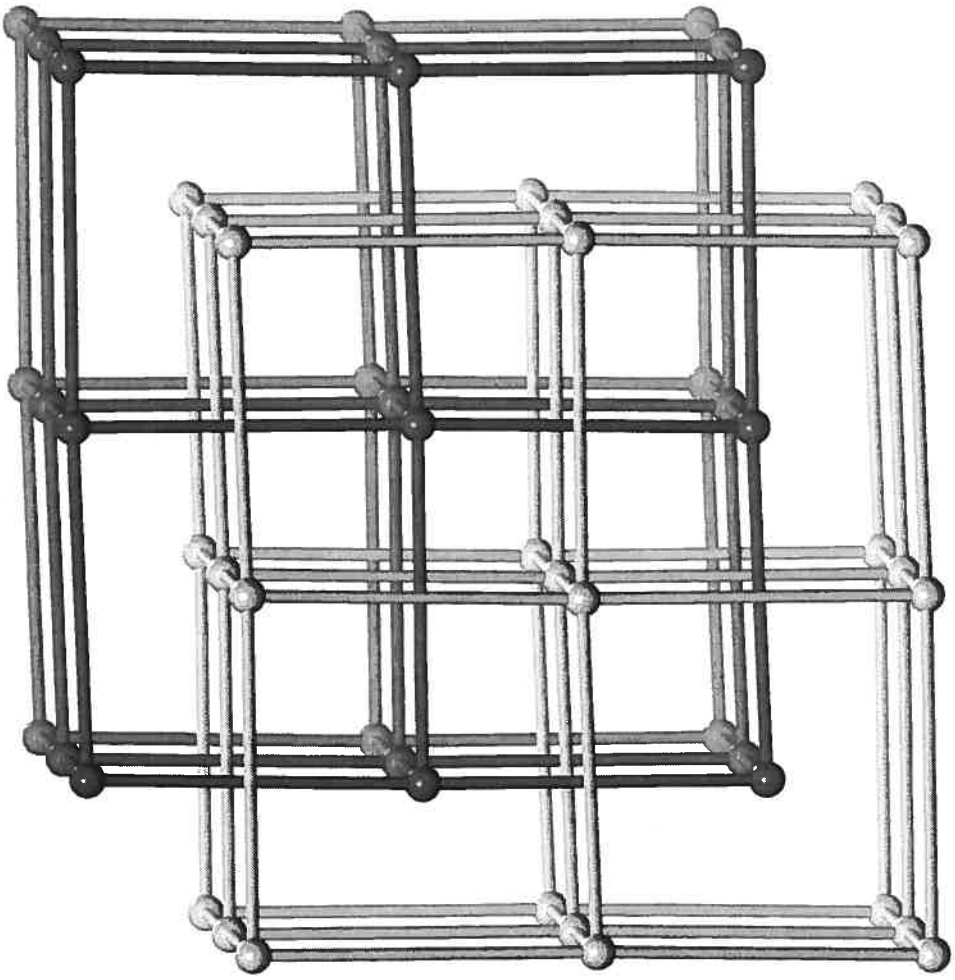

Figure 3. Representation of the two-fold interpenetration of the simple cubic (α-Po) networks defined by the association of tecton **2**. In this drawing, the central carbon atom of each tecton is represented by a sphere, and the solid lines represent interactions with the six neighboring hydrogen-bonding tectons. One independent network is shown in light gray and the other in dark gray.

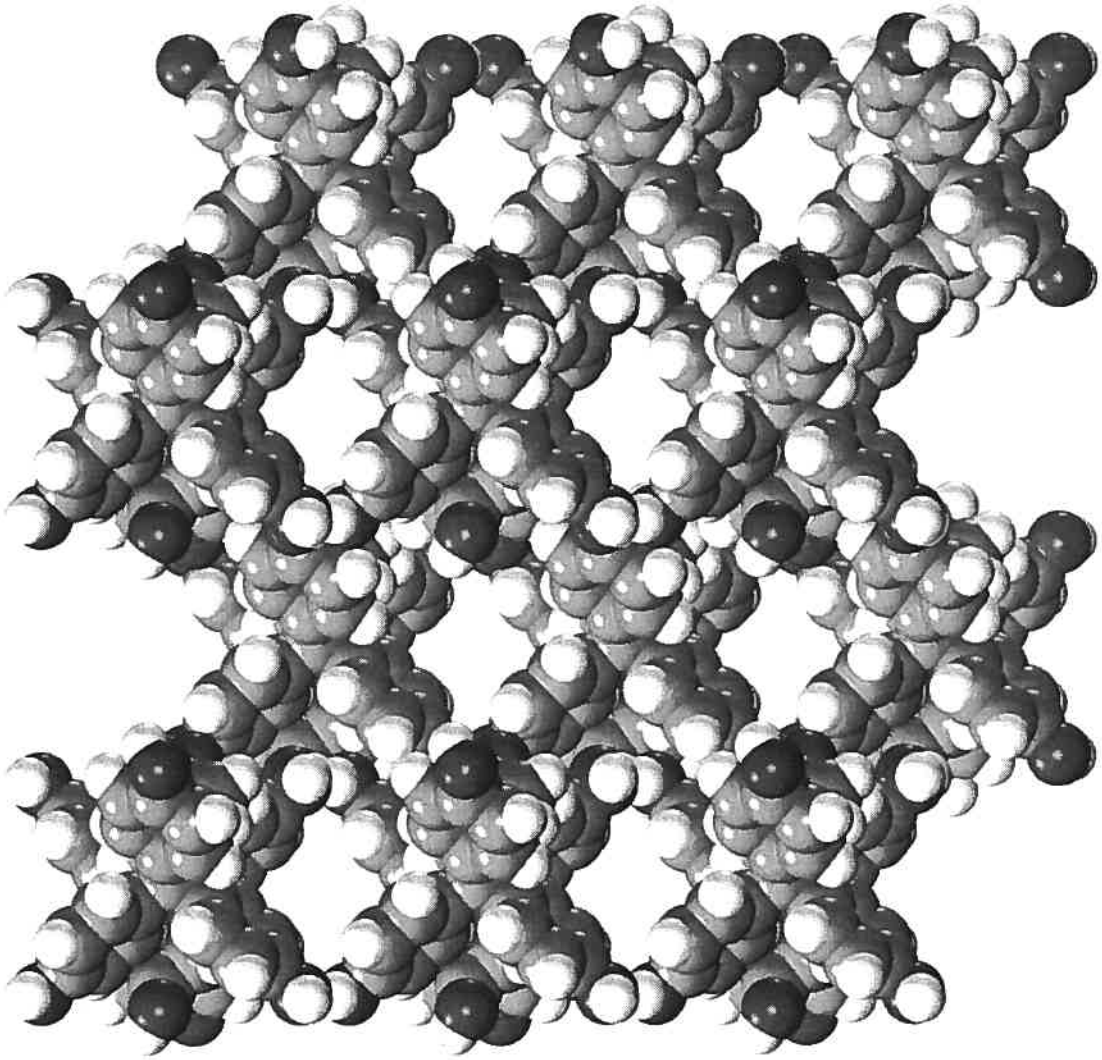

Figure 4. View along the *c* axis of the network constructed from tetraphenol **2** showing a 3 x 2 x 2 array of unit cells. Guests are omitted, and atoms are shown as spheres of van der Waals radii in order to reveal the cross sections of channels.

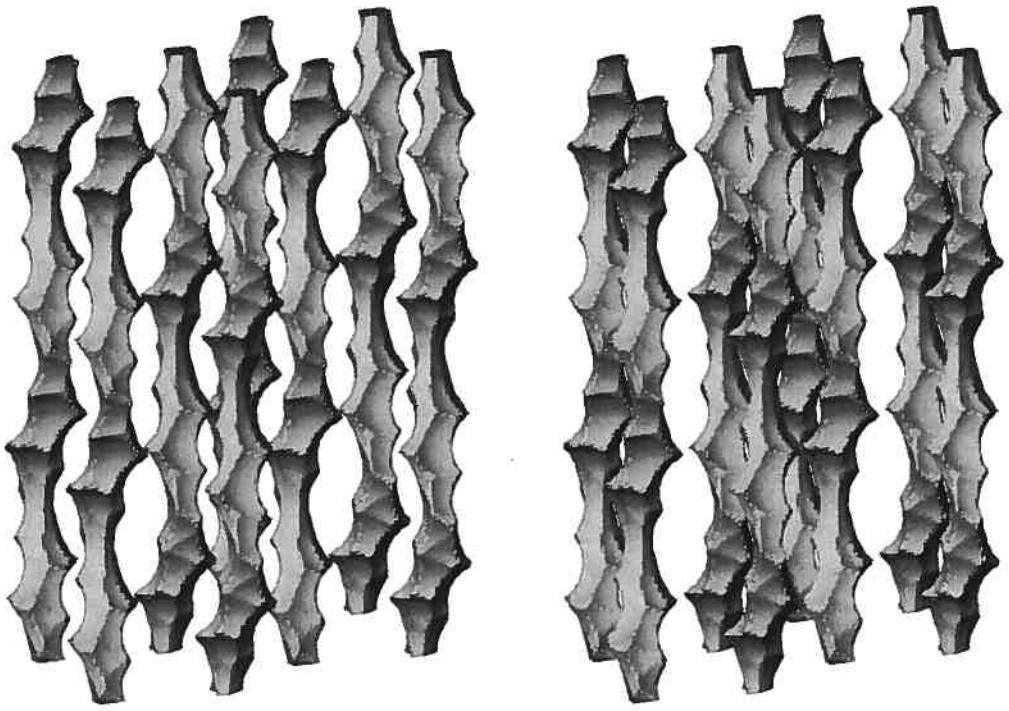

Figure 5. Stereoscopic representation of the channels defined by the network constructed from tetraphenol **2**. The image shows a 2 x 2 x 2 array of unit cells viewed with the *c* axis vertical. The outsides of the channels appear in light gray, and dark gray is used to show where the channels are cut by the boundaries of the array. The surface of the channels is defined by the possible loci of the center of a sphere of diameter 3 Å as it rolls over the surface of the ordered tectonic network.[18]

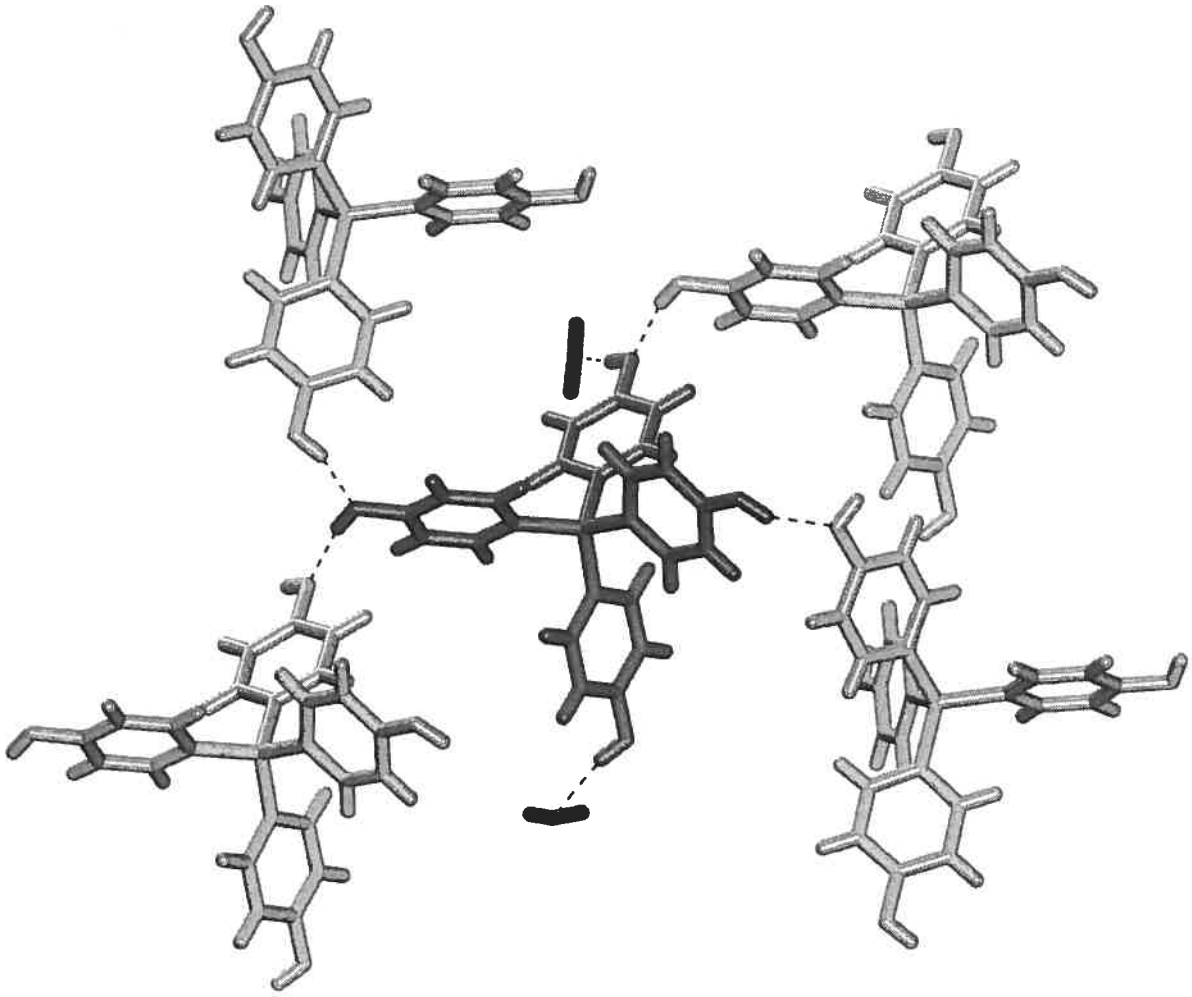

Figure 6. View of the structure of the monohydrate of tetrakis(4-hydroxyphenyl)silane (**3**), showing a central molecule (dark gray) surrounded by four hydrogen-bonded neighboring tectons (light gray) and two molecules of H_2O (black). Hydrogen bonds appear as broken lines.

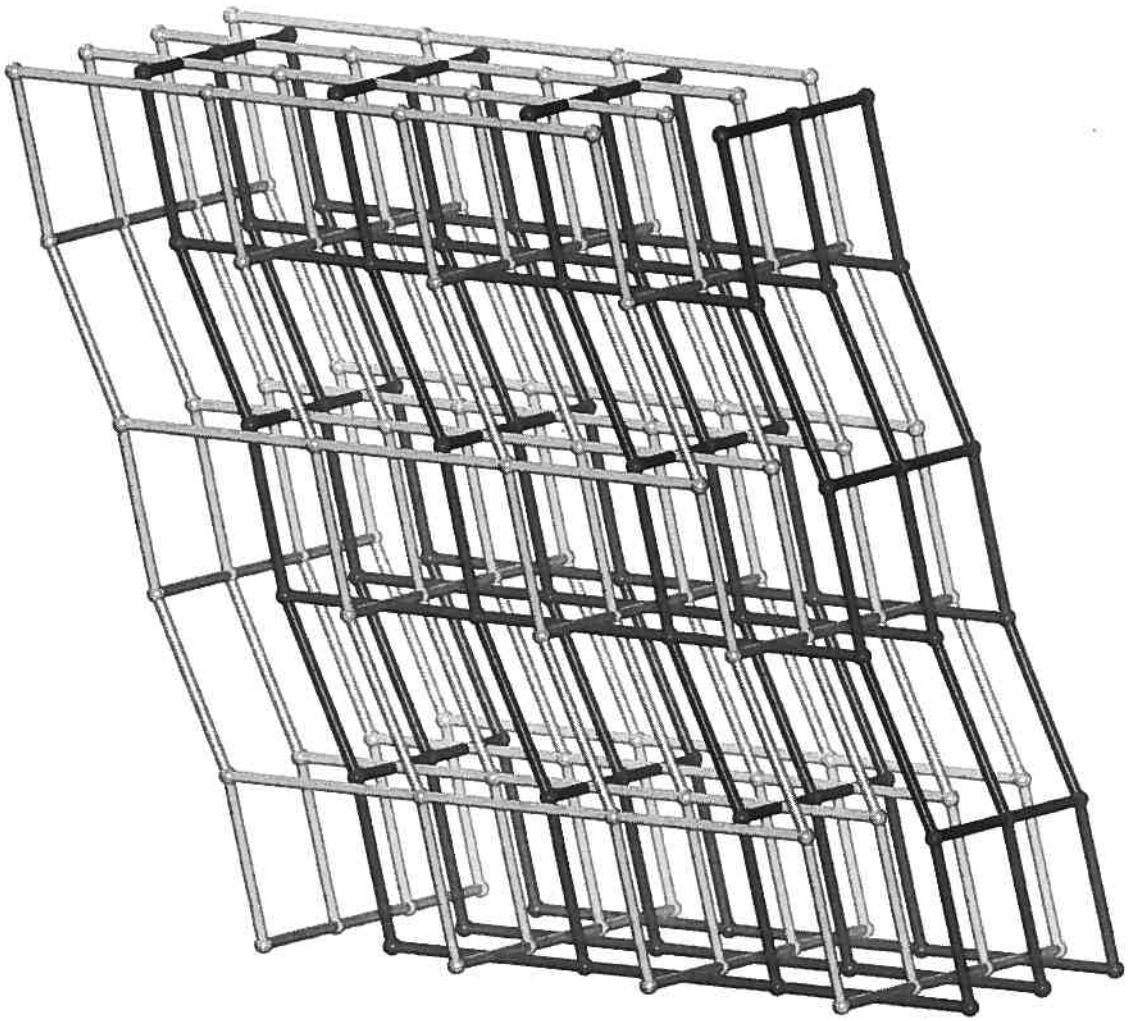

Figure 7. Representation of the two-fold interpenetration of the distorted NbO networks defined by the association of tecton **3**. In this drawing, the central silicon atom of each tecton is represented by a sphere, and the solid lines represent interactions with the four neighboring hydrogen-bonding tectons. One independent network is shown in light gray and the other in dark gray.

Chapitre 4

Utilisation des acides boroniques en tectonique moléculaire

4.1 Introduction

Le chapitre précédent a mis en lumière la difficulté d'utiliser l'association de simples phénols comme éléments directeurs pour la formation de réseaux supramoléculaires, l'absence de motif de reconnaissance récurrent étant le principal obstacle à leur utilisation. Les efforts subséquents se sont donc concentrés sur la recherche de nouveaux groupes de reconnaissance ayant des modes d'association plus fiables. Un objectif extrêmement attrayant est apparu alors dans l'utilisation des acides boroniques comme éléments de reconnaissance moléculaire. Les acides boroniques font maintenant désormais partie du paysage des fonctions familières en chimie organique, que ce soit pour leur utilité dans des réactions de couplages de type Suzuki[1], comme acide de Lewis en catalyse[2] ou encore pour la reconnaissance sélective de carbohydrates.[3] Peu d'exemples existent toutefois quant à leur utilisation comme groupement de reconnaissance moléculaire.

4.2 Mode d'association des acides arylboroniques à l'état solide.

Un examen des structures recensées dans la *Cambridge Structural Database* permet de constater qu'en date du mois d'avril 2002, seulement 14 structures de dérivés d'acides arylboroniques avaient été rapportées. De ce nombre, neuf d'entre-elles montrent la formation de dimères à l'état solide par le biais de ponts hydrogène.[4-11] Ainsi, la structure de l'acide phénylboronique permet de voir que chaque molécule établit deux ponts hydrogène avec une molécule voisine : chaque acide agit à la fois comme donneur et accepteur de ponts hydrogène (Figure 4.1).[4] Ce phénomène de dimérisation est également observé pour les composés illustrés à la Figure 4.2.[5-11]

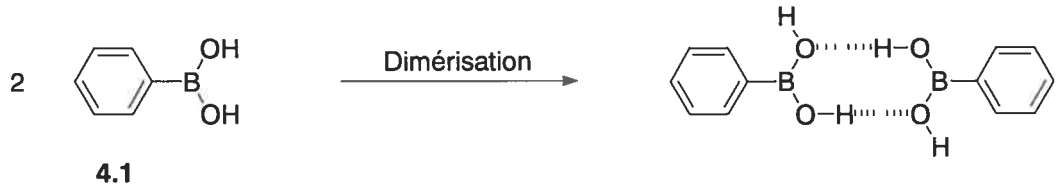

4.1

Figure 4.1 Dimérisation de l'acide phénylboronique à l'état solide.

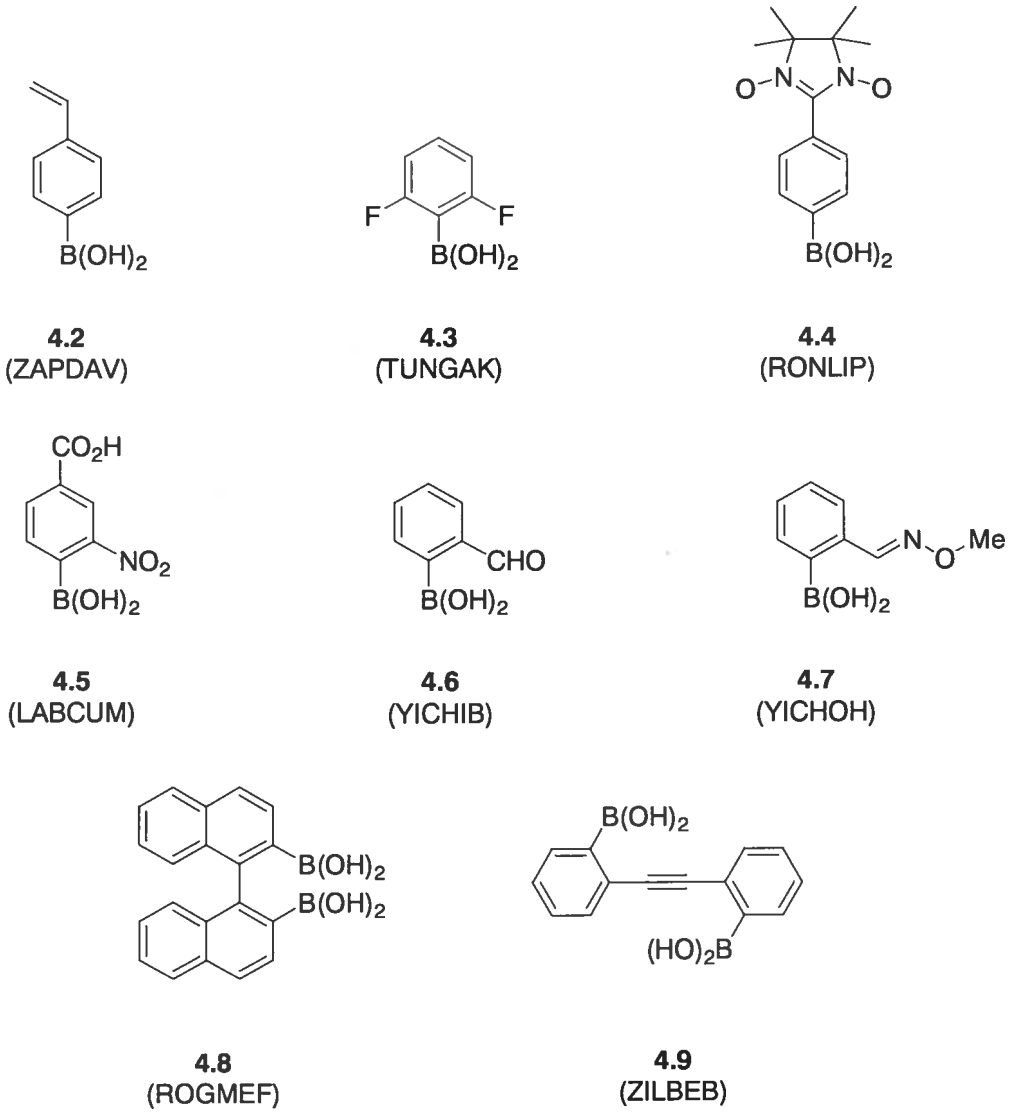

4.2 (ZAPDAV) **4.3** (TUNGAK) **4.4** (RONLIP)

4.5 (LABCUM) **4.6** (YICHIB) **4.7** (YICHOH)

4.8 (ROGMEF) **4.9** (ZILBEB)

Figure 4.2 Acides arylboroniques donnant lieu à la formation de dimères à l'état cristallin. Le code de référence de la *Cambridge Structural Database* est indiqué entre parenthèses.

Le composé **4.9** constitue certainement l'un des cas les plus intéressants d'un point de vue structural. En effet, la cristallisation de ce composé mène à la formation de l'arrangement supramoléculaire illustré à la Figure 4.3a. La présence de deux groupements acides boroniques sur chaque molécule mène à la formation de rubans infinis dans le cristal : chaque groupement acide boronique dimérise avec celui d'une

molécule voisine par le biais de ponts hydrogène. Cette propension à la dimérisation rappelle la même tendance observée parmis certaines classes de fonctions telles que les acides carboxyliques ou encore les 2-pyridones. De plus, la formation d'un tel arrangement n'est pas sans rappeler la formation de rubans observée lors de la cristallisation de la dipyridone **4.10** tel qu'illustré à la Figure 4.3b.[12]

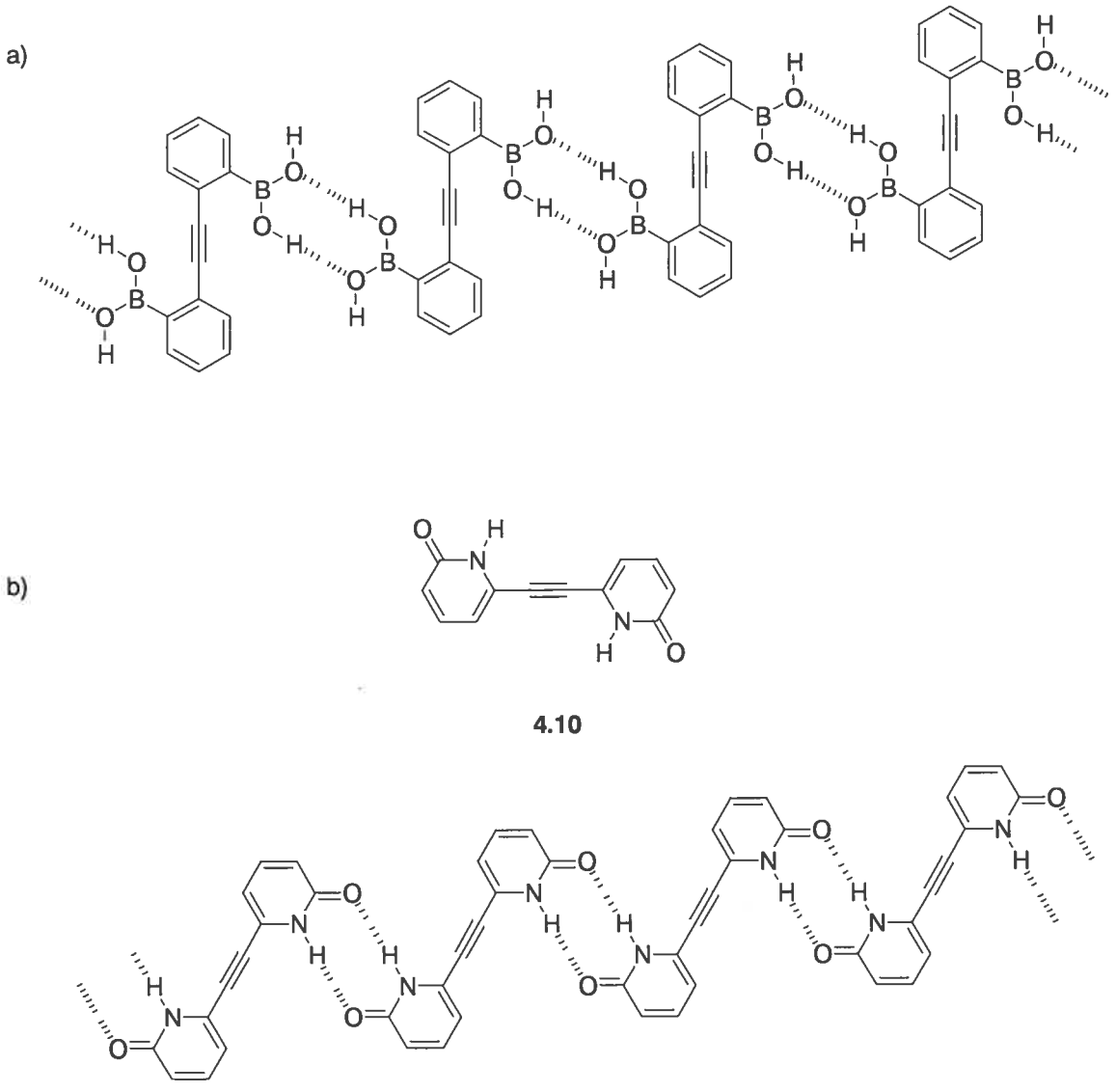

Figure 4.3 a) Formation de rubans infinis par dimérisation des acides boroniques lors de la cristallisation du composé **4.9**. b) Formation de rubans infinis par dimérisation de la dipyridone **4.10**.

L'exemple du composé **4.9** amène les questions suivantes : est-il possible d'utiliser les acides boroniques comme éléments de reconnaissance moléculaire et ce afin d'élaborer des réseaux supramoléculaires poreux comme il est possible de le faire en utilisant les acides carboxyliques ou les 2-pyridones ? La dimérisation des acides arylboroniques à l'état cristallin est-elle une association suffisamment forte pour contrebalancer efficacement la tendance à l'empilement compact et diriger la formation d'un réseau stable ? La synthèse, la caractérisation et l'étude par diffraction des rayons-X des composés **4.11** et **4.12** furent donc entreprises afin de vérifier le potentiel des acides boroniques comme groupement de reconnaissance pour le contrôle d'association intermoléculaire à l'état solide. Les résultats de ces études sont présentés dans les pages qui suivent sous forme d'article.

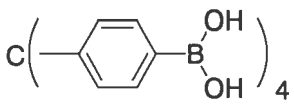

4.10

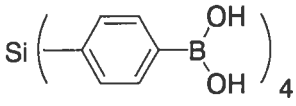

4.11

4.3 Références

1) Hassan, H.; Sévignon, M.; Gozzi, C.; Schulz, E.; Lemaire, M. *Chem. Rev.* **2002**, *102*, 1359. Suzuki, A. *J. Organomet. Chem.* **1999**, *576*, 147. Miyauran N.; Suzuki, A. *Chem. Rev.* **1995**, *95*, 2457.
2) Ishihara, K.; Yamamoto, H. *Eur. J. Org. Chem.* **1999**, 527. Rao, G.; Philipp, M. *J. Org. Chem.* **1991**, *56*, 1506.
3) Davis, C. J.; Lewix, P. T.; McCarroll, M. E.; Read, M. W.; Cueto, R.; Strongin, R. M. *Org. Lett.* **1999**, *1*, 331. James, T. D.; Samankumara Sandanayake, K. R. A.; Shinkai, S. *Angew. Chem., Int. Ed. Engl.* **1996**, *35*, 1910.
4) Rettig, S. J.; Trotter, J. *Can. J. Chem.* **1977**, *55*, 3071.

5) Soundararajan, S.; Duesler, E. S.; Hageman, J. H. *Acta, Crystallogr., Sect. C.* **1993**, *49*, 690.

6) Akita, T.; Kobayashi, K. *Adv. Mater.* **1997**, *9*, 346.

7) Bradley, D. C.; Harding, I. S.; Keefe, A. D.; Motevalli, M.; Zheng, D. H. *J. Chem. Soc., Dalton Trans.* **1996**, 3931.

8) Scouten, W. H.; Liu, X.-C.; Khangin, N.; Mullica, D. F.; Sappenfield, E. L. *J. Chem. Cryst.* **1994**, *24*, 621.

9) Gainsford, G. J.; Meinhold, R. H.; Woolhouse, A. D. *Acta, Crystallogr., Sect. C.* **1995**, *51*, 2694.

10) Schilling, B.; Kaiser, V.; Kaufmann, D. E. *Chem. Ber.* **1997**, *130*, 923.

11) Pilkington, M.; Wallis, J. D.; Larsen, S. *Chem. Commun.* **1995**, 1499.

12) Ducharme, Y.; Wuest, J. D. *J. Org. Chem.* **1988**, *53*, 5787.

Article 3

Fournier, J.-H.; Maris, T.; Wuest, J. D. Galoppini, E.; Guo, W. "Molecular Tectonics. Use of Hydrogen Bonding of Boronic Acids To Direct Supramolecular Construction" *Journal of American Chemical Society*, **2003**, *125*, 1002.

Molecular Tectonics. Use of the Hydrogen Bonding of Boronic Acids to Direct Supramolecular Construction

Jean-Hugues Fournier,[1] Thierry Maris, and James D. Wuest*

Département de Chimie, Université de Montréal
Montréal, Québec H3C 3J7 Canada

Wenzhuo Guo and Elena Galoppini*

Department of Chemistry, Rutgers University
Newark, New Jersey 07102 USA

*Authors to whom correspondence may be addressed: [redacted]

[redacted]

Abstract

Tetraboronic acids **1** and **2** have four $-B(OH)_2$ groups oriented tetrahedrally by cores derived from tetraphenylmethane and tetraphenylsilane. Crystallization produces isostructural diamondoid networks held together by hydrogen bonding of the $-B(OH)_2$ groups, in accord with the tendency of simple arylboronic acids to form cyclic hydrogen-bonded dimers in the solid state. Five-fold interpenetration of the networks is observed, but 60% and 64% of the volumes of crystals of tetraboronic acids **1** and **2**, respectively, remain available for the inclusion of disordered guests. Guests occupy two types of interconnected channels aligned with the *a* and *b* axes; those in crystals of tetraphenylmethane **1** measure approximately 5.9 x 5.9 $Å^2$ and 5.2 x 8.6 $Å^2$ in cross section at the narrowest points, whereas those in crystals of tetraphenylsilane **2** are approximately 6.4 x 6.4 $Å^2$ and 6.4 x 9.0 $Å^2$. These channels provide access to the interior and permit guests to be exchanged quantitatively without loss of crystallinity. Because the Si-C bonds at the core of tetraboronic acid **2** are longer (1.889(3) Å) than the C-C bonds at the core of tetraboronic acid **1** (1.519(6) Å), the resulting network is expanded rationally. By associating to form robust isostructural networks with predictable architectures and properties of porosity, compounds **1** and **2** underscore the usefulness of molecular tectonics as a strategy for making ordered materials.

Introduction

Molecular tectonics is a strategy for building predictably ordered networks from subunits called tectons, which are molecules designed to interact strongly with their neighbors in ways that are specific and directional.[2,3] The strategy provides chemists with a useful tool for achieving the spontaneous assembly of new ordered materials with predetermined structures and properties. Of particular interest is the observation that tectons cannot typically form normal close-packed structures in which their ability to take part in specific intermolecular interactions is fully exploited at the same time; instead, they tend to form open networks in which significant volumes are available for the inclusion of guests.

In a conceptually simple method for making tectons, multiple functional groups that promote strong intermolecular interactions can be attached to geometrically suitable cores. Many sticky functional groups have now been tested and found useful as the principal sites of association,[4] but the field remains rich in unexplored potential. For example, the crystallization of arylboronic acids typically produces cyclic hydrogen-bonded dimers (eq. 1),[5,6] but this interaction has not yet been exploited in supramolecular assembly,[7,8] despite the extensive use of boronic acids in

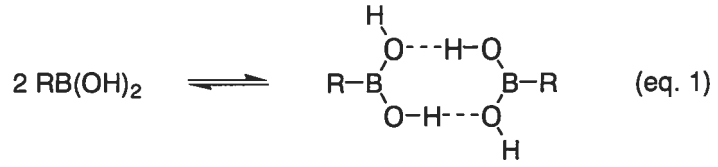

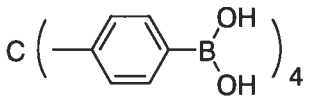

1

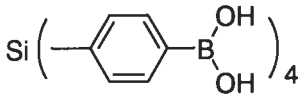

2

other areas of molecular recognition.[9] In this paper, we describe the crystal structures of tetraboronic acids **1** and **2**, and we confirm our expectation that they are predisposed to associate by hydrogen bonding according to eq. 1 and to thereby form open three-dimensional, four-connected networks with significant internal volumes for the inclusion of guests.

Results and Discussion

Synthesis. Tetraboronic acid **1** was prepared by minor modifications of the known method.[10] The analogous silane **2** was prepared in 84% overall yield by tetralithiation of tetrakis(4-bromophenyl)silane (BuLi),[11] followed by the addition of B(O-*i*-Pr)$_3$ and subsequent hydrolysis. Tetraboronic acids **1** and **2** are both of intrinsic interest as substrates for Suzuki couplings and as precursors for the synthesis of a wide range of tetrahedral molecular building blocks derived from tetraphenylmethane and tetraphenylsilane.[11]

General Description of Structures. Crystallization of compounds **1** and **2** was achieved by partial evaporation of solutions in wet ethyl acetate or by diffusion of hexane into solutions in wet ethyl acetate,[12] and the structures were determined by X-ray crystallography. Both compounds crystallize in the tetragonal space group I $4_1/a$ to give isostructural networks held together by hydrogen bonding of $-B(OH)_2$ groups, in accord with the characteristic motif shown in eq. 1.[13] Because the two structures are closely similar, only views of the network derived from tetraphenylsilane **2** are shown (Figures 1-4). The $-B(OH)_2$ groups are oriented tetrahedrally by the relatively rigid tetraphenylmethyl and tetraphenylsilyl cores to which they are attached, so both networks are predisposed to favor diamondoid connectivity,[14] which is observed, or a related three-dimensional, four-connected arrangement. The average intertectonic distances between the tetrahedral centers of neighboring hydrogen-bonded tetraboronic acids are 15.79 Å and 16.63 Å in the structures of compounds **1** and **2**, respectively. As a result, each diamondoid network is open enough to permit interpenetration by four independent diamondoid networks (Figure 2).[15]

Inclusion of Guests. Despite this five-fold interpenetration, the structures of compounds **1** and **2** both retain very significant volume for the inclusion of guests. Specifically, crystallization produces inclusion compounds of approximate composition **1** • 5 $CH_3COOC_2H_5$ • x H_2O and **2** • 5 $CH_3COOC_2H_5$ • y H_2O, as estimated by ^1H NMR spectroscopy of dissolved samples.[16] In both cases, the guests are highly disordered, and their location within the networks cannot be determined precisely. However, the volume available for inclusion defines two types of interconnected channels aligned with the

crystallographic *a* and *b* axes. In the network derived from tetraphenylmethane **1**, these channels have cross sections of approximately 5.9 x 5.9 Å^2 and 5.2 x 8.6 Å^2 at the narrowest points, whereas those in the isostructural network derived from tetraphenylsilane **2** are 6.4 x 6.4 Å^2 and 6.4 x 9.0 Å^2.[17] Both cross sections in the structure assembled from tecton **2** are clearly visible in the view along the *a* axis shown in Figure 3.

The channels themselves and their connectivity are represented by the surface shown in Figure 4.[18] This establishes that 1) the channels are highly interconnected; 2) their detailed shapes are much more complex than those suggested by the simple cross sections shown in Figure 3; and 3) guests that diffuse within the network can reach any point within the channels by multiple redundant pathways.[19] In principle, the high connectivity should help ensure that diffusion is not prevented by occasional obstacles or defects in the system of channels.

Overall, nearly 60% and 64% of the volume of crystals of tectons **1** and **2**, respectively, is available for including guests.[20,21] These values are notably high and far exceed the unused space in normal molecular crystals, typically close to 30%, that is created by inefficient packing.[22] In fact, the available volume in crystals of tectons **1** and **2** even exceeds that used to include water in many protein crystals, despite the characteristically large, complex, and irregular shapes of proteins.[23] In principle, the very simple shapes of tectons **1** and **2** would allow them to be packed with normal efficiency to create relatively compact periodic structures; indeed, tetraphenylmethane, tetraphenylsilane, and simple

substituted derivatives do not typically form inclusion compounds.[24] By not acting like normal molecules, compounds **1** and **2** show special behavior that fully supports the emerging principles of molecular tectonics. In particular, the inherent tendency of tectons to form strong directional interactions disfavors efficient molecular packing and promotes the formation of structures in which significant volume is available for the inclusion of guests.

Exchange of Guests. In the structures derived from tetraboronic acids **1** and **2**, each tecton participates in a total of eight hydrogen bonds with four neighbors to form a diamondoid network. Moreover, each diamondoid network is linked to the two adjacent interpenetrating diamondoid networks by supplementary hydrogen bonds between cyclic dimers, as shown in structure **3**. Similar inter-dimeric hydrogen bonding has also been observed in the structures of

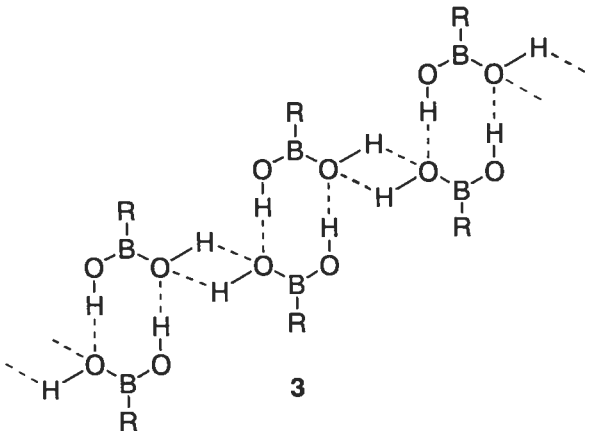

3

simpler arylboronic acids.[5,6] As a result, each tecton participates in a total of sixteen hydrogen bonds, eight involving neighbors in the same diamondoid network and eight

involving tectons in the adjacent interpenetrating networks. This extensive hydrogen bonding helps ensure that the structural integrity of the ordered assembly is high.

In contrast, the guests are disordered, potentially mobile, and located in channels that in principle provide multiple routes of escape from inside the crystal. As observed in other tectonic materials,[2] the exchange of guests can take place without destroying the ordered network. For example, single crystals of estimated composition **1** • 5 $CH_3COOC_2H_5$ • x H_2O and approximate dimensions 1 mm x 1 mm x 1 mm were suspended in tetrahydrofuran (THF)/hexane at 25 °C for 24 h. The recovered sample remained transparent and morphologically unchanged, continued to diffract and to exhibit uniform extinction between crossed polarizers, and showed closely similar unit cell parameters when studied by single-crystal X-ray diffraction. However, analysis of dissolved samples by ^{1}H NMR spectroscopy established that the initial guest, $CH_3COOC_2H_5$, had been replaced quantitatively by THF to give new crystals of approximate composition **1** • 5 THF • z H_2O.[16] In similar single-crystal to single-crystal transformations, $CH_3COOC_2H_5$ was also replaced quantitatively by two guests approximately twice as large, diethyl malonate and diethyl methylmalonate. The exchange of guests is feasible, at least within geometric limits imposed by the channels, but the removal of guests by exposure of crystals to air or vacuum leads to a loss of crystallinity.

The unit cell parameters before replacement of $CH_3COOC_2H_5$ by THF were $a = b =$ 10.627(11) Å, c = 41.608(6) Å, $\alpha = \beta = \gamma = 90°$, and V = 4699(7) Å^3, whereas those after exchange were $a = b$ = 10.794(17) Å, c = 42.08(7) Å, $\alpha = \beta = \gamma = 90°$, and V = 4902(5)

$Å^3$ at the same temperature (226 K). This observation shows that the replacement of $CH_3COOC_2H_5$ by THF induces a small expansion of the network, possibly associated with subtle changes in the conformation of tecton **1**, differences in internal solvation of the network by the included guests, or an increase in the number of guests.

Together, our studies of exchange demonstrate that 1) the crystalline network is robust enough to remain insoluble and to retain its original ordered architecture during the exchange of guests, yet 2) the network is deformable enough to accommodate small structural changes. In general, tectonic networks may prove to offer a unique balance between structural integrity and deformability that makes them distinctly different from both normal soft organic materials and hard inorganic materials.[25]

Channels in the structures derived from tectons **1** and **2** provide access to –OH groups involved in intertectonic hydrogen bonding. Because arylboronic acids are moderately acidic (pKa 8.83 for benzeneboronic acid itself),[26] porous crystals constructed by the association of boronic acids may prove to be useful in heterogeneous acidic catalysis or in the separation of bases according to size, shape, and other characteristics.[27]

Detailed Analysis and Comparison of Structures. The bond lengths and angles in the structures of tectons **1** and **2** are similar to those of simpler arylboronic acids. For example, the O···O distances in the dimeric units defined by eq. 1 are 2.693(5) Å and 2.713(3) Å in the networks derived from compounds **1** and **2**, respectively, whereas they are 2.743(2) Å in the dimer of phenylboronic acid itself.[5] Similar values are also found

for the O-B-O angles (118.7(8)° and 119.5(4)° in the structures derived from tectons **1** and **2**, respectively, and 116.2(2)° in the model dimer[5]), the average values for the angle between the planes defined by the aryl groups and the $-B(OH)_2$ groups (13.2° and 1.6° in the structures derived from compounds **1** and **2**, respectively, and 14.2° in the model dimer[5]), and other parameters.

In both structures derived from tetraboronic acids **1** and **2**, adjacent interpenetrating networks are related by a displacement along the *a* or *b* axes equal to the unit cell parameters ($a = b$ = 10.627(11) Å for tetraphenylmethane **1** and $a = b$ = 10.8370(15) Å for tetraphenylsilane **2**). The O···O distances for the inter-dimeric hydrogen bonds defined by structure **3** are 2.700(8) Å and 2.729(5) Å, respectively. These distances are slightly longer than those corresponding to the intra-dimeric hydrogen bonds, so it is appropriate to consider the cyclic arrangement shown in eq. 1 as the primary hydrogen-bonding motif present in the structures of tectons **1** and **2**. Nevertheless, the inter-dimeric hydrogen bonds also appear to make an important contribution.

Because the average Si-C distance at the core of tetraphenylsilane **1** (1.889(3) Å) is significantly greater than the average C-C distance at the core of tetraphenylmethane **2** (1.519(6) Å), the average intertectonic distances between the centers of hydrogen-bonded neighbors are correspondingly larger (15.79 Å vs. 16.63 Å). As a result, the dimensions of the channels, the percentage of volume available for inclusion, and various unit cell parameters are increased predictably. Specifically, the values of $a = b$ = 10.627(11) Å, c = 41.608(6) Å, and V = 4699(7) Å^3 in the structure of

tetraphenylmethane **1** are increased to $a = b = 10.8370(15)$ Å, $c = 45.602(9)$ Å, and $V = 5355.6(15)$ Å^3 in the structure of tetraphenylsilane **2**.

Although the networks constructed from tectons **1** and **2** are predictably similar, several minor differences are noteworthy. In particular, the C-C-C angles at the core of tetraphenylmethane **1** have values of either 102.1(4)° or 113.3(2)°, whereas the C-Si-C angles at the core of tetraphenylsilane **2** vary less widely (106.0(2)° or 111.2(1)°), despite the presumably greater flexibility of the tetraphenylsilyl core. In neither case, however, do deviations from ideal tetrahedral geometry give rise to non-diamondoid architectures.

Detailed prediction of the structures of molecular crystals remains impossible.[28] However, our study of the behavior of tectons **1** and **2** shows that the strategy of molecular tectonics gives chemists an effective tool for engineering new crystalline structures with important elements of predictability. As their design intends, tectons **1** and **2** self-associate by hydrogen bonding of $-B(OH)_2$ groups according to the standard motif (eq. 1), thereby forming isostructural three-dimensional, four-connected networks with significant degrees of openness that depend predictably on the size of the individual subunits.

Conclusions

Our studies of tetraboronic acids **1** and **2** are of broad chemical interest for the following reasons: 1) Both compounds are promising precursors for synthesizing a range of

tetrahedral molecular building blocks by Suzuki couplings; 2) their association establishes for the first time the usefulness of boronic acids in the self-assembly of supramolecular structures; and 3) their predictable behavior confirms that molecular tectonics is an effective strategy for making ordered supramolecular materials by design.

Experimental Section

Tetrahydrofuran (THF) was dried by distillation from the sodium ketyl of benzophenone. All other reagents were commercial products that were used without further purification.

(Methanetetrayltetra-4,1-phenylene)tetrakisboronic Acid (1).[10] A solution of tetrakis(4-bromophenyl)methane (1.27 g, 2.00 mmol)[29,30] in THF (125 mL) was stirred at -78 °C under dry N_2 and treated dropwise with a solution of butyllithium (6.4 mL, 2.5 M in hexane, 16 mmol). The resulting mixture was kept at –78 °C for 30 min, and then B(O-*i*Pr)$_3$ (5.50 mL, 23.8 mmol) was added dropwise. The mixture was stirred at -78 °C for 20 min and then at 25 °C for 1 h. After acidification with 1 M aqueous HCl (25 mL), the mixture was concentrated by partial evaporation of volatiles under reduced pressure. The concentrate was treated with aqueous 1 M NaOH and filtered, and the filtrate was acidified with 1 M aqueous HCl. This yielded a precipitate, which was separated by filtration and dried in air to afford (methanetetrayltetra-4,1-phenylene)tetrakisboronic acid (**1**; 0.914 g, 1.84 mmol, 92%) as a colorless solid: mp > 300 °C; IR (KBr) 3369 cm^{-1}; ^{1}H NMR (400 MHz, DMSO-d$_6$) δ 8.03 (s, 8H), 7.66 (d, 8H, ^3J = 8.4 Hz), 7.12 (d, 8H, ^3J = 8.4 Hz); ^{13}C NMR (100 MHz, DMSO-d$_6$) δ 149.3, 134.5, 132.3, 130.6, 65.9; MS (FAB,

glycerol) *m/e* 721. Anal. Calcd for $C_{25}H_{24}B_4O_8 \cdot 4\ H_2O$: C, 52.89; H, 5.68. Found: C, 53.51; H, 5.93.

(Silanetetrayltetra-4,1-phenylene)tetrakisboronic Acid (2). An analogous procedure converted tetrakis(4-bromophenyl)silane (1.30 g, 1.99 mmol)[11] into (silanetetrayltetra-4,1-phenylene)tetrakisboronic acid (**2**; 0.860 g, 1.68 mmol, 84%), which was isolated as a colorless solid: mp > 300 °C; IR (KBr) 3369 cm^{-1}; ^1H NMR (400 MHz, DMSO-d_6) δ 8.14 (s, 8H), 7.79 (d, 8H, ^3J = 7.8 Hz), 7.42 (d, 8H, ^3J = 7.8 Hz); ^{13}C NMR (100 MHz, DMSO-d_6) δ 136.9, 136.4, 135.9, 134.5; MS (FAB, glycerol) *m/e* 737. Anal. Calcd for $C_{24}H_{24}B_4O_8Si \cdot 1\ H_2O$: C, 54.41; H, 4.95. Found: C, 53.66; H, 4.79.

Crystallization of Tetraboronic Acids 1 and 2. In typical crystallizations, tetraboronic acid **1** or **2** (0.2 mmol) was treated with $CH_3COOC_2H_5$ (15 mL), and the mixture was shaken with H_2O.[12] The organic phase was separated and exposed to vapors of hexane. Crystals suitable for X-ray diffraction were obtained after two days. Alternatively, suitable crystals of tetraboronic acid **1** or **2** could also be obtained by slow evaporation of solutions in wet $CH_3COOC_2H_5$.

X-Ray Crystallographic Studies. The structures were solved by direct methods using SHELXS-97 and refined with SHELXL-97.[31] All non-hydrogen atoms were refined anisotropically, whereas hydrogen atoms were placed in ideal positions and refined as riding atoms. In both structures, the included guests were found to be highly disordered and could not be resolved. The SQUEEZE option of the PLATON program was used to

eliminate the contribution of the guests and to give final models based only on the ordered part of the structures.[21]

Structure of Tetraboronic Acid 1. Data were collected using a Bruker SMART 2000 CCD diffractometer with Cu Kα radiation at 226 K. Crystals of compound **1** belong to the tetragonal space group I 4_1/a (No. 88) with $a = b = 10.627(11)$ Å, $c = 41.608(6)$ Å, $V = 4699(7)$ Å^3, D_{calcd} (without solvent) = 0.701 g cm^{-3}, and $Z = 4$. Full-matrix least-squares refinements on F^2 led to final residuals $R_f = 0.0938$, $R_w = 0.2759$, and $GoF = 0.699$ for 358 reflections with $I>2\sigma(I)$.

Structure of Tetraboronic Acid 2. Data were collected using an Enraf-Nonius CAD-4 diffractometer with Cu Kα radiation at 210 K. Crystals of compound **2** belong to the tetragonal space group I 4_1/a (No. 88) with $a = b = 10.8370(15)$ Å, $c = 45.602(9)$ Å, $V = 5355.6(15)$ Å^3, D_{calcd} (without solvent) = 0.634 g cm^{-3}, and $Z = 4$. Full-matrix least-squares refinements on F^2 led to final residuals $R_f = 0.0701$, $R_w = 0.1717$, and $GoF = 0.666$ for 804 reflections with $I>2\sigma(I)$.

Exchange of Guests in Crystals of Tetraboronic Acid 1. Single crystals of estimated composition **1** • 5 $CH_3COOC_2H_5$ • x H_2O and approximate dimensions 1 mm x 1 mm x 1 mm were grown in the normal manner. The mother liquors were removed by pipette, and the crystals were immediately covered with a 1:9 mixture of THF/hexane and kept unstirred at 25 °C for 24 h. The liquid was removed by pipette, the recovered crystals were washed three times with hexane, and their content was determined by ^{1}H NMR

spectroscopy. Replacement of $CH_3COOC_2H_5$ by diethyl malonate and methyl diethylmalonate was carried under similar conditions and analysed by ^1H NMR spectroscopy of dissolved samples.

Acknowledgment. We thank Dr. Richard Gilardi for preliminary crystallographic studies and helpful discussions. We are grateful to the Natural Sciences and Engineering Research Council of Canada, the Ministère de l'Éducation du Québec, Merck Frosst, the U. S. National Science Foundation, and the Rutgers University Research Council for financial support. In addition, acknowledgment is made to the donors of the Petroleum Research Fund, administered by the American Chemical Society, for support of this research.

Supplementary Material Available: ORTEP drawings and tables of crystallographic data, atomic coordinates, anisotropic thermal parameters, and bond lengths and angles for tetraboronic acids **1** and **2**. This information is available free of charge via the internet at http://pubs.acs.org.

Notes and References

1) Fellow of the Ministère de l'Éducation du Québec, 2000-2002. Fellow of the Natural Sciences and Engineering Research Council of Canada, 1998-2000.

2) Brunet, P.; Simard, M.; Wuest, J. D. *J. Am. Chem. Soc.* **1997**, *119*, 2737. Su, D.; Wang, X.; Simard, M.; Wuest, J. D. *Supramolecular Chemistry* **1995**, *6*, 171. Wuest, J. D. In *Mesomolecules: From Molecules to Materials*; Mendenhall, G. D.; Greenberg, A.; Liebman, J. F., Eds.; Chapman & Hall: New York, 1995. Wang, X.;

Simard, M.; Wuest, J. D. *J. Am. Chem. Soc.* **1994**, *116*, 12119. Simard, M.; Su, D.; Wuest, J. D. *J. Am. Chem. Soc.* **1991**, *113*, 4696.

3) For recent studies of hydrogen-bonded supramolecular networks by other groups, see: Holman, K. T.; Pivovar, A. M.; Swift, J. A.; Ward, M. D. *Acc. Chem. Res.* **2001**, *34*, 107. Kuduva, S. S.; Bläser, D.; Boese, R.; Desiraju, G. R. *J. Org. Chem.* **2001**, *66*, 1621. Mak, T. C. W.; Xue, F. *J. Am. Chem. Soc.* **2000**, *122*, 9860. Sharma, C. V. K.; Clearfield, A. *J. Am. Chem. Soc.* **2000**, *122*, 4394. Corbin, P. S.; Zimmerman, S. C. *J. Am. Chem. Soc.* **2000**, *122*, 3779. Cantrill, S. J.; Pease, A. R.; Stoddart, J. F. *J. Chem. Soc., Dalton Trans.* **2000**, 3715. Batchelor, E.; Klinowski, J.; Jones, W. *J. Mater. Chem.* **2000**, *10*, 839. Videnova-Adrabinska, V.; Janeczko, E. *J. Mater. Chem.* **2000**, *10*, 555. Reddy, D. S.; Dewa, T.; Endo, K.; Aoyama, Y. *Angew. Chem., Int. Ed. Engl.* **2000**, *39*, 4266. Akazome, M.; Suzuki, S.; Shimizu, Y.; Henmi, K.; Ogura, K. *J. Org. Chem.* **2000**, *65*, 6917. Baumeister, B.; Matile, S. *J. Chem. Soc., Chem. Commun.* **2000**, 913. Chowdhry, M. M.; Mingos, D. M. P.; White, A. J. P.; Williams, D. J. *J. Chem. Soc., Perkin Trans. 1* **2000**, 3495. Gong, B.; Zheng, C.; Skrzypczak-Jankun, E.; Zhu, J. *Org. Lett.* **2000**, *2*, 3273. Krische, M. J.; Lehn, J.-M.; Kyritsakas, N.; Fischer, J.; Wegelius, E. K.; Rissanen, K. *Tetrahedron* **2000**, *56*, 6701. Aakeröy, C. B.; Beatty, A. M.; Nieuwenhuyzen, M.; Zou, M. *Tetrahedron* **2000**, *56*, 6693. Kobayashi, K.; Shirasaka, T.; Horn, E.; Furukawa, N. *Tetrahedron Lett.* **2000**, *41*, 89. Dahal, S.; Goldberg, I. *J. Phys. Org. Chem.* **2000**, *13*, 382. Bishop, R.; Craig, D. C.; Dance, I. G.; Scudder, M. L.; Ung, A. T. *J. Struct. Chem.* **1999**, *40*, 663. Fuchs, K.; Bauer, T.; Thomann, R.; Wang, C.; Friedrich, C.; Mühlhaupt, R. *Macromolecules* **1999**, *32*, 8404. Holý, P.; Závada, J.; Císarová, I.; Podlaha, J. *Angew. Chem., Int. Ed.*

Engl. **1999**, *38*, 381. Karle, I. L.; Ranganathan, D.; Kurur, S. *J. Am. Chem. Soc.* **1999**, *121*, 7156. Chin, D. N.; Palmore, G. T. R.; Whitesides, G. M. *J. Am. Chem. Soc.* **1999**, *121*, 2115. Hanessian, S.; Saladino, R.; Margarita, R.; Simard, M. *Chem. Eur. J.* **1999**, *5*, 2169. Biradha, K.; Dennis, D.; MacKinnon, V. A.; Sharma, C. V. K.; Zaworotko, M. J. *J. Am. Chem. Soc.* **1998**, *120*, 11894. Schauer, C. L.; Matwey, E.; Fowler, F. W.; Lauher, J. W. *J. Am. Chem. Soc.* **1997**, *119*, 10245. Bhyrappa, P.; Wilson, S. R.; Suslick, K. S. *J. Am. Chem. Soc.* **1997**, *119*, 8492. Lambert, J. B.; Zhao, Y.; Stern, C. L. *J. Phys. Org. Chem.* **1997**, *10*, 229. Félix, O.; Hosseini, M. W.; De Cian, A.; Fischer, J. *Angew. Chem., Int. Ed. Engl.* **1997**, *36*, 102. MacGillavray, L.; Atwood, J. *Nature* **1997**, *389*, 469. Adam, K. R.; Atkinson, I. M.; Davis, R. L.; Lindoy, L. F.; Mahinay, M. S.; McCool, B. J.; Skelton, B. W.; White, A. H. *J. Chem. Soc., Chem. Commun.* **1997**, 467. Schwiebert, K. E.; Chin, D. N.; MacDonald, J. C.; Whitesides, G. M. *J. Am. Chem. Soc.* **1996**, *118*, 4018. Kinbara, K.; Hashimoto, Y.; Sukegawa, M.; Nohira, H.; Saigo, K. *J. Am. Chem. Soc.* **1996**, *118*, 3441. Munakata, M.; Wu, L. P.; Yamamoto, M.; Kuroda-Sowa, T.; Maekawa, M. *J. Am. Chem. Soc.* **1996**, *118*, 3117. Hartgerink, J. D.; Granja, J. R.; Milligan, R. A.; Ghadiri, M. R. *J. Am. Chem. Soc.* **1996**, *118*, 43. Hollingsworth, M. D.; Brown, M. E.; Hillier, A. C.; Santarsiero, B. D.; Chaney, J. D. *Science* **1996**, *273*, 1355. Kolotuchin, S. V.; Fenlon, E. E.; Wilson, S. R.; Loweth, C. J.; Zimmerman, S. C. *Angew. Chem., Int. Ed. Engl.* **1995**, *34*, 2654. Lawrence, D. S.; Jiang, T.; Levett, M. *Chem. Rev.* **1995**, *95*, 2229. Ermer, O.; Eling, A. *J. Chem. Soc., Perkin Trans. 2* **1994**, 925. Venkataraman, D.; Lee, S.; Zhang, J.; Moore, J. S. *Nature* **1994**, *371*, 591.

4) Nangia, A.; Desiraju, G. R. *Top. Curr. Chem.* **1998**, *198*, 57.

5) Rettig, S. J.; Trotter, J. *Can. J. Chem.* **1977**, *55*, 3071.

6) Zhdankin, V. V.; Persichini, P. J. III; Zhang, L.; Fix, S.; Kiprof, P. *Tetrahedron Lett.* **1999**, *40*, 6705. Schilling, B.; Kaiser, V.; Kaufmann, D. E. *Chem. Ber.* **1997**, *130*, 923. Akita, T.; Kobayashi, K. *Adv. Mater.* **1997**, *9*, 346. Bradley, D. C.; Harding, I. S.; Keefe, A. D.; Motevalli, M.; Zheng, D. H. *J. Chem. Soc., Dalton Trans.* **1996**, 3931. Pilkington, M.; Wallis, J. D.; Larsen, S. *J. Chem. Soc., Chem. Commun.* **1995**, 1499. Gainsford, G. J.; Meinhold, R. H.; Woolhouse, A. D. *Acta Crystallogr.* **1995**, *C51*, 2694. Scouten, W. H.; Liu, X.-C.; Khangin, N.; Mullica, D. F.; Sappenfield, E. L. *J. Chem. Cryst.* **1994**, *24*, 621. Soundararajan, S.; Duesler, E. N.; Hageman, J. H. *Acta Crystallogr.* **1993**, *C49*, 690. Feulner, H.; Linti, G.; Noth, H. *Chem. Ber.* **1990**, *123*, 1841. Zvonkova, Z. V.; Gluskova, V. P. *Kristallografija, SSSR* **1958**, *3*, 559.

7) The dimers of boronic acids have been overlooked in previous systematic studies of cyclic hydrogen-bonded motifs. Davis, R. E.; Bernstein, J. *Trans. Am. Crystallogr. Assoc.* **1999**, *33*, 7. Allen, F. H.; Raithby, P. R.; Shields, G. P.; Taylor, R. *J. Chem. Soc., Chem. Commun.* **1998**, 1043.

8) Hydrogen bonding of a monoester of a phenylboronic acid has recently been observed in a molecular network. Davis, C. J.; Lewis, P. T.; Billodeaux, D. R.; Fronczek, F. R.; Escobedo, J. O.; Strongin, R. M. *Org. Lett.* **2001**, *3*, 2443.

9) For example, see: Takeuchi, M.; Ikeda, M.; Sugasaki, A.; Shinkai, S. *Acc. Chem. Res.* **2001**, *34,* 865.

10) Wilson, L. M.; Griffin, A. C. *J. Mater. Chem.* **1993**, *3*, 991.

11) Fournier, J.-H.; Wang, X.; Wuest, J. D., submitted for publication.

12) Wet ethyl acetate was used to disfavor the formation of boroxines by dehydration of tetraboronic acids **1** and **2**.

13) Crystallization of tetraboronic acids **1** and **2** from primarily aqueous mixtures appears to yield a different structure that is currently being studied.

14) For a review of diamondoid hydrogen-bonded networks, see: Zaworotko, M. J. *Chem. Soc. Rev.* **1994**, *23*, 283.

15) For discussions of interpenetration in networks, see: Batten, S. R. *Cryst. Eng. Commun.* **2001**, *18*, 1; Batten, S. R.; Robson, R. *Angew. Chem., Int. Ed. Engl.* **1998**, *37*, 1460.

16) Small amounts of H_2O may be included, but the quantity could not be determined accurately by ^1H NMR spectroscopy. In addition, rapid loss of guests from crystals removed from their mother liquors prevented us from using thermogravimetric analysis to estimate the composition.

17) The dimensions of a channel in a particular direction correspond to the cross section of an imaginary cylinder that could be passed through the hypothetical empty network in the given direction in contact with the van der Waals surface. Such values are inherently conservative because 1) they measure the cross section at the most narrow constriction, and 2) they systematically underestimate the sizes of channels that are not uniform and linear.

18) Representations of channels were generated by the Cavities option in the program ATOMS Version 5.1 (Shape Software, 521 Hidden Valley Road, Kingsport, Tennessee 37663 USA; www.shapesoftware.com). We are grateful to Eric Dowty of Shape Software for integrating this capacity in ATOMS at our suggestion.

19) For a discussion of pathways for diffusion in microporous materials, see: Venuto, P. B. *Microporous Mater.* **1994**, *2*, 297.

20) The percentage of volume accessible to guests was estimated by the PLATON program.[21]

21) Spek, A. L. *PLATON, A Multipurpose Crystallographic Tool*; Utrecht University: Utrecht, The Netherlands, 2001. van der Sluis, P.; Spek, A. L. *Acta Crystallogr.* **1990**, *A46*, 194.

22) Kitaigorodskii, A. I. *Organic Chemical Crystallography*; Consultants Bureau: New York, 1961.

23) Quillin, M. L.; Matthews, B. W. *Acta Crystallogr.* **2000**, *D56*, 791. Andersson, K. M.; Hovmöller, S. *Acta Crystallogr.* **2000**, *D56*, 789.

24) Galoppini, E.; Gilardi, R. *J. Chem. Soc., Chem. Commun.* **1999**, 173. Oldham, W. J., Jr.; Lachicotte, R.; Bazan, G. C. *J. Am. Chem. Soc.* **1998**, *120*, 2987. Thaimattam, R.; Reddy, D. S.; Xue, F.; Mak, T. C. W.; Nangia, A.; Desiraju, G. R. *New J. Chem.* **1998**, 143. Lloyd, M. A.; Brock, C. P. *Acta Crystallogr.* **1997**, *B53*, 780. Reddy, D. S.; Craig, D. C.; Desiraju, G. R. *J. Am. Chem. Soc.* **1996**, *118*, 4090. Charissé, M.; Gauthey, V.; Dräger, M. *J. Organomet. Chem.* **1993**, *448*, 47. Charissé, M.; Roller, S.; Dräger, M. *J. Organomet. Chem.* **1992**, *427*, 23. Gruhnert, V.; Kirfel, A.; Will, G.; Wallrafen, F.; Recker, K. *Z. Krist.* **1983**, *163*, 53. Robbins, A.; Jeffrey, G. A.; Chesick, J. P.; Donohue, J.; Cotton, F. A.; Frenz, B. A.; Murillo, C. A. *Acta Crystallogr.* **1975**, *B31*, 2395.

25) For related work, see: Thaimattam, R.; Xue, F.; Sarma, J. A. R. P.; Mak, T. C. W.; Desiraju, G. R. *J. Am. Chem. Soc.* **2001**, *123*, 4432.

26) Nakatani, H.; Morita, T.; Hiromi, K. *Biochim. Biophys. Acta* **1978**, *525*, 423. Juillard, J.; Geugue, N. *C. R. Acad. Paris C* **1967**, *264*, 259.

27) For a review of the ability of arylboronic acids to serve as acid catalysts, see: Ishihara, K.; Yamamoto, H. *Eur. J. Org. Chem.* **1999**, 527.

28) For a discussion, see: Gavezzotti, A. *Acc. Chem. Res.* **1994**, *27*, 309.

29) Grimm, M.; Kirste, B.; Kurreck, H. *Angew. Chem., Int. Ed. Engl.* **1986**, *25*, 1097. Other methods for the synthesis of tetrakis(4-bromophenyl)methane have been published subsequently.[10,30]

30) Hoskins, B. F.; Robson, R. *J. Am. Chem. Soc.* **1990**, *112*, 1546.

31) Sheldrick, G. M. *SHELXS-97, Program for the Solution of Crystal Structures* and *SHELXL-97, Program for the Refinement of Crystal Structures*; Universität Göttingen: Germany, 1997.

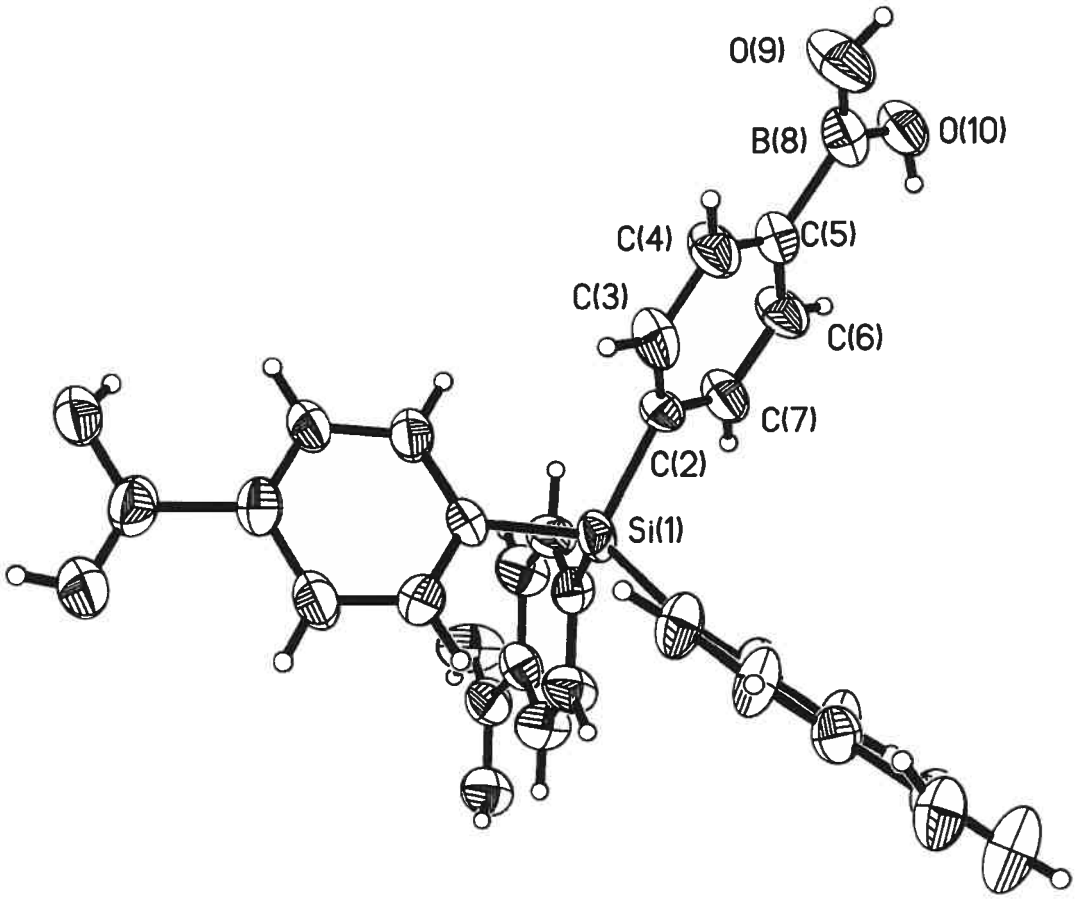

Figure 1. ORTEP view of the structure of tetraboronic acid **2.** Disordered guests are omitted, non-hydrogen atoms are represented by ellipsoids corresponding to 30% probability, and hydrogen atoms are shown as spheres of arbitrary size.

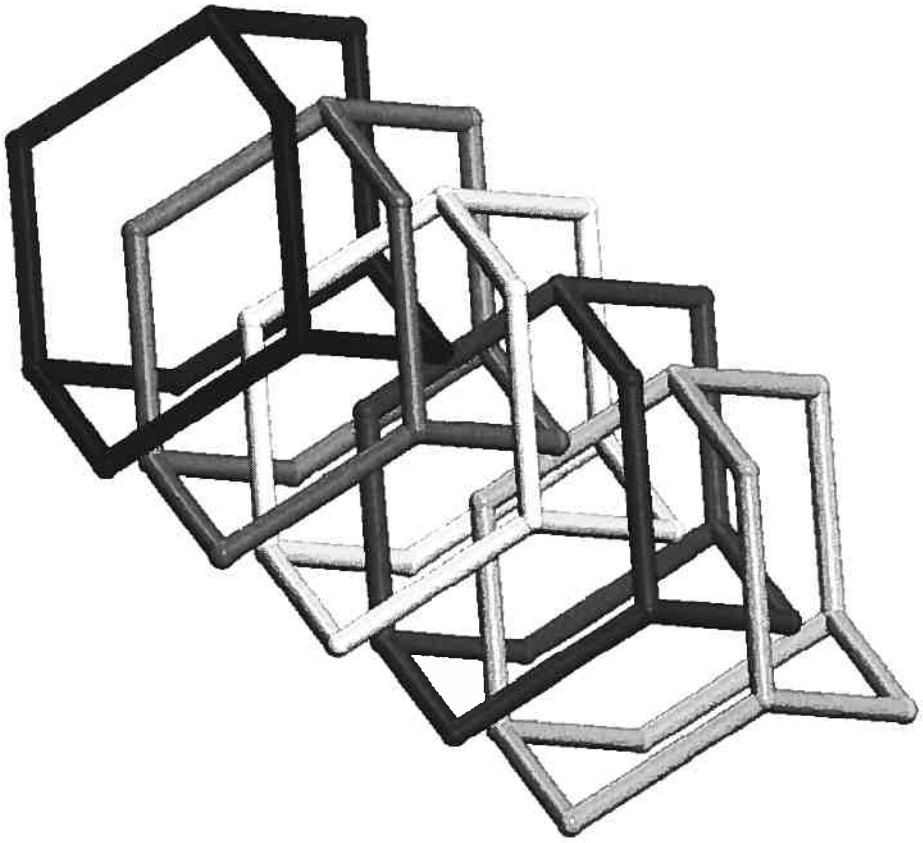

Figure 2. Representation of the system of five-fold interpenetrated diamondoid networks generated by tetraboronic acid **2**. In this drawing, the tectons lie at the intersections of solid lines that represent their interactions with four neighbors by hydrogen bonding according to the motif shown in eq. 1. The independent networks are shown in different shades of gray.

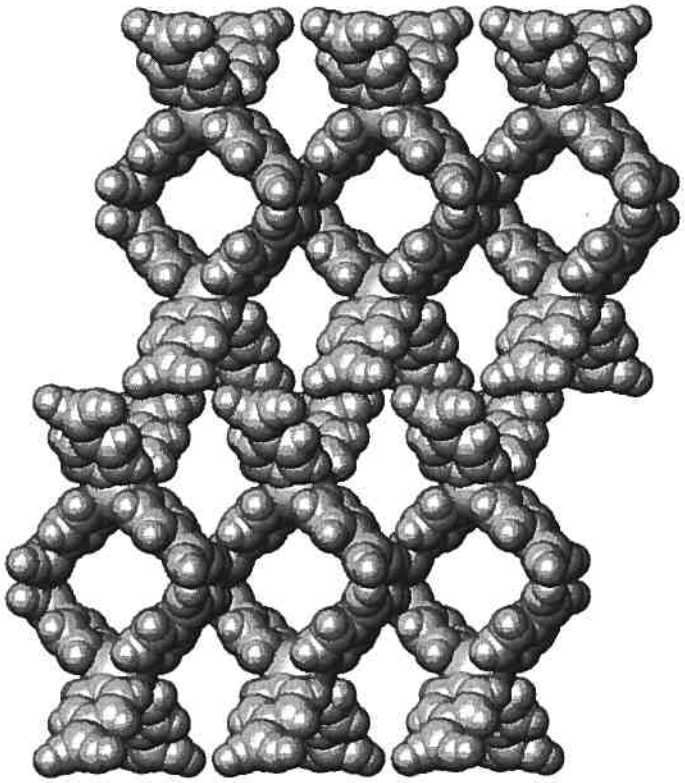

Figure 3. View along the *a* axis of the network constructed from tetraboronic acid **2** showing a 3 x 3 x 1 array of unit cells with disordered guests omitted.

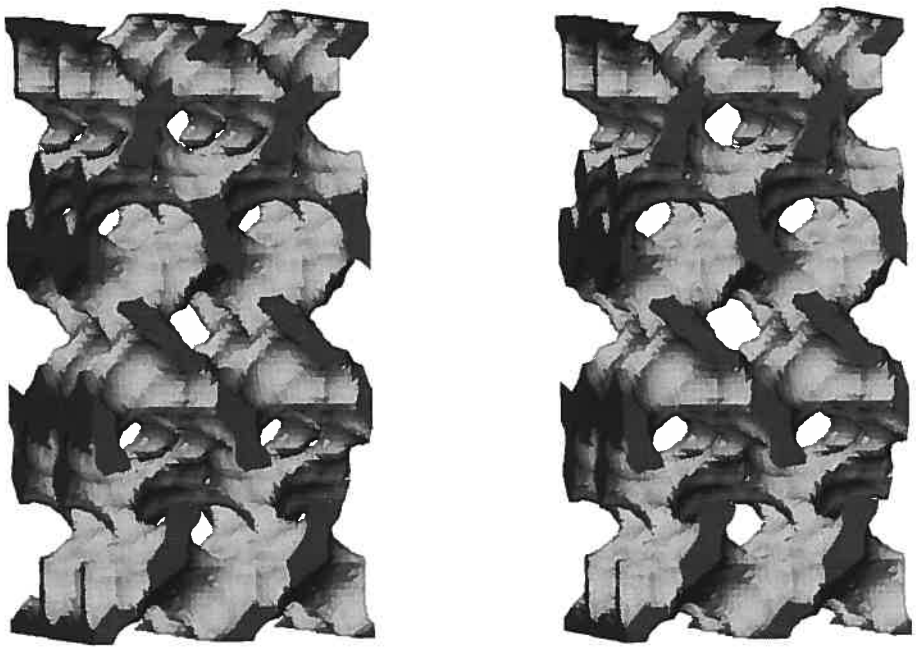

Figure 4. Stereoscopic representation of the interconnected channels defined by the network constructed from tetraboronic acid **2**. The image shows a 2 x 2 x 1 array of unit cells viewed with the *c* axis vertical. The outsides of the channels appear in light gray, and dark gray is used to show where the channels are cut by the boundaries of the array. The surface of the channels is defined by the possible loci of the center of a sphere of diameter 3 Å as it rolls over the surface of the ordered tectonic network.[18]

Chapitre 5

Utilisation des dérivés du 9,9'-spirobifluorène en tectonique moléculaire

5.1 Introduction

Les études résumées dans les chapitres précédents avaient pour but d'évaluer le potentiel de certains groupements fonctionnels pour l'élaboration de réseaux supramoléculaires poreux. Ainsi que mentionné au Chapitre 1, le choix du groupement d'association intermoléculaire s'avère crucial pour la création de matériaux tectoniques. Un autre facteur devant être considéré lors de l'élaboration de tectons est celui du squelette moléculaire servant de support aux groupes d'association.

Le squelette moléculaire du tecton est responsable de l'orientation spatiale des groupes de reconnaissance moléculaire : la nature de sa géométrie conditionne la géométrie obtenue pour l'assemblage supramoléculaire. Ainsi, les chapitres précédents ont mis en lumière comment les dérivés du tétraphénylméthane ont été employés à de nombreuses reprises pour l'élaboration de réseaux supramoléculaires tridimensionnels. Toutefois, rien ne limite *a priori* le design de tectons tétraédriques à cette seule classe de dérivés. C'est afin d'identifier d'autres types de squelettes moléculaires pouvant maintenir des groupes d'association intermoléculaire dans une orientation spatiale tridimensionnelle que les études sur les dérivés du 9,9'-spirobifluorène (**5.1**) ont été entreprises.

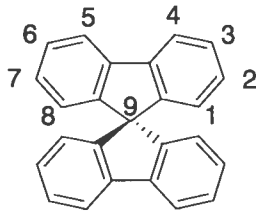

5.1

5.2 Le 9,9-spirobifluorène : synthèse et réactivité.

Le 9,9'-spirobifluorène (**5.1**) apparaît au premier coup d'œil comme un analogue contraint géométriquement du tétraphénylméthane. Synthétisé pour la première fois par le groupe de Gomberg à l'Université du Michigan en 1930, il fallut attendre jusqu'au

début des années 70 pour la résolution de sa structure par diffraction des rayons-X.[1,2] Cette étude, réalisée par Schenk en 1972, montre clairement l'orthogonalité des deux systèmes aromatiques fluorène (Figure 5.1). En fait, le 9,9'-spirobifluorène doit être considéré comme constitué de deux systèmes aromatiques indépendants l'un de l'autre.

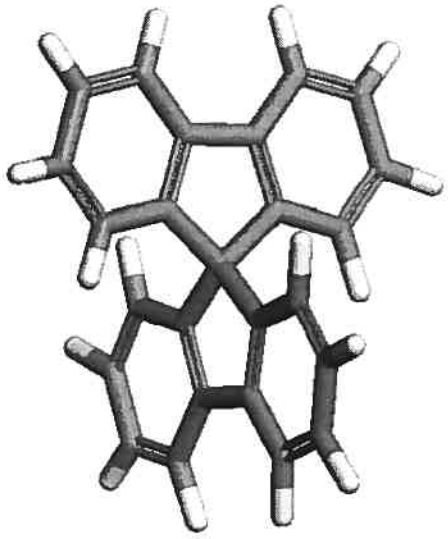

Figure 5.1 Structure du 9,9'-spirobifluorène obtenue par diffraction des rayons-X.[2]

La synthèse du 9,9'-spirobifluorène utilise encore essentiellement la voie initialement développée par Gomberg, soit une réaction d'addition du dérivé lithié du 2-iodobiphényl sur la fonction carbonyle de la 9-fluorènone suivie d'une alkylation interne de Friedel-Crafts catalysée en milieu acide (Figure 5.2).[1,3]

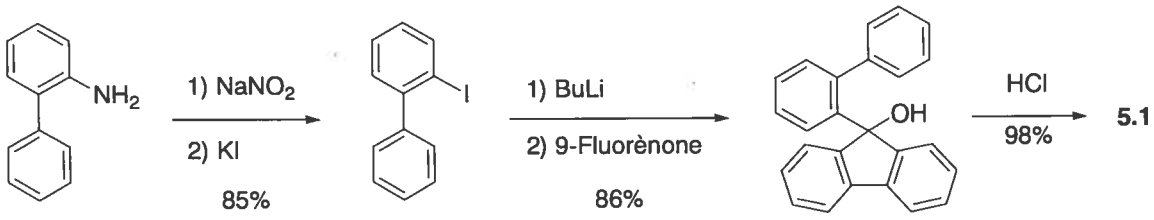

Figure 8.2 Synthèse du 9,9'-spirobifluorène (**5.1**).

Les dérivés du 9,9'spirobifluorène sont synthétisés en mettant à profit la grande régiosélectivité des réactions de substitution électrophile aromatique observées pour ce système. En effet, l'addition d'électrophiles sur le 9,9'-spirobifluorène **(5.1)** est uniquement observée aux positions 2 et 7. Cette régiosélectivité peut être rationalisée en

Attaque aux positions 2 et 7

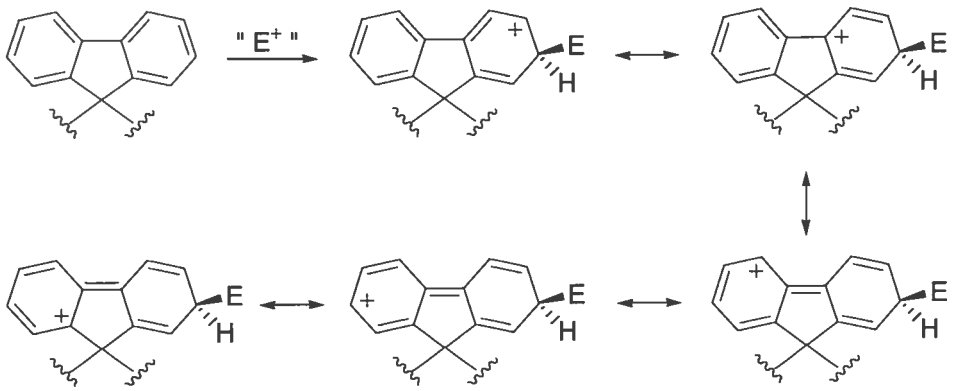

Attaque aux positions 3 et 6

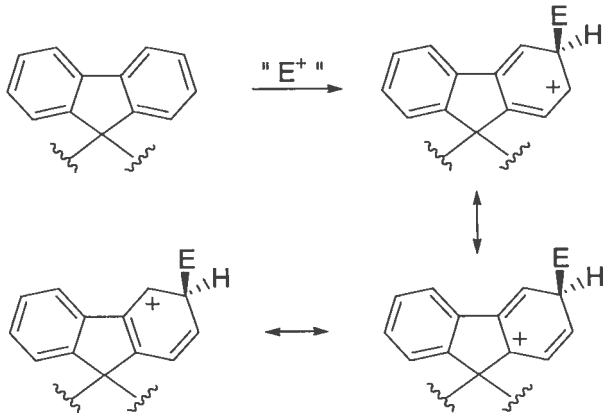

Figure 5.3 Stabilisation de des états de transition lors de réactions de substitution électrophile aromatique sur le 9,9'-spirobifluorène.

invoquant la plus grande stabilité du carbocation généré lors de l'addition de l'électrophiles à ces positions.[3] L'addition d'électrophile à la position 2 ou 7 profite d'une plus grande délocalisation de charge que lors d'une attaque aux positions 3 et 6 ainsi que le montre la Figure 5.3. Cette remarquable sélectivité permet d'obtenir par exemple les dérivés tétrabromé ou tétraiodé dans d'excellents rendements (Figure 5.4).[3]

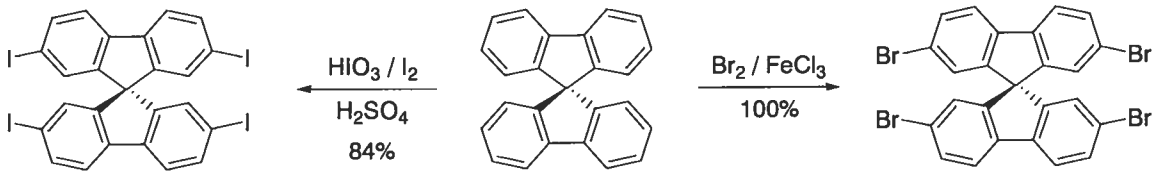

5.1

Figure 8.4 Halogénation du 9,9'-spirobifluorène (**5.1**).

5.3 Utilisation des dérivés du 9,9'-spirobifluorène en chimie supramoléculaire.

Du fait de sa conformation figée, le 9,9'-spirobifluorène constitue un « bloc de construction » intéressant pour la synthèse de systèmes de reconnaissance nécessitant une certaine rigidité. Ainsi, le groupe de Prelog a utilisé des dérivés de ce système à la fois comme espaceur rigide et élément d'asymétrie dans l'élaboration d'éther-couronnes chirales pour la reconnaissance sélective d'ester d'acides aminés (Figure 5.5).[4]

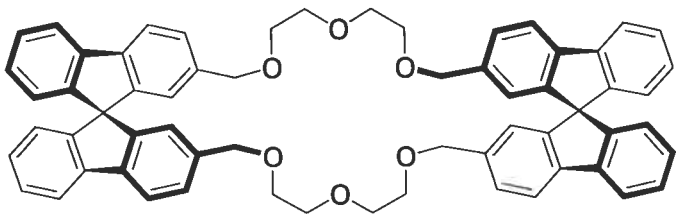

Figure 5.5 Incorporation de l'unité 9,9'-spirobifluorène dans un récepteur chiral pour acide aminé.

Plus récemment, le groupe de Diederich a également employé l'unité spirobifluorène dans l'élaboration du récepteur chiral **5.2**, utilisé pour la reconnaissance sélective d'acides dicarboxyliques chiraux (Figure 5.6).[5]

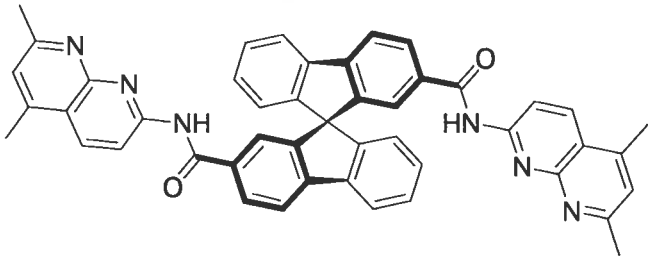

5.2

Figure 5.6 Récepteur chiral pour la reconnaissance sélective d'acides dicarboxyliques chiraux.

La littérature montre également quelques exemples d'utilisation de dérivés du 9,9'-spirobifluorène pour la formation de composés d'inclusion. Ainsi, le 9,9-spirobifluorène forme des complexes d'inclusion avec de nombreux hydrocarbures tel que l'a démontré Weber et ses collaborateurs au milieu des années 80.[6] Weber a également étudié la formation de complexes d'inclusion entre le diacide **5.3** et différents hôtes.[7] Par exemple, le diacide **5.3** forme un complexe de composition **5.3** • 2 DMF lorsque il est cristallisé dans ce solvant. Les molécules de DMF s'associent alors par ponts hydrogène aux groupements carboxyliques. Il est à noter cependant que ces complexes d'inclusion ne sont pas des structures poreuses mais plutôt des solides dans lesquels les molécules incluses sont trappées à l'intérieur de cages fermées.

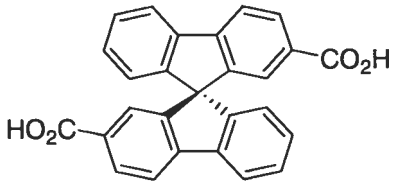

5.3

5.4 Utilisation de l'unité 9,9'-spirobifluorène dans la conception de tectons.

La structure du 9,9'-spirobifluorène présente un potentiel intéressant pour l'élaboration de tectons notamment en raison de sa structure rigide mais également du fait de la tendance à la formation de composés d'inclusion observée chez cette classe de composés. Un système substitué aux positions 3 et 6 est évidemment un choix attrayant notamment en raison de l'analogie avec certains tectons précédemment synthétisés appartenant aux dérivés du tétraphénylméthane. Ce choix se heurte cependant au fait qu'il n'existe aucun dérivés du 9,9'-spirobifluorene tétrasubstitués à ces positions. Une autre possibilité pour l'élaboration de matériaux tectoniques consisterait à utiliser des dérivés tétrasubstitués aux positions 2 et 7, composés beaucoup plus accessibles synthétiquement par des réactions de substitution électrophile.

Des études ont donc été entreprises afin d'évaluer le potentiel des dérivés du 9,9'-spirobifluorène pour l'élaboration de matériaux poreux. Deux principaux objectifs ont guidé cette étude :

- Synthétiser de nouveaux tectons utilisant la tétrasubstitution des positions 2 et 7, facilement accessibles d'un point de vue synthétique.

- Développer une approche permettant l'accès à la fonctionalisation des positions 3 et 6 et utiliser ces dérivés pour la synthèse de nouveaux tectons.

Les résultats de ces études apparaissent dans les pages qui suivent sous forme d'article.

5.5 Références

1) Clarkson, R. G.; Gomberg, M. *J. Am. Chem. Soc.* **1930**, *52*, 2881.
2) Schenk, H. *Acta Crystallogr., Sect. B.* **1972**, *28*, 625.

3) Wu, R.; Schumm, J. S.; Pearson, D. L.; Tour, J. M. *J. Org. Chem.* **1996**, *61*, 6906.

4) Dobler, M.; Dumic, M.; Egli, M.; Prelog, V. *Angew. Chem., Int. Ed. Engl.* **1985**, *24*, 792. Prelog, V.; Mutak, S. *Helv. Chim. Acta* **1983**, *66*, 2274. Prelog, V. *Pure Appl. Chem.* **1978**, *50*, 893. Prelog, V.; Bedekovic, D. *Helv. Chim. Acta* **1979**, *62*, 2285. Prelog, V.; Haas, G. *Helv. Chim. Acta* **1969**, *52*, 1202.

5) Cuntze, J.; Owens, L.; Alcázar, V.; Seiler, P.; Diederich, F. *Helv. Chim. Acta* **1995**, *78*, 367.

6) Weber, E.; Ahrendt, J.; Czugler, M.; Csöregh, I. *Angew. Chem., Int. Ed. Engl.* **1986**, *25*, 746.

7) Czugler, M.; Stezowski, J. J.; Weber, E. *J. Chem. Soc., Chem. Commun.* **1983**, 154.

Article 4

Fournier, J.-H.; Maris, T.; Wuest, J. D. "Molecular Tectonics. Construction of Porous Hydrogen-Bonded Networks from 9,9'-spirobifluorenes" *Journal of Organic Chemistry*, accepté pour publication, **2003**.

In press in *J. Org. Chem.*
Version 1 of September 10, 2003

Molecular Tectonics. Porous Hydrogen-Bonded Networks Built from Derivatives of 9,9'-Spirobifluorene

Jean-Hugues Fournier,[1] Thierry Maris, and James D. Wuest*

Département de Chimie, Université de Montréal

Montréal, Québec H3C 3J7 Canada

*Author to whom correspondence may be addressed:

[redacted]

Abstract

Molecules with multiple sites that induce strong directional association tend to form open networks with significant volumes available for the inclusion of guests. Such molecules can be conveniently synthesized by grafting diverse sticky sites onto geometrically suitable cores. The characteristic inability of 9,9'-spirobifluorene to form close-packed crystals suggests that it should serve as a particularly effective core for the elaboration of molecules designed to form highly porous networks. To test this hypothesis, various new tetrasubstituted 9,9'-spirobifluorenes with hydrogen-bonding sites at the 3,3',6,6'-positions or 2,2',7,7'-positions were synthesized by multi-step routes. Four of these compounds were crystallized, and their structures were determined by X-ray crystallography. In all cases, the compounds form extensively hydrogen-bonded networks with high porosity. In particular, 43% of the volume of crystals of 3,3',6,6'-tetrahydroxy-9,9'-spirobifluorene (**28**) is available for the inclusion of guests, whereas the porosity is only 28% in crystals of tetrakis(4-hydroxyphenyl)methane, a close model that lacks the spirobifluorene core. Similarly, the porosities found in crystals of 2,2',7,7'-tetra(acetamido)-9,9'-spirobifluorene (**33**) and 2,2',7,7'-tetrasubstituted tetrakis(diaminotriazine) **39** are 33% and 60%, respectively. Moreover, the porosity of crystals of 2,2',7,7'-tetrasubstituted tetrakis(triaminotriazine) **40** is 75%, the highest value yet observed in crystals built from small molecules. These observations demonstrate that a particularly effective strategy for engineering molecules able to form highly porous networks is to graft multiple sticky sites onto spirobifluorenes or other cores intrinsically resistant to close packing.

Introduction

Learning how to make molecular materials by design is one of the most challenging problems in modern science. Meeting this challenge requires shrewd selection of individual molecular components and artful control of how neighboring molecules are arranged and interact, so that the resulting material has the desired composition, architecture, and properties. Unfortunately, no universal strategy has yet emerged for reaching this ambitious goal.

In the particular field of solid-state chemistry, however, rapid progress in crystal engineering is providing new ways to make predictably ordered molecular materials.[2] An effective strategy in crystal engineering, which has been called molecular tectonics,[3-4] exploits compounds with strong predispositions to associate according to various well-established motifs,[5-12] which have been named supramolecular synthons.[13] The individual associating molecules, called tectons from the Greek word for builder, can be considered to have multiple peripheral sticky sites that direct molecular association, linked to a core that holds the sticky sites in specific orientations. The core is not merely an anchor point for attaching the sticky sites; it is also an active component that can be chosen judiciously to introduce desirable molecular properties such as luminescence, chirality, catalytic activity, and many others. Because the sticky sites and cores can both be varied widely, molecular tectonics is a potentially powerful tool for creating ordered materials by design.

Crystallization is a complex process of molecular recognition governed by the combined thermodynamic effects of strong directional forces and weak diffuse interactions, as well as by kinetic factors that remain poorly understood.[14] The crystallization of tectons differs from that of normal molecules because specific directional effects are much more important. Like normal molecules, tectons will attempt to form closely packed structures stabilized by weak diffuse interactions; at the same time, however, they must attempt to obey the specific dictates of a small number of strong directional forces. In tectonic association, these forces typically predominate, and close packing is thereby disfavored. Although tectons can be specifically engineered to form close-packed structures in which directional interactions are optimized simultaneously,[7] tectonic association normally leads to the formation of open networks with significant space for the inclusion of guests.

The tendency of tectonic association to favor inclusion is a striking phenomenon of substantial fundamental interest and potential utility. Inclusion typically shows selectivity, and in many cases tectonic networks are robust enough to allow guests to be exchanged in single crystals without loss of crystallinity. Such crystals therefore behave as microporous molecular solids analogous to zeolites, and similar applications in separation, sensing, catalysis, and other areas are being explored. As a result, the control of porosity in ordered molecular materials is a subject of substantial importance. In this paper, we describe an effective strategy for enhancing porosity, and we show how it can be used to make the most porous crystal yet obtained from simple molecular precursors.

Results and Discussion

Factors that Help Determine Porosity in Tectonic Networks. Derivatives of tetraphenylmethane (**1**) and tetraphenylsilane (**2**) have been widely used in molecular tectonics

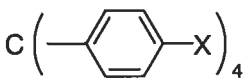

1 (X = H)
3 (X = $B(OH)_2$)

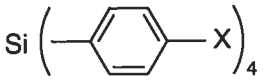

2 (X = H)
4 (X = $B(OH)_2$)

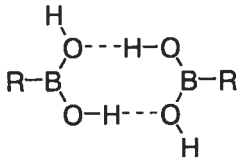

5

because their cores can hold sticky sites in a tetrahedral orientation, allowing diamondoid networks or related three-dimensional, four-connected structures to be created by self-assembly.[15] For example, crystallization of tetraboronic acids **3** and **4** from $CH_3COOC_2H_5$ induces the formation of isostructural diamondoid networks held together by predictable hydrogen bonding, defined by supramolecular synthon **5**.[5] Each diamondoid network is open enough to permit interpenetration by four independent diamondoid networks.[16-17]

Despite this interpenetration, approximately 60% and 64% of the volume of crystals of tectons **3** and **4**, respectively, is available for including guests.[18-19] These values far

exceed those found in crystals of normal molecular analogues such as tetraphenylmethane, tetraphenylsilane, and simple substituted derivatives, which do not typically form inclusion compounds.[20-22] By forming open networks with predetermined architectures, compounds **3** and **4** show special behavior that supports the emerging principles of molecular tectonics and reveals how profoundly packing in crystals can be changed and controlled by the judicious addition of a small number of sites that take part in strong directional interactions.

To place recent achievements of the field in proper perspective, Chart 1 provides a comparison of the porosity of representative inclusion compounds built from neutral molecules,[10,12,23-33] as measured by the percentage of volume available for guests.[18] Many

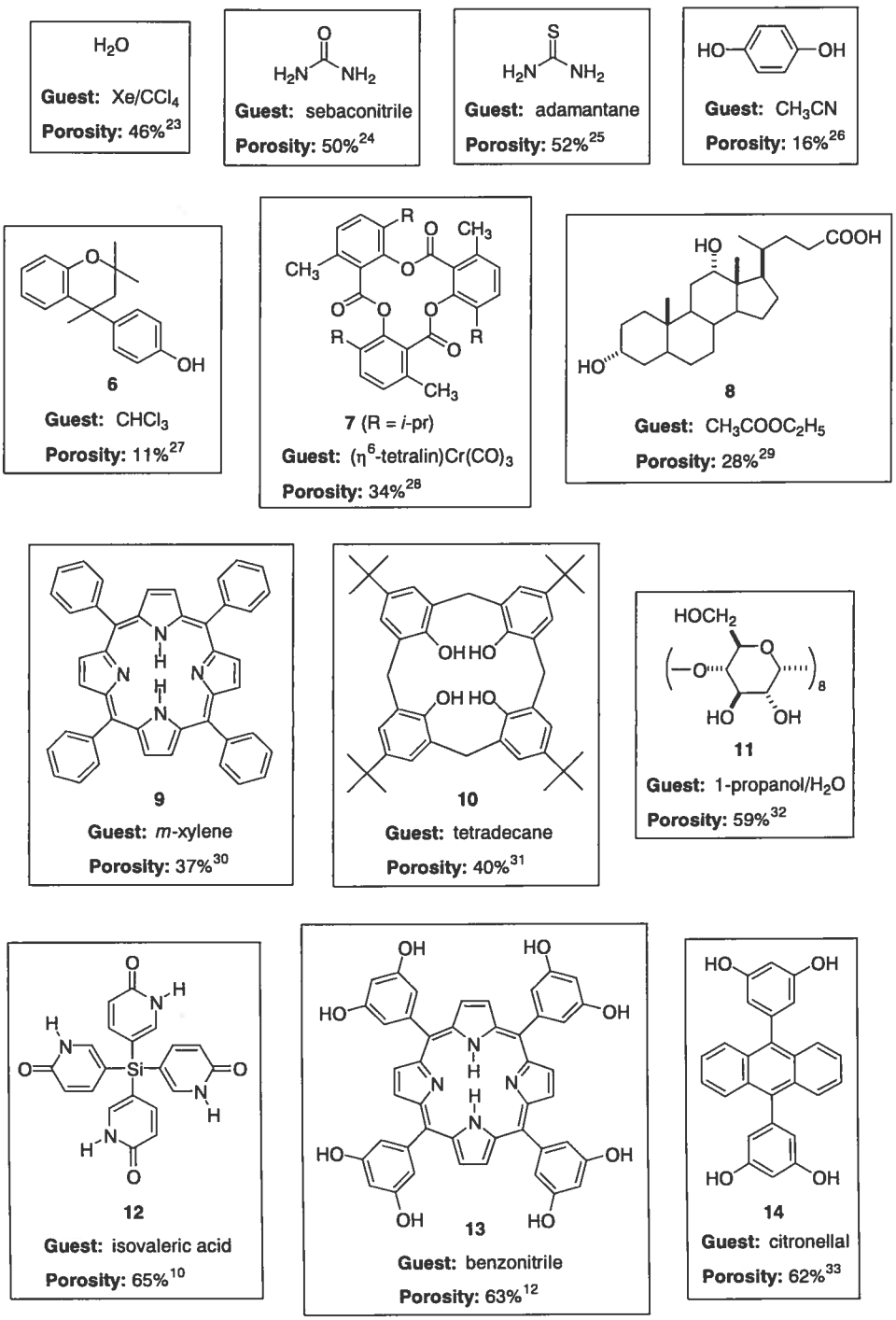

Chart 1. Selected small neutral molecules that crystallize to form families of inclusion compounds. The specific guests shown are those for which the porosity, as measured by the percentage of volume accessible to guests,[18] is near the upper limit observed in each family of inclusion compounds.

additional examples, all drawn primarily from the November 2002 version of the Cambridge Structural Database (Version 5.24), appear in the Supporting Information. Chart 1 comprises classic families of inclusion compounds, including those formed by water, urea, thiourea, hydroquinone, Dianin's compound (**6**), tri-*ortho*-thymotide (**7**), deoxycholic acid (**8**), 5,10,15,20-tetraphenylporphyrin (**9**), calix[4]arene **10**, and γ-cyclodextrin (**11**). In addition, Chart 1 includes newer compounds **12-14**, which have been selected from the recent literature as particularly well-studied examples of small neutral molecules specifically designed to form open hydrogen-bonded networks and to create new families of inclusion compounds. For each molecule in Chart 1, the particular inclusion compound illustrated is one for which the porosity is among the highest observed, so the data in Chart 1 provide an estimate of the upper limits of porosity attained in previously known families of inclusion compounds.

Chart 1 and the further examples in the Supporting Information are not intended to provide a systematic analysis of porosity in molecular solids; nevertheless, the data help set useful guidelines for further research. For example, the porosity of structures assembled from tectons **3**, **4**, **12**, **13**, and **14** (60%, 64%, 65%, 63%, and 62%, respectively) greatly exceeds that of structures formed by models **1**,[21] **2**,[22] **15**,[34] **9**,[30] and **16**,[35] which have similar geometries but lack hydrogen-bonding sites. In all these models the porosities are 0%, except in the case of tetraphenylporphyrin **9** (37%). This comparison confirms that grafting sticky sites to core structures can have a profound effect on packing across a wide range of molecular topologies. In addition, Chart 1 suggests that the highest levels of porosity in hydrogen-bonded networks cannot be

attained with small molecules, such as water and urea, presumably because larger molecules tend to have more complex topologies that pack less efficiently in crystals. This accounts for the high percentages of volume often available in protein crystals for the inclusion of water and other guests.[36] Despite the relatively small size and simple symmetric shapes of tectons **3**, **4**, **12**, **13**, and **14**, the porosity of their networks is impressive, even in comparison with that of the most highly porous protein crystals. This is a notable achievement of crystal engineering, and it provides a strong impetus to learn how even higher porosity can be attained.

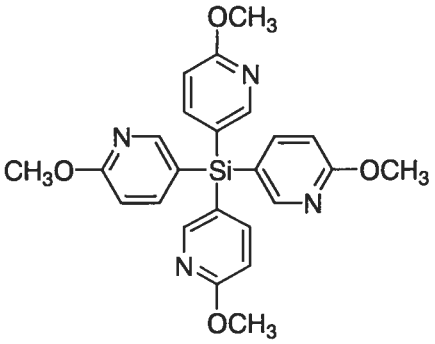

15

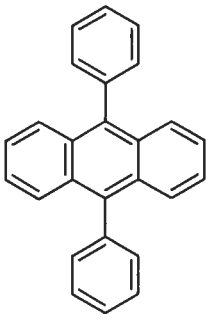

16

A potential strategy is suggested by the small but significant increase in porosity caused by replacing the central carbon-carbon bonds in tetraboronic acid **3** with longer silicon-carbon bonds in analogue **4**, which places the sticky sites farther from the core. In principle, lengthening the connections between the cores and sticky sites of tectons offers a general strategy for increasing the openness of the resulting networks. Tetraboronic acids **3** and **4** exemplify a case in which this strategy works; in other systems, however, such changes often simultaneously lead to higher degrees of interpenetration, with no net increase in porosity.

An alternative strategy is based on the observation that inclusion compounds of porphyrinic tecton **13** can have exceptional porosities (up to 63%),[12] among the highest values we have been able to find for crystals derived from small neutral molecules. In this case, the high porosity can be attributed in part to the well-known inability of the core itself, 5,10,15,20- tetraphenylporphyrin (**9**), to pack efficiently without including significant numbers of guests.[30,37] Grafting sites for hydrogen bonding onto core **9** then causes further deviations from close packing. This suggests that the search for tectons able to form crystals with significantly higher porosity should focus on targets with core structures intrinsically unable to pack efficiently.

Tectons Derived from Spirobifluorenes. Particularly attractive candidates for new cores are 9,9'-spirobifluorene (**17**) and the analogous silane **18**. Unlike their close relatives

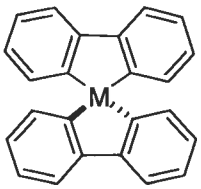

17 (M = C)
18 (M = Si)

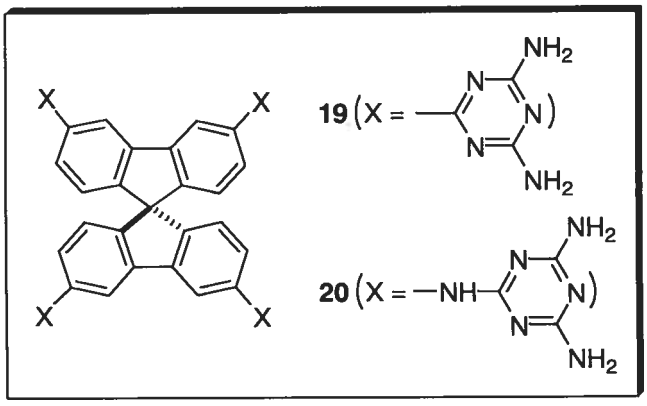

tetraphenylmethane and tetraphenylsilane, which form close-packed crystals, spirobifluorenes **17** and **18** are known to form inclusion compounds when crystallized under diverse conditions.[38-39] In particular, crystallization of silane **18** from

tetrahydrofuran yields a structure in which 43% of the volume is available for the inclusion of guests.[39] The markedly different behaviors of tetraphenylmethane and 9,9'-spirobifluorene (**17**), as well as the dissimilarity of the analogous pair of silanes **2** and **18**, can be attributed to the enhanced rigidity of the spirocyclic cores. This prevents rotation of the aryl groups around bonds joining them to the central atom of the core and thereby prohibits conformational changes needed to attain close packing.

For these reasons, replacing tectons derived from tetraphenylmethane and tetraphenylsilane with analogues derived from spirobifluorenes **17** and **18** can be expected to have major effects on packing, possibly leading to new architectures with enhanced porosity and lower levels of interpenetration. Although the 9,9'-spirobifluorene core has been used to create molecular receptors,[40] liquid crystals,[41] polymers,[42] and optical and electronic materials,[43-44] no systematic effort to exploit it in crystal engineering has yet been reported.

Synthesis of Tectons Derived from 3,3',6,6'-Tetrasubstituted 9,9'-Spirobifluorenes. Derivatives of tetraphenylmethane previously used in crystal engineering have normally been *para*-substituted, so the synthesis of analogous tectons with sticky sites attached to the 3,3',6,6'-positions of 9,9'-spirobifluorene was undertaken first. Our principal targets were tectons **19** and **20**, which incorporate four symmetrically located aminotriazine groups. These groups were selected because they can participate in multiple hydrogen bonds according to established motifs, are easily introduced, and have already demonstrated their usefulness in supramolecular chemistry.[6,8] Moreover, the structures of

the two analogous tectons derived from tetraphenylmethane are both known,[8,45] allowing potentially illuminating comparisons of architecture and porosity.

Electrophilic substitution of 9,9'-spirobifluorene occurs primarily at the 2,2',7,7'-positions,[44] so the synthesis of 3,3',6,6'-tetrasubstituted tectons **19** and **20** required the indirect approach summarized in Schemes 1 and 2. Regioselective monobromination of 3,3'-dimethoxybiphenyl

Scheme 1

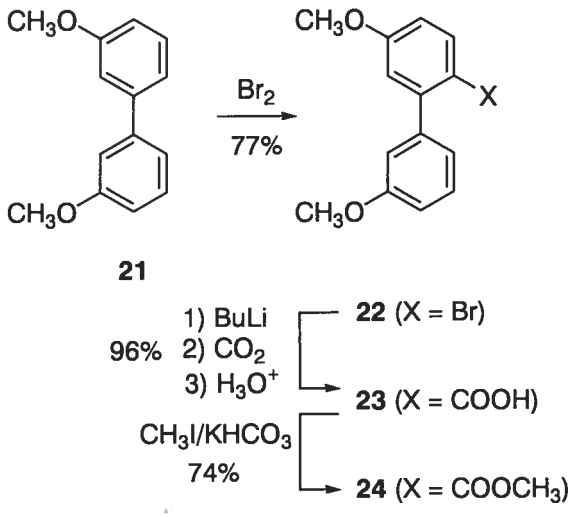

(**21**) gave bromide **22**[46] in 77% yield (Scheme 1). Subsequent lithiation (BuLi), addition of CO_2, and acidification then provided a 96% yield of acid **23**.[46-47] Finally, esterification ($CH_3I/KHCO_3$) gave intermediate **24** in 74% yield.

Dilithiation of 2,2'-dibromo-5,5'-dimethoxybiphenyl (**25**)[48-49] and subsequent addition to ester **24** gave a 50% yield of carbinol **26**, which was transformed under acidic conditions

into spirobifluorene **27** in 82% yield (Scheme 2). Deprotection (BBr_3) gave a 91% yield of tetraphenol **28**, which was subsequently converted into triflate **29** in 70% yield. Palladium-catalyzed cyanation with $Zn(CN)_2$ in DMF[50] then gave a 67% yield of tetranitrile **30**, which was converted into target **19** in 72% yield by treatment with dicyandiamide and a catalytic amount of KOH in refluxing 2-methoxyethanol.[51]

Scheme 2

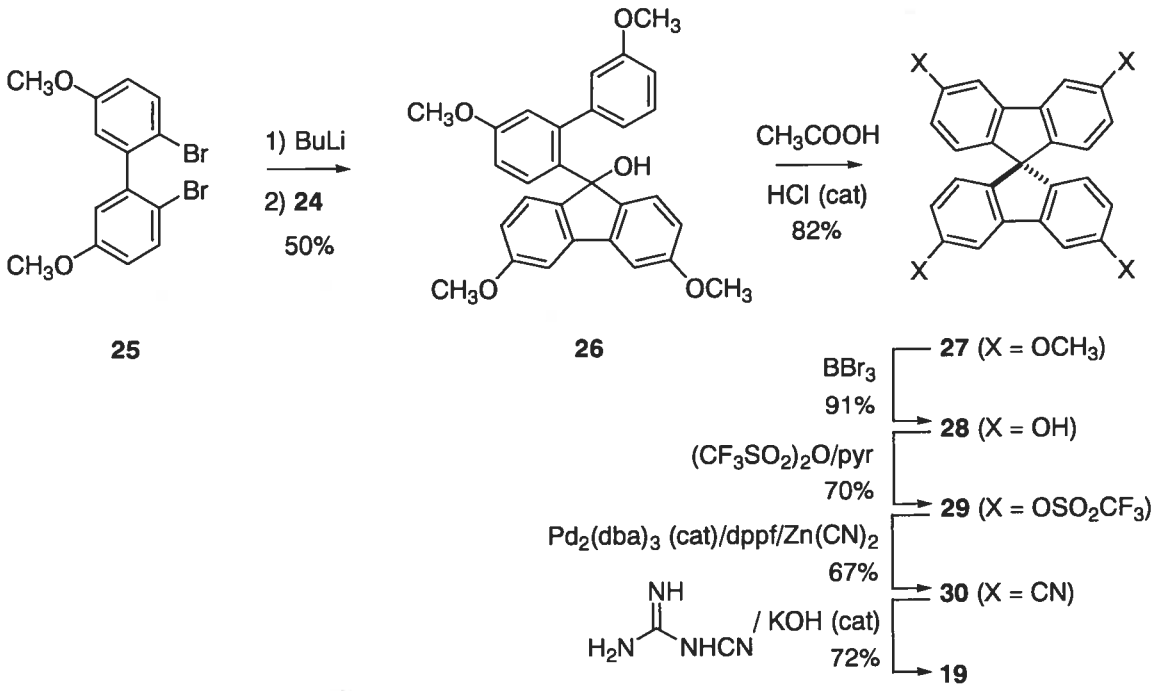

The synthesis of tecton **20** required a different approach, outlined in Scheme 3. Regioselective nitration of 9,9'-spirobifluorene (**17**)[44] at the 2,2',7,7'-positions gave tetranitro derivative **31** in 75% yield. Reduction of the nitro groups gave tetraamine **32** (98%), and subsequent acetylation gave tetraamide **33** (98%), which was again nitrated to give compound **34** in 97% yield. After hydrolysis of the amide groups to give intermediate **35** (96%), reductive deamination[52] gave a 31% yield of tetranitro compound **36**, which was reduced under standard conditions to provide tetraamine **37** in 93% yield.

This compound was then converted into target **20** in 62% overall yield by a two-step procedure involving treatment with cyanuric chloride at 0 °C, followed by addition of NH_3.

Scheme 3

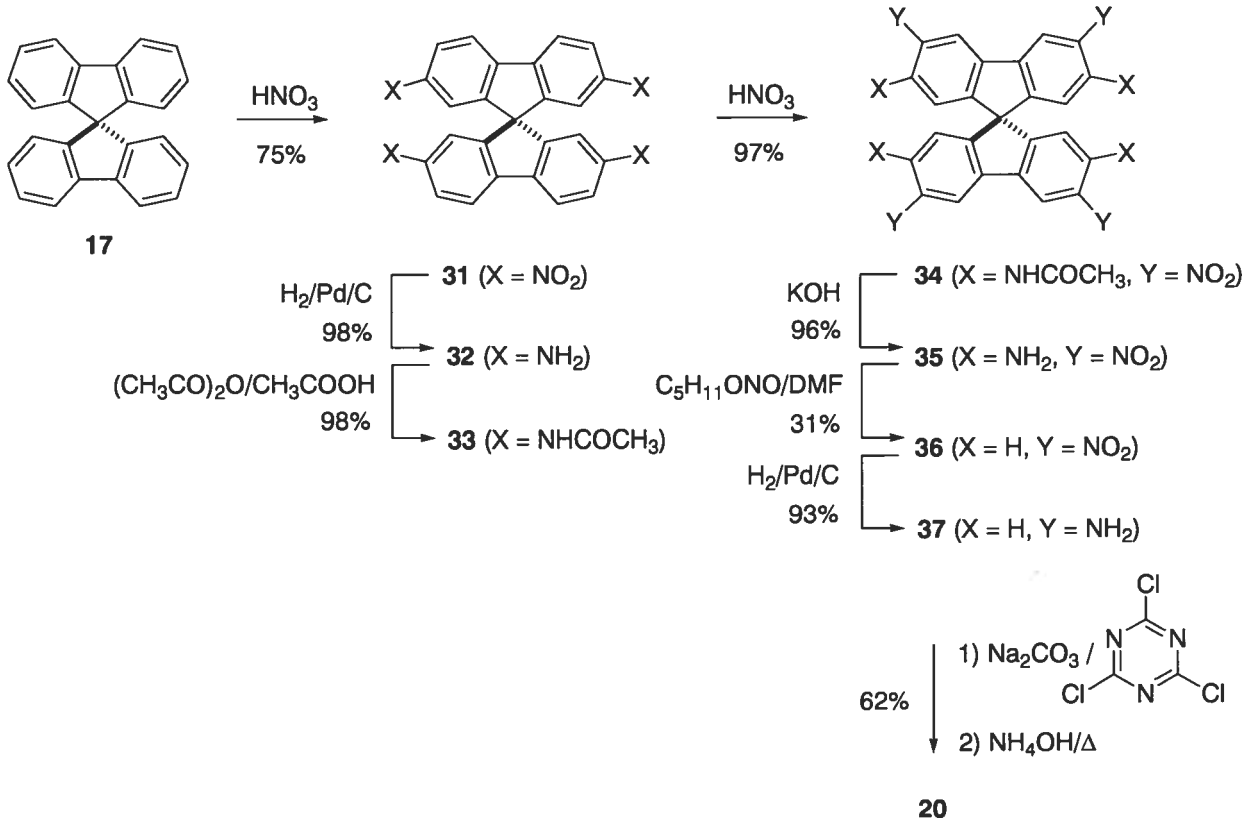

Structures of Tectons with 3,3',6,6'-Tetrasubstituted 9,9'-Spirobifluorene Cores. In general, the intermediate spirobifluorenes **27-37** have molecular structures that favor self-association and crystallization with inclusion of guests, making all of them worthy candidates for X-ray crystallographic studies. Unfortunately, the compounds of principal interest, tectons **19** and **20**, did not yield crystals suitable for X-ray diffraction despite

multiple attempts to grow them. However, we were able to crystallize 3,3',6,6'-tetrasubstituted tetraphenol **28** and solve its structure.

Crystals were obtained by diffusion of hexane into solutions of tecton **28** in $CH_3COOC_2H_5$. The crystals belong to the triclinic space group P-1 and correspond to an inclusion compound with the composition **28** • 2 $CH_3COOC_2H_5$. Views of the structure are shown in Figures 1-3. Each molecule of tetraphenol **28** forms hydrogen bonds with three neighboring tectons and with two molecules of $CH_3COOC_2H_5$ as shown in Figure 1. The resulting network is held together by four hydrogen bonds per tecton, and two additional hydrogen bonds per tecton are used to bind the guests. The network is primarily one-dimensional and can be considered to define parallel ladders that are stacked as shown in Figure 2. No hydrogen bonds are formed between individual ladders. The included molecules of $CH_3COOC_2H_5$ occupy parallel channels that have a cross section of approximately 3.6 x 3.2 $Å^2$ and lie along the *b* axis (Figure 3).[53]

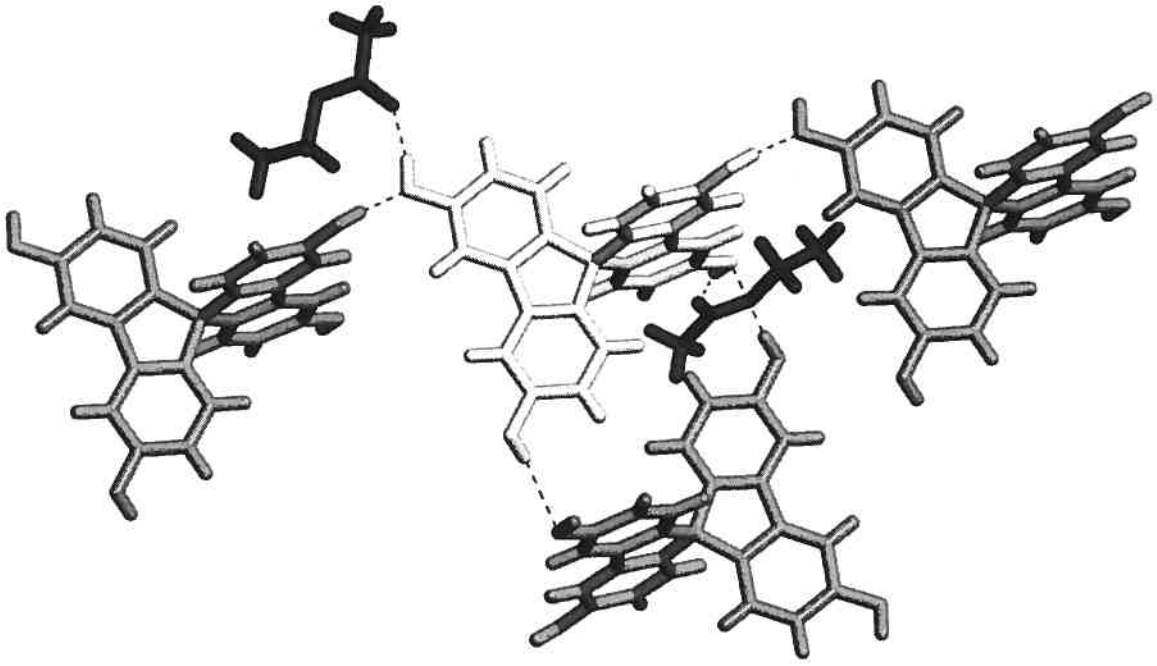

Figure 1. View of the structure of 3,3',6,6'-tetrahydroxy-9,9'-spirobifluorene (**28**) and included $CH_3COOC_2H_5$, showing a central tecton (white) surrounded by its hydrogen-bonded neighbors, which include three other tectons (gray) and two molecules of $CH_3COOC_2H_5$ (black). Hydrogen bonds appear as broken lines. The central tecton (white) uses two of its hydroxyl groups simultaneously as a donor and acceptor of hydrogen bonds to interact with two neighboring tectons and two molecules of $CH_3COOC_2H_5$, and the remaining two hydroxyl groups of the central tecton serve as simple hydrogen-bond donors.

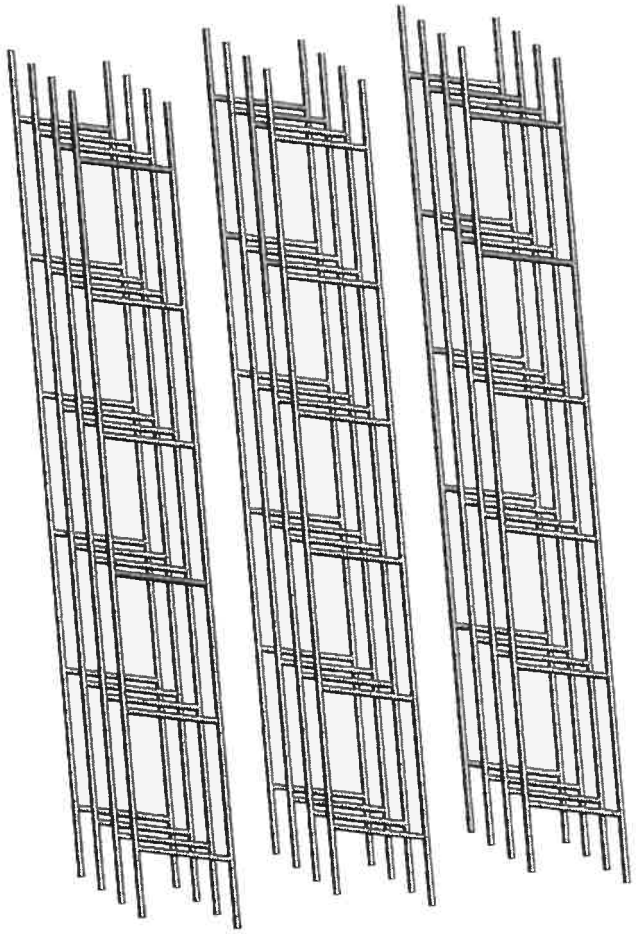

Figure 2. Representation of the network generated by the self-association of 3,3',6,6'-tetrahydroxy-9,9'-spirobifluorene (**28**). In this drawing, the central spirocyclic carbon atoms of the tectons are considered to lie at the intersections of the solid lines, and the lines themselves connect the center of each tecton with the centers of its three hydrogen-bonded neighbors.

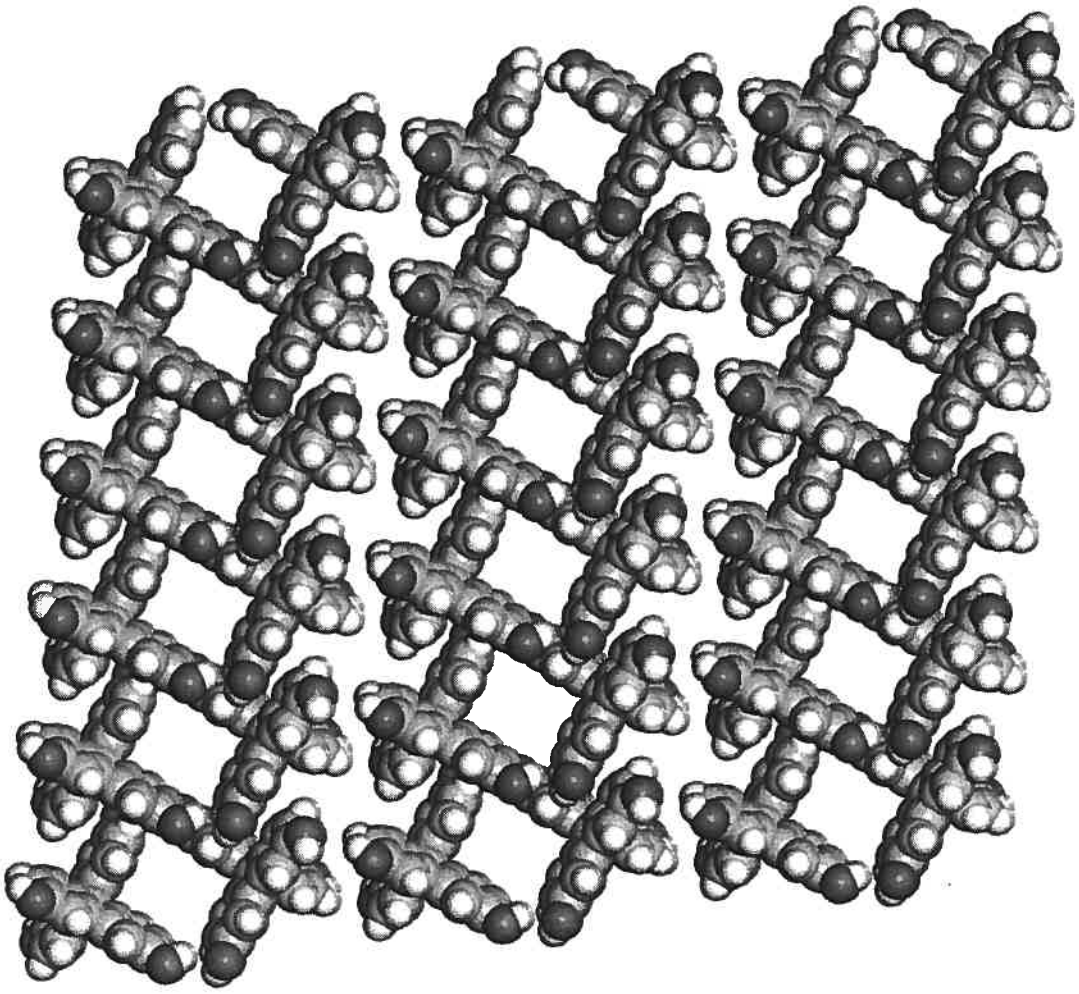

Figure 3. View along the *b* axis of the network constructed from 3,3',6,6'-tetrahydroxy-9,9'-spirobifluorene (**28**) showing a 6 x 2 x 3 array of unit cells. Guests are omitted, and atoms are shown as spheres of van der Waals radii in order to reveal the cross sections of the channels. Atoms of hydrogen appear in white, atoms of carbon in light gray, and atoms of oxygen in dark gray.

Approximately 43% of the volume of crystals of tetrahydroxyspirobifluorene **28** is available for the inclusion of guests.[18] Although this porosity is modest by current standards, it is significantly higher than that of crystals of a very close relative, tetrakis(4-hydroxyphenyl)methane (**38**), when grown under identical conditions (28%).[7] Detailed comparison of the two structures clearly reveals the major effects that replacing a tetraphenylmethane core by a spirobifluorene core can have in molecular tectonics. In particular, spirobifluorene **28** forms an inclusion compound with stoichiometry **28** • 2 $CH_3COOC_2H_5$, whereas the analogous tetraphenylmethane **38** yields crystals with composition **38** • 1 $CH_3COOC_2H_5$. Moreover, spirobifluorene **28** has fewer hydrogen-bonded neighboring tectons (3) than does the closely related tetraphenylmethane **38** (4). Together, these observations confirm that the characteristic rigidity and topology of the spirobifluorene core can be used to good effect in molecular tectonics to produce crystals 1) with greater porosity than that found in crystals built from analogous tetraphenylmethanes and 2) with structures in which each tecton has a smaller number of hydrogen-bonded neighbors. As a result, we were encouraged to continue exploring the consequences of attaching sites for hydrogen bonding to the spirobifluorene core.

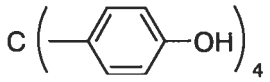

38

Synthesis of Tectons Derived from 2,2',7,7'-Tetrasubstituted 9,9'-Spirobifluorenes. Because 2,2',7,7'-tetrasubstituted derivatives of 9,9'-spirobifluorene are readily accessible by direct electrophilic substitution of 9,9'-spirobifluorene, we decided to undertake the synthesis of tectons **39** and **40** according to the route summarized in Scheme 4. The

reaction of CuCN[54] with the known tetrabromospirobifluorene **41**[44] afforded tetranitrile **42** in 80% yield. Conversion to tecton **39** was accomplished in 84% yield by treatment with dicyandiamide and a catalytic amount of KOH.[51] Tecton **40** was made from tetraamine **32** (Scheme 3) in 72% overall yield by reaction with cyanuric chloride followed by aminolysis. Unlike 3,3',6,6'-tetrasubstituted tectons **19** and **20**, 2,2',7,7'-tetrasubstituted isomers **39** and **40** both gave crystals suitable for X-ray analysis, as did 2,2',7,7'-tetrasubstituted tetraacetamide **33** (Scheme 3).

Scheme 4

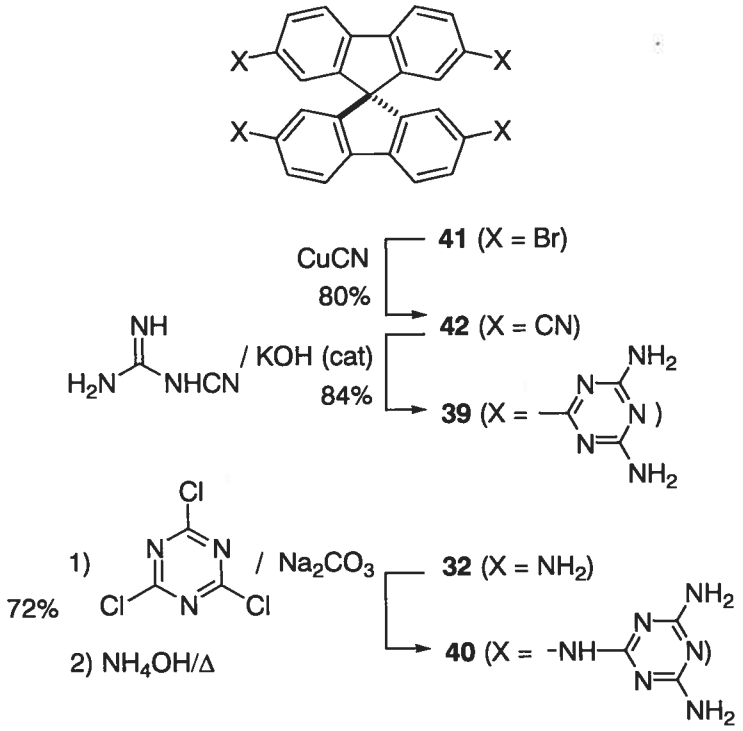

Structures of Tectons with 2,2',7,7'-Tetrasubstituted 9,9'-Spirobifluorene Cores. Crystals of tetraamide **33** were grown from acetone/DMF and were found to belong to the monoclinic space group C2/c and to have the composition **33** • 2 acetone. Self-association produces the extensively hydrogen-bonded network shown in Figure 4. The included

acetone is ordered but does not form hydrogen bonds with the network. Each tecton participates in a total of eight hydrogen bonds with six neighboring tectons, of which only three are shown in Figure 4. The resulting network defines parallel channels that have no significant connections, and the included molecules of acetone lie in these channels. Approximately 33% of the volume is available for the inclusion of guests,[18] confirming again the suitability of the spirobifluorene core for engineering porous crystals.

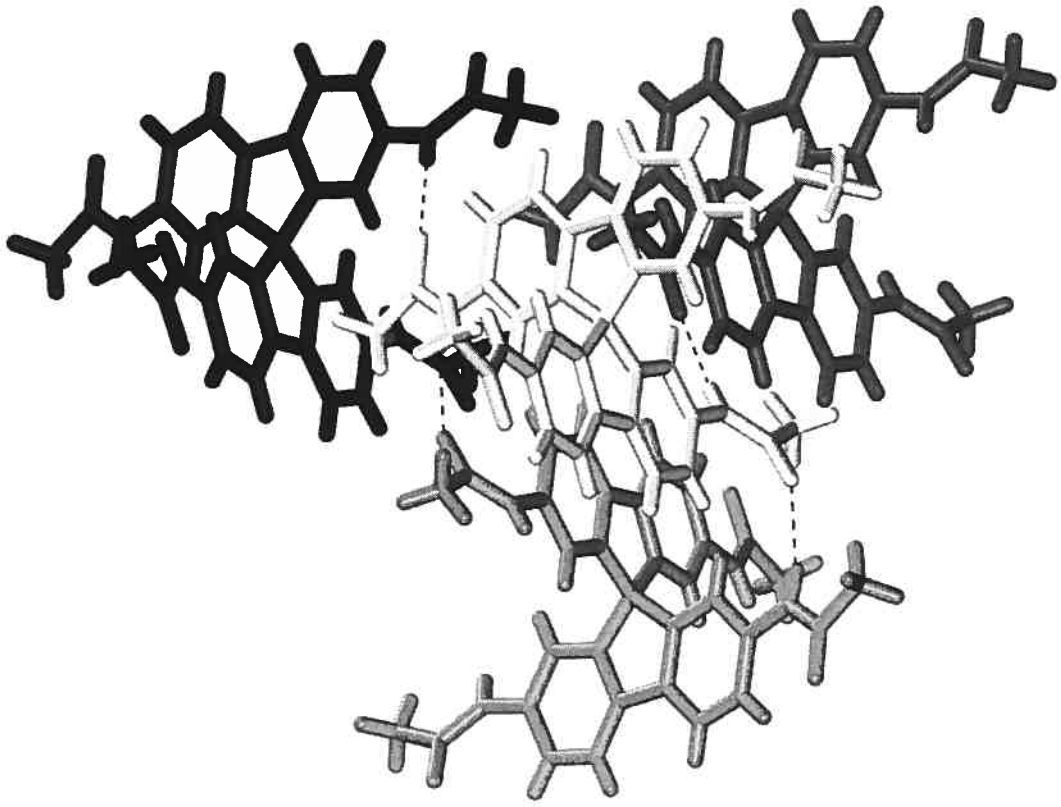

Figure 4. Representation of the structure of crystals of tetraacetamide **33** grown from acetone/DMF, showing a tecton (white) surrounded by three of a total of six hydrogen-bonded neighboring tectons. The other three neighbors are equivalent by symmetry and are omitted for clarity, as are included molecules of acetone. Hydrogen bonds appear as broken lines. Each acetamido group serves simultaneously as a donor and acceptor of hydrogen bonds. Two neighbors (one shown in light gray, with a second equivalent by symmetry and omitted) each accept one hydrogen bond and donate another, two other neighbors (dark gray) each accept a single hydrogen bond, and the final two neighbors (black) each donate a single hydrogen bond.

Crystallization of the 2,2',7,7'-tetrasubstituted tetrakis(diaminotriazine) **39** from DMSO/dioxane gave an inclusion compound of approximate composition **39** • 4 DMSO • 7 dioxane • x H_2O,[55] and the structure was determined by X-ray diffraction. Views of the structure are shown in Figures 5-6. As expected, tecton **39** self-associates by hydrogen bonding of the diaminotriazine groups, thereby forming an open three-dimensional network. The resulting network has significant space for both interpenetration and inclusion of guest molecules. Each tecton participates in a total of sixteen hydrogen bonds with six neighbors, creating the assembly shown in Figure 5. As previously observed in other networks constructed from diaminotriazines,[6] hydrogen bonding occurs according to motifs **43-45**.

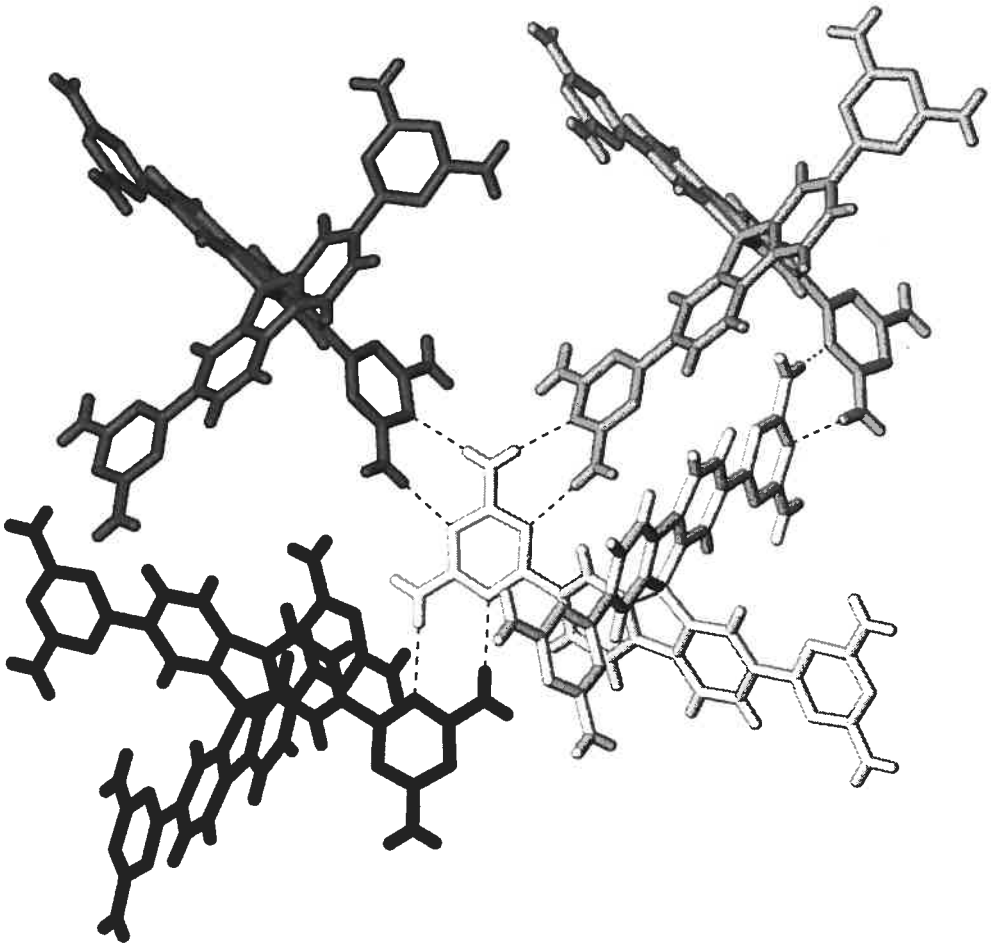

Figure 5. Representation of the structure of crystals of tetrakis(diaminotriazine) **39** grown from DMSO/dioxane, showing a tecton (white) surrounded by three of a total of six hydrogen-bonded neighboring tectons. The other three neighbors are equivalent by symmetry and are omitted for clarity, as are all guests. Hydrogen bonds appear as broken lines. Two of the six neighbors (one shown in dark gray, with a second equivalent by symmetry and omitted) each form two hydrogen bonds with the central tecton (white), creating motifs of type **43**. Two other neighbors (light gray) each form four hydrogen bonds with the central tecton, creating distorted motifs of type **44**, and the remaining two neighbors (black) each form two hydrogen bonds with the central tecton according to motif **45.**

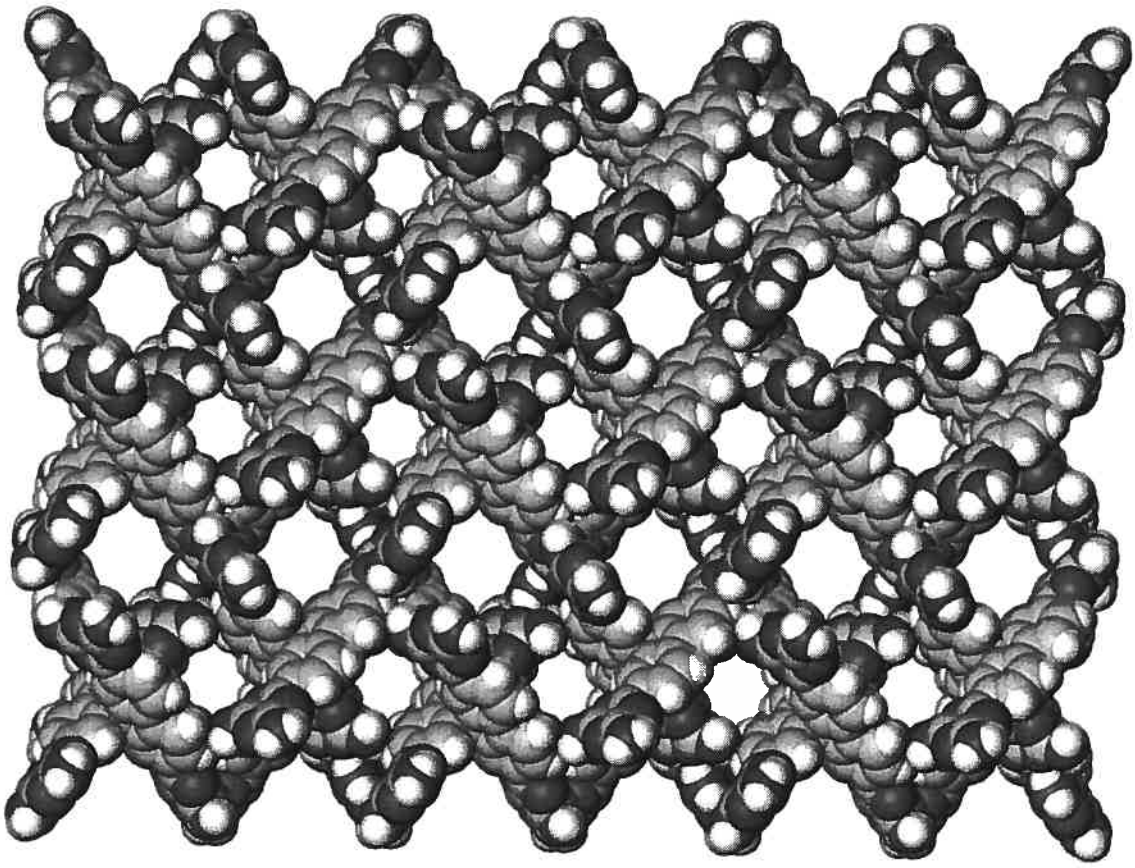

Figure 6. View along the *a* axis of the network constructed from tecton **39** showing a 2 x 3 x 3 array of unit cells. Guests are omitted, and atoms are shown as spheres of van der Waals radii in order to reveal the cross sections of the channels. Atoms of hydrogen appear in white, atoms of carbon in light gray, and atoms of nitrogen in dark gray.

Motif **43** involves the more accessible N-3/N-3' nitrogen atoms and is therefore expected to be stronger than the alternative N-1/N-3' and N-1/N-1' motifs **44** and **45**. In the network built from tecton **39**, two of the six neighbors each form two hydrogen bonds with the central tecton according to motif **43**. In this case, the spirocyclic centers of the central tecton and each neighbor are separated by 15.4 Å. Together, the tectons that interact in this way define square grids that are stacked in parallel along the *c* axis. Two other neighbors each form four hydrogen bonds with the central tecton, creating distorted motifs of type **44**. In this case, the intertectonic distances are 11.6 Å. The remaining two neighbors are separated from the central tecton by 15.3 Å, and each forms two hydrogen bonds with the central tecton according to motif **45**. Together, the central tecton and the four neighbors that interact according to motifs **44** and **45** define a diamondoid network with two-fold interpenetration. The complex interpenetration of diamondoid and square planar networks may arise because the intertectonic separation is too small to permit three-fold diamondoid interpenetration, yet too large to prevent the incorporation of another type of network.

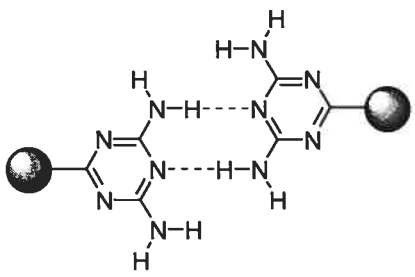

43

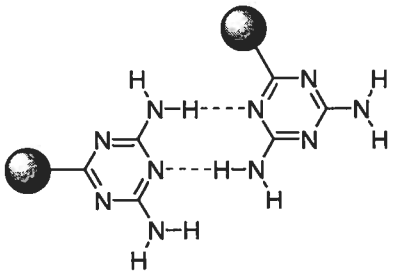

44

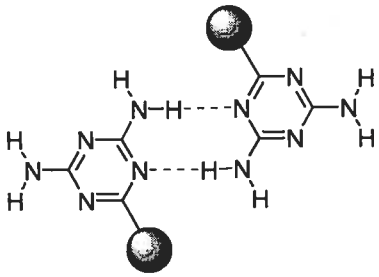

45

Despite the presence of multiple interpenetrating networks, nearly 60% of the volume of crystals built from tecton **39** remains available for the inclusion of guests.[18] The guests are highly disordered and lie in two types of channels aligned with the *a* axis (Figure 6).

The cross sections of these channels measure approximately 4.2 x 4.2 $Å^2$ and 3.9 x 3.9 $Å^2$ at the narrowest points.[53] The behavior of tecton **39** provides further evidence that attaching multiple hydrogen-bonding sites to the spirobifluorene core is an effective strategy for creating molecules predisposed to form highly porous crystals.

Even higher porosity was found in crystals of the 2,2',7,7'-tetrasubstituted tetrakis(triaminotriazine) **40**, which were grown from DMSO/dioxane. The crystals proved to belong to the tetragonal space group P-4b2 and to have the approximate composition **40** • 8 DMSO • 8 dioxane • x H_2O.[55] Views of the structure are shown in Figures 7-10. The triaminotriazine groups associate extensively according to hydrogen-bonding motifs **43** and **45**, thereby generating a network in which each tecton forms a total of sixteen hydrogen bonds with eight symmetrically oriented neighboring tectons (Figure 7). Each triaminotriazine group participates in two hydrogen bonds of type **43** with one set of four neighbors that are equivalent by symmetry (dark gray), and each triaminotriazine group also forms two other hydrogen bonds according to motif **45** with a second set of four equivalent neighbors (black). The tectons linked by motif **43** define a four-fold interpenetrated diamondoid network (Figure 8), whereas those joined by motif **45** generate a square planar network.

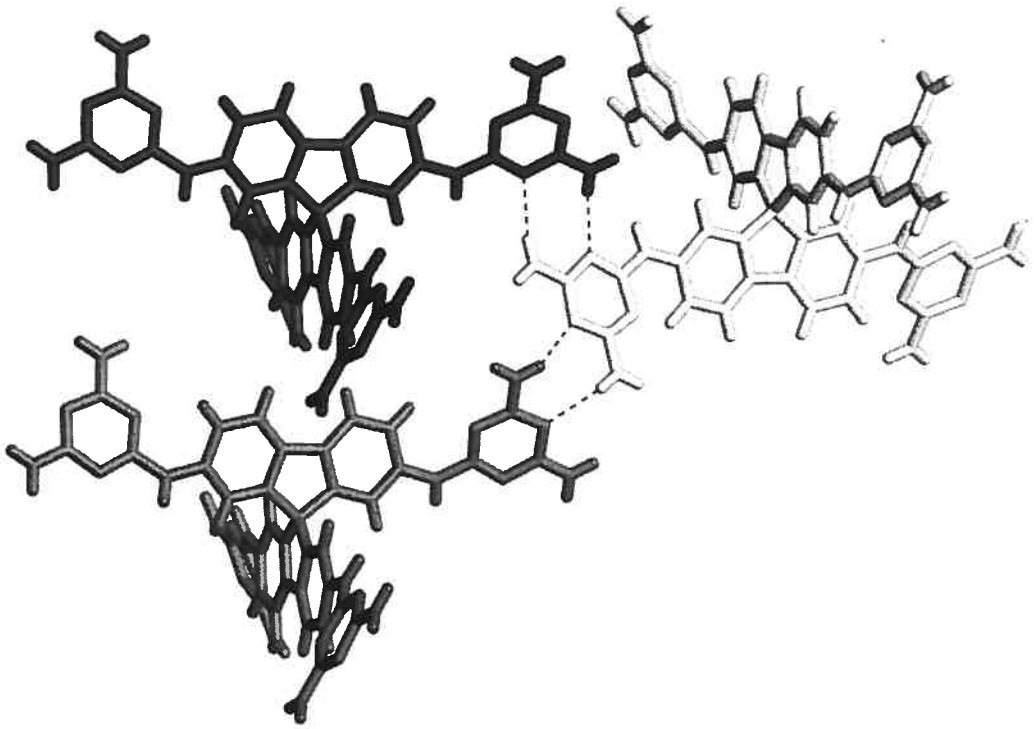

Figure 7. Representation of the structure of crystals of tetrakis(triaminotriazine) **40** grown from DMSO/dioxane, showing a tecton (white) surrounded by two of a total of eight hydrogen-bonded neighboring tectons (dark gray and black). Each of the two illustrated neighbors is equivalent by symmetry to three others, which are omitted for clarity, as are all guests. Hydrogen bonds appear as broken lines. The central tecton (white) shares two hydrogen bonds with each neighboring tecton according to motif **43** (dark gray) or motif **45** (black).

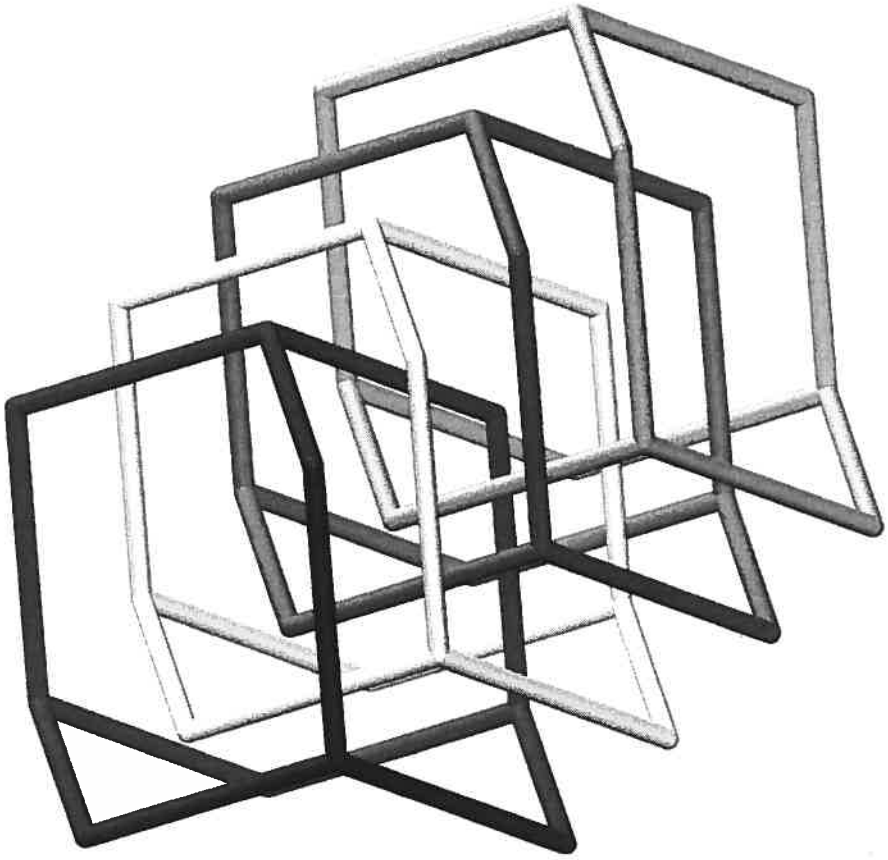

Figure 8. Representation of the four-fold interpenetrated diamondoid networks generated by association of tecton **40**. In this drawing, the central spirocyclic carbon atom of each tecton lies at the intersections of solid lines that represent hydrogen bonding to four neighbors according to motif **43**. The independent networks are shown in different shades of gray.

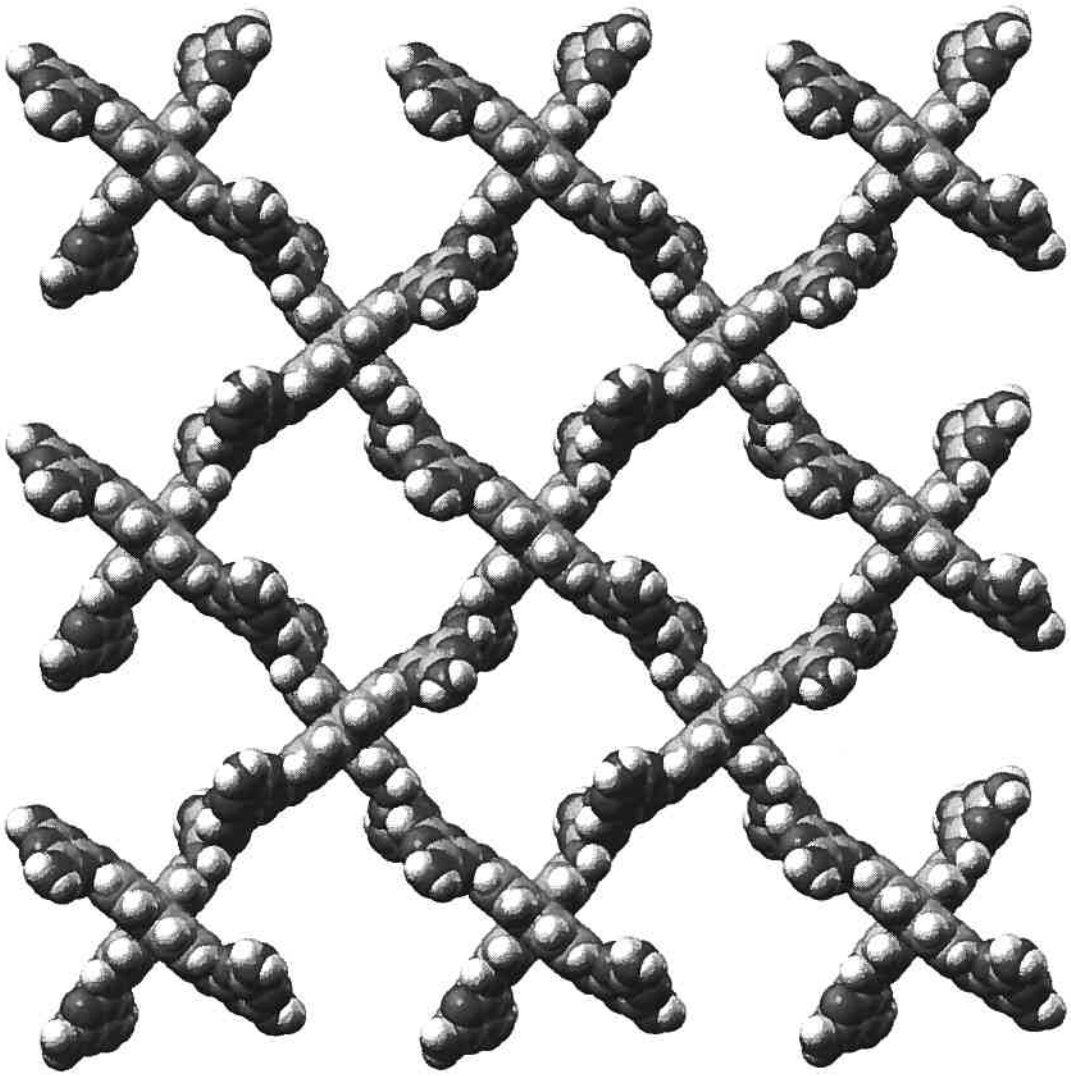

Figure 9. View along the *c* axis of the network constructed from tecton **40** showing a 2 x 2 x 4 array of unit cells. Guests are omitted, and atoms are shown as spheres of van der Waals radii in order to reveal the cross sections of the channels. Atoms of hydrogen appear in white, atoms of carbon in light gray, and atoms of nitrogen in dark gray.

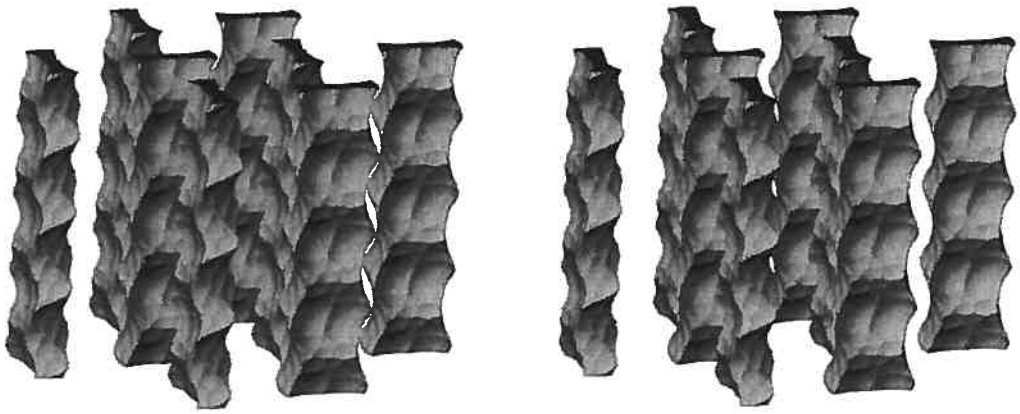

Figure 10. Stereoscopic representation of the parallel helical channels defined by the network constructed from tecton **40**. The image shows a 2 x 2 x 4 array of unit cells viewed with the *c* axis vertical. The outsides of the channels appear in light gray, and dark gray is used to show where the channels are cut by the boundaries of the array. The surface of the channels is defined by the possible loci of the centre of a sphere of diameter 7 Å as it rolls over the surface of the ordered tectonic network.[56]

Despite this complex interpenetration, the resulting structure contains impressive channels parallel to the *c* axis (Figures 9-10). Their cross section (Figure 9) measures approximately 13 x 13 Å^2,[53] and the channels themselves are represented by the surface shown in Figure 10.[56] This view establishes that the channels have an irregular helical shape with no significant interconnections; although the individual channels are chiral, equal numbers of helices of opposite handedness are present. Fully 75% of the volume of the crystals remains available for the inclusion of guests.[18] To our knowledge, the porosity of this system is the highest ever reported for a crystal built from small molecules.

Conclusions

The detailed structures of molecular crystals cannot yet be predicted with accuracy,[57] but research in crystal engineering is providing increasingly powerful tools for designing molecules that are predisposed to form structures with particular features. Especially rapid progress has been made in learning how to make molecular crystals in which significant volume is available for the inclusion of guests. A particularly promising strategy for making porous crystals is to build them from molecules that interact with their neighbors by strongly directional forces, thereby disfavoring close packing and leading to the formation of open networks. Such molecules can be made conveniently by grafting sticky sites onto suitable cores. If the cores are chosen to have topologies that make efficient packing inherently impossible, then the resulting molecules should yield

especially porous crystals. This hypothesis is supported by the behavior of tectons **28**, **33**, **39**, and **40**, in which multiple sites for hydrogen bonding are attached to a spirobifluorene core. In particular, crystals of tecton **40** have a porosity of 75%, the highest value ever reported for a crystal built from small molecules. We are optimistic that this strategy can be exploited to make molecular crystals with even higher porosity and useful applications in separation, catalysis, and other areas.

Experimental Section

2-Bromo-3',5-dimethoxy-[1,1'-biphenyl] (22).[46] A solution of 3,3'-dimethoxy-[1,1'-biphenyl] (**21**; 12.7 g, 59.3 mmol) in CCl_4 (70 mL) was stirred at 0 °C and treated dropwise with a solution of Br_2 (3.3 mL, 64 mmol) in CCl_4 (20 mL). The resulting mixture was stirred at 25 °C for 1.5 h, and then saturated aqueous $Na_2S_2O_3$ was added (50 mL). The mixture was extracted with CH_2Cl_2, and the organic phase was washed with water and brine, dried over $MgSO_4$, and filtered. Volatiles were removed by evaporation under reduced pressure, and the resulting oil was purified by flash chromatography (silica, toluene (80%)/ether (20%)) to afford 2-bromo-3',5-dimethoxy-[1,1'-biphenyl] (**22**; 13.3 g, 45.4 mmol, 77%)[46] as a colorless oil: IR (film, NaCl) 1590, 1566, 1464, 1232, 1031 cm^{-1}; ^1H NMR (400 MHz, $CDCl_3$) d 7.56 (d, 1H, ^3J = 8.8 Hz), 7.37 (t, 1H, ^3J = 7.7 Hz), 7.03-6.95 (m, 3H), 6.92 (d, 1H, ^4J = 3.1 Hz), 6.81 (dd, 1H, ^3J = 8.8 Hz, ^4J = 3.1 Hz), 3.87 (s, 3H), 3.83 (s, 3H); ^{13}C NMR (100 MHz, $CDCl_3$) d 159.5, 159.2, 143.7, 142.9, 134.1, 129.4, 122.1, 117.0, 115.4, 115.2, 113.7, 113.4, 55.9, 55.7; MS (EI +) 292; HRMS (EI +) calcd for $C_{14}H_{13}BrO_2$ *m/e* 292.009891, found 292.009680.

3',5-Dimethoxy-[1,1'-biphenyl]-2-carboxylic acid (23).[46-47] A solution of 2-bromo-3',5-dimethoxy-[1,1'-biphenyl] (**22**; 13.3 g, 45.4 mmol)[46] in diethyl ether (400 mL) was stirred at -10 °C under dry N_2 and treated dropwise with a solution of butyllithium (25 mL, 2.5 M in hexane, 62 mmol). After 15 min, gaseous CO_2 was bubbled through the mixture, and the temperature was allowed to rise to 25 °C. The resulting mixture was acidified with aqueous 1 M HCl and extracted with diethyl ether. The organic phase was washed with water and brine, dried over $MgSO_4$, and filtered. Volatiles were removed by evaporation under reduced pressure, and the residue was crystallized from acetone/pentane to afford 3',5-dimethoxy-[1,1'-biphenyl]-2-carboxylic acid (**23**; 11.3 g, 43.8 mmol, 96%)[46-47] as a light yellow solid: mp 126-128 °C (lit.[47] 126-128 °C); IR (KBr) 3200-2400, 1692, 1666, 1600, 1566, 1452, 1436, 1294, 1282, 1224, 1023 cm^{-1}; ^1H NMR (400 MHz, $CDCl_3$) d 7.99 (d, 1H, ^3J = 8.7 Hz), 7.30 (t, 1H, ^3J = 8.0 Hz), 6.94-6.87 (m, 4H), 6.84 (d, 1H, ^4J = 2.6 Hz), 3.87 (s, 3H), 3.83 (s, 3H); ^{13}C NMR (100.1 MHz, CD_3OD) d 170.6, 162.2, 159.7, 145.4, 143.4, 132.3, 128.9, 123.6, 120.9, 116.4, 114.2, 112.7, 112.3, 55.0, 54.7; MS (FAB, 3-nitrobenzyl alcohol) *m/e* 258. Anal. Calcd for $C_{15}H_{14}O_4$: C, 69.76; H, 5.46. Found C, 69.58; H, 5.49.

Methyl 3',5-Dimethoxy-[1,1'-biphenyl]-2-carboxylate (24). A solution of 3',5-dimethoxy-[1,1'-biphenyl]-2-carboxylic acid (**23**; 11.3 g, 43.8 mmol)[46-47] in anhydrous DMF (100 mL) was treated with $KHCO_3$ (11.5 g, 115 mmol). The mixture was stirred at 25 °C and treated dropwise with CH_3I (7.0 mL, 110 mmol). After 24 h, the mixture was diluted with water (200 mL) and extracted with diethyl ether (3 x 100 mL). The organic

phase was washed thoroughly with water (5 x 100 mL) and brine (100 mL), dried over $MgSO_4$, and filtered. Volatiles were removed by evaporation under reduced pressure, and the residue was purified by flash chromatography (silica, $CH_3COOC_2H_5$ (15%)/hexane (85%)) to afford methyl 3',5-dimethoxy-[1,1'-biphenyl]-2-carboxylate (**24**; 8.76 g, 32.2 mmol, 74%) as a colorless oil: IR (film, NaCl) 1718, 1600, 1568, 1484, 1464, 1434, 1286, 1255, 1236, 1038 cm^{-1}; ^1H NMR (400 MHz, $CDCl_3$) d 7.89 (d, 1H, ^3J = 8.6 Hz), 7.32 (t, 1H, ^3J = 7.9 Hz), 6.94-6.87 (m, 5H), 3.86 (s, 3H), 3.84 (s, 3H), 3.65 (s, 3H); ^{13}C NMR (100 MHz, $CDCl_3$) d 168.6, 162.1, 159.6, 145.5, 143.5, 132.7, 129.3, 123.1, 121.3, 116.5, 114.3, 113.1, 113.1, 55.9, 55.6, 52.1; MS (FAB, 3-nitrobenzyl alcohol) *m/e* 272. Anal. Calcd for $C_{16}H_{16}O_4$: C, 70.58; H, 5.92. Found C, 70.17; H, 6.08.

9-(3',5-Dimethoxy-[1,1'-biphenyl]-2-yl)-3,6-dimethoxy-9*H*-fluoren-9-ol (26). A solution of 2,2'-dibromo-5,5'-dimethoxy-[1,1'-biphenyl] (**25**; 2.42 g, 6.50 mmol)[48] in diethyl ether (50 mL) was stirred under N_2 at -10 °C and treated dropwise with butyllithium (5.2 mL, 2.5 M in hexane, 13 mmol). The mixture was kept at -10 °C for 30 min, and a solution of methyl 5,3'-dimethoxybiphenyl-2-carboxylate (**24**; 1.77 g, 6.50 mmol) in diethyl ether (25 mL) was added dropwise. The resulting mixture was stirred at -10 °C for 30 min and at 25 °C for 2 h. Water was added and the phases were separated. The organic layer was washed with water and brine, dried over Na_2SO_4, and filtered. Volatiles were removed under reduced pressure, and the residue was purified by flash chromatography (silica, CH_2Cl_2 (98%)/acetone (2%)) to afford 9-(3',5-dimethoxy-[1,1'-biphenyl]-2-yl)-3,6-dimethoxy-9*H*-fluoren-9-ol (**26**; 1.48 g, 3.26 mmol, 50%) as a colorless solid. The product was unstable and was used directly without any further

purification: ^{1}H NMR (400 MHz, $CDCl_3$) δ 8.33 (d, 1H, ^3J = 8.8 Hz), 7.09-7.01 (m, 3H), 6.68 (t, 2H, ^3J = 8.3 Hz), 6.65-6.55 (m, 3H), 6.47 (d, 1H, ^4J = 2.8 Hz), 6.43-6.40 (m, 1H), 5.63 (d, 1H, ^3J = 7.5 Hz), 5.57 (m, 1H), 3.79 (s, 6H), 3.78 (s, 3H), 3.41 (s, 3H); MS (FAB, 3-nitrobenzyl alcohol) *m/e* 454.

3,3',6,6'-Tetramethoxy-9,9'-spirobi[9*H*-fluorene] (27). A solution of 9-(3',5-dimethoxy-[1,1'-biphenyl]-2-yl)-3,6-dimethoxy-9*H*-fluoren-9-ol (**26**; 702 mg, 1.54 mmol) in a mixture of concentrated aqueous HCl (1 mL) and acetic acid (10 mL) was heated at reflux for 2 h. The mixture was then cooled, diluted with water, and extracted with $CH_3COOC_2H_5$ (2 x 25 mL). The combined organic extracts were washed with saturated aqueous $NaHCO_3$ (3 x 25 mL), water (25 mL), and brine (25 mL). After the organic phase was dried over Na_2SO_4 and filtered, volatiles were removed under reduced pressure. The residue was dissolved in the minimum amount of CH_2Cl_2 and filtered through a plug of silica gel, using CH_2Cl_2 as the eluent. The filtrate was concentrated under reduced pressure, and the residue was crystallized from $CHCl_3$/hexane to afford 3,3',6,6'-tetramethoxy-9,9'-spirobi[9*H*-fluorene] (**27**; 553 mg, 1.27 mmol, 82%) as a colorless solid: mp 197-198 °C; IR (KBr) 1610, 1581, 1492, 1460, 1430, 1305, 1286, 1276, 1244, 1227, 1200, 1175, 1160, 1031 cm^{-1}; ^{1}H NMR (400 MHz, $CDCl_3$) d 7.34 (d, 4H, ^4J = 2.2 Hz), 6.69 (dd, 4H, ^3J = 8.3 Hz, ^4J = 2.2 Hz), 6.66 (d, 4H, ^3J = 8.3 Hz), 3.90 (s, 12H); ^{13}C NMR (100 MHz, $CDCl_3$) d 159.6, 142.6, 141.9, 124.4, 113.8, 105.0, 63.4, 55.4; MS (FAB, 3-nitrobenzyl alcohol) *m/e* 436. Anal. Calcd for $C_{29}H_{24}O_4$: C, 79.80; H, 5.54. Found C, 79.57; H, 5.53.

3,3',6,6'-Tetrahydroxy-9,9'-spirobi[9*H*-fluorene] (28). A solution of 3,3',6,6'-tetramethoxy-9,9'-spirobi[9*H*-fluorene] (**27**; 538 mg, 1.23 mmol) in anhydrous CH_2Cl_2 (10 mL) was stirred under N_2 at 0 °C and treated dropwise with BBr_3 (15 mL, 1.0 M in CH_2Cl_2, 15 mmol). The mixture was stirred at 0 °C for 30 min and at 25 °C for 24 h. Water was then added, and the organic layer was extracted with 1 N aqueous NaOH (4 x 15 mL). The combined aqueous extracts were acidified with concentrated aqueous HCl and extracted with $CH_3COOC_2H_5$. The organic phase was dried over $MgSO_4$ and filtered, and volatiles were then removed under reduced pressure. The residue was dissolved in the minimum amount of $CH_3COOC_2H_5$, and the solution was filtered through a plug of silica gel using $CH_3COOC_2H_5$ as the eluent. The filtrate was concentrated under reduced pressure, and the residue was crystallized from $CH_3COOC_2H_5$/hexane to afford 3,3',6,6'-tetrahydroxy-9,9'-spirobi[9*H*-fluorene] (**28**; 425 mg, 1.12 mmol, 91%) as a colorless solid: mp 196-198 °C; IR (KBr) 3420, 1611, 1587, 1452, 1384, 1303, 1236, 1163 cm^{-1}; H NMR (400 MHz, acetone-d_6) d 8.28 (bs, 4H), 7.27 (d, 4H, ^4J = 2.2 Hz), 6.60 (dd, 4H, ^3J = 8.1 Hz, ^4J = 2.2 Hz), 6.46 (d, 4H, ^3J = 8.1 Hz); ^{13}C NMR (100 MHz, acetone-d_6) d 157.7, 143.3, 141.6, 124.6, 115.3, 106.9, 60.0; MS (EI +) 380.1; HRMS (EI +) calcd for $C_{25}H_{16}O_4$ *m/e* 380.104859, found 380.104254.

Tetrakis(trifluoromethanesulfonate) (29) of 3,3',6,6'-Tetrahydroxy-9,9'-spirobi[9*H*-fluorene] (28). A solution of 3,3',6,6'-tetrahydroxy-9,9'-spirobi[9*H*-fluorene] (**28**; 423 mg, 1.11 mmol) in pyridine (10 mL) was stirred at -20 °C under N_2 and treated dropwise with $(CF_3SO_2)_2O$ (1.2 mL, 7.1 mmol). The mixture was stirred at -20 °C for 1 h and at 25 °C for 24 h. The mixture was then diluted with water and extracted with diethyl ether.

The organic layer was washed with water and brine, dried over $MgSO_4$, and filtered. Volatiles were then removed under reduced pressure, and the residue was dissolved in the minimum amount of CH_2Cl_2 and filtered through a plug of silica gel using CH_2Cl_2 as the eluent. The filtrate was concentrated under reduced pressure to afford the tetrakis(trifluoromethanesulfonate) of 3,3',6,6'-tetrahydroxy-9,9'-spirobi[9*H*-fluorene] (**29**; 706 mg; 0.777 mmol, 70%) as a colorless solid that was used without any further purification: mp 171-172 °C; IR (KBr) 1433, 1248, 1216, 1139, 893 cm^{-1}; ^1H NMR (400 MHz, $CDCl_3$) d 7.77 (d, 4H, ^4J = 2.2 Hz), 7.14 (dd, 4H, ^3J = 8.4 Hz, ^4J = 2.2 Hz), 6.84 (d, 4H, ^3J = 8.4 Hz); ^{13}C NMR (100.1 MHz, $CDCl_3$) δ 150.4, 147.3, 142.6, 126.3, 122.6, 119.1 (q, $J_{C\text{-}F}$ = 320 Hz), 114.7, 64.7; ^{19}F NMR (376.5 MHz, $CDCl_3$) δ -75.5; MS (FAB, 3-nitrobenzyl alcohol) *m/e* 907; HRMS (FAB, 3-nitrobenzyl alcohol) calcd for $C_{29}H_{12}F_{12}O_{12}S_4$ *m/e* 907.90198, found 907.90400.

3,3',6,6'-Tetracyano-9,9'-spirobi[9*H*-fluorene] (30). A solution of $Pd_2(dba)_3$ (27 mg, 0.029 mmol)[58] and 1,1'-bis(diphenylphosphino)ferrocene (58.1 mg, 0.105 mmol) in dry DMF (3 mL) was stirred at 25 °C under N_2, the tetrakis(trifluoromethanesulfonate) of 3,3',6,6'-tetrahydroxy-9,9'-spirobi[9*H*-fluorene] (**29**; 300 mg, 0.330 mmol) was added, and the resulting mixture was heated at 80 °C. $Zn(CN)_2$ (102 mg, 0.869 mmol) was then added in 20 portions over a 3 h period, and the mixture was stirred at 80 °C for 24 h. The resulting suspension was cooled, filtered, and partitioned between CH_2Cl_2 and water. The organic layer was washed with water and brine, dried over $MgSO_4$, filtered, and concentrated under reduced pressure. The residue was then dissolved in a 7:3 mixture of $CH_3COOC_2H_5$ and hexane (5 mL) and filtered through a plug of silica gel using the same

mixture of solvents as eluent (100 mL). The filtrate was then concentrated under reduced pressure, and the residue was purified by flash chromatography (silica, CH_2Cl_2 (99%)/acetone (1%)) to afford 3,3',6,6'-tetracyano-9,9'-spirobi[9*H*-fluorene] (**30**; 90 mg, 0.22 mmol, 67%) as a colorless solid: mp > 300 °C; IR (KBr) 2228, 1610, 1486, 1401, 824 cm^{-1}; ^1H NMR (400 MHz, acetone-d_6) d 8.65 (s, 4H), 7.71 (dd, 4H, ^3J = 7.9 Hz, ^4J = 1.3 Hz), 7.08 (d, 4H, ^3J = 7.9 Hz); ^{13}C NMR (75.5 MHz, acetone-d_6) d 151.9, 142.3, 134.0, 126.4, 126.2, 119.0, 113.9, 67.4; MS (EI +) 416; HRMS (EI +) calcd for $C_{29}H_{12}N_4$ *m/e* 416.106197, found 416.106329.

Tecton 19. A mixture of 3,3',6,6'-tetracyano-9,9'-spirobi[9*H*-fluorene] (**30**; 305 mg, 0.732 mmol), dicyandiamide (985 mg, 11.7 mmol), and powdered KOH (104 mg, 1.85 mmol) in 2-methoxyethanol (10 mL) was heated at reflux for 24 h. The mixture was then cooled, and water (20 mL) was added. The resulting solid was filtered, washed thoroughly with hot water, and then dried in vacuo to give tecton **19** (398 mg, 0.529 mmol, 72%) as a colorless solid: mp > 300 °C; IR (KBr) 3400, 1607, 1541, 1457, 1433, 1381, 815 cm^{-1}; ^1H NMR (400 MHz, DMSO-d_6) d 8.83 (s, 4H), 8.10 (d, 4H, ^3J = 8.0 Hz), 6.83 (d, 4H, ^3J = 8.0 Hz), 6.98-6.67 (bs, 16H); ^{13}C NMR (100.1 MHz, CF_3COOD) d 165.4, 161.6, 156.0, 143.6, 131.7, 130.8, 127.2, 123.0, 68.6. MS (FAB, 3-nitrobenzyl alcohol) *m/e* 753.8 (M + 1); HRMS (FAB, 3-nitrobenzyl alcohol) calcd for $C_{37}H_{29}N_{20}$ *m/e* 753.288406, found 753.287000.

2,2',7,7'-Tetranitro-9,9'-spirobi[9*H*-fluorene] (31). Fuming nitric acid (40 mL) was stirred at 0 °C, and 9,9'-spirobi[9*H*-fluorene] (**17**; 7.18 g, 22.7 mmol)[44] was added in

small portions during 20 min. The resulting mixture was kept at 0 °C for 1 h, and a mixture of acetic anhydride (15 mL) and acetic acid (25 mL) was slowly added. The resulting precipitate was filtered, washed abundantly with acetic acid and water, and dried in vacuo to afford 2,2',7,7'-tetranitro-9,9'-spirobi[9*H*-fluorene] (**31**; 8.42 g, 17.0 mmol, 75%) as a light yellow solid. A sample of analytical purity was obtained by crystallization from THF/hexane: mp > 300 °C; IR (KBr) 1589, 1522, 1340, 1077 cm^{-1}; ^1H NMR (400 MHz, DMSO-d_6) d 8.58 (d, 4H, ^3J = 8.5 Hz), 8.45 (dd, 4H, ^3J = 8.5 Hz, ^4J = 2.0 Hz), 7.63 (d, 4H, ^4J = 2.0 Hz); ^{13}C NMR (100.1 MHz, DMSO-d_6) d 149.3, 148.5, 146.7, 126.2, 124.8, 120.0, 65.9; HRMS (FAB, 3-nitrobenzyl alcohol) calcd for $C_{25}H_{13}N_4O_8$ *m/e* 497.073339, found 497.075500. Anal. Calcd for $C_{25}H_{12}N_4O_8$: C, 60.49; H, 2.44. Found C, 60.59; H, 2.43.

2,2',7,7'-Tetraamino-9,9'-spirobi[9*H*-fluorene] (32). A suspension of 2,2',7,7'-tetranitro-9,9'-spirobi[9*H*-fluorene] (**31**; 8.30 g, 16.7 mmol) and 10% Pd/C (800 mg) in THF (250 mL) was stirred for 24 h in a Parr reactor at 25 °C under H_2 (160 psi). The resulting mixture was filtered through Celite using THF as eluent, and the filtrate was concentrated under reduced pressure. This yielded a residue of 2,2',7,7'-tetraamino-9,9'-spirobi[9*H*-fluorene] (**32**; 6.16 g, 16.4 mmol, 98%) as a colorless solid, which was used without further purification: mp > 210 °C (decomposition); IR (KBr) 3427, 3383, 3344, 1699, 1620, 1579, 1439, 1313, 1232, 1120, 880 cm^{-1}; ^1H NMR (400 MHz, DMSO-d_6) d 7.38 (d, 4H, ^3J = 8.0 Hz), 6.59 (dd, 4H, ^3J = 8.0 Hz, ^4J = 2.0 Hz), 5.93 (d, 4H, ^4J = 2.0 Hz), 4.35 (bs, 8H); ^{13}C NMR (100.1 MHz, DMSO-d_6) d 151.3, 147.9, 131.7, 119.5,

113.8, 110.4, 65.7; MS (EI +) *m/e* 376; HRMS (EI +) calcd for $C_{25}H_{20}N_4$ *m/e* 376.168797, found 376.168412.

2,2',7,7'-Tetra(acetamido)-9,9'-spirobi[9H-fluorene] (33). A solution of 2,2',7,7'-tetraamino-9,9'-spirobi[9*H*-fluorene] (**32**; 6.38 g, 16.9 mmol) in acetic acid (200 mL) was stirred vigorously at 0 °C and treated dropwise with acetic anhydride (200 mL) over a 30 min period. The resulting suspension was stirred at 25 °C for 18 h and then diluted with CH_2Cl_2 (500 mL). The resulting precipitate was filtered and dissolved in DMF (150 mL), and the solution was poured into cold water with vigorous stirring. The resulting precipitate was separated by filtration, washed with water, and dried to afford a pure sample of 2,2',7,7'-tetra(acetamido)-9,9'-spirobi[9*H*-fluorene] (**33**; 8.98 g, 16.5 mmol, 98%) as an off-white solid: mp > 300 °C; IR (KBr) 3300, 1668, 1596, 1548, 1469, 1412, 1370, 1312, 1255, 815 cm^{-1}; ^1H NMR (300 MHz, DMSO-d_6) d 9.80 (s, 4H), 7.80 (d, 4H, ^3J = 8.3 Hz), 7.59 (dd, 4H, ^3J = 8.3 Hz, ^4J = 1.8 Hz), 6.86 (d, 4H, ^4J = 1.8 Hz), 1.89 (s, 12H); ^{13}C NMR (75.5 MHz, DMSO-d_6) d 168.9, 149.9, 139.6, 136.8, 121.0, 119.5, 114.7, 66.3, 24.8; HRMS (FAB, 3-nitrobenzyl alcohol) calcd for $C_{33}H_{29}N_4O_4$ *m/e* 545.218881, found 545.220400.

2,2',7,7'-Tetra(acetamido)-3,3',6,6'-tetranitro-9,9'-spirobi[9*H*-fluorene] (34). 2,2',7,7'-Tetra(acetamido)-9,9'-spirobi[9*H*-fluorene] (**33**; 2.18 g, 4.00 mmol) was added in small portions over a 10 min period to fuming nitric acid (20 mL) stirred at -10 °C. The mixture was kept at this temperature for 20 min and was then poured into cold water (400 mL). The resulting precipitate was filtered, washed with water, and dried. The solid was

crystallized from THF/hexane to afford 2,2',7,7'-tetra(acetamido)-3,3',6,6'-tetranitro-9,9'-spirobi[9*H*-fluorene] (**34**; 2.80 g, 3.86 mmol, 97%) as a yellow solid: mp > 300 °C; IR (KBr) 3400, 1702, 1623, 1585, 1483, 1418, 1384, 1330, 1290, 1232 cm^{-1}; ^1H NMR (400 MHz, DMSO-d_6) d 10.19 (s, 4H), 8.88 (s, 4H), 6.96 (s, 4H), 1.90 (s, 12H); ^{13}C NMR (100.1 MHz, DMSO-d_6) d 167.9, 150.2, 143.5, 135.9, 131.1, 119.8, 118.2, 64.3, 22.6; MS (FAB, 3-nitrobenzyl alcohol) *m/e* 725 (M+1); HRMS (FAB, 3-nitrobenzyl alcohol) calcd for $C_{33}H_{24}N_8O_{12}$ *m/e* 725.159194, found 725.161500.

2,2',7,7'-Tetraamino-3,3',6,6'-tetranitro-9,9'-spirobi[9*H*-fluorene] (35). A suspension of 2,2',7,7'-tetra(acetamido)-3,3',6,6'-tetranitro-9,9'-spirobi[9*H*-fluorene] (**34**; 1.78 g, 2.46 mmol) in aqueous 3 N KOH (50 mL) was stirred at 50 °C for 24 h. The suspension was cooled, and the resulting precipitate was filtered, washed with water, and dried in vacuo. The solid was crystallized from THF/hexane to afford 2,2',7,7'-tetraamino-3,3',6,6'-tetranitro-9,9'-spirobi[9*H*-fluorene] (**35**; 1.31 g, 2.35 mmol, 96%) as a red solid: mp > 250 °C (dec); IR (KBr) 3478, 3367, 1637, 1591, 1495, 1463, 1431, 1392, 1333, 1308, 1271, 1225, 1187 cm^{-1}; ^1H NMR (400 MHz, DMSO-d_6) d 8.70 (s, 4H), 7.40 (s, 8H), 6.45 (s, 4H); ^{13}C NMR (100.1 MHz, DMSO-d_6) d 156.4, 147.2, 131.8, 128.5, 118.0, 114.6, 64.3; MS (FAB, 3-nitrobenzyl alcohol) *m/e* 556; HRMS (FAB, 3-nitrobenzyl alcohol) calcd for $C_{25}H_{17}N_8O_8$ *m/e* 557.116935, found 557.118800. Anal. Calcd for $C_{25}H_{16}N_8O_8 \cdot 0.5$ THF $\cdot H_2O$: C, 53.12; H, 3.63; N, 18.35. Found C, 53.04; H, 3.37; N, 18.39.

3,3',6,6'-Tetranitro-9,9'-spirobi[9*H*-fluorene] (36). A mixture of isoamyl nitrite (40 mL) in anhydrous DMF (75 mL) was stirred at 65 °C under N_2 and treated dropwise with

a solution of 2,2',7,7'-tetraamino-3,3',6,6'-tetranitro-9,9'-spirobi[9*H*-fluorene] (**35**; 3.01 g, 5.41 mmol) in DMF (75 mL). The mixture was stirred at 65 °C for 3 h, cooled to room temperature, and partitioned between $CH_3COOC_2H_5$ and water. The organic phase was washed several times with water, aqueous 1 N HCl, and brine. It was then dried over Na_2SO_4, filtered, and concentrated under reduced pressure. The residue was dissolved in the minimum amount of CH_2Cl_2 and filtered through a plug of silica gel using CH_2Cl_2 as eluent. The filtrate was concentrated under reduced pressure, and the residue was purified by flash chromatography (silica, CH_2Cl_2 (80%)/hexane (20%)) to afford 3,3',6,6'-tetranitro-9,9'-spirobi[9*H*-fluorene] (**36**; 0.834 g, 1.68 mmol, 31%) as a light yellow solid: mp > 300 °C; IR (KBr) 1516, 1343 cm^{-1}; ^1H NMR (300 MHz, $CDCl_3$) d 8.86 (d, 4H, ^4J = 2.0 Hz), 8.17 (dd, 4H, ^3J = 8.4 Hz, ^4J = 2.0 Hz), 6.92 (d, 4H, ^3J = 8.4 Hz); ^{13}C NMR (100.1 MHz, DMSO-d_6) d 153.3, 149.8, 142.4, 126.0, 125.6, 118.9, 65.7; MS (EI +) *m/e* 496; HRMS (EI +) calcd for $C_{25}H_{12}N_4O_8$ *m/e* 496.065514, found 496.065354.

3,3',6,6'-Tetraamino-9,9'-spirobi[9*H*-fluorene] (37). A procedure analogous to the one used to reduce tetranitrospirobifluorene **31** was carried out using 3,3',6,6'-tetranitro-9,9'-spirobi[9*H*-fluorene] (**36**; 805 mg, 1.62 mmol) in contact with 10% Pd/C (380 mg) and H_2 during 72 h. The reaction provided 3,3',6,6'-tetraamino-9,9'-spirobi[9*H*-fluorene] (**37**; 565 mg, 1.50 mmol, 93%) as a light yellow solid: mp > 300 °C; IR (KBr) 3409, 2924, 2859, 1612, 1497, 1460, 1309, 1255, 1177, 1053 cm^{-1}; ^1H NMR (400 MHz, DMSO-d_6) d 6.85 (d, 4H, ^4J = 1.9 Hz), 6.26 (dd, 4H, ^3J = 8.0 Hz, ^4J = 1.9 Hz), 6.18 (d, 4H, ^3J = 8.0 Hz), 5.00 (bs, 8H); ^{13}C NMR (100.1 MHz, DMSO-d_6) d 148.8, 142.9, 139.1, 124.3,

114.4, 105.5, 63.7; HRMS (FAB, 3-nitrobenzyl alcohol) calcd for $C_{25}H_{21}N_4$ *m/e* 377.176622, found 377.175900.

Tecton 20. A solution of cyanuric chloride (738 mg, 4.00 mmol) in acetone (10 mL) was stirred at -10 °C and treated dropwise with a solution of 3,3',6,6'-tetraamino-9,9'-spirobi[9*H*-fluorene] (**37**; 347 mg, 0.922 mmol) in acetone (10 mL). The mixture was stirred at -10 °C for 1 h, and Na_2CO_3 (424 mg, 4.00 mmol) was added. The resulting suspension was poured into cold water (100 mL), and the precipitate was filtered, washed thoroughly with cold water, and dried. The solid was then dissolved in dioxane (10 mL), and the mixture was treated with concentrated aqueous NH_4OH (10 mL) and heated at reflux for 18 h. The resulting suspension was cooled, and water (25 mL) was added. The precipitate was filtered, washed thoroughly with water, and dried to afford tecton **20** (468 mg, 0.576 mmol, 62%) as an off-white solid: mp > 300 °C; IR (KBr) 3400, 1607, 1552, 1438, 1407, 812 cm^{-1}; ^1H NMR (400 MHz, DMSO-d_6, 25 °C) 8.85 (m, 4H), 8.11 (m, 4H), 7.44 (m, 4H), 6.44 (m, 4H), 6.30 (bs, 16H); ^{13}C NMR (100.1 MHz, DMSO-d_6, 25 °C) d 168.2, 165.9, 143.4, 142.4, 141.0, 123.9, 121.5, 113.2, 66.0; MS (FAB, 3-nitrobenzyl alcohol) *m/e* 813 (M + 1); HRMS (FAB, 3-nitrobenzyl alcohol) calcd for $C_{37}H_{33}N_{24}$ *m/e* 813.332003, found 813.334300.

2,2',7,7'-Tetracyano-9,9'-spirobi[9*H*-fluorene] (42). A mixture of 2,2',7,7'-tetrabromo-9,9'-spirobi[9*H*-fluorene] (**41**; 1.26 g, 1.99 mmol)[44] and CuCN (0.806 g, 9.00 mmol) in DMF (10 mL) was heated at reflux for 24 h under N_2. The resulting mixture was cooled, diluted with water (100 mL) and ethylenediamine (10 mL), and extracted with CH_2Cl_2 (3

x 75 mL). The combined organic extracts were washed with 10% aqueous NaCN, water, and brine. The organic phase was then dried over $MgSO_4$ and filtered. Volatiles were removed under reduced pressure, and the residue was purified by flash chromatography (silica, CH_2Cl_2) to afford 2,2',7,7'-tetracyano-9,9'-spirobi[9*H*-fluorene] (**42**; 0.662 g, 1.60 mmol, 80%) as a colorless solid: mp > 300 °C; IR (KBr) 2231, 1604, 1573, 1501, 1448, 1406, 1073, 910, 833 cm^{-1}; ^1H NMR (400 MHz, $CDCl_3$) d 8.07 (d, 4H, ^3J = 8.0 Hz), 7.84 (dd, 4H, ^3J = 8.0 Hz, ^4J = 1.3 Hz), 7.02 (d, 4H, ^4J = 1.3 Hz); ^{13}C NMR (100.1 MHz, $CDCl_3$) d 147.5, 144.3, 134.0, 128.2, 122.9, 118.3, 113.9, 65.5; MS (FAB, 3-nitrobenzyl alcohol) *m/e* 417 (M+1); HRMS (FAB, 3-nitrobenzyl alcohol) calcd for $C_{29}H_{13}N_4$ *m/e* 417.114022, found 417.113100.

Tecton 39. A procedure analogous to the one used to synthesize tecton **19** was carried out using 2,2',7,7'-tetracyano-9,9'-spirobi[9*H*-fluorene] (**42**; 227 mg, 0.545 mmol). This provided tecton **39** (343 mg, 0.456 mmol, 84%) as a colorless solid: mp > 300 °C; IR (KBr) 3469, 3387, 1609, 1537, 1418, 1382, 814 cm^{-1}; ^1H NMR (300 MHz, DMSO-d_6) d 8.42 (d, 4H, ^3J = 8.1 Hz), 8.25 (d, 4H, ^3J = 8.1 Hz), 7.57 (s, 4H), 6.68 (bs, 16H); ^{13}C NMR (75.5 MHz, DMSO-d_6) d 168.7, 166.7, 148.0, 143.0, 137.2, 127.9, 122.2, 120.6, 64.8; MS (FAB, 3-nitrobenzyl alcohol) *m/e* 753 (M+1); HRMS (FAB, 3-nitrobenzyl alcohol) calcd for $C_{37}H_{29}N_{20}$ *m/e* 753.28839, found 753.29010.

Tecton 40. A procedure analogous to the one used to synthesize tecton **20** was carried out using 2,2',7,7'-tetraamino-9,9'-spirobi[9*H*-fluorene] (**32**; 376 mg, 0.999 mmol). This provided tecton **40** (585 mg, 0.720 mmol, 72%) as a colorless solid: mp > 300 °C; IR

(KBr) 3390, 1618, 1547, 1467, 1448, 1419, 1384 cm^{-1}; ^1H NMR (400 MHz, DMSO-d_6) d 8.58 (s, 4H), 8.23 (d, 4H, ^3J = 8.4 Hz), 7.73 (d, 4H, ^3J = 8.4 Hz), 6.55 (s, 4H), 6.19 (bs, 16H); ^{13}C NMR (100.1 MHz, DMSO-d_6) d 167.9, 165.5, 149.8, 140.4, 135.7, 120.7, 120.0, 115.7, 66.2; MS (FAB, 3-nitrobenzyl alcohol) *m/e* 813 (M + 1). Anal. Calcd for $C_{37}H_{32}N_{24}$ • 1 dioxane • 1 H_2O: C, 53.59; H, 4.61. Found C, 53.39; H, 4.32.

X-Ray Crystallographic Studies. The structures were solved by direct methods using SHELXS-97 and refined with SHELXL-97.[59] All non-hydrogen atoms were refined anisotropically, whereas hydrogen atoms were placed in ideal positions and refined as riding atoms.

Structure of 3,3',6,6'-Tetrahydroxy-9,9'-spirobi[9*H*-fluorene] (28). Crystals of the compound **28** belong to the triclinic space group P-1 with a = 7.5560(3) Å, b = 11.3326(4) Å, c = 17.5119(7) Å, α = 85.896(2)°, β = 77.828(3)°, γ = 73.671(2)°, V = 1406.57(9) $Å^3$, D_{calcd} = 1.314 g cm^{-3}, and Z = 2. Full-matrix least-squares refinements on F^2 led to final residuals R_f = 0.0597 and R_w = 0.1649 for 3767 reflections with $I > 2\sigma(I)$.

Structure of 2,2',7,7'-Tetra(acetamido)-9,9'-spirobi[9*H*-fluorene] (33). Crystals of compound **33** belong to the monoclinic space group C2/c with a = 20.504(8) Å, b = 12.2870(7) Å, c = 16.8890(4) Å, β = 120.36(5)°, V = 3671.4(14) $Å^3$, D_{calcd} = 1.195 g cm^{-3}, and Z = 4.

Full-matrix least-squares refinements on F^2 led to final residuals R_f = 0.0663 and R_w = 0.2090 for 3418 reflections with $I > 2\sigma(I)$.

Structure of Tecton 39. Crystals of compound **39** belong to the orthorhombic space group Pcca with a = 21.506(8) Å, b = 15.279(5) Å, c = 21.305(7) Å, V = 7001(4) Å^3, D_{calcd} = 1.425 g cm^{-3}, and Z = 4. Only part of the included molecules could be resolved. The SQUEEZE option of the program PLATON[19] was used to eliminate the contribution of included molecules (dioxane) that were highly disordered, thereby giving final models based only on the ordered part of the structure. Full-matrix least-squares refinements on F^2 led to final residuals R_f = 0.0913 and R_w = 0.2847 for 5042 reflections with $I > 2\sigma(I)$.

Structure of Tecton 40. Crystals of compound **40** belong to the tetragonal space group P-4b2 with $a = b$ = 23.519(4) Å, c = 10.2647(13) Å, V = 5677.8(14) Å^3, D_{calcd} = 1.253 g cm^{-3}, and Z = 2. Only part of the included molecules could be resolved. The SQUEEZE option of the program PLATON[19] was used to eliminate the contribution of included molecules that were highly disordered, thereby giving final models based only on the ordered part of the structure. Full-matrix least-squares refinements on F^2 led to final residuals R_f = 0.0743 and R_w = 0.1838 for 4057 reflections with $I > 2\sigma(I)$.

Acknowledgment. We are grateful to the Natural Sciences and Engineering Research Council of Canada, the Ministère de l'Éducation du Québec, the Canada Foundation for Innovation, the Canada Research Chairs Program, and Merck Frosst for financial support.

In addition, acknowledgment is made to the donors of the Petroleum Research Fund, administered by the American Chemical Society, for support of this research.

Supporting Information Available: General experimental procedures; crystallization of compounds **28**, **33**, **39**, and **40**; ORTEP drawings and tables of crystallographic data, atomic coordinates, anisotropic thermal parameters, and bond lengths and angles for compounds **28**, **33**, **39**, and **40**; comparison of the porosities of selected molecular crystals; and ^{1}H and ^{13}C NMR spectra for compounds **19-20**, **26**, **28-30**, **32-34**, **36-37**, **39**, and **42**. This information is available free of charge via the Internet at http://pubs.acs.org.

Notes and References

1. Fellow of the Ministère de l'Éducation du Québec, 2000-2002. Fellow of the Natural Sciences and Engineering Research Council of Canada, 1998-2000.
2. Desiraju, G. R. *Crystal Engineering: The Design of Organic Solids*; Elsevier: Amsterdam, 1989.
3. Mann, S. *Nature* **1993**, *365*, 499.
4. Simard, M.; Su, D.; Wuest, J. D. *J. Am. Chem. Soc.* **1991**, *113*, 4696.
5. Fournier, J.-H.; Maris, T.; Wuest, J. D.; Guo, W.; Galoppini, E. *J. Am. Chem. Soc.* **2003**, *125*, 1002.
6. Sauriat-Dorizon, H.; Maris, T.; Wuest, J. D.; Enright, G. D. *J. Org. Chem.* **2003**, *68*, 240.
7. Fournier, J.-H.; Maris, T.; Simard, M.; Wuest, J. D. *Cryst. Growth Des.* **2003**, *3*, 535.

8. Brunet, P.; Simard, M.; Wuest, J. D. *J. Am. Chem. Soc.* **1997**, *119*, 2737.

9. Vaillancourt, L.; Simard, M.; Wuest, J. D. *J. Org. Chem.* **1998**, *63*, 9746. Su, D.; Wang, X.; Simard, M.; Wuest, J. D. *Supramolecular Chem.* **1995**, *6*, 171. Wuest, J. D. In *Mesomolecules: From Molecules to Materials*; Mendenhall, G. D., Greenberg, A., Liebman, J. F.; Chapman & Hall: New York, 1995; p 107.

10. Wang, X.; Simard, M.; Wuest, J. D. *J. Am. Chem. Soc.* **1994**, *116*, 12119.

11. For other recent studies of crystal engineering using molecules designed to associate by hydrogen bonding, see: Tanaka, T.; Tasaki, T.; Aoyama, Y. *J. Am. Chem. Soc.* **2002**, *124*, 12453. Moorthy, J. N.; Natarajan, R.; Mal, P.; Venugopalan, P. *J. Am. Chem. Soc.* **2002**, *124*, 6530. Diskin-Posner, Y.; Patra, G. K.; Goldberg, I. *CrystEngComm* **2002**, *4*, 296. Beatty, A. M.; Schneider, C. M.; Simpson, A. E.; Zaher, J. L. *CrystEngComm* **2002**, *4*, 282. Bhogala, B. R.; Vishweshwar, P.; Nangia, A. *Cryst. Growth Des.* **2002**, *2*, 325. Ma, B.-Q.; Zhang, Y.; Coppens, P. *Cryst. Growth Des.* **2002**, *2*, 7. Field, J. E.; Combariza, M. Y.; Vachet, R. W.; Venkataraman, D. *J. Chem. Soc., Chem. Commun.*, **2002**, 2260. Ferlay, S.; Félix, O.; Hosseini, M. W.; Planeix, J.-M.; Kyritsakas, N. *J. Chem. Soc., Chem. Commun.* **2002**, 702. Aitipamula, S.; Thallapally, P. K.; Thaimattam, R.; Jaskólski, M.; Desiraju, G. R. *Org. Lett.* **2002**, *4*, 921. Nguyen, V. T.; Ahn, P. D.; Bishop, R.; Scudder, M. L.; Craig, D. C. *Eur. J. Org. Chem.* **2001**, 4489. Holman, K. T.; Pivovar, A. M.; Swift, J. A.; Ward, M. D. *Acc. Chem. Res.* **2001**, *34*, 107. Mak, T. C. W.; Xue, F. *J. Am. Chem. Soc.* **2000**, *122*, 9860. Sharma, C. V. K.; Clearfield, A. *J. Am. Chem. Soc.* **2000**, *122*, 4394. Corbin, P. S.; Zimmerman, S. C. *J. Am. Chem. Soc.* **2000**, *122*, 3779. Cantrill, S. J.; Pease, A. R.; Stoddart, J. F. *J. Chem. Soc., Dalton Trans.* **2000**, 3715. Batchelor,

E.; Klinowski, J.; Jones, W. *J. Mater. Chem.* **2000**, *10*, 839. Videnova-Adrabinska, V.; Janeczko, E. *J. Mater. Chem.* **2000**, *10*, 555. Akazome, M.; Suzuki, S.; Shimizu, Y.; Henmi, K.; Ogura, K. *J. Org. Chem.* **2000**, *65*, 6917. Baumeister, B.; Matile, S. *J. Chem. Soc., Chem. Commun.* **2000**, 913. Chowdhry, M. M.; Mingos, D. M. P.; White, A. J. P.; Williams, D. J. *J. Chem. Soc., Perkin Trans. 1* **2000**, 3495. Gong, B.; Zheng, C.; Skrzypczak-Jankun, E.; Zhu, J. *Org. Lett.* **2000**, *2*, 3273. Krische, M. J.; Lehn, J.-M.; Kyritsakas, N.; Fischer, J.; Wegelius, E. K.; Rissanen, K. *Tetrahedron* **2000**, *56*, 6701. Aakeröy, C. B.; Beatty, A. M.; Nieuwenhuyzen, M.; Zou, M. *Tetrahedron* **2000**, *56*, 6693. Kobayashi, K.; Shirasaka, T.; Horn, E.; Furukawa, N. *Tetrahedron Lett.* **2000**, *41*, 89. Fuchs, K.; Bauer, T.; Thomann, R.; Wang, C.; Friedrich, C.; Mülhaupt, R. *Macromolecules* **1999**, *32*, 8404. Holý, P.; Závada, J.; Císarová, I.; Podlaha, J. *Angew. Chem., Int. Ed. Engl.* **1999**, *38*, 381. Karle, I. L.; Ranganathan, D.; Kurur, S. *J. Am. Chem. Soc.* **1999**, *121*, 7156. Chin, D. N.; Palmore, G. T. R.; Whitesides, G. M. *J. Am. Chem. Soc.* **1999**, *121*, 2115. Hanessian, S.; Saladino, R.; Margarita, R.; Simard, M. *Chem. Eur. J.* **1999**, *5*, 2169. Biradha, K.; Dennis, D.; MacKinnon, V. A.; Sharma, C. V. K.; Zaworotko, M. J. *J. Am. Chem. Soc.* **1998**, *120*, 11894. Schauer, C. L.; Matwey, E.; Fowler, F. W.; Lauher, J. W. *J. Am. Chem. Soc.* **1997**, *119*, 10245. Lambert, J. B.; Zhao, Y.; Stern, C. L. *J. Phys. Org. Chem.* **1997**, *10*, 229. MacGillivray, L. R.; Atwood, J. L. *Nature* **1997**, *389*, 469. Adam, K. R.; Atkinson, I. M.; Davis, R. L.; Lindoy, L. F.; Mahinay, M. S.; McCool, B. J.; Skelton, B. W.; White, A. H. *J. Chem. Soc., Chem. Commun.* **1997**, 467. Kinbara, K.; Hashimoto, Y.; Sukegawa, M.; Nohira, H.; Saigo, K. *J. Am. Chem. Soc.* **1996**, *118*, 3441. Munakata, M.; Wu, L. P.; Yamamoto, M.; Kuroda-Sowa, T.; Maekawa, M. *J.*

Am. Chem. Soc. **1996**, *118*, 3117. Hartgerink, J. D.; Granja, J. R.; Milligan, R. A.; Ghadiri, M. R. *J. Am. Chem. Soc.* **1996**, *118*, 43. Hollingsworth, M. D.; Brown, M. E.; Hillier, A. C.; Santarsiero, B. D.; Chaney, J. D. *Science* **1996**, *273*, 1355. Lawrence, D. S.; Jiang, T.; Levett, M. *Chem. Rev.* **1995**, *95*, 2229. Ermer, O.; Eling, A. *J. Chem. Soc., Perkin Trans. 2* **1994**, 925. Venkataraman, D.; Lee, S.; Zhang, J.; Moore, J. S. *Nature* **1994**, *371*, 591.

12. Bhyrappa, P.; Wilson, S. R.; Suslick, K. S. *J. Am. Chem. Soc.* **1997**, *119*, 8492.
13. Nangia, A.; Desiraju, G. R. *Top. Curr. Chem.* **1998**, *198*, 57. Desiraju, G. R. *Angew. Chem., Int. Ed. Engl.* **1995**, *34*, 2311.
14. Mullin, J. W. *Crystallization*; Butterworth-Heinemann: Oxford, 1997.
15. For a review of diamondoid hydrogen-bonded networks, see: Zaworotko, M. J. *Chem. Soc. Rev.* **1994**, *23*, 283.
16. For discussions of interpenetration in networks, see: Batten, S. R. *CrystEngComm* **2001**, *18*, 1. Batten, S. R.; Robson, R. *Angew. Chem., Int. Ed. Engl.* **1998**, *37*, 1460.
17. An updated list of examples of interpenetration is available on the web site of Dr. Stuart R. Batten at Monash University (www.chem.monash.edu.au).
18. The percentage of volume accessible to guests was estimated by the PLATON program.[19] PLATON calculates the accessible volume by allowing a spherical probe of variable radius to roll over the internal van der Waals surface of the crystal structure. PLATON uses a default value of 1.20 Å for the radius of the probe, which is an appropriate model for small guests such as water. The van der Waals radii used to define surfaces for these calculations are as follows: C: 1.70 Å, H: 1.20 Å, N: 1.55 Å, O: 1.52 Å, and S: 1.80 Å. If V is the volume of the unit cell and V_g is the guest-

accessible volume as calculated by PLATON, then the porosity P in % is given by $100V_g/V$.

19. Spek, A. L. *PLATON, A Multipurpose Crystallographic Tool*; Utrecht University: Utrecht, The Netherlands, 2001. van der Sluis, P.; Spek, A. L. *Acta Crystallogr.* **1990**, *A46*, 194.

20. Galoppini, E.; Gilardi, R. *J. Chem. Soc., Chem. Commun.* **1999**, 173. Oldham, W. J., Jr.; Lachicotte, R. J.; Bazan, G. C. *J. Am. Chem. Soc.* **1998**, *120*, 2987. Thaimattam, R.; Reddy, D. S.; Xue, F.; Mak, T. C. W.; Nangia, A.; Desiraju, G. R. *New J. Chem.* **1998**, 143. Lloyd, M. A.; Brock, C. P. *Acta Crystallogr.* **1997**, *B53*, 780. Reddy, D. S.; Craig, D. C.; Desiraju, G. R. *J. Am. Chem. Soc.* **1996**, *118*, 4090. Charissé, M.; Gauthey, V.; Dräger, M. *J. Organomet. Chem.* **1993**, *448*, 47. Charissé, M.; Roller, S.; Dräger, M. *J. Organomet. Chem.* **1992**, *427*, 23.

21. Robbins, A.; Jeffrey, G. A.; Chesick, J. P.; Donohue, J.; Cotton, F. A.; Frenz, B. A.; Murillo, C. A. *Acta Crystallogr.* **1975**, *B31*, 2395.

22. Gruhnert, V.; Kirfel, A.; Will, G.; Wallrafen, F.; Recker, K. *Z. Kristallogr.* **1983**, *163*, 53.

23. McMullan, R. K.; Kvick, Å. *Acta Crystallogr.* **1990**, *B46*, 390.

24. Hollingsworth, M. D.; Santarsiero, B. D.; Harris, K. D. M. *Angew. Chem., Int. Ed. Engl.* **1994**, *33*, 649.

25. Gopal, R.; Robertson, B. E.; Rutherford, J. S. *Acta Crystallogr.* **1989**, *C45*, 257.

26. Chan, T.-L.; Mak, T. C. W. *J. Chem. Soc., Perkin Trans. 2* **1983**, 777.

27. Flippen, J. L.; Karle, J.; Karle, I. L. *J. Am. Chem. Soc.* **1970**, *92*, 3749.

28. Tam, W.; Eaton, D. F.; Calabrese, J. C.; Williams, I. D.; Wang, Y.; Anderson, A. G. *Chem. Mater.* **1989**, *1*, 128.

29. van der Sluis, P.; Schouten, A.; Kanters, J. A. *Acta Crystallogr.* **1990**, *C46*, 2165.

30. Byrn, M. P.; Curtis, C. J.; Khan, S. I.; Sawin, P. A.; Tsurumi, R.; Strouse, C. E. *J. Am. Chem. Soc.* **1990**, *112*, 1865.

31. Brouwer, E. B.; Udachin, K. A.; Enright, G. D.; Ripmeester, J. A.; Ooms, K. J.; Halchuk, P. A. *J. Chem. Soc., Chem. Commun.* **2001**, 565.

32. Lindner, K.; Saenger, W. *Biochem. Biophys. Res. Commun.* **1980**, *92*, 933.

33. Sawaki, T.; Endo, K.; Kobayashi, K.; Hayashida, O.; Aoyama, Y. *Bull. Chem. Soc. Jpn.* **1997**, *70*, 3075.

34. Saied, O.; Maris, T.; Wuest, J. D., unpublished results.

35. Langer, V.; Becker, H. D. *Z. Kristallogr.* **1992**, *199*, 313.

36. Quillin, M. L.; Matthews, B. W. *Acta Crystallogr.* **2000**, *D56*, 791. Andersson, K. M.; Hovmöller, S. *Acta Crystallogr.* **2000**, *D56*, 789.

37. Byrn, M. P.; Curtis, C. J.; Hsiou, Y.; Khan, S. I.; Sawin, P. A.; Tendick, S. K.; Terzis, A.; Strouse, C. E. *J. Am. Chem. Soc.* **1993**, *115*, 9480.

38. Weber, E.; Ahrendt, J.; Czugler, M.; Csöregh, I. *Angew. Chem., Int. Ed. Engl.* **1986**, *25*, 746. Czugler, M.; Stezowski, J. J.; Weber, E. *J. Chem. Soc., Chem. Commun.* **1983**, 154. Schenk, H. *Acta Crystallogr.* **1972**, *B28*, 625.

39. Spek, A. L., private communication (Refcode VEXNUH in the November 2002 version of the Cambridge Structural Database).

40. Tejeda, A.; Oliva, A. I.; Simón, L.; Grande, M.; Caballero, M. C.; Morán, J. R. *Tetrahedron Lett.* **2000**, *41*, 4563. Smith, D. K.; Zingg, A.; Diederich, F. *Helv. Chim.*

Acta **1999**, *82*, 1225. Das, G.; Hamilton, A. D. *Tetrahedron Lett.* **1997**, *38*, 3675. Egli, M.; Dobler, M. *Helv. Chim. Acta* **1986**, *69*, 626. Dobler, M.; Dumic, M.; Egli, M.; Prelog, V. *Angew. Chem., Int. Ed. Engl.* **1985**, *24*, 792.

41. Palmieri, P.; Samorì, B. *J. Am. Chem. Soc.* **1981**, *103*, 6818.
42. Chou, C.-H.; Reddy, D. S.; Shu, C.-F. *J. Polym. Sci., Part A* **2002**, *40*, 3615.
43. Wong, K.-T.; Chien, Y.-Y.; Chen, R.-T.; Wang, C.-F.; Lin, Y.-T.; Chiang, H.-H.; Hsieh, P.-Y.; Wu, C.-C.; Chou, C. H.; Su, Y. O.; Lee, G.-H.; Peng, S.-M. *J. Am. Chem. Soc.* **2002**, *124*, 11576. Wu, F.-I.; Dodda, R.; Reddy, D. S.; Shu, C.-F. *J. Mater. Chem.* **2002**, *12*, 2893. Katsis, D.; Geng, Y. H.; Ou, J. J.; Culligan, S. W.; Trajkovska, A.; Chen, S. H.; Rothberg, L. J. *Chem. Mater.* **2002**, *14*, 1332. Pei, J.; Ni, J.; Zhou, X.-H.; Cao, X.-Y.; Lai, Y.-H. *J. Org. Chem.* **2002**, *67*, 4924. Crispin, A.; Crispin, X.; Fahlman, M.; dos Santos, D. A.; Cornil, J.; Johansson, N.; Bauer, J.; Weissörtel, F.; Salbeck, J.; Brédas, J. L.; Salaneck, W. R. *J. Chem. Phys.* **2002**, *116*, 8159. Tian, H.; Chen, B.; Liu, P.-H. *Chem. Lett.* **2001**, 990. Marsitzky, D.; Murray, J.; Scott, J. C.; Carter, K. R. *Chem. Mater.* **2001**, *13*, 4285. Wang, S.; Oldham, W. J., Jr.; Hudack, R. A., Jr.; Bazan, G. C. *J. Am. Chem. Soc.* **2000**, *122*, 5695. Johansson, N.; Salbeck, J.; Bauer, J.; Weissörtel, F.; Bröms, P.; Andersson, A.; Salaneck, W. R. *Synth. Met.* **1999**, *101*, 405. Kim, S. Y.; Lee, M.; Boo, B. H. *J. Chem. Phys.* **1998**, *109*, 2593. Bach, U.; Lupo, D.; Comte, P.; Moser, J. E.; Weissörtel, F.; Salbeck, J.; Spreitzer, H.; Grätzel, M. *Nature* **1998**, *395*, 583.
44. Wu, R.; Schumm, J. S.; Pearson, D. L.; Tour, J. M. *J. Org. Chem.* **1996**, *61*, 6906.
45. Hetzel, S.; Maris, T.; Simard, M.; Wuest, J. D., unpublished results.

46. Geiger, S.; Joannic, M.; Pesson, M.; Techer, H.; Lagrange, E.; Aurousseau, M. *Chim. Thér.* **1966**, 425.

47. Chew, W.; Hynes, R. C.; Harpp, D. N. *J. Org. Chem.* **1993**, *58*, 4398. Chuang, C.; Lapin, S. C.; Schrock, A. K.; Schuster, G. B. *J. Am. Chem. Soc.* **1985**, *107*, 4238.

48. Campbell, N.; Scott, A. H. *J. Chem. Soc. (C)* **1966**, 1050.

49. Rothuis, R.; Font Freide, J. J. H. M.; Buck, H. M. *Recl. Trav. Chim. Pays-Bas* **1973**, *92*, 1308.

50. Drechsler, U.; Hanack, M. *Synlett* **1998**, 1207.

51. Simons, J. K.; Saxton, M. R. *Organic Syntheses*; Wiley: New York, 1963; Coll. Vol. IV, p 78.

52. Doyle, M. P.; Dellaria, J. F., Jr.; Siegfried, B.; Bishop, S. W. *J. Org. Chem.* **1977**, *42*, 3494.

53. The dimensions of a channel in a particular direction correspond to the cross section of an imaginary cylinder that could be passed through the hypothetical open network in the given direction in contact with the van der Waals surface. Such values are inherently conservative because 1) they measure the cross section at the most narrow constriction, and 2) they systematically underestimate the sizes of channels that are not uniform and linear.

54. Ellis, G. P.; Romney-Alexander, T. M. *Chem. Rev.* **1987**, *87*, 779.

55. The composition was estimated by X-ray crystallography and by ^{1}H NMR spectroscopy of dissolved samples. The amount of included H_2O could not be determined accurately.

56. Representations of channels were generated by the Cavities option in the program ATOMS (*ATOMS*, Version 5.1; Shape Software: 521 Hidden Valley Road, Kingsport, TN 37663; www.shapesoftware.com). We are grateful to Eric Dowty of Shape Software for integrating this capacity in ATOMS at our suggestion.

57. Dunitz, J. D. *J. Chem. Soc., Chem. Commun.* **2003**, 545. Desiraju, G. R. *Nature Materials* **2002**, *1*, 77. Gavezzotti, A. *Acc. Chem. Res.* **1994**, *27*, 309.

58. Ukai, T.; Kawazura, H.; Ishii, Y.; Bonnet, J. J.; Ibers, J. A. *J. Organomet. Chem.* **1974**, *65*, 253.

59. Sheldrick, G. M. *SHELXS-97, Program for the Solution of Crystal Structures* and *SHELXL-97, Program for the Refinement of Crystal Structures*; Universität Göttingen: Germany, 1997.

Chapitre 6

Conclusion

Conclusion

Les travaux présentés tout au long des chapitres précédents se sont concentrés principalement autour de deux thèmes majeurs soit l'étude du potentiel de certaines fonctions comme groupements d'association intermoléculaire et le développement de nouveaux squelettes pouvant servir à l'élaboration de nouveaux tectons.

L'étude du potentiel des phénols comme groupe de reconnaissance en tectonique moléculaire a mis en lumière la difficulté d'utiliser de façon fiable cette fonction pour l'élaboration de réseaux supramoléculaires, la principale difficulté étant l'absence de motif d'association récurrent. En effet, la fonction phénolique ne semble pas présenter une tendance à répéter un motif d'association précis, rendant ainsi son utilisation moins intéressante étant donné l'incertitude quant à la nature de l'association intermoléculaire adoptée.

Les acides boroniques semblent présenter un meilleur potentiel d'utilisation comme éléments directeurs pour l'élaboration de réseaux supramoléculaires. Le motif d'association dimérique analogue à celui des acides carboxyliques a pu être utilisé avec succès dans l'élaboration de réseaux supramoléculaires poreux. Ces résultats sont intéressants à plusieurs niveaux. Premièrement, notre étude montre pour la première fois la possibilité d'utiliser les acides boroniques comme élément d'association intermoléculaire, un potentiel qui n'avait pas encore été examiné jusque là. Deuxièmement, l'étude montre que des modifications rationnelles au niveau de la structure moléculaire du tecton ont un impact sur les propriétés du matériau créé. En effet, lorsque nous passons de l'acide boronique dérivé du tétraphénylméthane à celui dérivé du tétraphénylsilane, il y a augmentation de la longueur de chacune des branches tétraédriques composant le tecton, du fait de la plus grande longueur de la liaison Si-C. Cette augmentation de la longueur au niveau moléculaire se répercute au niveau supramoléculaire par un agrandissement de la dimension des cavités et, par le fait même, de la porosité du solide. Ces observations tendent à supporter une des hypothèses de base de la tectonique moléculaire voulant que de simples modifications au niveau de la

structure moléculaire des tectons modifient de façon prévisible les propriétés du matériau créé.

La tectonique moléculaire repose également sur l'utilisation de squelettes moléculaires choisis soigneusement. Parmi ceux-ci, les dérivés du tétraphénylméthane et du tétraphénylsilane occupent une place importante du fait de leur capacité à orienter efficacement dans une orientation tétraédrique des groupes d'association intermoléculaire. Le développement d'une approche efficace pour la fonctionalisation de ces squelettes moléculaires tétraédriques élargit le nombre de différents dérivés possibles, rendant ainsi cette classe de molécules encore plus attrayante en tant que blocs de construction pour l'élaboration de réseaux supramoléculaires. Les différents dérivés du tétraphénylméthane et du tétraphénylsilane présentés au Chapitre 2 constituent une gamme de blocs de construction d'autant plus attrayants du fait qu'ils sont disponibles en quelques étapes simples à partir de simples précurseurs. De plus, ces dérivés sont isolés aisément par de simples processus de cristallisation, ce qui évite les purifications par chromatographie, souvent peu couronnées de succès dans le cas des molécules appartenant à la famille du tétraphénylméthane ou du tétraphénylsilane.

L'étude du 9,9'-spirobifluorène comme squelette moléculaire dans la synthèse de tectons a été entreprise notamment afin de comparer le comportement de tectons basés sur cette molécule avec celui des analogues dérivés du tétraphénylméthane. Bien que la cristallisation des tectons *para*-substitués du 9,9'-spirobifluorène n'ait pu être achevée, empêchant ainsi une comparaison directe avec leurs analogues dérivés du tétraphénylméthane, cette étude s'est révélée intéressante à plusieurs points de vue. Premièrement, des approches synthétiques pour la synthèse de dérivés tétrasubstitués aux positions 3,3',6 et 6', inaccessibles jusque là, ont été développées. Les différents intermédiaires synthétisés au cours de cette étude pourraient se révéler intéressant en eux-même comme blocs de construction supramoléculaire. Un autre élément intéressant de cette étude découle de l'utilisation de dérivés tétrasubstitués aux positions 2,2',7 et 7'. Nous avons démontré qu'il est possible d'accomplir la formation de réseaux supramoléculaire poreux en utilisant de tels dérivés avec des résultats parfois surprenants.

Ainsi, il a été possible de créer un réseau supramoléculaire poreux dans lequel près de 74% du volume est disponible pour l'inclusion de molécules invitées. Cette valeur est jusqu'à ce jour la plus grande porosité jamais observée dans le cas d'un solide organique non-ionique dans lequel de simples ponts hydrogène assurent le maintien des associations intermoléculaires.

Les dérivés du 9,9'-spirobifluorène présentent un potentiel important pour l'élaboration de réseaux supramoléculaires, potentiel d'autant plus important puisque relativement peu exploré jusqu'à présent. Des études se poursuivent afin d'étendre l'utilisation du 9,9'-spirobifluorène en chimie supramoléculaire.

Annexe

Supporting Information

Derivatives of Tetraphenylmethane and Tetraphenylsilane. Synthesis of New Tetrahedral Building Blocks for Molecular Construction

Jean-Hugues Fournier, Xin Wang, James D. Wuest

Département de chimie, Université de Montréal, Montréal, Québec H3C 3J7 Canada

Contents : ^{1}H and ^{1}C NMR spectra of tetrakis[(4-chloromethyl)phenyl]silane (13)

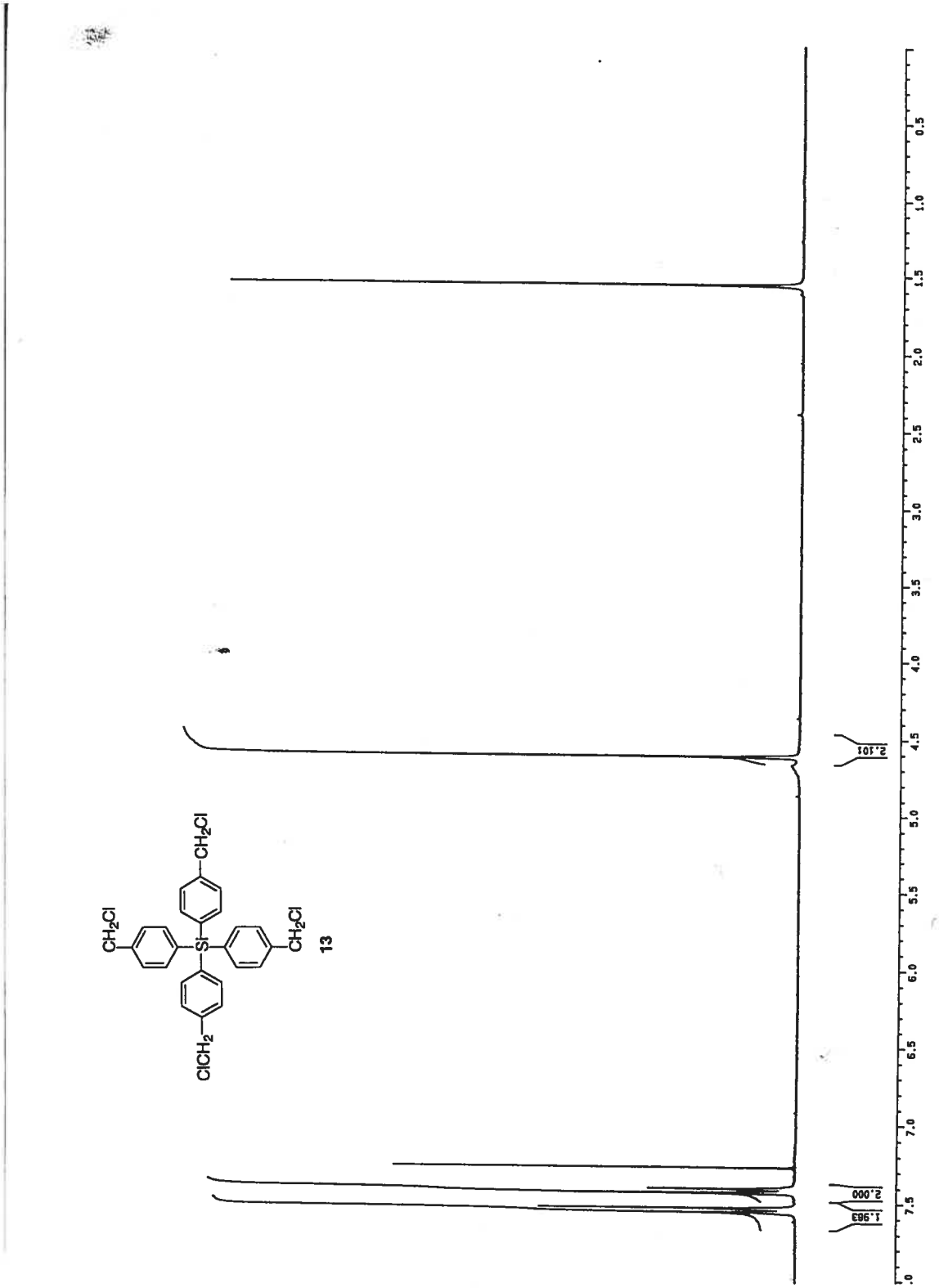
CH2Cl
CH2Cl
CH2Cl
ClCH2
Si
13
2.103
1.983
2.000

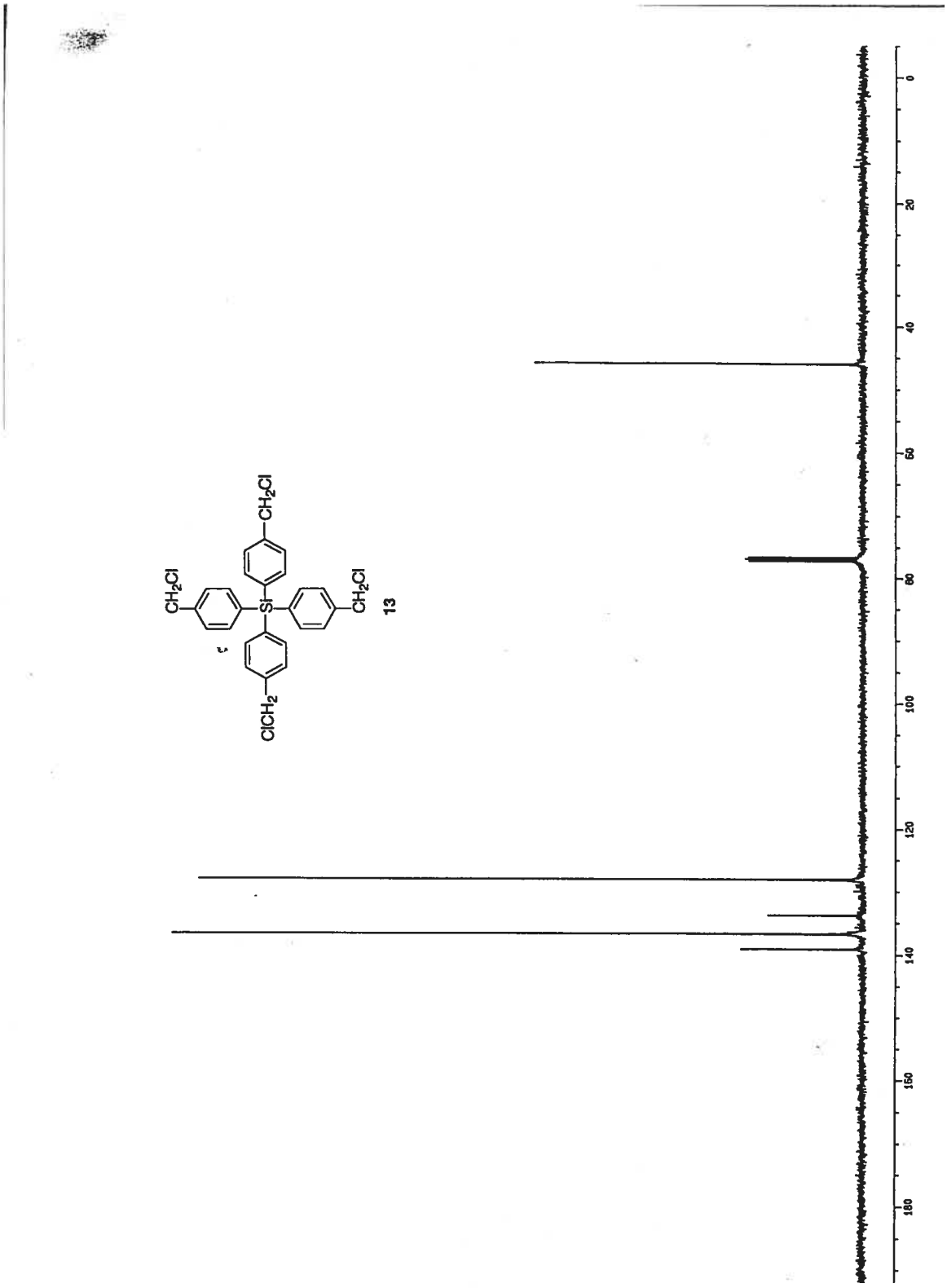
CH2Cl
CH2Cl
CH2Cl
ClCH2
Si
13
0
20
40
60
80
100
120
140
150
180

Supporting Information

Molecular Tectonics. Hydrogen-Bonded Networks Built from Tetraphenols Derived from Tetraphenylmethane and Tetraphenylsilane

Jean-Hugues Fournier,[1] Thierry Maris, Michel Simard, and James D. Wuest*

Département de Chimie, Université de Montréal
Montréal, Québec H3C 3J7 Canada

Contents

*Author to whom correspondence may be addressed:
[redacted]

Université de Montréal

CRYSTAL AND MOLECULAR STRUCTURE OF

C24 H20 O4 Si COMPOUND (JIW376)

Equipe WUEST

Département de chimie, Université de Montréal,

C.P. 6128, Succ. Centre-Ville, Montréal, Québec, H3C 3J7 (Canada)

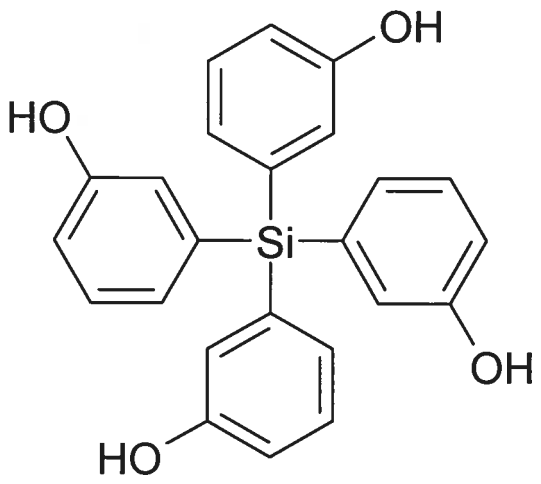

Structure solved and refined in the laboratory of X-ray diffraction, Université de Montréal by Dr. Thierry Maris.

Table 1. Crystal data and structure refinement for C24 H20 O4 Si.

Identification code	JIW376
Empirical formula	C24 H20 O4 Si
Formula weight	400.49
Temperature	226(2) K
Wavelength	1.54178 Å
Crystal system	Tetragonal
Space group	$I4_1/a$
Unit cell dimensions	a = 17.1641(2) Å $\alpha = 90°$ b = 17.1641(2) Å $\beta = 90°$ c = 7.26760(10) Å $\gamma = 90°$
Volume	2141.08(5)Å^3
Z	4
Density (calculated)	1.242 Mg/m^3
Absorption coefficient	1.188 mm^{-1}
F(000)	840
Crystal size	0.50 x 0.50 x 0.30 mm
Theta range for data collection	5.15 to 72.81°
Index ranges	$-21 \leq h \leq 21$, $-20 \leq k \leq 17$, $-8 \leq \ell \leq 8$
Reflections collected	12866
Independent reflections	1062 [R_{int} = 0.064]
Absorption correction	Semi-empirical from equivalents
Max. and min. transmission	1.0000 and 0.4900
Refinement method	Full-matrix least-squares on F^2
Data / restraints / parameters	1062 / 0 / 67
Goodness-of-fit on F^2	1.157
Final R indices [I>2sigma(I)]	R_1 = 0.0445, wR_2 = 0.1319
R indices (all data)	R_1 = 0.0446, wR_2 = 0.1321
Extinction coefficient	0.0016(5)
Largest diff. peak and hole	0.315 and -0.164 e/Å^3

Table 2. Atomic coordinates ($\times 10^4$) and equivalent isotropic displacement parameters ($Å^2 \times 10^3$) for C24 H20 O4 Si.

U_{eq} is defined as one third of the trace of the orthogonalized Uij tensor.

	x	y	z	U_{eq}
Si(1)	0	2500	6250	26(1)
O(12)	1688(1)	4785(1)	3539(2)	50(1)
C(10)	165(1)	3367(1)	4731(2)	29(1)
C(11)	862(1)	3777(1)	4764(2)	30(1)
C(12)	990(1)	4395(1)	3562(2)	34(1)
C(13)	415(1)	4626(1)	2353(2)	42(1)
C(14)	-286(1)	4226(1)	2328(3)	48(1)
C(15)	-407(1)	3596(1)	3474(2)	41(1)

Table 3. Hydrogen coordinates ($\times 10^4$) and isotropic displacement parameters ($Å^2 \times 10^3$) for C24 H20 O4 Si.

	x	y	z	U_{eq}
H(12)	1984	4594	4322	74
H(11)	1252	3637	5587	39
H(13)	496	5043	1559	55
H(14)	-682	4383	1540	62
H(15)	-868	3313	3399	53

Table 4. Anisotropic parameters ($Å^2 \times 10^3$) for C24 H20 O4 Si.

The anisotropic displacement factor exponent takes the form:

$$-2\pi^2 [h^2 a^{*2} U_{11} + \ldots + 2 h k a^* b^* U_{12}]$$

	U11	U22	U33	U23	U13	U12
Si(1)	23(1)	23(1)	33(1)	0	0	0
O(12)	34(1)	43(1)	72(1)	25(1)	-9(1)	-11(1)
C(10)	28(1)	25(1)	34(1)	0(1)	0(1)	0(1)
C(11)	27(1)	26(1)	38(1)	3(1)	-1(1)	2(1)
C(12)	29(1)	27(1)	45(1)	4(1)	1(1)	-3(1)
C(13)	46(1)	38(1)	43(1)	14(1)	-6(1)	-5(1)
C(14)	42(1)	54(1)	46(1)	16(1)	-17(1)	-8(1)
C(15)	35(1)	44(1)	45(1)	8(1)	-10(1)	-10(1)

Table 5. Bond lengths [Å] and angles [°] for C24 H20 O4 Si

Si(1)-C(10)#1	1.8740(14)	C(14)-C(15)	1.380(2)
Si(1)-C(10)	1.8740(14)	C(10)#1-Si(1)-C(10)	107.80(9)
Si(1)-C(10)#2	1.8740(14)	C(10)#1-Si(1)-C(10)#2	110.32(5)
Si(1)-C(10)#3	1.8740(14)	C(10)-Si(1)-C(10)#2	110.32(4)
O(12)-C(12)	1.374(2)	C(10)#1-Si(1)-C(10)#3	110.32(4)
C(10)-C(11)	1.389(2)	C(10)-Si(1)-C(10)#3	110.32(5)
C(10)-C(15)	1.397(2)	C(10)#2-Si(1)-C(10)#3	107.80(9)
C(11)-C(12)	1.392(2)	C(11)-C(10)-C(15)	118.30(13)
C(12)-C(13)	1.379(2)	C(11)-C(10)-Si(1)	121.45(11)
C(13)-C(14)	1.386(3)	C(15)-C(10)-Si(1)	120.20(11)
		C(10)-C(11)-C(12)	120.72(13)
		O(12)-C(12)-C(13)	118.43(14)
		O(12)-C(12)-C(11)	121.11(14)
		C(13)-C(12)-C(11)	120.46(14)
		C(12)-C(13)-C(14)	119.14(15)
		C(15)-C(14)-C(13)	120.70(15)
		C(14)-C(15)-C(10)	120.63(15)

Symmetry transformations used to generate equivalent atoms:

#1 -x,-y+1/2,z #2 -y+1/4,x+1/4,-z+5/4 #3 y-1/4,-x+1/4,-z+5/4

Table 6. Torsion angles [°] for C24 H20 O4 Si.

C(10)#1-Si(1)-C(10)-C(11-	118.12(13)	Si(1)-C(10)-C(11)-C(12)	176.75(12)
C(10)#2-Si(1)-C(10)-	C(11)121.37(15)	C(10)-C(11)-C(12)-O(12) -	177.58(15)
C(10)#3-Si(1)-C(10)-C(11)	2.39(12)	C(10)-C(11)-C(12)-C(13)	2.0(2)
C(10)#1-Si(1)-C(10)-C(15)	59.25(12)	O(12)-C(12)-C(13)-C(14)	178.43(18)
C(10)#2-Si(1)-C(10)-C(15)-	61.26(10)	C(11)-C(12)-C(13)-C(14)	-1.1(3)
C(10)#3-Si(1)-C(10)-	C(15)179.75(14)	C(12)-C(13)-C(14)-C(15)	-1.0(3)
C(15)-C(10)-C(11)-C(12)	- 0.7(2)	C(13)-C(14)-C(15)-C(10)	2.3(3)
		C(11)-C(10)-C(15)-C(14)	-1.4(3)
		Si(1)-C(10)-C(15)-C(14) -	178.90(15)

Symmetry transformations used to generate equivalent atoms:

#1 -x,-y+1/2,z #2 -y+1/4,x+1/4,-z+5/4 #3 y-1/4,-x+1/4,-z+5/4

Table 7. Bond lengths [Å] and angles [°] related to the hydrogen bonding for C24 H20 O4 Si.

D-H	..A	d(D-H)	d(H..A)	d(D..A)	<DHA
O(12)-H(12)	O(12)#4	0.83	1.90	2.7304(13)	176.4

Symmetry transformations used to generate equivalent atoms:

#1 -x,-y+1/2,z #2 -y+1/4,x+1/4,-z+5/4
#3 y-1/4,-x+1/4,-z+5/4 #4 -y+3/4,x+1/4,z+1/4

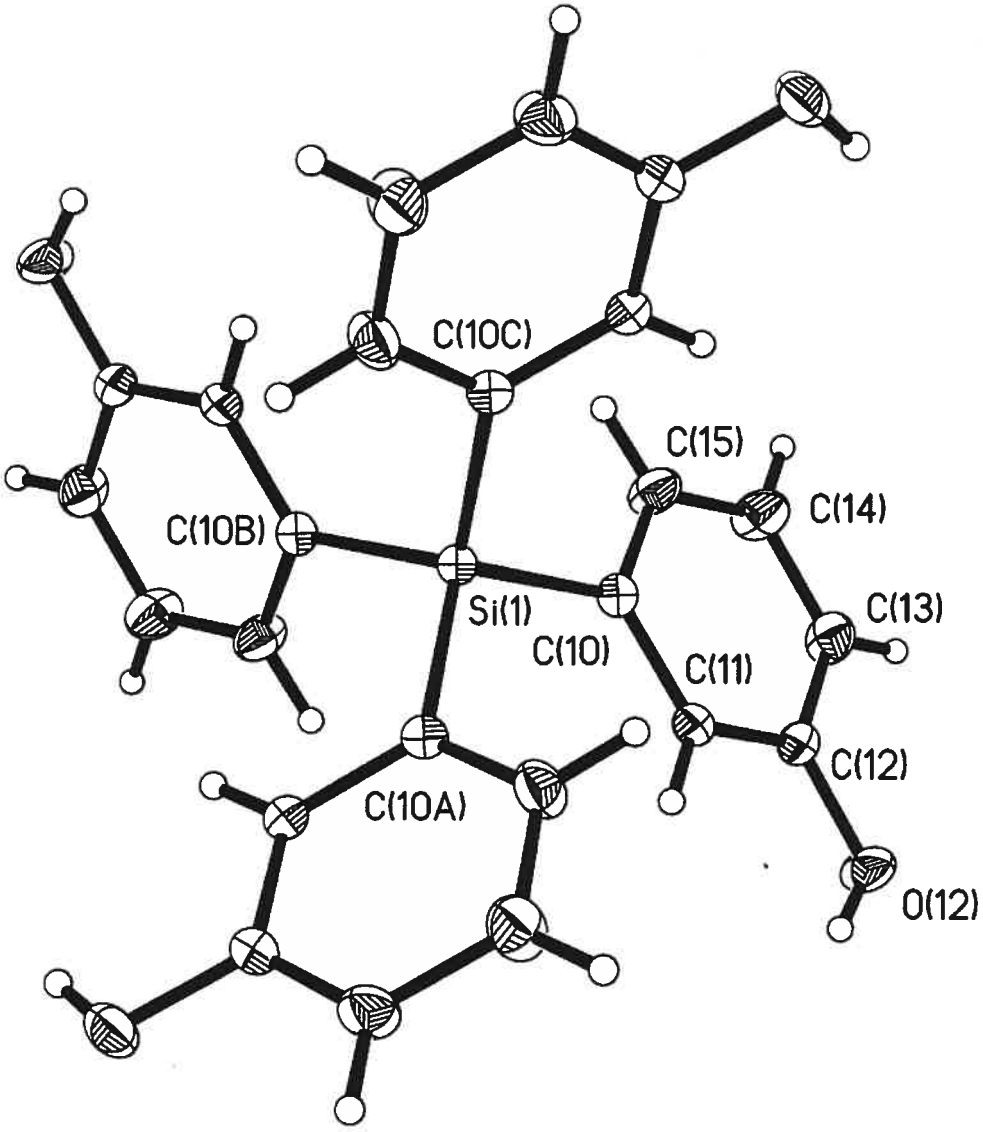

ORTEP view of the C24 H20 O4 Si compound with the numbering scheme adopted. Ellipsoids drawn at 30% probability level. Hydrogens represented by sphere of arbitrary size.

REFERENCES

International Tables for Crystallography (1992). Vol. C. Tables 4.2.6.8 and
6.1.1.4, Dordrecht: Kluwer Academic Publishers.

SAINT (1999) Release 6.06; Integration Software for Single Crystal Data. Bruker AXS Inc., Madison, WI 53719-1173.

Sheldrick, G.M. (1996). SADABS, Bruker Area Detector Absorption Corrections.
Bruker AXS Inc., Madison, WI 53719-1173.

Sheldrick, G.M. (1997). SHELXS97, Program for the Solution of Crystal Structures. Univ. of Gottingen, Germany.

Sheldrick, G.M. (1997). SHELXL97, Program for the Refinement of Crystal Structures. Univ. of Gottingen, Germany.

SHELXTL (1997) Release 5.10; The Complete Software Package for Single Crystal Structure Determination. Bruker AXS Inc., Madison, WI 53719-1173.

SMART (1999) Release 5.059; Bruker Molecular Analysis Research Tool. Bruker AXS Inc., Madison, WI 53719-1173.

Spek, A.L. (2000). PLATON, Molecular Geometry Program, 2000 version. University of Utrecht, Utrecht, Holland.

XPREP (1997) Release 5.10; X-ray data Preparation and Reciprocal space Exploration Program. Bruker AXS Inc., Madison, WI 53719-1173.

Université de Montréal

CRYSTAL AND MOLECULAR STRUCTURE OF

C29 H28 O6 COMPOUND (JIW226)

Equipe WUEST

Département de chimie, Université de Montréal,

C.P. 6128, Succ. Centre-Ville, Montréal, Québec, H3C 3J7 (Canada)

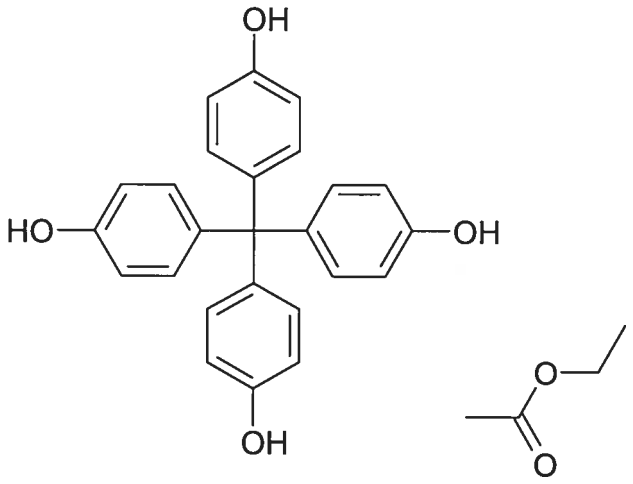

Structure solved and refined in the laboratory of X-ray diffraction, Université de Montréal by Dr. Thierry Maris.

Table 1. Crystal data and structure refinement for C29 H28 O6.

Identification code	JIW226
Empirical formula	C29 H28 O6
Formula weight	472.51
Temperature	223(2) K
Wavelength	1.54178 Å
Crystal system	Monoclinic
Space group	$P2_1/c$
Unit cell dimensions	a = 10.243(4) Å α = 90° b = 15.673(6) Å β = 100.86(4)° c = 15.412(8) Å γ = 90°
Volume	2429.9(18)Å^3
Z	4
Density (calculated)	1.292 Mg/m^3
Absorption coefficient	0.732 mm^{-1}
F(000)	1000
Crystal size	0.24 x 0.22 x 0.20 mm
Theta range for data collection	4.06 to 70.02°
Index ranges	$0 \le h \le 12$, $0 \le k \le 19$, $-18 \le \ell \le 18$
Reflections collected	4603
Independent reflections	4603 [R_{int} = 0.040]
Absorption correction	None
Max. and min. transmission	0.8700 and 0.8400
Refinement method	Full-matrix least-squares on F^2
Data / restraints / parameters	4603 / 0 / 317
Goodness-of-fit on F^2	1.117
Final R indices [I>2sigma(I)]	R_1 = 0.0584, wR_2 = 0.1740
R indices (all data)	R_1 = 0.0715, wR_2 = 0.1835
Extinction coefficient	0.0034(5)
Largest diff. peak and hole	0.470 and -0.452 e/Å^3

Table 2. Atomic coordinates (x 10^4) and equivalent isotropic displacement parameters ($Å^2$ x 10^3) for C29 H28 O6.

U_{eq} is defined as one third of the trace of the orthogonalized Uij tensor.

	x	y	z	U_{eq}
C(1)	2620(2)	2742(1)	-59(1)	32(1)
O(14)	3353(2)	5148(1)	-2715(1)	47(1)
C(11)	2748(2)	3358(1)	-823(1)	34(1)
C(12)	3869(2)	3889(1)	-714(1)	39(1)
C(13)	4057(2)	4473(1)	-1349(2)	40(1)
C(14)	3111(2)	4556(1)	-2115(1)	38(1)
C(15)	1985(2)	4052(1)	-2227(1)	42(1)
C(16)	1809(2)	3462(1)	-1586(1)	39(1)
O(24)	-1585(1)	292(1)	-737(1)	40(1)
C(21)	1395(2)	2149(1)	-258(1)	33(1)
C(22)	1223(2)	1615(1)	-996(1)	37(1)
C(23)	224(2)	1012(1)	-1152(1)	37(1)
C(24)	-628(2)	915(1)	-557(1)	34(1)
C(25)	-470(2)	1419(1)	185(1)	38(1)
C(26)	538(2)	2027(1)	332(1)	36(1)
O(34)	6841(1)	293(1)	496(1)	40(1)
C(31)	3807(2)	2116(1)	114(1)	33(1)
C(32)	4620(2)	1981(1)	-501(1)	36(1)
C(33)	5622(2)	1369(1)	-368(1)	37(1)
C(34)	5834(2)	887(1)	388(1)	33(1)
C(35)	5016(2)	990(1)	1008(1)	37(1)
C(36)	4007(2)	1587(1)	858(1)	37(1)
O(44)	2273(2)	5046(1)	2768(1)	53(1)
C(41)	2549(2)	3337(1)	729(1)	34(1)
C(42)	3514(2)	3390(1)	1486(1)	40(1)
C(43)	3419(2)	3966(2)	2156(2)	44(1)
C(44)	2342(2)	4507(1)	2074(1)	40(1)
C(45)	1368(2)	4483(1)	1320(2)	43(1)
C(46)	1483(2)	3908(1)	658(2)	41(1)
O(50)	8541(2)	1662(1)	2365(1)	62(1)
O(51)	7587(3)	2910(2)	2501(2)	105(1)
C(50)	7308(5)	1880(3)	3499(3)	127(2)
C(52)	7867(3)	2124(2)	2729(2)	62(1)
C(53)	8327(4)	3308(3)	1776(3)	102(1)
C(54)	7365(5)	3245(3)	1077(4)	167(3)

Table 3. Hydrogen coordinates ($\times 10^4$) and isotropic displacement parameters ($Å^2 \times 10^3$) for C29 H28 O6.

	x	y	z	U_{eq}
H(14)	2711	5168	-3133	71
H(12)	4511	3845	-193	47
H(13)	4826	4814	-1262	48
H(15)	1332	4109	-2742	50
H(16)	1034	3127	-1674	46
H(24)	-1982	249	-317	60
H(22)	1803	1668	-1398	45
H(23)	121	668	-1660	45
H(25)	-1041	1354	591	45
H(26)	642	2365	844	44
H(34)	7074	180	1029	59
H(32)	4488	2311	-1019	43
H(33)	6153	1287	-797	44
H(35)	5150	657	1524	44
H(36)	3438	1639	1267	44
H(44)	1843	5479	2581	79
H(42)	4256	3027	1549	48
H(43)	4088	3986	2665	53
H(45)	634	4853	1259	51
H(46)	825	3900	143	49
H(51A)	7874	1455	3840	191
H(51B)	6425	1644	3305	191
H(51C)	7252	2378	3864	191
H(53A)	8586	3903	1909	123
H(53B)	9110	2974	1709	123
H(54A)	7671	3469	564	250
H(54B)	6600	3568	1176	250
H(54C)	7119	2650	978	250

Table 4. Anisotropic parameters ($Å^2$ x 10^3) for C29 H28 O6.

The anisotropic displacement factor exponent takes the form:

$$-2\pi^2 [h^2 a^{*2} U_{11} + ... + 2 h k a^* b^* U_{12}]$$

	U11	U22	U33	U23	U13	U12
C(1)	30(1)	33(1)	33(1)	0(1)	5(1)	-1(1)
O(14)	49(1)	46(1)	48(1)	13(1)	11(1)	2(1)
C(11)	32(1)	32(1)	36(1)	0(1)	6(1)	2(1)
C(12)	36(1)	38(1)	40(1)	4(1)	1(1)	-2(1)
C(13)	36(1)	35(1)	48(1)	4(1)	5(1)	-3(1)
C(14)	40(1)	32(1)	43(1)	5(1)	10(1)	6(1)
C(15)	39(1)	43(1)	40(1)	4(1)	2(1)	4(1)
C(16)	31(1)	40(1)	43(1)	2(1)	4(1)	-1(1)
O(24)	37(1)	37(1)	46(1)	-4(1)	9(1)	-6(1)
C(21)	29(1)	31(1)	37(1)	0(1)	5(1)	0(1)
C(22)	35(1)	40(1)	39(1)	-4(1)	11(1)	-2(1)
C(23)	38(1)	37(1)	38(1)	-7(1)	9(1)	-2(1)
C(24)	28(1)	30(1)	42(1)	-1(1)	4(1)	1(1)
C(25)	36(1)	40(1)	39(1)	-5(1)	12(1)	-2(1)
C(26)	38(1)	35(1)	37(1)	-6(1)	9(1)	-3(1)
O(34)	36(1)	37(1)	46(1)	6(1)	8(1)	5(1)
C(31)	29(1)	32(1)	36(1)	1(1)	5(1)	-3(1)
C(32)	36(1)	35(1)	36(1)	5(1)	8(1)	1(1)
C(33)	36(1)	37(1)	38(1)	3(1)	11(1)	1(1)
C(34)	28(1)	29(1)	42(1)	1(1)	6(1)	-3(1)
C(35)	38(1)	35(1)	39(1)	8(1)	9(1)	-1(1)
C(36)	34(1)	37(1)	42(1)	5(1)	12(1)	0(1)
O(44)	75(1)	41(1)	44(1)	-9(1)	12(1)	-6(1)
C(41)	33(1)	32(1)	37(1)	1(1)	6(1)	-5(1)
C(42)	34(1)	41(1)	43(1)	0(1)	3(1)	-1(1)
C(43)	46(1)	45(1)	39(1)	-1(1)	1(1)	-8(1)
C(44)	53(1)	32(1)	38(1)	-4(1)	13(1)	-12(1)
C(45)	43(1)	36(1)	49(1)	-5(1)	9(1)	0(1)
C(46)	39(1)	38(1)	43(1)	-6(1)	0(1)	1(1)
O(50)	63(1)	48(1)	79(1)	-7(1)	25(1)	4(1)
O(51)	154(3)	56(1)	125(2)	12(1)	73(2)	32(2)
C(50)	208(6)	66(2)	144(4)	2(2)	126(4)	18(3)
C(52)	63(2)	44(1)	82(2)	-12(1)	24(2)	-2(1)
C(53)	70(2)	80(2)	151(4)	-35(3)	6(2)	7(2)
C(54)	118(4)	143(5)	206(6)	-94(5)	-54(4)	32(3)

Table 5. Bond lengths [Å] and angles [°] for C29 H28 O6

C(1)-C(41)	1.544(3)
C(1)-C(21)	1.545(3)
C(1)-C(31)	1.546(3)
C(1)-C(11)	1.548(3)
O(14)-C(14)	1.364(3)
C(11)-C(16)	1.382(3)
C(11)-C(12)	1.402(3)
C(12)-C(13)	1.379(3)
C(13)-C(14)	1.386(3)
C(14)-C(15)	1.381(3)
C(15)-C(16)	1.390(3)
O(24)-C(24)	1.376(2)
C(21)-C(26)	1.392(3)
C(21)-C(22)	1.396(3)
C(22)-C(23)	1.380(3)
C(23)-C(24)	1.389(3)
C(24)-C(25)	1.373(3)
C(25)-C(26)	1.392(3)
O(34)-C(34)	1.376(2)
C(31)-C(32)	1.390(3)
C(31)-C(36)	1.398(3)
C(32)-C(33)	1.391(3)
C(33)-C(34)	1.372(3)
C(34)-C(35)	1.395(3)
C(35)-C(36)	1.380(3)
O(44)-C(44)	1.376(3)
C(41)-C(42)	1.382(3)
C(41)-C(46)	1.399(3)
C(42)-C(43)	1.388(3)
C(43)-C(44)	1.379(3)
C(44)-C(45)	1.381(3)
C(45)-C(46)	1.384(3)
O(50)-C(52)	1.208(3)
O(51)-C(52)	1.299(4)
O(51)-C(53)	1.590(5)
C(50)-C(52)	1.463(5)
C(53)-C(54)	1.319(6)

C(41)-C(1)-C(21)	111.26(16)
C(41)-C(1)-C(31)	113.58(16)
C(21)-C(1)-C(31)	103.61(17)
C(41)-C(1)-C(11)	104.15(17)
C(21)-C(1)-C(11)	113.98(16)
C(31)-C(1)-C(11)	110.55(16)
C(16)-C(11)-C(12)	117.07(19)
C(16)-C(11)-C(1)	125.17(18)
C(12)-C(11)-C(1)	117.66(17)
C(13)-C(12)-C(11)	121.98(19)
C(12)-C(13)-C(14)	119.9(2)
O(14)-C(14)-C(15)	123.9(2)
O(14)-C(14)-C(13)	117.00(19)
C(15)-C(14)-C(13)	119.1(2)
C(14)-C(15)-C(16)	120.6(2)
C(11)-C(16)-C(15)	121.37(19)
C(26)-C(21)-C(22)	116.88(18)
C(26)-C(21)-C(1)	122.78(18)
C(22)-C(21)-C(1)	119.71(18)
C(23)-C(22)-C(21)	121.89(19)
C(22)-C(23)-C(24)	119.78(19)
C(25)-C(24)-O(24)	123.01(19)
C(25)-C(24)-C(23)	119.81(18)
O(24)-C(24)-C(23)	117.16(18)
C(24)-C(25)-C(26)	119.79(19)
C(25)-C(26)-C(21)	121.81(19)
C(32)-C(31)-C(36)	117.05(19)

C(32)-C(31)-C(1) 122.10(18)		C(41)-C(42)-C(43)	121.8(2)
		C(44)-C(43)-C(42)	119.9(2)
C(36)-C(31)-C(1)	120.43(18)	O(44)-C(44)-C(43)	117.6(2)
C(31)-C(32)-C(33)	121.65(19)	O(44)-C(44)-C(45)	122.4(2)
C(34)-C(33)-C(32)	119.94(19)	C(43)-C(44)-C(45)	119.9(2)
C(33)-C(34)-O(34)	118.10(18)	C(44)-C(45)-C(46)	119.3(2)
C(33)-C(34)-C(35)	119.92(18)	C(45)-C(46)-C(41)	122.1(2)
O(34)-C(34)-C(35)	121.96(18)	C(52)-O(51)-C(53)	116.8(3)
C(36)-C(35)-C(34)	119.41(19)	O(50)-C(52)-O(51)	124.0(3)
C(35)-C(36)-C(31)	121.91(19)	O(50)-C(52)-C(50)	124.5(3)
C(42)-C(41)-C(46)	116.82(19)	O(51)-C(52)-C(50)	111.5(3)
C(42)-C(41)-C(1)	124.61(18)	C(54)-C(53)-O(51)	99.4(4)
C(46)-C(41)-C(1)	118.42(17)		

Table 6. Bond lengths [Å] and angles [°] related to the hydrogen bonding for C29 H28 O6.

D-H	..A	d(D-H)	d(H..A)	d(D..A)	<DHA
O(14)-H(14)	O(24)#1	0.83	1.91	2.719(3)	165.1
O(24)-H(24)	O(34)#2	0.83	1.90	2.714(2)	168.1
O(34)-H(34)	O(44)#3	0.83	1.86	2.687(3)	173.0
O(44)-H(44)	O(50)#4	0.83	1.90	2.662(3)	152.0

Symmetry transformations used to generate equivalent atoms:

#1 -x,y+1/2,-z-1/2 #2 x-1,y,z
#3 -x+1,y-1/2,-z+1/2 #4 -x+1,y+1/2,-z+1/2

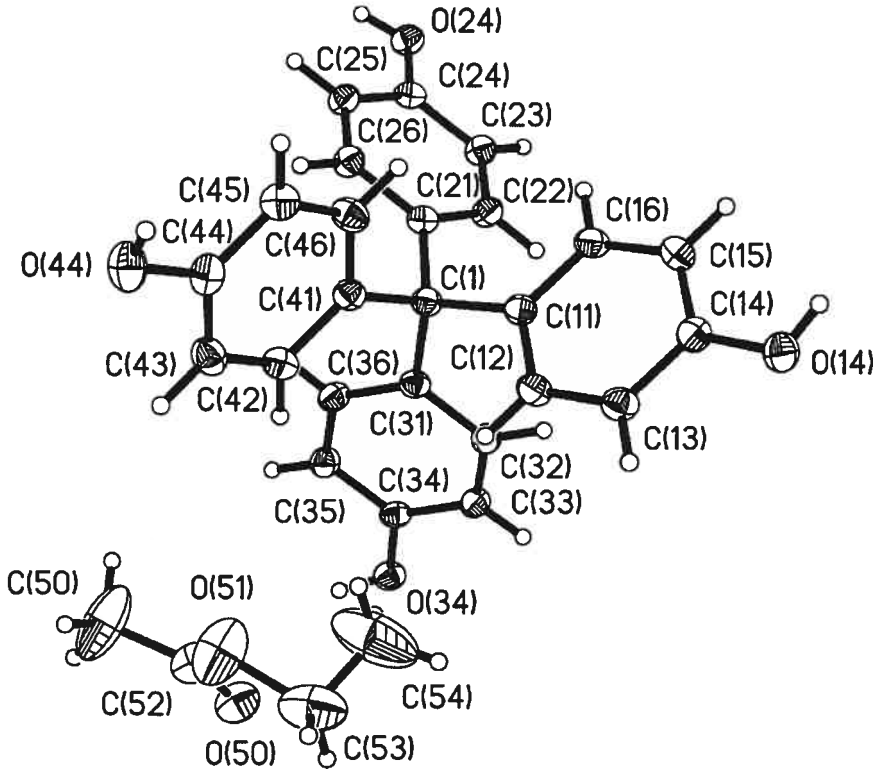

ORTEP view of the C29 H28 O6 compound with the numbering scheme adopted. Ellipsoids drawn at 30% probability level. Hydrogens represented by sphere of arbitrary size.

REFERENCES

Ahmed, F.R., Hall, S.R., Pippy, M.E. and Huber, C.P. (1973). NRC Crystallographic Computer Programs for the IBM/360. Accession Nos. 133-147 in J. Appl. Cryst. 6, 309-346.

Enraf-Nonius (1989). CAD-4 Software, Version 5.0. Enraf-Nonius, Delft, Holland.

Gabe, E.J., Le Page, Y., Charland, J.-P., Lee, F.L. and White, P.S. (1989). J. Appl. Cryst. 22, 384-387.

International Tables for Crystallography (1992). Vol. C. Tables 4.2.6.8 and 6.1.1.4, Dordrecht: Kluwer Academic Publishers.

Sheldrick, G.M. (1997). SHELXS97, Program for the Solution of Crystal Structures Univ. of Gottingen, Germany.

Sheldrick, G.M. (1997). SHELXL97, Program for the Refinement of Crystal Structures. Univ. of Gottingen, Germany.

SHELXTL (1997) Release 5.10; The Complete Software Package for Single Crystal Structure Determination. Bruker AXS Inc., Madison, WI 53719-1173.

Spek, A.L. (2000). PLATON, Molecular Geometry Program, 2000 version. University of Utrecht, Utrecht, Holland.

Université de Montréal

CRYSTAL AND MOLECULAR STRUCTURE OF

C24 H22 O5 Si COMPOUND (JIW262)

Equipe WUEST

Département de chimie, Université de Montréal,

C.P. 6128, Succ. Centre-Ville, Montréal, Québec, H3C 3J7 (Canada)

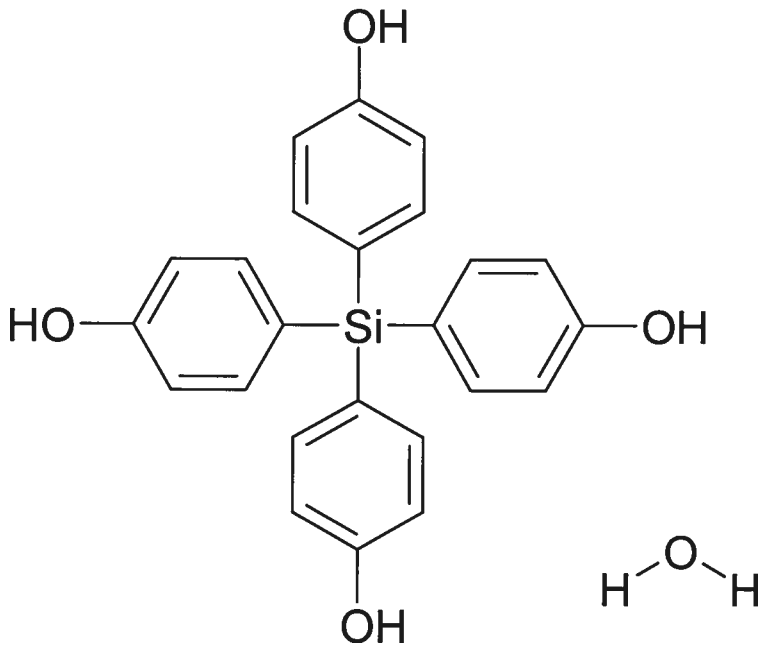

Structure solved and refined in the laboratory of X-ray diffraction, Université de Montréal by Dr. Thierry Maris.

Table 1. Crystal data and structure refinement for C24 H22 O5 Si.

Identification code	JIW262
Empirical formula	C24 H22 O5 Si
Formula weight	418.51
Temperature	210(2) K
Wavelength	1.54178 Å
Crystal system	Monoclinic
Space group	C2/c
Unit cell dimensions	a = 14.962(9) Å α = 90° b = 15.855(11) Å β = 111.49(5)° c = 19.697(13) Å γ = 90°
Volume	4348(5)Å^3
Z	8
Density (calculated)	1.279 Mg/m^3
Absorption coefficient	1.226 mm^{-1}
F(000)	1760
Crystal size	0.30 x 0.20 x 0.10 mm
Theta range for data collection	4.23 to 69.93°
Index ranges	$0 \leq h \leq 18$, $0 \leq k \leq 19$, $-23 \leq \ell \leq 22$
Reflections collected	4117
Independent reflections	4117 [R_{int} = 0.070]
Absorption correction	None
Max. and min. transmission	0.8900 and 0.7100
Refinement method	Full-matrix least-squares on F^2
Data / restraints / parameters	4117 / 2 / 279
Goodness-of-fit on F^2	1.064
Final R indices [I>2sigma(I)]	R_1 = 0.0784, wR_2 = 0.1879
R indices (all data)	R_1 = 0.1210, wR_2 = 0.2049
Largest diff. peak and hole	0.524 and -0.658 e/Å^3

Table 2. Atomic coordinates ($\times 10^4$) and equivalent isotropic displacement parameters ($Å^2 \times 10^3$) for C24 H22 O5 Si.

U_{eq} is defined as one third of the trace of the orthogonalized Uij tensor.

	x	y	z	U_{eq}
Si(1)	2420(1)	768(1)	2489(1)	43(1)
C(1)	1847(3)	1297(3)	3074(2)	42(1)
C(2)	1067(3)	961(3)	3228(2)	44(1)
C(3)	707(3)	1371(3)	3693(2)	46(1)
C(4)	1102(3)	2105(3)	4020(2)	43(1)
C(5)	1871(3)	2467(3)	3888(2)	50(1)
C(6)	2219(3)	2054(3)	3412(3)	54(1)
O(7)	732(2)	2489(2)	4489(2)	55(1)
C(11)	3571(3)	262(3)	3097(2)	41(1)
C(12)	3855(3)	-516(3)	2933(3)	56(1)
C(13)	4719(3)	-889(3)	3378(3)	58(1)
C(14)	5299(3)	-464(3)	3991(2)	48(1)
C(15)	5051(3)	316(3)	4172(2)	48(1)
C(16)	4186(3)	668(3)	3716(2)	50(1)
O(17)	6127(2)	-867(2)	4435(2)	62(1)
C(21)	2681(3)	1585(3)	1917(2)	43(1)
C(22)	2075(3)	2262(3)	1611(2)	53(1)
C(23)	2242(3)	2845(3)	1148(2)	54(1)
C(24)	3069(3)	2749(3)	980(2)	46(1)
C(25)	3677(3)	2094(3)	1265(2)	51(1)
C(26)	3506(3)	1520(3)	1727(2)	48(1)
O(27)	3229(2)	3325(2)	519(2)	61(1)
C(31)	1653(3)	-67(3)	1882(2)	42(1)
C(32)	1284(3)	-762(3)	2144(2)	52(1)
C(33)	764(3)	-1386(3)	1695(2)	54(1)
C(34)	604(3)	-1362(3)	961(2)	47(1)
C(35)	969(3)	-711(3)	679(2)	56(1)
C(36)	1475(3)	-72(3)	1135(2)	54(1)
O(37)	61(2)	-1992(2)	520(2)	65(1)
O(100)	7415(3)	78(3)	5386(3)	94(1)

Table 3. Hydrogen coordinates (x 10^4) and isotropic displacement parameters ($Å^2$ x 10^3) for C24 H22 O5 Si.

	x	y	z	U_{eq}
H(2)	784	445	3008	53
H(3)	178	1136	3784	55
H(5)	2149	2982	4115	60
H(6)	2737	2303	3315	65
H(71)	926	2990	4561	74
H(12)	3454	-806	2509	67
H(13)	4902	-1426	3259	69
H(15)	5457	606	4594	57
H(16)	4010	1209	3833	60
H(171)	6495	-514	4722	50
H(22)	1516	2327	1727	63
H(23)	1808	3298	951	64
H(25)	4232	2032	1144	61
H(26)	3947	1072	1922	58
H(27)	2948	3778	536	91
H(32)	1402	-797	2651	63
H(33)	513	-1837	1889	65
H(35)	873	-701	175	68
H(36)	1710	382	933	64
H(371)	173	-2012	132	122
H(101)	7210(80)	520(40)	5080(40)	260(60)
H(102)	7830(50)	-230(50)	5750(30)	180(40)

Table 4. Anisotropic parameters ($Å^2$ x 10^3) for C24 H22 O5 Si.

The anisotropic displacement factor exponent takes the form:

$$-2\pi^2 [h^2 a^{*2} U_{11} + ... + 2 h k a^* b^* U_{12}]$$

	U11	U22	U33	U23	U13	U12
Si(1)	32(1)	57(1)	49(1)	-1(1)	26(1)	0(1)
C(1)	29(2)	58(3)	45(2)	0(2)	23(2)	1(2)
C(2)	28(2)	61(3)	47(2)	-2(2)	18(2)	-7(2)
C(3)	29(2)	66(3)	51(3)	1(2)	23(2)	-3(2)
C(4)	32(2)	61(3)	45(2)	1(2)	23(2)	3(2)
C(5)	41(2)	58(3)	64(3)	-7(2)	36(2)	-8(2)
C(6)	42(2)	67(3)	70(3)	-13(3)	40(2)	-10(2)
O(7)	54(2)	69(2)	64(2)	0(2)	47(2)	6(2)
C(11)	34(2)	51(3)	50(3)	-1(2)	28(2)	1(2)
C(12)	44(2)	65(3)	59(3)	-9(3)	19(2)	0(2)
C(13)	47(2)	62(3)	66(3)	-10(3)	22(2)	8(2)
C(14)	36(2)	59(3)	54(3)	3(2)	23(2)	2(2)
C(15)	40(2)	55(3)	50(3)	-3(2)	18(2)	-1(2)
C(16)	40(2)	58(3)	56(3)	-6(2)	24(2)	1(2)
O(17)	38(2)	66(2)	73(2)	-6(2)	10(2)	5(2)
C(21)	35(2)	53(3)	50(3)	-2(2)	27(2)	-1(2)
C(22)	36(2)	67(3)	66(3)	12(3)	32(2)	11(2)
C(23)	41(2)	67(3)	63(3)	11(3)	32(2)	12(2)
C(24)	39(2)	58(3)	49(3)	4(2)	24(2)	-2(2)
C(25)	36(2)	61(3)	68(3)	5(2)	34(2)	3(2)
C(26)	35(2)	60(3)	60(3)	5(2)	31(2)	8(2)
O(27)	58(2)	65(2)	75(2)	18(2)	43(2)	7(2)
C(31)	35(2)	54(3)	46(2)	2(2)	24(2)	5(2)
C(32)	55(3)	63(3)	50(3)	0(2)	33(2)	-5(2)
C(33)	54(3)	64(3)	60(3)	-7(3)	40(2)	-13(2)
C(34)	41(2)	63(3)	50(3)	-10(2)	31(2)	-9(2)
C(35)	62(3)	71(3)	49(3)	-7(3)	36(2)	-12(3)
C(36)	48(2)	73(3)	53(3)	-1(2)	34(2)	-10(2)
O(37)	61(2)	87(3)	68(2)	-27(2)	50(2)	-30(2)
O(100)	76(3)	89(3)	89(3)	14(3)	-4(3)	-11(3)

Table 5. Bond lengths [Å] and angles [°] for C24 H22 O5 Si

Si(1)-C(21)	1.850(4)
Si(1)-C(31)	1.868(5)
Si(1)-C(1)	1.869(4)
Si(1)-C(11)	1.879(4)
C(1)-C(6)	1.387(6)
C(1)-C(2)	1.413(5)
C(2)-C(3)	1.383(5)
C(3)-C(4)	1.356(6)
C(4)-O(7)	1.379(4)
C(4)-C(5)	1.393(5)
C(5)-C(6)	1.391(6)
C(11)-C(12)	1.381(6)
C(11)-C(16)	1.388(6)
C(12)-C(13)	1.399(6)
C(13)-C(14)	1.377(6)
C(14)-C(15)	1.376(6)
C(14)-O(17)	1.383(5)
C(15)-C(16)	1.394(6)
C(21)-C(22)	1.392(6)
C(21)-C(26)	1.417(5)
C(22)-C(23)	1.384(6)
C(23)-C(24)	1.403(5)
C(24)-C(25)	1.359(6)
C(24)-O(27)	1.368(5)
C(25)-C(26)	1.376(6)
C(31)-C(36)	1.396(6)
C(31)-C(32)	1.412(6)
C(32)-C(33)	1.364(6)
C(33)-C(34)	1.377(6)
C(34)-C(35)	1.377(6)
C(34)-O(37)	1.378(5)
C(35)-C(36)	1.382(6)

C(21)-SI1-C(31)	108.90(19)
C(21)-SI1-C(1)	108.0(2)
C(31)-SI1-C(1)	113.53(18)
C(21)-SI1-C(11)	109.77(18)
C(31)-SI1-C(11)	108.1(2)
C(1)-SI1-C(11)	108.57(19)
C(6)-C(1)-C(2)	116.2(4)
C(6)-C(1)-SI1	119.4(3)
C(2)-C(1)-SI1	124.4(3)
C(3)-C(2)-C(1)	121.1(4)
C(4)-C(3)-C(2)	120.8(4)
C(3)-C(4)-O(7)	119.1(3)
C(3)-C(4)-C(5)	120.7(4)
O(7)-C(4)-C(5)	120.3(4)
C(6)-C(5)-C(4)	118.1(4)
C(1)-C(6)-C(5)	123.2(4)
C(12)-C(11)-C(16)	117.3(4)
C(12)-C(11)-SI1	121.4(3)
C(16)-C(11)-SI1	121.3(3)
C(11)-C(12)-C(13)	121.6(5)
C(14)-C(13)-C(12)	119.0(5)
C(15)-C(14)-C(13)	121.5(4)
C(15)-C(14)-O(17)	121.0(4)
C(13)-C(14)-O(17)	117.4(4)
C(14)-C(15)-C(16)	118.0(4)
C(11)-C(16)-C(15)	122.7(4)
C(22)-C(21)-C(26)	115.8(4)
C(22)-C(21)-SI1	123.6(3)
C(26)-C(21)-SI1	120.5(3)
C(23)-C(22)-C(21)	123.6(4)
C(22)-C(23)-C(24)	118.1(4)
C(25)-C(24)-O(27)	122.1(4)
C(25)-C(24)-C(23)	120.0(4)
O(27)-C(24)-C(23)	117.9(4)
C(24)-C(25)-C(26)	121.4(4)
C(25)-C(26)-C(21)	121.1(4)
C(36)-C(31)-C(32)	115.5(4)
C(36)-C(31)-SI1	120.9(3)
C(32)-C(31)-SI1	123.4(3)

C(33)-C(32)-C(31)	122.4(4)	C(35)-C(34)-O(37)	
C(32)-C(33)-C(34)	119.9(4)	121.2(4)	
C(33)-C(34)-C(35)	120.2(4)	C(34)-C(35)-C(36)	119.4(4)
C(33)-C(34)-O(37)	118.6(4)	C(35)-C(36)-C(31)	122.5(4)

Table 6. Bond lengths [Å] and angles [°] related to the hydrogen bonding for C24 H22 O5 Si.

D-H	..A	d(D-H)	d(H..A)	d(D..A)	<DHA
O(7)-H(71)	O(17)#1	0.84	1.87	2.683(5)	163.2
O(17)-H(171)	O(100)	0.84	1.78	2.611(6)	169.9
O(27)-H(27)	O(100)#2	0.84	1.96	2.781(6)	165.6
O(37)-H(371)	O(7)#3	0.84	1.91	2.692(4)	153.9

Symmetry transformations used to generate equivalent atoms:

#1 x-1/2,y+1/2,z #2 x-1/2,-y+1/2,z-1/2
#3 x,-y,z-1/2 #4 x+1/2,-y+1/2,z+1/2

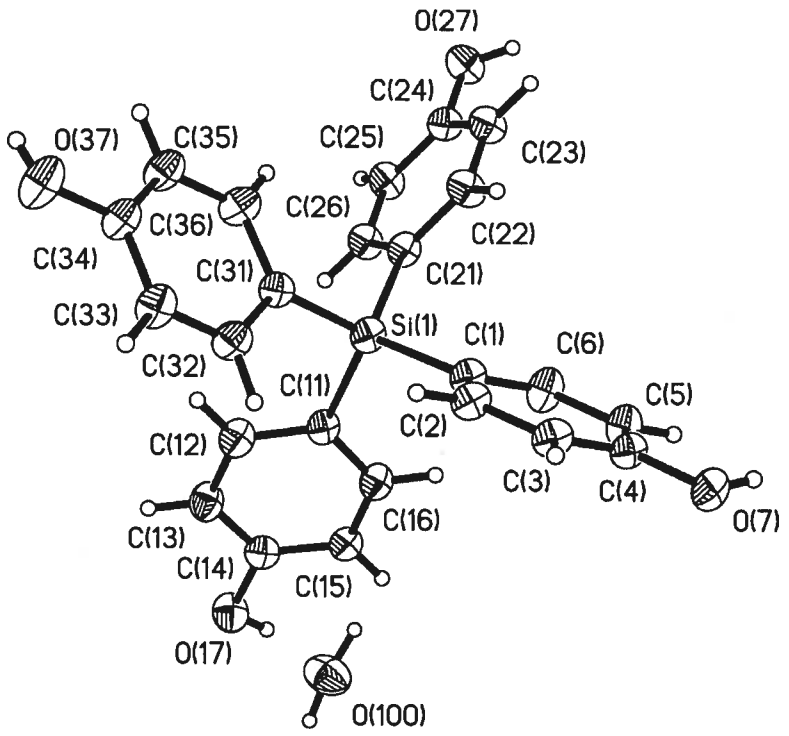

ORTEP view of the C24 H22 O5 Si compound with the numbering scheme adopted. Ellipsoids drawn at 30% probability level. Hydrogens represented by sphere of arbitrary size.

REFERENCES

Ahmed, F.R., Hall, S.R., Pippy, M.E. and Huber, C.P. (1973).
NRC Crystallographic Computer Programs for the IBM/360.
Accession Nos. 133-147 in J. Appl. Cryst. 6, 309-346.

Enraf-Nonius (1989). CAD-4 Software, Version 5.0. Enraf-Nonius, Delft, Holland.

Gabe, E.J., Le Page, Y., Charland, J.-P., Lee, F.L. and White, P.S. (1989). J.
Appl. Cryst. 22, 384-387.

International Tables for Crystallography (1992). Vol. C. Tables 4.2.6.8 and
6.1.1.4, Dordrecht: Kluwer Academic Publishers.

Sheldrick, G.M. (1997). SHELXS97, Program for the Solution of Crystal Structures
Univ. of Gottingen, Germany.

Sheldrick, G.M. (1997). SHELXL97, Program for the Refinement of Crystal Structures. Univ. of Gottingen, Germany.

SHELXTL (1997) Release 5.10; The Complete Software Package for Single Crystal Structure Determination. Bruker AXS Inc., Madison, WI 53719-1173.

Spek, A.L. (2000). PLATON, Molecular Geometry Program, 2000 version.
University of Utrecht, Utrecht, Holland.

Supporting Information

Molecular Tectonics. Use of the Hydrogen Bonding of Boronic Acids to Direct Supramolecular Construction

Jean-Hugues Fournier,[1] Thierry Maris, and James D. Wuest*

Département de Chimie, Université de Montréal
Montréal, Québec H3C 3J7 Canada

Wenzhuo Guo and Elena Galoppini*

Department of Chemistry, Rutgers University
Newark, New Jersey 07102 USA

Contents

*Authors to whom correspondence may be addressed: [redacted]

[redacted]

Université de Montréal

CRYSTAL AND MOLECULAR STRUCTURE OF

C25 H24 B4 O8 COMPOUND (JIW360)

Wednesday, January 29, 2003

Equipe WUEST

Département de chimie, Université de Montréal,

C.P. 6128, Succ. Centre-Ville, Montréal, Québec, H3C 3J7 (Canada)

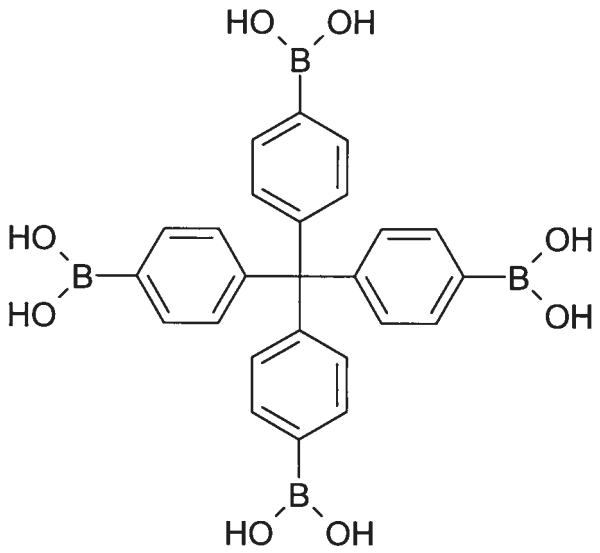

Structure solved and refined in the laboratory of X-ray diffraction, Université de Montréal by Dr. Thierry Maris.

Table 1. Crystal data and structure refinement for C25 H24 B4 O8.

Identification code	JIW360
Empirical formula	C25 H24 B4 O8
Formula weight	495.68
Temperature	226(2)K
Wavelength	1.54178 Å
Crystal system	Tetragonal
Space group	I41/a
Unit cell dimensions	a = 10.627(11) Å α = 90° b = 10.627(11) Å β = 90° c = 41.608(6) Å γ = 90°
Volume	4699(7)Å^3
Z	4
Density (without solvent)	0.701 Mg/m^3
Absorption coefficient	0.414 mm^{-1}
F(000)	1032
Crystal size	0.60 x 0.60 x 0.40 mm
Theta range for data collection	5.24 to 73.48°
Index ranges	$-11 \leq h \leq 13$, $-13 \leq k \leq 13$, $-51 \leq \ell \leq 39$
Reflections collected	11933
Independent reflections	2308 [R_{int} = 0.0758]
Absorption correction	Semi-empirical from equivalents
Max. and min. transmission	1 and 0.3446
Refinement method	Full-matrix least-squares on F^2
Data / restraints / parameters	2308 / 60 / 85
Goodness-of-fit on F^2	0.981
Final R indices [I>2sigma(I)]	R_1 = 0.0978, wR_2 = 0.1410
R indices (all data)	R_1 = 0.3307, wR_2 = 0.1594
Largest diff. peak and hole	0.229 and -0.237 e/Å^3

Table 2. Atomic coordinates (x 10^4) and equivalent isotropic displacement parameters ($Å^2$ x 10^3) for C25 H24 B4 O8.

U_{eq} is defined as one third of the trace of the orthogonalized Uij tensor.

	x	y	z	U_{eq}
C(1)	5000	7500	1250	51(3)
C(2)	5971(6)	6967(6)	1019(1)	64(2)
C(3)	6743(6)	7816(5)	860(1)	68(2)
C(4)	7603(5)	7328(6)	641(1)	69(2)
C(5)	7760(6)	6100(7)	573(1)	67(2)
C(6)	6932(6)	5316(5)	725(1)	82(2)
C(7)	6083(6)	5732(6)	950(1)	80(2)
B(8)	8715(10)	5565(9)	330(2)	75(3)
O(9)	8651(4)	4385(4)	232(1)	101(2)
O(10)	9669(3)	6282(3)	222(1)	74(1)

Table 3. Hydrogen coordinates (x 10^4) and isotropic displacement parameters ($Å^2$ x 10^3) for C25 H24 B4 O8.

	x	y	z	U_{eq}
H(3)	6687	8686	899	81
H(4)	8118	7905	531	82
H(6)	6944	4455	673	98
H(7)	5572	5146	1058	96
H(9)	9207	4255	95	151
H(10)	9545	7026	273	110

Table 4. Anisotropic parameters ($Å^2$ x 10^3) for C25 H24 B4 O8.

The anisotropic displacement factor exponent takes the form:

$$-2\pi^2 [h^2 a^{*2} U_{11} + ... + 2 h k a^* b^* U_{12}]$$

	U11	U22	U33	U23	U13	U12
C(1)	36(6)	36(6)	80(10)	0	0	0
C(2)	86(4)	56(4)	48(3)	-1(3)	16(3)	7(4)
C(3)	87(4)	63(4)	54(3)	-9(3)	18(3)	0(3)
C(4)	89(4)	61(4)	56(3)	-7(3)	20(3)	2(3)
C(5)	84(3)	58(3)	59(3)	0(3)	19(3)	-7(3)
C(6)	102(4)	72(4)	71(3)	0(3)	31(3)	2(3)
C(7)	103(4)	72(4)	64(3)	-1(3)	39(3)	8(4)
B(8)	119(6)	49(6)	57(5)	27(5)	7(5)	9(6)
O(9)	145(4)	88(4)	70(3)	-29(3)	56(2)	6(3)
O(10)	113(4)	59(3)	49(2)	-20(2)	7(2)	-5(2)

Table 5. Bond lengths [Å] and angles [°] for C25 H24 B4 O8

C(1)-C(2)#1	1.521(6)	B(8)-O(9)	1.320(8)
C(1)-C(2)#2	1.521(6)	B(8)-O(10)	1.345(9)
C(1)-C(2)	1.521(6)		
C(1)-C(2)#3	1.521(6)	C(2)#1-C(1)-C(2)#2	101.4(4)
C(2)-C(7)	1.349(6)	C(2)#1-C(1)-C(2)	113.6(2)
C(2)-C(3)	1.386(6)	C(2)#2-C(1)-C(2)	113.6(2)
C(3)-C(4)	1.391(6)	C(2)#1-C(1)-C(2)#3	113.6(2)
C(4)-C(5)	1.345(6)	C(2)#2-C(1)-C(2)#3	113.6(2)
C(5)-C(6)	1.366(6)	C(2)-C(1)-C(2)#3	101.4(4)
C(5)-B(8)	1.544(9)	C(7)-C(2)-C(3)	118.8(6)
C(6)-C(7)	1.375(6)	C(7)-C(2)-C(1)	123.7(6)
		C(3)-C(2)-C(1)	117.4(5)
		C(2)-C(3)-C(4)	117.2(6)
		C(5)-C(4)-C(3)	125.5(6)
		C(4)-C(5)-C(6)	114.5(6)
		C(4)-C(5)-B(8)	125.2(7)
		C(6)-C(5)-B(8)	120.1(7)
		C(5)-C(6)-C(7)	122.8(7)
		C(2)-C(7)-C(6)	120.9(6)
		O(9)-B(8)-O(10)	118.2(9)
		O(9)-B(8)-C(5)	121.3(8)
		O(10)-B(8)-C(5)	120.4(8)

Symmetry transformations used to generate equivalent atoms:
#1 -y+5/4,x+1/4,-z+1/4 #2 y-1/4,-x+5/4,-z+1/4 #3 -x+1,-y+3/2,z+0

Table 6. Torsion angles [°] for C25 H24 B4 O8.

C(2)#1-C(1)-C(2)-C(7) 135.0(7)	C(2)-C(3)-C(4)-C(5) -0.9(9)
C(2)#2-C(1)-C(2)-C(7) 19.7(5)	C(3)-C(4)-C(5)-C(6) 4.0(9)
C(2)#3-C(1)-C(2)-C(7) -102.7(6)	C(3)-C(4)-C(5)-B(8) 179.9(6)
C(2)#1-C(1)-C(2)-C(3) -47.9(4)	C(4)-C(5)-C(6)-C(7) -5.6(8)
C(2)#2-C(1)-C(2)-C(3) -163.2(6)	B(8)-C(5)-C(6)-C(7) 178.2(5)
C(2)#3-C(1)-C(2)-C(3) 74.5(5)	C(3)-C(2)-C(7)-C(6) -0.9(9)
C(7)-C(2)-C(3)-C(4) -0.8(9)	C(1)-C(2)-C(7)-C(6) 176.2(4)
C(1)-C(2)-C(3)-C(4) -178.0(4)	C(5)-C(6)-C(7)-C(2) 4.3(9)
	C(4)-C(5)-B(8)-O(9) -166.9(6)
	C(6)-C(5)-B(8)-O(9) 8.8(10)
	C(4)-C(5)-B(8)-O(10) 15.8(10)
	C(6)-C(5)-B(8)-O(10) -168.5(6)

Symmetry transformations used to generate equivalent atoms:

#1 -y+5/4,x+1/4,-z+1/4 #2 y-1/4,-x+5/4,-z+1/4 #3 -x+1,-y+3/2,z+0

Table 7. Bond lengths [Å] and angles [°] related to the hydrogen bonding for C25 H24 B4 O8.

D-H	..A	d(D-H)	d(H..A)	d(D..A)	<DHA
O(9)-H(9)	O(10)#4	0.83	1.87	2.691(5)	171.0
O(10)-H(10)	O(10)#5	0.83	1.99	2.683(8)	139.9

Symmetry transformations used to generate equivalent atoms:

#1 -y+5/4,x+1/4,-z+1/4 #2 y-1/4,-x+5/4,-z+1/4
#3 -x+1,-y+3/2,z+0 #4 -x+2,-y+1,-z
#5 -x+2,-y+3/2,z+0

Least-squares planes (x,y,z in crystal coordinates) and deviations from them
(* indicates atom used to define plane)

PLANE 1 C2 to C7 (phenyl ring)

7.2140 (0.0177) x - 1.0131 (0.0221) y + 30.2944 (0.0669) z = 6.6892 (0.0185)

*	0.0055	(0.0040)	C2
*	-0.0066	(0.0039)	C3
*	-0.0069	(0.0040)	C4
*	0.0218	(0.0040)	C5
*	-0.0237	(0.0042)	C6
*	0.0099	(0.0042)	C7

Rms deviation of fitted atoms = 0.0144

PLANE 2 O -B - O group

6.0054 (0.0827) x - 3.0922 (0.0520) y + 32.1220 (0.3077) z = 4.5749 (0.0470)

Angle to previous plane (with approximate esd) = **13.24** (0.97)

*	0.0000	(0.0001)	B8
*	0.0000	(0.0000)	O9
*	0.0000	(0.0000)	O10

Rms deviation of fitted atoms = 0.0000

PLANE 3 C1 to C7 (central carbon + phenyl ring)

7.1136 (0.0152) x - 1.0102 (0.0252) y + 30.6575 (0.0503) z = 6.6512 (0.0220)

Angle to previous plane (with approximate esd) = **12.90** (0.97)

*	-0.0198	(0.0024)	C1
*	0.0226	(0.0045)	C2
*	-0.0029	(0.0030)	C3
*	0.0045	(0.0032)	C5
*	-0.0274	(0.0043)	C6
*	0.0230	(0.0043)	C7

Rms deviation of fitted atoms = 0.0192

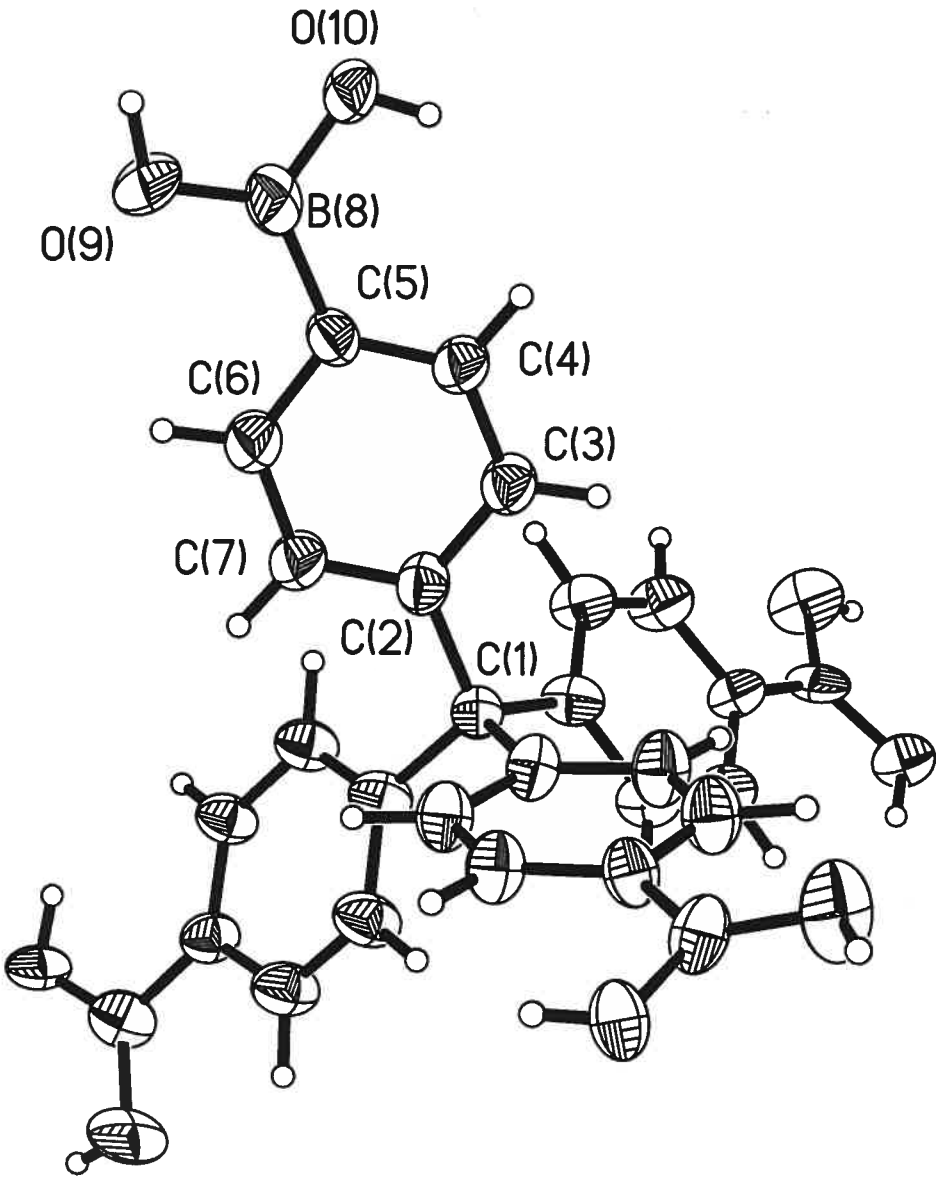

ORTEP view of the C25 H24 B4 O8 compound with the numbering scheme adopted. Ellipsoids drawn at 30% probability level. Hydrogens represented by sphere of arbitrary size.

REFERENCES

International Tables for Crystallography (1992). Vol. C. Tables 4.2.6.8 and
6.1.1.4, Dordrecht: Kluwer Academic Publishers.

SAINT (1999) Release 6.06; Integration Software for Single Crystal Data. Bruker AXS Inc., Madison, WI 53719-1173.

Sheldrick, G.M. (1996). SADABS, Bruker Area Detector Absorption Corrections.
Bruker AXS Inc., Madison, WI 53719-1173.

Sheldrick, G.M. (1997). SHELXS97, Program for the Solution of Crystal Structures. Univ. of Gottingen, Germany.

Sheldrick, G.M. (1997). SHELXL97, Program for the Refinement of Crystal Structures. Univ. of Gottingen, Germany.

SHELXTL (1997) Release 5.10; The Complete Software Package for Single Crystal Structure Determination. Bruker AXS Inc., Madison, WI 53719-1173.

SMART (1999) Release 5.059; Bruker Molecular Analysis Research Tool. Bruker AXS Inc., Madison, WI 53719-1173.

Spek, A.L. (2000). PLATON, Molecular Geometry Program, 2000 version. University of Utrecht, Utrecht, Holland.

XPREP (1997) Release 5.10; X-ray data Preparation and Reciprocal space Exploration Program. Bruker AXS Inc., Madison, WI 53719-1173.

Université de Montréal

CRYSTAL AND MOLECULAR STRUCTURE OF

C24 H24 B4 O8 Si COMPOUND (JIW368)

Wednesday, January 29, 2003

Equipe WUEST

Département de chimie, Université de Montréal,

C.P. 6128, Succ. Centre-Ville, Montréal, Québec, H3C 3J7 (Canada)

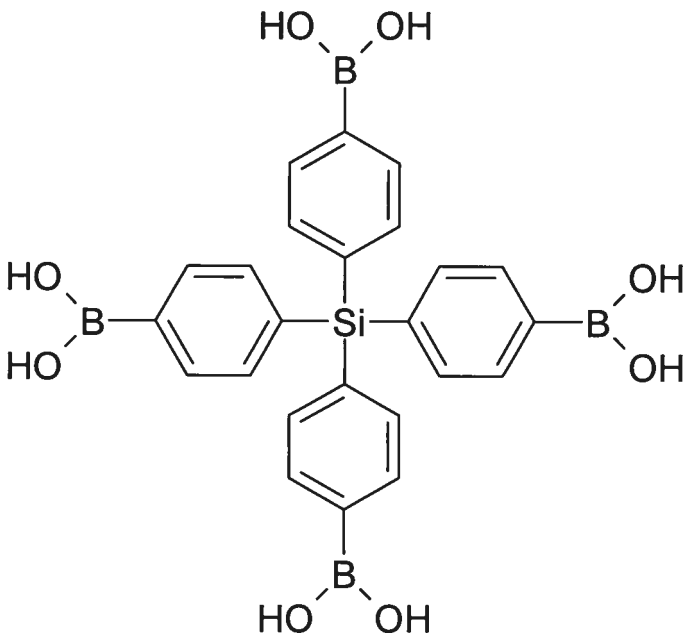

Structure solved and refined in the laboratory of X-ray diffraction Université de Montréal by Dr. Thierry Maris.

Table 1. Crystal data and structure refinement for C24 H24 B4 O8 Si.

Identification code	JIW368
Empirical formula	C24 H24 B4 O8 Si
Formula weight	511.76
Temperature	210(2)K
Wavelength	1.54178 Å
Crystal system	Tetragonal
Space group	$I4_1/a$
Unit cell dimensions	a = 10.8370(15) Å $\alpha = 90°$ b = 10.8370(15) Å $\beta = 90°$ c = 45.603(9) Å $\gamma = 90°$
Volume	5355.6(15)Å^3
Z	4
Density (without solvent)	0.635 Mg/m^3
Absorption coefficient	0.578 mm^{-1}
F(000)	1064
Crystal size	0.45 x 0.35 x 0.20 mm
Theta range for data collection	3.88 to 70.26°
Index ranges	$-13 \le h \le 13$, $-13 \le k \le 13$, $0 \le \ell \le 55$
Reflections collected	10175
Independent reflections	2563 [R_{int} = 0.0789]
Absorption correction	Gaussian
Max. and min. transmission	0.8931 and 0.7809
Refinement method	Full-matrix least-squares on F^2
Data / restraints / parameters	2563 / 0 / 84
Goodness-of-fit on F^2	0.840
Final R indices [I>2sigma(I)]	R_1 = 0.0758, wR_2 = 0.1250
R indices (all data)	R_1 = 0.1508, wR_2 = 0.1367
Largest diff. peak and hole	0.185 and -0.192 e/Å^3

Table 2. Atomic coordinates (x 10^4) and equivalent isotropic displacement parameters ($Å^2$ x 10^3) for C24 H24 B4 O8 Si.

U_{eq} is defined as one third of the trace of the orthogonalized Uij tensor.

	x	y	z	U_{eq}
Si(1)	10000	2500	1250	71(1)
C(2)	8766(3)	3141(4)	998(1)	63(1)
C(3)	8834(4)	4266(4)	888(1)	90(1)
C(4)	8058(4)	4722(4)	677(1)	99(1)
C(5)	7085(4)	3951(4)	583(1)	83(1)
C(6)	6977(4)	2783(4)	691(1)	92(1)
C(7)	7820(4)	2389(4)	902(1)	90(1)
B(8)	6180(5)	4472(6)	327(1)	96(2)
O(9)	6272(3)	5598(3)	222(1)	131(1)
O(10)	5225(3)	3743(2)	232(1)	101(1)

Table 3. Hydrogen coordinates (x 10^4) and isotropic displacement parameters ($Å^2$ x 10^3) for C24 H24 B4 O8 Si.

	x	y	z	U_{eq}
H(3)	9456	4791	960	107
H(4)	8169	5515	597	118
H(6)	6348	2255	625	110
H(7)	7743	1592	982	108
H(9)	5763	5693	88	196
H(10)	5390	3007	264	152

Table 4. Anisotropic parameters ($Å^2$ x 10^3) for C24 H24 B4 O8 Si.

The anisotropic displacement factor exponent takes the form:

$$-2\pi^2 [h^2 a^{*2} U_{11} + ... + 2 h k a^* b^* U_{12}]$$

	U11	U22	U33	U23	U13	U12
Si(1)	86(1)	86(1)	42(1)	0	0	0
C(2)	74(3)	70(3)	45(2)	12(2)	-4(2)	3(2)
C(3)	111(4)	96(3)	62(2)	8(2)	-18(2)	-32(3)
C(4)	136(4)	97(3)	63(2)	21(2)	-27(2)	-15(3)
C(5)	97(3)	98(4)	54(2)	-2(2)	-15(2)	5(3)
C(6)	126(4)	79(3)	71(2)	29(2)	-27(2)	-12(3)
C(7)	122(4)	89(3)	59(2)	10(2)	-26(2)	-17(3)
B(8)	100(5)	113(5)	73(3)	-7(3)	-10(3)	-15(4)
O(9)	161(3)	119(3)	112(2)	41(2)	-58(2)	-37(2)
O(10)	130(3)	107(2)	68(1)	15(2)	-25(2)	-13(2)

Table 5. Bond lengths [Å] and angles [°] for C24 H24 B4 O8 Si

Si(1)-C(2)#1	
1.895(3)	
Si(1)-C(2)#2	
1.895(3)	
Si(1)-C(2)	
1.895(3)	
Si(1)-C(2)#3	
1.895(3)	
C(2)-C(3)	
1.320(5)	
C(2)-C(7)	
1.380(4)	
C(3)-C(4)	
1.374(5)	
C(4)-C(5)	
1.412(5)	
C(5)-C(6)	
1.364(5)	
C(5)-B(8)	
1.625(6)	
C(6)-C(7)	
1.394(4)	
B(8)-O(9)	
1.315(6)	
B(8)-O(10)	
1.374(5)	
C(2)#1-Si(1)-C(2)#2	
105.36(18)	
C(2)#1-Si(1)-C(2)	
111.57(9)	
C(2)#2-Si(1)-C(2)	
111.57(9)	
C(2)#1-Si(1)-C(2)#3	111.57(9)
C(2)#2-Si(1)-C(2)#3	111.57(9)
C(2)-Si(1)-C(2)#3	105.36(18)
C(3)-C(2)-C(7)	117.8(3)
C(3)-C(2)-Si(1)	121.9(3)
C(7)-C(2)-Si(1)	120.0(3)
C(2)-C(3)-C(4)	124.4(4)
C(3)-C(4)-C(5)	117.2(4)
C(6)-C(5)-C(4)	120.3(4)
C(6)-C(5)-B(8)	122.1(4)
C(4)-C(5)-B(8)	117.5(4)
C(5)-C(6)-C(7)	118.6(4)
C(2)-C(7)-C(6)	121.6(4)
O(9)-B(8)-O(10)	118.4(4)
O(9)-B(8)-C(5)	122.6(5)
O(10)-B(8)-C(5)	118.8(5)

Symmetry transformations used to generate equivalent atoms:

#1 y+3/4,-x+5/4,-z+1/4 #2 -y+5/4,x-3/4,-z+1/4 #3 -x+2,-y+1/2,z+0

Table 6. Torsion angles [°] for C24 H24 B4 O8 Si.

C(2)#1-Si(1)-C(2)-C(3)	36.2(3)	C(2)-C(3)-C(4)-C(5)	3.6(6)
C(2)#2-Si(1)-C(2)-C(3)	153.7(3)	C(3)-C(4)-C(5)-C(6)	-3.1(6)
C(2)#3-Si(1)-C(2)-C(3)	-85.1(3)	C(3)-C(4)-C(5)-B(8)	-178.7(3)
C(2)#1-Si(1)-C(2)-C(7)	-149.9(3)	C(4)-C(5)-C(6)-C(7)	2.1(6)
C(2)#2-Si(1)-C(2)-C(7)	-32.3(3)	B(8)-C(5)-C(6)-C(7)	177.5(3)
C(2)#3-Si(1)-C(2)-C(7)	88.9(3)	C(3)-C(2)-C(7)-C(6)	1.6(5)
C(7)-C(2)-C(3)-C(4)	-2.8(6)	Si(1)-C(2)-C(7)-C(6)	-172.6(3)
Si(1)-C(2)-C(3)-C(4)	171.2(3)	C(5)-C(6)-C(7)-C(2)	-1.4(6)
		C(6)-C(5)-B(8)-O(9)	179.7(4)
		C(4)-C(5)-B(8)-O(9)	-4.8(6)
		C(6)-C(5)-B(8)-O(10)	4.5(6)
		C(4)-C(5)-B(8)-O(10)	180.0(4)

Symmetry transformations used to generate equivalent atoms:

#1 y+3/4,-x+5/4,-z+1/4 #2 -y+5/4,x-3/4,-z+1/4 #3 -x+2,-y+1/2,z+0

Table 7. Bond lengths [Å] and angles [°] related to the hydrogen bonding for C24 H24 B4 O8 Si.

D-H	..A	d(D-H)	d(H..A)	d(D..A)	<DHA
O(9)-H(9)	O(10)#4	0.83	1.91	2.725(3)	167.1
O(10)-H(10)	O(10)#5	0.83	2.02	2.737(5)	144.9

Symmetry transformations used to generate equivalent atoms:

#1 y+3/4,-x+5/4,-z+1/4 #2 -y+5/4,x-3/4,-z+1/4
#3 -x+2,-y+1/2,z+0 #4 -x+1,-y+1,-z
#5 -x+1,-y+1/2,z+0

Least-squares planes (x,y,z in crystal coordinates) and deviations from them
(* indicates atom used to define plane)

PLANE 1 c2 to C7 (phenyl ring)

6.4651 (0.0117) x - 3.8105 (0.0152) y - 32.8988 (0.0398) z = 1.1714 (0.0141)

*	0.0058	(0.0023)	C2
*	-0.0150	(0.0025)	C3
*	0.0185	(0.0025)	C4
*	-0.0139	(0.0025)	C5
*	0.0053	(0.0025)	C6
*	-0.0007	(0.0025)	C7

Rms deviation of fitted atoms = 0.0117

PLANE 2 B8 O9 O10

6.2711 (0.0513) x - 3.7186 (0.0347) y - 33.7392 (0.2281) z = 1.1079 (0.0239)

Angle to previous plane (with approximate esd) = **1.55** (0.68)

*	0.0000	(0.0000)	B8
*	0.0000	(0.0000)	O9
*	0.0000	(0.0000)	O10

Rms deviation of fitted atoms = 0.0000

PLANE 3 Si1 to C7 (Si + phenyl ring)

6.1610 (0.0089) x - 3.6549 (0.0147) y - 34.2186 (0.0178) z = 0.8938 (0.0121)

Angle to previous plane (with approximate esd) = **0.90** (0.68)

*	0.0761	(0.0014)	Si1
*	-0.0664	(0.0024)	C2
*	-0.0576	(0.0026)	C3
*	0.0353	(0.0025)	C4
*	0.0333	(0.0026)	C5
*	0.0225	(0.0026)	C6
*	-0.0431	(0.0027)	C7

Rms deviation of fitted atoms = 0.0511

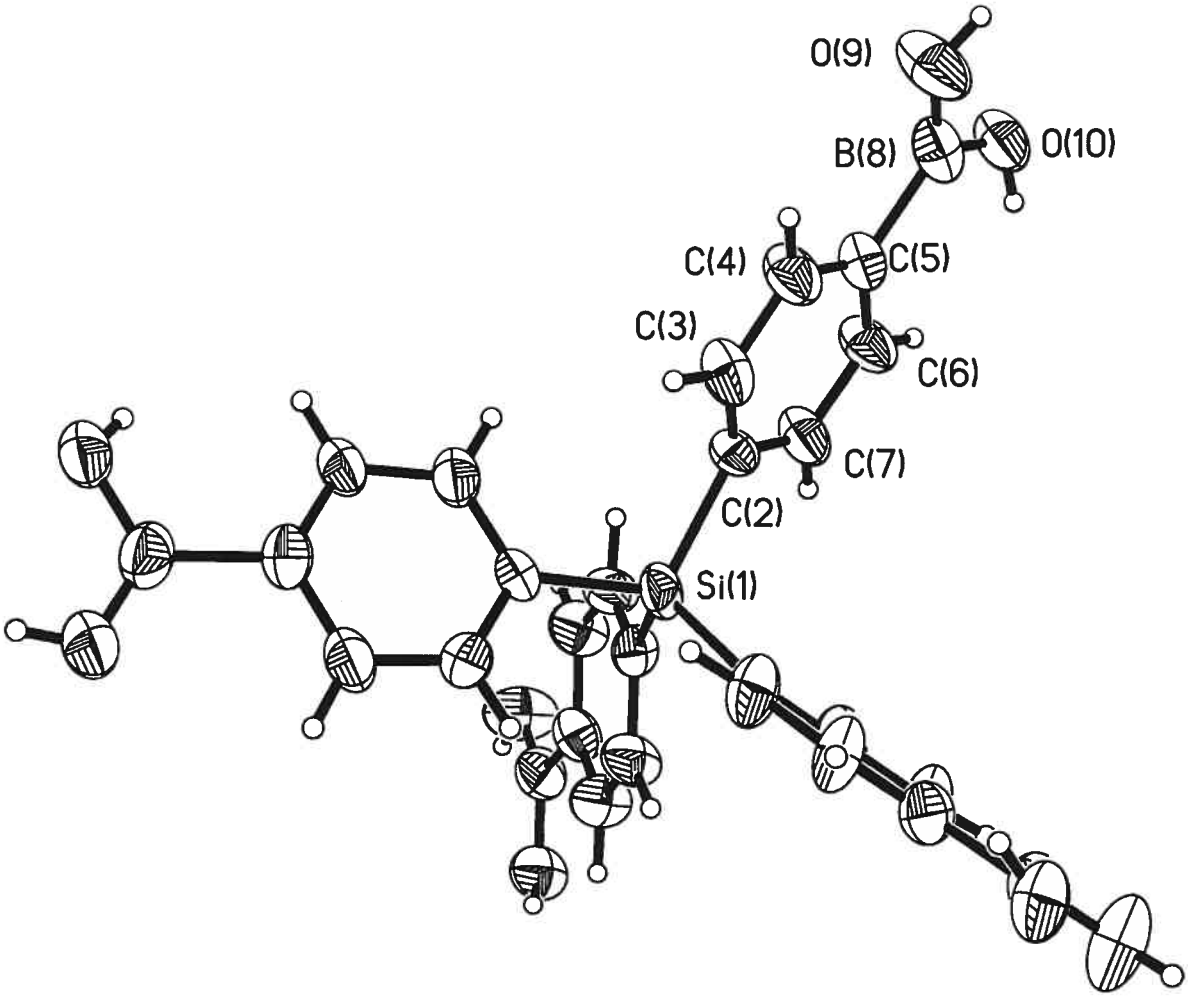

ORTEP view of the C24 H24 B4 O8 Si compound with the numbering scheme adopted. Ellipsoids drawn at 30% probability level. Hydrogens represented by sphere of arbitrary size.

REFERENCES

Ahmed, F.R., Hall, S.R., Pippy, M.E. and Huber, C.P. (1973). NRC Crystallographic Computer Programs for the IBM/360. Accession Nos. 133-147 in J. Appl. Cryst. 6, 309-346.

Enraf-Nonius (1989). CAD-4 Software, Version 5.0. Enraf-Nonius, Delft, Holland.

Gabe, E.J., Le Page, Y., Charland, J.-P., Lee, F.L. and White, P.S. (1989). J. Appl. Cryst. 22, 384-387.

International Tables for Crystallography (1992). Vol. C. Tables 4.2.6.8 and 6.1.1.4, Dordrecht: Kluwer Academic Publishers.

Sheldrick, G.M. (1997). SHELXS97, Program for the Solution of Crystal Structures Univ. of Gottingen, Germany.

Sheldrick, G.M. (1997). SHELXL97, Program for the Refinement of Crystal Structures. Univ. of Gottingen, Germany.

SHELXTL (1997) Release 5.10; The Complete Software Package for Single Crystal Structure Determination. Bruker AXS Inc., Madison, WI 53719-1173.

Spek, A.L. (2000). PLATON, Molecular Geometry Program, 2000 version. University of Utrecht, Utrecht, Holland.

Université de Montréal

CRYSTAL AND MOLECULAR STRUCTURE OF

C33 H32 O8 COMPOUND (JIW540)

Wednesday, January 29, 2003

Equipe WUEST

Département de chimie, Université de Montréal,

C.P. 6128, Succ. Centre-Ville, Montréal, Québec, H3C 3J7 (Canada)

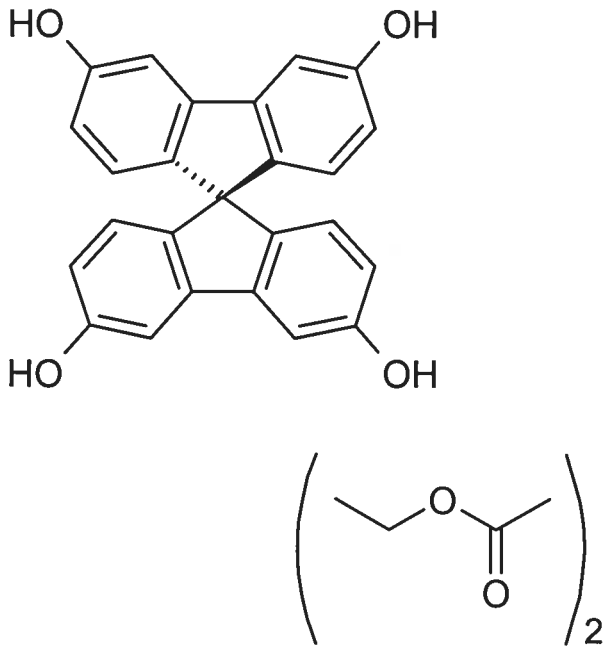

Structure solved and refined in the laboratory of X-ray diffraction, Université de Montréal by Dr. Thierry Maris.

Table 1. Crystal data and structure refinement for C33 H32 O8.

Identification code	JIW540
Empirical formula	C33 H32 O8
Formula weight	556.59
Temperature	223(2)K
Wavelength	1.54178 Å
Crystal system	Triclinic
Space group	P-1
Unit cell dimensions	a = 7.5560(3) Å α = 85.896(2)°
	b = 11.3326(4) Å β = 77.828(3)°
	c = 17.5119(7) Å γ = 73.671(2)°
Volume	1406.57(9)Å^3
Z	2
Density (calculated)	1.314 Mg/m^3
Absorption coefficient	0.771 mm^{-1}
F(000)	588
Crystal size	0.6 x 0.6 x 0.4 mm
Theta range for data collection	2.58 to 59.01°
Index ranges	$-7 \leq h \leq 8$, $-12 \leq k \leq 12$, $-19 \leq \ell \leq 19$
Reflections collected	8047
Independent reflections	3767 [R_{int} = 0.031]
Absorption correction	Semi-empirical from equivalents
Max. and min. transmission	1.0000 and 0.4400
Refinement method	Full-matrix least-squares on F^2
Data / restraints / parameters	3767 / 0 / 370
Goodness-of-fit on F^2	1.005
Final R indices [I>2sigma(I)]	R_1 = 0.0597, wR_2 = 0.1649
R indices (all data)	R_1 = 0.0671, wR_2 = 0.1745

Largest diff. peak and hole 0.292 and -0.246 e/Å^3

Table 2. Atomic coordinates (x 10^4) and equivalent isotropic displacement parameters (Å^2 x 10^3) for C33 H32 O8.

U_{eq} is defined as one third of the trace of the orthogonalized Uij tensor.

	x	y	z	U_{eq}
C(1)	5502(3)	4151(2)	2442(1)	36(1)
O(1)	4564(2)	-206(2)	4040(1)	47(1)
C(2)	6898(3)	3464(2)	1749(1)	36(1)
O(2)	10350(3)	1145(2)	4(1)	72(1)
C(3)	7168(3)	2198(2)	1841(1)	35(1)
O(3)	7733(3)	7705(2)	3829(1)	53(1)
C(4)	6035(3)	1959(2)	2600(1)	34(1)
O(4)	-581(2)	7991(2)	1730(1)	60(1)
C(5)	5055(3)	3083(2)	2953(1)	35(1)
C(6)	3877(3)	3107(2)	3679(1)	41(1)
C(7)	3690(3)	2015(2)	4048(1)	42(1)
C(8)	4694(3)	894(2)	3692(1)	37(1)
C(9)	5857(3)	855(2)	2967(1)	37(1)
C(10)	8342(3)	1397(2)	1268(1)	41(1)
C(11)	9232(4)	1897(2)	600(1)	47(1)
C(12)	9018(3)	3150(2)	518(1)	47(1)
C(13)	7836(3)	3942(2)	1093(1)	41(1)
C(14)	6284(3)	5003(2)	2833(1)	36(1)
C(15)	7842(3)	4716(2)	3172(1)	42(1)
C(16)	8305(3)	5641(2)	3494(1)	44(1)
C(17)	7199(3)	6856(2)	3485(1)	41(1)
C(18)	5651(3)	7154(2)	3129(1)	39(1)
C(19)	5189(3)	6222(2)	2806(1)	35(1)
C(20)	3626(3)	6264(2)	2418(1)	36(1)
C(21)	2169(3)	7237(2)	2254(1)	42(1)
C(22)	850(3)	7005(2)	1885(1)	44(1)
C(23)	980(3)	5821(2)	1683(1)	45(1)
C(24)	2444(3)	4843(2)	1849(1)	43(1)
C(25)	3765(3)	5059(2)	2210(1)	36(1)
C(30)	7964(8)	3549(4)	5242(2)	120(2)
C(31)	7604(5)	2411(3)	5106(2)	78(1)
O(32)	8728(3)	1936(2)	4357(1)	64(1)
C(33)	8893(4)	786(2)	4211(1)	49(1)
C(34)	10139(4)	379(3)	3454(2)	63(1)
O(35)	8123(3)	118(2)	4653(1)	59(1)
C(40)	3351(5)	10642(3)	1352(2)	81(1)
C(41)	4964(4)	9537(3)	1216(2)	68(1)
O(42)	4540(3)	8709(2)	738(1)	62(1)
C(43)	5685(4)	7577(3)	657(2)	52(1)
C(44)	5087(5)	6799(3)	168(2)	74(1)
O(46)	7029(3)	7222(2)	967(1)	63(1)

Table 3. Hydrogen coordinates (x 10^4) and isotropic displacement parameters ($Å^2$ x 10^3) for C33 H32 O8.

	x	y	z	U_{eq}
H(1)	3855	-80	4476	50
H(2)	10359	421	121	107
H(3)	6821	8316	3945	50
H(4)	-1285	7747	1511	50
H(6)	3209	3862	3920	49
H(7)	2886	2028	4538	50
H(9)	6516	99	2726	45
H(10)	8530	543	1329	49
H(12)	9677	3464	71	56
H(13)	7676	4794	1036	49
H(15)	8584	3898	3184	50
H(16)	9376	5450	3721	52
H(18)	4925	7974	3107	47
H(21)	2075	8043	2390	50
H(23)	76	5678	1433	54
H(24)	2527	4038	1714	51
H(30A)	7213	3877	5740	180
H(30B)	7634	4133	4828	180
H(30C)	9288	3405	5249	180
H(31A)	6265	2548	5104	94
H(31B)	7931	1817	5523	94
H(34A)	10589	1057	3198	94
H(34B)	9445	107	3126	94
H(34C)	11201	-296	3539	94
H(40A)	3614	11212	1672	121
H(40B)	2235	10409	1619	121
H(40C)	3144	11033	855	121
H(41A)	6101	9766	951	81
H(41B)	5185	9137	1715	81
H(44A)	3973	7282	-15	111
H(44B)	4806	6105	477	111
H(44C)	6093	6503	-276	111

Table 4. Anisotropic parameters ($Å^2$ x 10^3) for C33 H32 O8.

The anisotropic displacement factor exponent takes the form:

$$-2\pi^2 [h^2 a^{*2} U_{11} + ... + 2 h k a^* b^* U_{12}]$$

	U11	U22	U33	U23	U13	U12
C(1)	43(1)	30(1)	37(1)	-6(1)	-4(1)	-15(1)
O(1)	55(1)	36(1)	49(1)	0(1)	-1(1)	-21(1)
C(2)	37(1)	35(1)	39(1)	-6(1)	-5(1)	-16(1)
O(2)	92(2)	46(1)	58(1)	-15(1)	31(1)	-19(1)
C(3)	37(1)	34(1)	39(1)	-4(1)	-7(1)	-17(1)
O(3)	59(1)	47(1)	63(1)	-15(1)	-17(1)	-22(1)
C(4)	33(1)	34(1)	38(1)	-5(1)	-6(1)	-15(1)
O(4)	48(1)	52(1)	84(1)	10(1)	-22(1)	-15(1)
C(5)	40(1)	32(1)	38(1)	-5(1)	-5(1)	-16(1)
C(6)	45(1)	34(1)	44(1)	-10(1)	-2(1)	-12(1)
C(7)	44(1)	43(1)	41(1)	-3(1)	0(1)	-20(1)
C(8)	39(1)	36(1)	43(1)	0(1)	-8(1)	-21(1)
C(9)	40(1)	30(1)	44(1)	-6(1)	-7(1)	-14(1)
C(10)	44(1)	35(1)	46(1)	-8(1)	0(1)	-18(1)
C(11)	50(1)	45(2)	44(1)	-13(1)	6(1)	-21(1)
C(12)	51(1)	48(2)	44(1)	-4(1)	2(1)	-26(1)
C(13)	49(1)	35(1)	44(1)	-3(1)	-7(1)	-21(1)
C(14)	41(1)	34(1)	36(1)	-5(1)	-1(1)	-17(1)
C(15)	48(1)	33(1)	45(1)	-5(1)	-7(1)	-12(1)
C(16)	44(1)	46(2)	47(1)	-5(1)	-11(1)	-19(1)
C(17)	51(1)	42(1)	37(1)	-6(1)	-4(1)	-25(1)
C(18)	46(1)	34(1)	40(1)	-5(1)	-4(1)	-17(1)
C(19)	40(1)	34(1)	32(1)	-3(1)	0(1)	-18(1)
C(20)	38(1)	34(1)	35(1)	-2(1)	1(1)	-16(1)
C(21)	42(1)	36(1)	47(1)	-5(1)	0(1)	-16(1)
C(22)	38(1)	48(2)	46(1)	3(1)	-3(1)	-16(1)
C(23)	40(1)	56(2)	45(1)	-1(1)	-7(1)	-23(1)
C(24)	46(1)	43(1)	44(1)	-6(1)	-4(1)	-21(1)
C(25)	40(1)	37(1)	35(1)	-4(1)	-1(1)	-19(1)
C(30)	197(5)	107(3)	68(2)	-28(2)	30(3)	-94(3)
C(31)	99(2)	69(2)	65(2)	-19(2)	18(2)	-39(2)
O(32)	76(1)	56(1)	58(1)	-8(1)	10(1)	-29(1)
C(33)	47(1)	54(2)	51(1)	-4(1)	-11(1)	-18(1)
C(34)	47(2)	83(2)	57(2)	-16(1)	-1(1)	-18(1)
O(35)	63(1)	55(1)	59(1)	-2(1)	0(1)	-26(1)
C(40)	75(2)	84(3)	83(2)	-13(2)	-17(2)	-19(2)
C(41)	57(2)	77(2)	76(2)	-16(2)	-18(1)	-21(2)
O(42)	59(1)	70(1)	65(1)	-3(1)	-19(1)	-27(1)
C(43)	53(2)	64(2)	47(1)	3(1)	-9(1)	-30(1)
C(44)	94(2)	75(2)	73(2)	2(2)	-36(2)	-40(2)
O(46)	57(1)	73(1)	68(1)	-4(1)	-18(1)	-28(1)

Table 5. Bond lengths [Å] and angles [°] for C33 H32 O8

C(1)-C(5)	1.525(3)
C(1)-C(2)	1.525(3)
C(1)-C(14)	1.529(3)
C(1)-C(25)	1.534(3)
O(1)-C(8)	1.368(3)
C(2)-C(13)	1.378(3)
C(2)-C(3)	1.394(3)
O(2)-C(11)	1.371(3)
C(3)-C(10)	1.386(3)
C(3)-C(4)	1.473(3)
O(3)-C(17)	1.362(3)
C(4)-C(9)	1.393(3)
C(4)-C(5)	1.394(3)
O(4)-C(22)	1.376(3)
C(5)-C(6)	1.387(3)
C(6)-C(7)	1.383(3)
C(7)-C(8)	1.396(3)
C(8)-C(9)	1.379(3)
C(10)-C(11)	1.389(3)
C(11)-C(12)	1.383(4)
C(12)-C(13)	1.384(3)
C(14)-C(15)	1.377(3)
C(14)-C(19)	1.399(3)
C(15)-C(16)	1.384(3)
C(16)-C(17)	1.396(3)
C(17)-C(18)	1.388(3)
C(18)-C(19)	1.391(3)
C(19)-C(20)	1.469(3)
C(20)-C(21)	1.385(3)
C(20)-C(25)	1.408(3)
C(21)-C(22)	1.386(3)
C(22)-C(23)	1.384(4)
C(23)-C(24)	1.391(4)
C(24)-C(25)	1.372(3)
C(30)-C(31)	1.436(5)
C(31)-O(32)	1.450(3)
O(32)-C(33)	1.312(3)
C(33)-O(35)	1.219(3)
C(33)-C(34)	1.475(3)
C(40)-C(41)	1.474(4)
C(41)-O(42)	1.442(3)
O(42)-C(43)	1.328(4)
C(43)-O(46)	1.208(3)
C(43)-C(44)	1.486(4)

C(5)-C(1)-C(2)	101.03(17)
C(5)-C(1)-C(14)	114.96(17)
C(2)-C(1)-C(14)	113.35(17)
C(5)-C(1)-C(25)	113.55(17)
C(2)-C(1)-C(25)	113.15(17)
C(14)-C(1)-C(25)	101.39(17)
C(13)-C(2)-C(3)	120.5(2)
C(13)-C(2)-C(1)	128.5(2)
C(3)-C(2)-C(1)	111.07(18)

C(10)-C(3)-C(2)	120.9(2)
C(10)-C(3)-C(4)	130.7(2)
C(2)-C(3)-C(4)	108.41(18)
C(9)-C(4)-C(5)	120.98(19)

C(9)-C(4)-C(3)	130.59(19)	C(18)-C(19)-C(14)	120.3(2)
C(5)-C(4)-C(3)	108.43(19)	C(18)-C(19)-C(20)	130.7(2)
C(6)-C(5)-C(4)	119.7(2)	C(14)-C(19)-C(20)	108.97(18)
C(6)-C(5)-C(1)	129.28(19)	C(21)-C(20)-C(25)	120.3(2)
C(4)-C(5)-C(1)	111.04(18)	C(21)-C(20)-C(19)	131.2(2)
C(7)-C(6)-C(5)	119.8(2)	C(25)-C(20)-C(19)	108.46(19)
C(6)-C(7)-C(8)	120.0(2)	C(20)-C(21)-C(22)	119.0(2)
O(1)-C(8)-C(9)	117.19(19)	O(4)-C(22)-C(23)	121.6(2)
O(1)-C(8)-C(7)	121.84(19)	O(4)-C(22)-C(21)	117.6(2)
C(9)-C(8)-C(7)	121.0(2)	C(23)-C(22)-C(21)	120.8(2)
C(8)-C(9)-C(4)	118.6(2)	C(22)-C(23)-C(24)	120.2(2)
C(3)-C(10)-C(11)	117.9(2)	C(25)-C(24)-C(23)	119.6(2)
O(2)-C(11)-C(12)	118.7(2)	C(24)-C(25)-C(20)	120.1(2)
O(2)-C(11)-C(10)	120.0(2)	C(24)-C(25)-C(1)	129.5(2)
C(12)-C(11)-C(10)	121.4(2)	C(20)-C(25)-C(1)	110.45(19)
C(11)-C(12)-C(13)	120.2(2)	C(30)-C(31)-O(32)	108.8(3)
C(2)-C(13)-C(12)	119.1(2)	C(33)-O(32)-C(31)	117.0(2)
C(15)-C(14)-C(19)	120.4(2)	O(35)-C(33)-O(32)	124.1(2)
C(15)-C(14)-C(1)	128.9(2)	O(35)-C(33)-C(34)	123.3(3)
C(19)-C(14)-C(1)	110.70(19)	O(32)-C(33)-C(34)	112.6(2)
C(14)-C(15)-C(16)	119.4(2)	O(42)-C(41)-C(40)	108.3(2)
C(15)-C(16)-C(17)	120.6(2)	C(43)-O(42)-C(41)	117.2(2)
O(3)-C(17)-C(18)	123.0(2)	O(46)-C(43)-O(42)	123.2(2)
O(3)-C(17)-C(16)	116.8(2)	O(46)-C(43)-C(44)	124.3(3)
C(18)-C(17)-C(16)	120.2(2)	O(42)-C(43)-C(44)	112.5(3)
C(17)-C(18)-C(19)	119.1(2)		

Table 6. Torsion angles [°] for C33 H32 O8.

C(5)-C(1)-C(2)-C(13)	-178.8(2)	C(10)-C(3)-C(4)-C(5)	-178.4(2)
C(14)-C(1)-C(2)-C(13)	-55.2(3)	C(2)-C(3)-C(4)-C(5)	1.3(2)
C(25)-C(1)-C(2)-C(13)	59.5(3)	C(9)-C(4)-C(5)-C(6)	-0.3(3)
C(5)-C(1)-C(2)-C(3)	1.3(2)	C(3)-C(4)-C(5)-C(6)	180.00(19)
C(14)-C(1)-C(2)-C(3)	124.8(2)	C(9)-C(4)-C(5)-C(1)	179.28(18)
C(25)-C(1)-C(2)-C(3)	-120.4(2)	C(3)-C(4)-C(5)-C(1)	-0.4(2)
C(13)-C(2)-C(3)-C(10)	-1.8(3)	C(2)-C(1)-C(5)-C(6)	179.0(2)
C(1)-C(2)-C(3)-C(10)	178.11(19)	C(14)-C(1)-C(5)-C(6)	56.6(3)
C(13)-C(2)-C(3)-C(4)	178.44(19)	C(25)-C(1)-C(5)-C(6)	-59.5(3)
C(1)-C(2)-C(3)-C(4)	-1.6(2)	C(2)-C(1)-C(5)-C(4)	-0.5(2)
C(10)-C(3)-C(4)-C(9)	1.9(4)	C(14)-C(1)-C(5)-C(4)	-122.9(2)
C(2)-C(3)-C(4)-C(9)	-178.4(2)	C(25)-C(1)-C(5)-C(4)	120.97(19)
		C(4)-C(5)-C(6)-C(7)	0.2(3)

```
  C(1)-C(5)-C(6)-C(7)      -
179.3(2)
  C(5)-C(6)-C(7)-C(8)
0.4(3)
  C(6)-C(7)-C(8)-O(1)
179.3(2)
  C(6)-C(7)-C(8)-C(9)        -
1.1(3)
  O(1)-C(8)-C(9)-C(4)      -
179.36(18)
  C(7)-C(8)-C(9)-C(4)
1.0(3)
  C(5)-C(4)-C(9)-C(8)        -
0.3(3)
  C(3)-C(4)-C(9)-C(8)
179.3(2)
  C(2)-C(3)-C(10)-C(11)      -
0.1(3)
  C(4)-C(3)-C(10)-C(11)
179.5(2)
  C(3)-C(10)-C(11)-O(2)    -
177.5(2)
  C(3)-C(10)-C(11)-C(12)
2.4(4)
  O(2)-C(11)-C(12)-C(13)
177.2(2)
  C(10)-C(11)-C(12)-C(13)    -
2.8(4)
  C(3)-C(2)-C(13)-C(12)
1.5(3)
  C(1)-C(2)-C(13)-C(12)    -
178.4(2)
  C(11)-C(12)-C(13)-C(2)
0.7(4)
  C(5)-C(1)-C(14)-C(15)
56.3(3)
  C(2)-C(1)-C(14)-C(15)     -
59.2(3)
  C(25)-C(1)-C(14)-C(15)
179.2(2)

C(5)-C(1)-C(14)-C(19)    -
124.49(19)
C(2)-C(1)-C(14)-C(19)     120.0(2)
C(25)-C(1)-C(14)-C(19)     -1.6(2)
C(19)-C(14)-C(15)-C(16)     0.7(3)
C(1)-C(14)-C(15)-C(16)    179.8(2)
C(14)-C(15)-C(16)-C(17)     0.7(3)
C(15)-C(16)-C(17)-O(3)
178.7(2)
C(15)-C(16)-C(17)-C(18)    -2.1(3)
O(3)-C(17)-C(18)-C(19)   -
178.76(19)
C(16)-C(17)-C(18)-C(19)     2.1(3)
C(17)-C(18)-C(19)-C(14)    -0.7(3)
C(17)-C(18)-C(19)-C(20)   178.2(2)
C(15)-C(14)-C(19)-C(18)    -0.7(3)
C(1)-C(14)-C(19)-C(18)   -
179.98(18)
C(15)-C(14)-C(19)-C(20)  -
179.80(19)
C(1)-C(14)-C(19)-C(20)      0.9(2)
C(18)-C(19)-C(20)-C(21)     0.7(4)
C(14)-C(19)-C(20)-C(21)   179.6(2)
C(18)-C(19)-C(20)-C(25)  -178.7(2)
C(14)-C(19)-C(20)-C(25)     0.2(2)
C(25)-C(20)-C(21)-C(22)     0.3(3)
C(19)-C(20)-C(21)-C(22)  -179.1(2)
C(20)-C(21)-C(22)-O(4)   -
179.99(19)
C(20)-C(21)-C(22)-C(23)     0.0(3)
O(4)-C(22)-C(23)-C(24)   -180.0(2)
C(21)-C(22)-C(23)-C(24)     0.0(3)
C(22)-C(23)-C(24)-C(25)    -0.4(3)
C(23)-C(24)-C(25)-C(20)     0.7(3)
C(23)-C(24)-C(25)-C(1)   -179.2(2)
C(21)-C(20)-C(25)-C(24)    -0.7(3)
C(19)-C(20)-C(25)-C(24)
178.85(18)
C(21)-C(20)-C(25)-C(1)
179.22(18)
C(19)-C(20)-C(25)-C(1)     -1.3(2)
C(5)-C(1)-C(25)-C(24)     -54.6(3)
C(2)-C(1)-C(25)-C(24)      59.9(3)
C(14)-C(1)-C(25)-C(24)   -178.4(2)
C(5)-C(1)-C(25)-C(20)
125.58(19)
C(2)-C(1)-C(25)-C(20)    -120.0(2)
C(14)-C(1)-C(25)-C(20)      1.7(2)
C(30)-C(31)-O(32)-C(33)   165.7(3)
C(31)-O(32)-C(33)-O(35)     2.1(4)
C(31)-O(32)-C(33)-C(34)  -177.1(3)
C(40)-C(41)-O(42)-C(43)  -169.2(3)
C(41)-O(42)-C(43)-O(46)     0.6(4)
C(41)-O(42)-C(43)-C(44)   178.6(2)
```

Table 7. Bond lengths [Å] and angles [°] related to the hydrogen bonding for C33 H32 O8.

D-H	..A	d(D-H)	d(H..A)	d(D..A)	<DHA
O(1)-H(1)	O(35)#1	0.83	1.91	2.707(2)	162.2
O(2)-H(2)	O(2)#2	0.83	2.03	2.792(4)	152.3
O(3)-H(3)	O(1)#3	0.83	2.01	2.836(2)	170.4
O(4)-H(4)	O(46)#4	0.83	1.98	2.806(3)	177.9

Symmetry transformations used to generate equivalent atoms:

#1 -x+1,-y,-z+1 #2 -x+2,-y,-z
#3 x,y+1,z #4 x-1,y,z

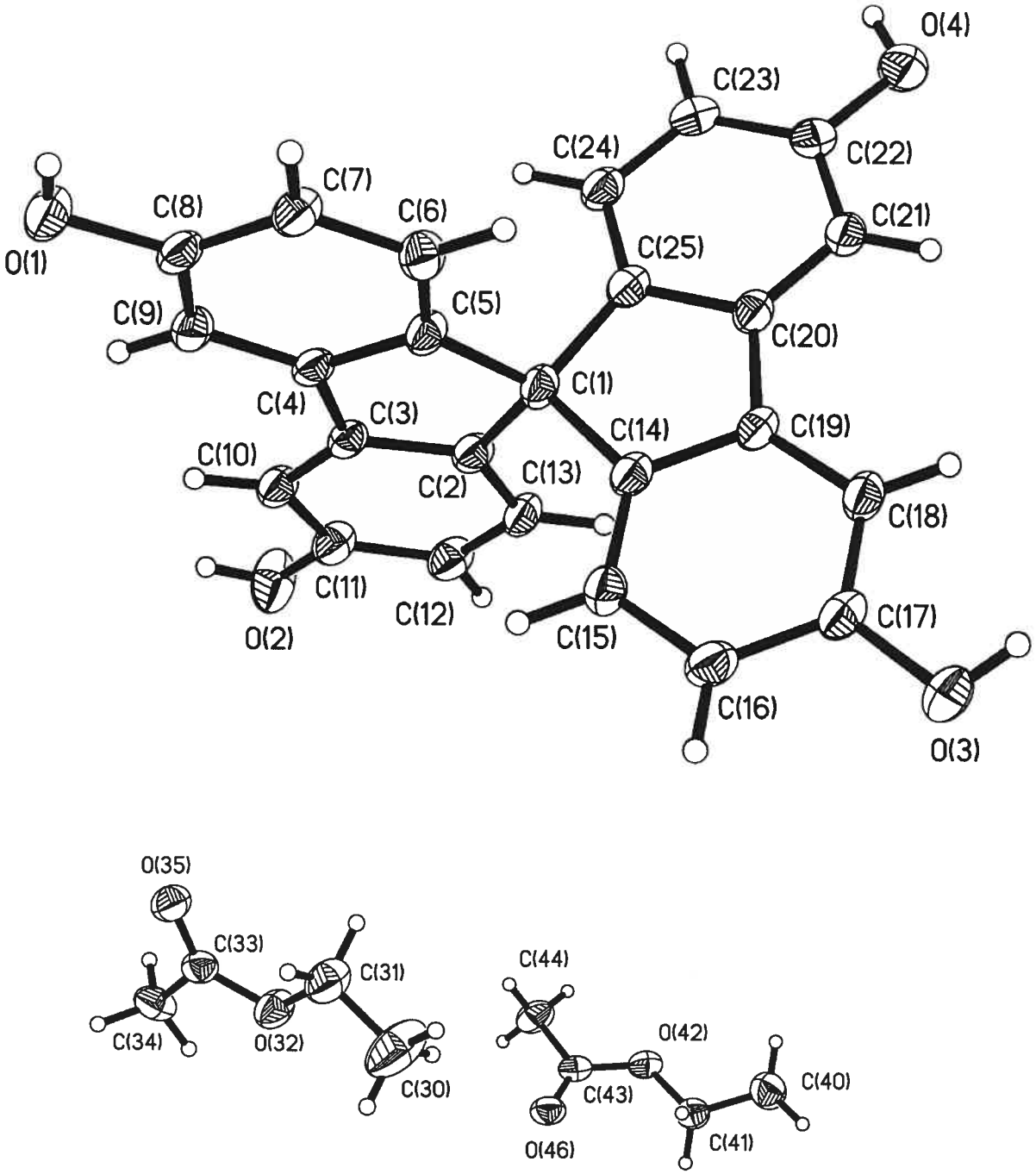

ORTEP view of the C33 H32 O8 compound with the numbering scheme adopted. Ellipsoids drawn at 30% probability level. Hydrogens represented by sphere of arbitrary size.

REFERENCES

International Tables for Crystallography (1992). Vol. C. Tables 4.2.6.8 and
6.1.1.4, Dordrecht: Kluwer Academic Publishers.

SAINT (1999) Release 6.06; Integration Software for Single Crystal Data. Bruker AXS Inc., Madison, WI 53719-1173.

Sheldrick, G.M. (1996). SADABS, Bruker Area Detector Absorption Corrections.
Bruker AXS Inc., Madison, WI 53719-1173.

Sheldrick, G.M. (1997). SHELXS97, Program for the Solution of Crystal Structures. Univ. of Gottingen, Germany.

Sheldrick, G.M. (1997). SHELXL97, Program for the Refinement of Crystal Structures. Univ. of Gottingen, Germany.

SHELXTL (1997) Release 5.10; The Complete Software Package for Single Crystal Structure Determination. Bruker AXS Inc., Madison, WI 53719-1173.

SMART (1999) Release 5.059; Bruker Molecular Analysis Research Tool. Bruker AXS Inc., Madison, WI 53719-1173.

Spek, A.L. (2000). PLATON, Molecular Geometry Program, 2000 version. University of Utrecht, Utrecht, Holland.

XPREP (1997) Release 5.10; X-ray data Preparation and Reciprocal space Exploration Program. Bruker AXS Inc., Madison, WI 53719-1173.

Université de Montréal

CRYSTAL AND MOLECULAR STRUCTURE OF

C39 H40 N4 O6 COMPOUND (JIW627)

Wednesday, January 29, 2003

Equipe WUEST

Département de chimie, Université de Montréal,

C.P. 6128, Succ. Centre-Ville, Montréal, Québec, H3C 3J7 (Canada)

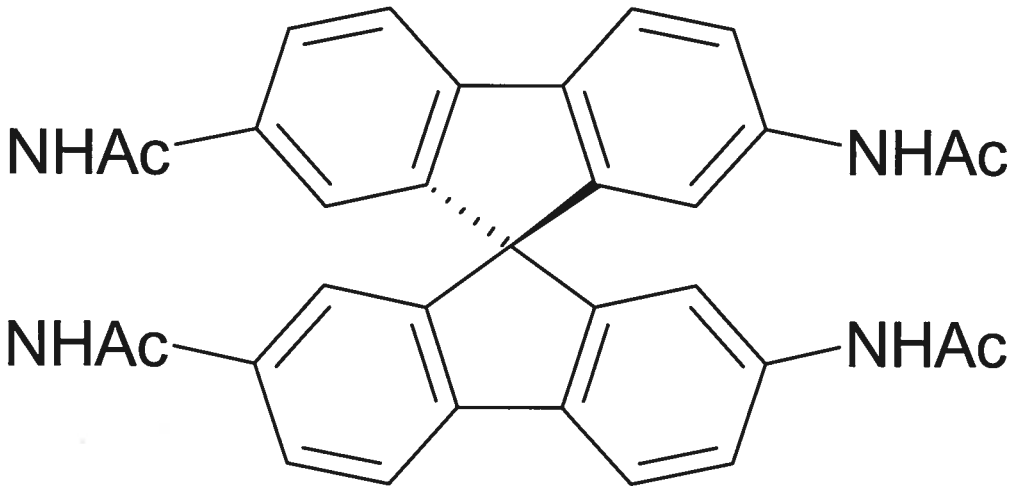

Solvent : Acetone

Structure solved and refined in the laboratory of X-ray diffraction, Université de Montréal by Dr. Thierry Maris.

Table 1. Crystal data and structure refinement for C39 H40 N4 O6.

Identification code	JIW627
Empirical formula	C39 H40 N4 O6
Formula weight	660.75
Temperature	223(2)K
Wavelength	1.54178 Å
Crystal system	Monoclinic
Space group	C2/c
Unit cell dimensions	a = 20.504(8) Å α = 90° b = 12.2870(7) Å β = 120.36(5)° c = 16.8890(4) Å γ = 90°
Volume	3671.4(14)Å^3
Z	4
Density (calculated)	1.195 Mg/m^3
Absorption coefficient	0.659 mm^{-1}
F(000)	1400
Crystal size	0.45 x 0.30 x 0.25 mm
Theta range for data collection	4.38 to 69.90°
Index ranges	$-24 \leq h \leq 24$, $-14 \leq k \leq 14$, $-20 \leq \ell \leq 19$
Reflections collected	11743
Independent reflections	3418 [R_{int} = 0.033]
Absorption correction	Semi-empirical from equivalents
Max. and min. transmission	0.8526 and 0.7558
Refinement method	Full-matrix least-squares on F^2
Data / restraints / parameters	3418 / 0 / 223
Goodness-of-fit on F^2	1.070
Final R indices [I>2sigma(I)]	R_1 = 0.0663, wR_2 = 0.2090
R indices (all data)	R_1 = 0.0722, wR_2 = 0.2166

Largest diff. peak and hole 0.522 and -0.391 e/Å^3

Table 2. Atomic coordinates (x 10^4) and equivalent isotropic displacement parameters (Å^2 x 10^3) for C39 H40 N4 O6.

U_{eq} is defined as one third of the trace of the orthogonalized Uij tensor.

	x	y	z	U_{eq}
O(1)	475(1)	13376(1)	10423(1)	57(1)
O(2)	3025(1)	6674(2)	8141(2)	101(1)
N(1)	1761(1)	6891(1)	7243(1)	47(1)
N(2)	-415(1)	12190(1)	9449(1)	49(1)
C(1)	0	9507(2)	7500	34(1)
C(2)	721(1)	8835(1)	7838(1)	35(1)
C(3)	1245(1)	9079(2)	8751(1)	37(1)
C(4)	1950(1)	8574(2)	9178(1)	44(1)
C(5)	2123(1)	7841(2)	8693(1)	44(1)
C(6)	1604(1)	7612(1)	7775(1)	39(1)
C(7)	889(1)	8107(2)	7347(1)	38(1)
C(8)	197(1)	10170(1)	8358(1)	36(1)
C(9)	917(1)	9898(2)	9074(1)	39(1)
C(10)	1198(1)	10381(2)	9933(1)	49(1)
C(11)	766(1)	11150(2)	10058(1)	50(1)
C(12)	53(1)	11428(2)	9339(1)	42(1)
C(13)	-239(1)	10929(2)	8481(1)	39(1)
C(14)	-186(1)	13104(2)	9963(1)	47(1)
C(15)	-803(2)	13761(2)	9963(2)	76(1)
C(16)	2436(1)	6474(2)	7441(2)	66(1)
C(17)	2412(2)	5728(3)	6721(2)	100(1)
C(20)	3546(5)	10956(8)	11531(7)	214(4)
O(20)	3289(4)	10131(6)	11050(6)	286(4)
C(21)	3680(7)	11860(10)	11136(7)	281(5)
C(22)	3595(12)	11004(11)	12309(9)	520(18)

Table 3. Hydrogen coordinates (x 10^4) and isotropic displacement parameters ($Å^2$ x 10^3) for C39 H40 N4 O6.

	x	y	z	U_{eq}
H(1A)	1375	6690	6723	56
H(2A)	-898	12054	9156	58
H(4)	2306	8733	9793	53
H(5)	2596	7491	8984	53
H(7)	530	7943	6734	45
H(10)	1676	10185	10423	59
H(11)	955	11487	10632	60
H(13)	-724	11108	7996	47
H(15A)	-1288	13422	9559	113
H(15B)	-800	14492	9748	113
H(15C)	-721	13793	10581	113
H(17A)	1897	5683	6209	150
H(17B)	2583	5009	6980	150
H(17C)	2738	6012	6508	150
H(21A)	3589	11671	10531	422
H(21B)	4200	12093	11518	422
H(21C)	3344	12447	11085	422
H(22A)	3479	10297	12462	780
H(22B)	3240	11540	12291	780
H(22C)	4105	11213	12770	780

Table 4. Anisotropic parameters ($Å^2$ x 10^3) for C39 H40 N4 O6.

The anisotropic displacement factor exponent takes the form:

$$-2\pi^2 [h^2 a^{*2} U_{11} + ... + 2 h k a^* b^* U_{12}]$$

	U11	U22	U33	U23	U13	U12
O(1)	42(1)	52(1)	57(1)	-6(1)	11(1)	-4(1)
O(2)	31(1)	141(2)	101(2)	-60(2)	12(1)	12(1)
N(1)	31(1)	52(1)	49(1)	-7(1)	15(1)	3(1)
N(2)	31(1)	56(1)	51(1)	-13(1)	15(1)	-1(1)
C(1)	25(1)	41(1)	34(1)	0	13(1)	0
C(2)	24(1)	41(1)	36(1)	4(1)	12(1)	-1(1)
C(3)	30(1)	43(1)	35(1)	4(1)	14(1)	1(1)
C(4)	34(1)	52(1)	35(1)	4(1)	10(1)	7(1)
C(5)	29(1)	50(1)	45(1)	7(1)	14(1)	8(1)
C(6)	31(1)	40(1)	47(1)	2(1)	19(1)	1(1)
C(7)	27(1)	46(1)	37(1)	-1(1)	14(1)	-1(1)
C(8)	28(1)	41(1)	34(1)	2(1)	13(1)	-3(1)
C(9)	31(1)	45(1)	34(1)	2(1)	13(1)	2(1)
C(10)	36(1)	63(1)	35(1)	-2(1)	7(1)	8(1)
C(11)	42(1)	62(1)	36(1)	-7(1)	12(1)	6(1)
C(12)	33(1)	47(1)	42(1)	-4(1)	16(1)	-1(1)
C(13)	27(1)	47(1)	38(1)	-1(1)	11(1)	-2(1)
C(14)	41(1)	47(1)	43(1)	-4(1)	15(1)	0(1)
C(15)	56(2)	65(2)	93(2)	-25(1)	28(2)	7(1)
C(16)	32(1)	77(2)	77(2)	-27(1)	18(1)	4(1)
C(17)	49(2)	125(3)	108(2)	-59(2)	28(2)	10(2)
C(20)	270(9)	197(7)	245(9)	-82(7)	183(8)	-131(7)
O(20)	240(6)	216(6)	328(8)	-86(6)	89(6)	-56(5)
C(21)	415(16)	236(10)	262(12)	-3(8)	222(12)	-69(10)
C(22)	1170(50)	276(13)	407(18)	-111(13)	610(30)	-240(20)

Table 5. Bond lengths [Å] and angles [°] for C39 H40 N4 O6

+

O(1)-C(14)	1.220(3)	C(20)-C(22)	1.269(11)
O(2)-C(16)	1.213(3)	C(20)-C(21)	1.392(11)
N(1)-C(16)	1.350(3)	C(16)-N(1)-C(6)	128.06(18)
N(1)-C(6)	1.409(2)	C(14)-N(2)-C(12)	126.51(16)
N(2)-C(14)	1.351(3)	C(8)-C(1)-C(8)#1	115.5(2)
N(2)-C(12)	1.418(2)	C(8)-C(1)-C(2)#1	112.63(9)
C(1)-C(8)	1.527(2)	C(8)#1-C(1)-C(2)#1	100.99(10)
C(1)-C(8)#1	1.527(2)	C(8)-C(1)-C(2)	100.99(10)
C(1)-C(2)#1	1.530(2)		
C(1)-C(2)	1.530(2)		
C(2)-C(7)	1.377(3)		
C(2)-C(3)	1.395(2)		
C(3)-C(4)	1.393(3)		
C(3)-C(9)	1.461(3)		
C(4)-C(5)	1.379(3)		
C(5)-C(6)	1.396(3)		
C(6)-C(7)	1.403(2)		
C(8)-C(13)	1.379(2)		
C(8)-C(9)	1.396(3)		
C(9)-C(10)	1.395(3)		
C(10)-C(11)	1.382(3)		
C(11)-C(12)	1.391(3)		
C(12)-C(13)	1.399(3)		
C(14)-C(15)	1.501(3)		
C(16)-C(17)	1.504(4)		
C(20)-O(20)	1.237(8)		

C(8)#1-C(1)-C(2)	112.63(9)
C(2)#1-C(1)-C(2)	114.7(2)
C(7)-C(2)-C(3)	121.21(16)
C(7)-C(2)-C(1)	127.88(15)
C(3)-C(2)-C(1)	110.86(15)
C(4)-C(3)-C(2)	119.64(17)
C(4)-C(3)-C(9)	131.83(17)
C(2)-C(3)-C(9)	108.51(15)
C(5)-C(4)-C(3)	119.64(18)
C(4)-C(5)-C(6)	120.71(17)
C(5)-C(6)-C(7)	119.77(17)
C(5)-C(6)-N(1)	122.86(16)
C(7)-C(6)-N(1)	117.36(17)
C(2)-C(7)-C(6)	119.00(17)
C(13)-C(8)-C(9)	120.88(16)
C(13)-C(8)-C(1)	128.51(15)
C(9)-C(8)-C(1)	110.61(15)
C(10)-C(9)-C(8)	120.00(17)
C(10)-C(9)-C(3)	130.96(16)
C(8)-C(9)-C(3)	109.02(16)
C(11)-C(10)-C(9)	119.31(17)
C(10)-C(11)-C(12)	120.47(18)
C(11)-C(12)-C(13)	120.47(18)
C(11)-C(12)-N(2)	121.99(17)
C(13)-C(12)-N(2)	117.50(17)
C(8)-C(13)-C(12)	118.84(17)
O(1)-C(14)-N(2)	123.42(19)
O(1)-C(14)-C(15)	121.18(19)
N(2)-C(14)-C(15)	115.36(19)
O(2)-C(16)-N(1)	123.7(2)
O(2)-C(16)-C(17)	121.4(2)
N(1)-C(16)-C(17)	114.8(2)
O(20)-C(20)-C(22)	120.1(1)
O(20)-C(20)-C(21)	117.5(1)
C(22)-C(20)-C(21)	121.8(9)

Symmetry transformations used to generate equivalent atoms:
#1 -x,y,-z+3/2

Table 6. Torsion angles [°] for C39 H40 N4 O6.

C(8)-C(1)-C(2)-C(7)	-177.27(17)
C(8)#1-C(1)-C(2)-C(7)	-53.5(3)
C(2)#1-C(1)-C(2)-C(7)	61.34(17)
C(8)-C(1)-C(2)-C(3)	0.29(18)
C(8)#1-C(1)-C(2)-C(3)	124.10(16)
C(2)#1-C(1)-C(2)-C(3)	-121.11(15)
C(7)-C(2)-C(3)-C(4)	-0.3(3)
C(1)-C(2)-C(3)-C(4)	-178.04(16)
C(7)-C(2)-C(3)-C(9)	178.03(16)
C(1)-C(2)-C(3)-C(9)	0.29(19)
C(2)-C(3)-C(4)-C(5)	0.1(3)
C(9)-C(3)-C(4)-C(5)	-177.78(18)
C(3)-C(4)-C(5)-C(6)	1.1(3)
C(4)-C(5)-C(6)-C(7)	-2.1(3)
C(4)-C(5)-C(6)-N(1)	178.31(18)
C(16)-N(1)-C(6)-C(5)	-13.1(3)
C(16)-N(1)-C(6)-C(7)	167.3(2)
C(3)-C(2)-C(7)-C(6)	-0.7(3)
C(1)-C(2)-C(7)-C(6)	176.67(16)
C(5)-C(6)-C(7)-C(2)	1.8(3)
N(1)-C(6)-C(7)-C(2)	-178.52(16)
C(8)#1-C(1)-C(8)-C(13)	58.66(16)
C(2)#1-C(1)-C(8)-C(13)	-56.7(2)
C(2)-C(1)-C(8)-C(13)	-179.54(17)
C(8)#1-C(1)-C(8)-C(9)	-122.60(15)
C(2)#1-C(1)-C(8)-C(9)	122.07(16)
C(2)-C(1)-C(8)-C(9)	-0.80(18)
C(13)-C(8)-C(9)-C(10)	1.3(3)
C(1)-C(8)-C(9)-C(10)	-177.56(17)
C(13)-C(8)-C(9)-C(3)	179.87(15)
C(1)-C(8)-C(9)-C(3)	1.0(2)
C(4)-C(3)-C(9)-C(10)	-4.4(4)
C(2)-C(3)-C(9)-C(10)	177.6(2)
C(4)-C(3)-C(9)-C(8)	177.24(19)
C(2)-C(3)-C(9)-C(8)	-0.8(2)
C(8)-C(9)-C(10)-C(11)	-1.9(3)
C(3)-C(9)-C(10)-C(11)	179.9(2)
C(9)-C(10)-C(11)-C(12)	1.0(3)
C(10)-C(11)-C(12)-C(13)	0.4(3)
C(10)-C(11)-C(12)-N(2)	178.13(19)
C(14)-N(2)-C(12)-C(11)	37.3(3)
C(14)-N(2)-C(12)-C(13)	-144.9(2)
C(9)-C(8)-C(13)-C(12)	0.1(3)
C(1)-C(8)-C(13)-C(12)	178.76(17)
C(11)-C(12)-C(13)-C(8)	-1.0(3)
N(2)-C(12)-C(13)-C(8)	-178.82(16)
C(12)-N(2)-C(14)-O(1)	-1.7(3)
C(12)-N(2)-C(14)-C(15)	-179.5(2)
C(6)-N(1)-C(16)-O(2)	0.3(5)
C(6)-N(1)-C(16)-C(17)	-179.6(3)

Symmetry transformations used to generate equivalent atoms:

#1 -x,y,-z+3/2

Table 7. Bond lengths [Å] and angles [°] related to the hydrogen bonding for C39 H40 N4 O6.

D-H	..A	d(D-H)	d(H..A)	d(D..A)	<DHA
N(1)-H(1A)	O(1)#2	0.87	2.03	2.884(3)	165.4
N(2)-H(2A)	O(2)#3	0.87	2.05	2.893(3)	162.5

Symmetry transformations used to generate equivalent atoms:

#1 -x,y,-z+3/2 #2 x,-y+2,z-1/2 #3 x-1/2,y+1/2,z

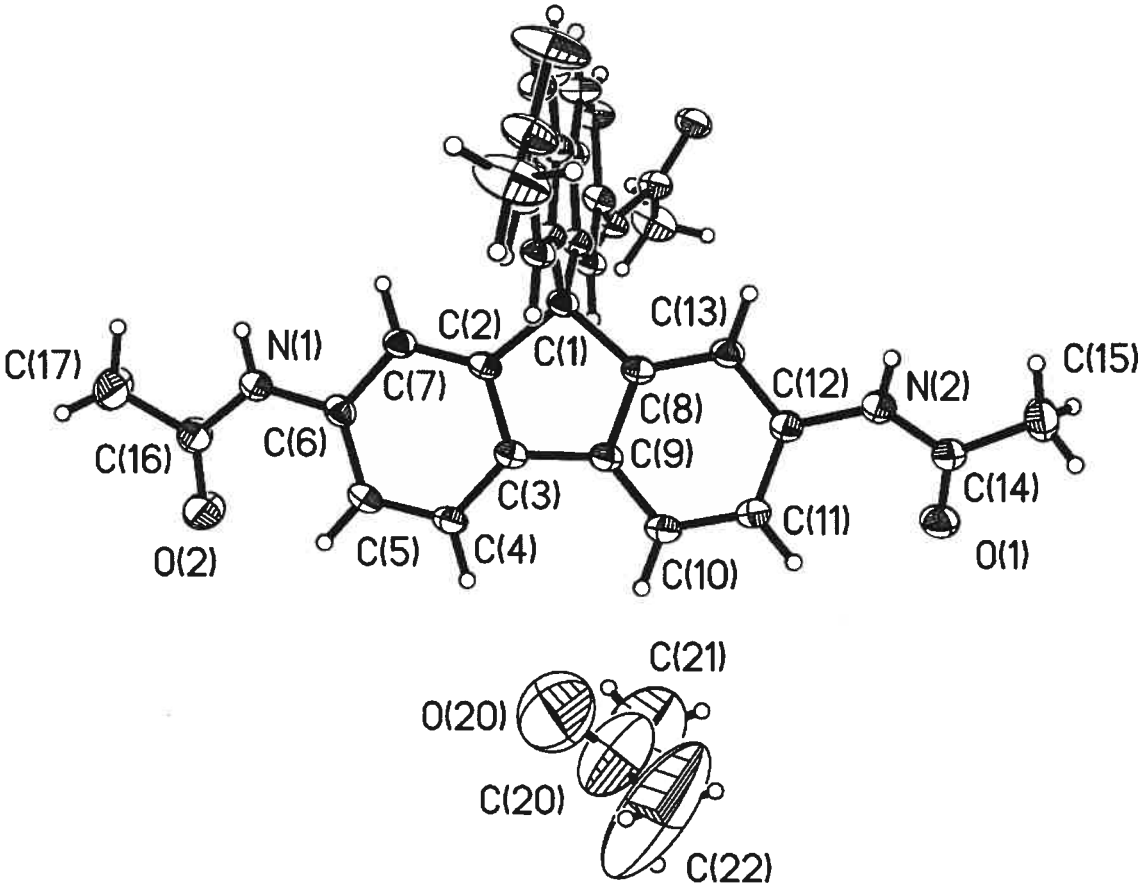

ORTEP view of the C39 H40 N4 O6 compound with the numbering scheme adopted. Ellipsoids drawn at 30% probability level. Hydrogens represented by sphere of arbitrary size.

REFERENCES

International Tables for Crystallography (1992). Vol. C. Tables 4.2.6.8 and
6.1.1.4, Dordrecht: Kluwer Academic Publishers.

SAINT (1999) Release 6.06; Integration Software for Single Crystal Data. Bruker AXS Inc., Madison, WI 53719-1173.

Sheldrick, G.M. (1996). SADABS, Bruker Area Detector Absorption Corrections.
Bruker AXS Inc., Madison, WI 53719-1173.

Sheldrick, G.M. (1997). SHELXS97, Program for the Solution of Crystal Structures. Univ. of Gottingen, Germany.

Sheldrick, G.M. (1997). SHELXL97, Program for the Refinement of Crystal Structures. Univ. of Gottingen, Germany.

SHELXTL (1997) Release 5.10; The Complete Software Package for Single Crystal Structure Determination. Bruker AXS Inc., Madison, WI 53719-1173.

SMART (1999) Release 5.059; Bruker Molecular Analysis Research Tool. Bruker AXS Inc., Madison, WI 53719-1173.

Spek, A.L. (2000). PLATON, Molecular Geometry Program, 2000 version. University of Utrecht, Utrecht, Holland.

XPREP (1997) Release 5.10; X-ray data Preparation and Reciprocal space Exploration Program. Bruker AXS Inc., Madison, WI 53719-1173.

Université de Montréal

CRYSTAL AND MOLECULAR STRUCTURE OF

C65 H88 N20 O14 S4 COMPOUND (JIW533)

Wednesday, January 29, 2003

Equipe WUEST

Département de chimie, Université de Montréal,

C.P. 6128, Succ. Centre-Ville, Montréal, Québec, H3C 3J7 (Canada)

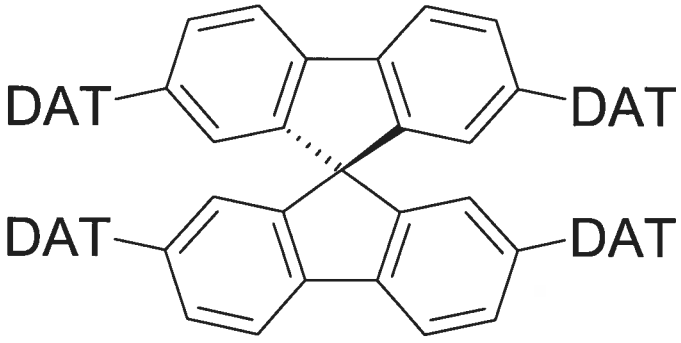

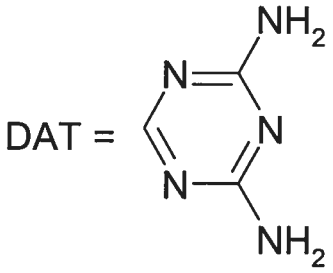

Solvant : DMSO / Dioxane

Structure solved and refined in the laboratory of X-ray diffraction, Université de Montréal by Dr. Thierry Maris.

Table 1. Crystal data and structure refinement for C65 H88 N20 O14 S4.

Identification code	JIW533
Empirical formula	C65 H88 N20 O14 S4
Formula weight	1501.79
Temperature	223(2)K
Wavelength	1.54178 Å
Crystal system	Orthorhombic
Space group	Pcca
Unit cell dimensions	a = 21.506(8) Å α = 90° b = 15.279(5) Å β = 90° c = 21.305(7) Å γ = 90°
Volume	7001(4)Å^3
Z	4
Density (calculated)	1.425 Mg/m^3
Absorption coefficient	1.914 mm^{-1}
F(000)	3176
Crystal size	0.50 x 0.30 x 0.30 mm
Theta range for data collection	2.89 to 59.03°
Index ranges	$-23 \le h \le 23$, $-13 \le k \le 16$, $-22 \le \ell \le 23$
Reflections collected	30231
Independent reflections	5042 [R_{int} = 0.054]
Absorption correction	Semi-empirical from equivalents
Max. and min. transmission	1.0000 and 0.4700
Refinement method	Full-matrix least-squares on F^2
Data / restraints / parameters	5042 / 0 / 354
Goodness-of-fit on F^2	1.103
Final R indices [I>2sigma(I)]	R_1 = 0.0913, wR_2 = 0.2847
R indices (all data)	R_1 = 0.1046, wR_2 = 0.2944

Largest diff. peak and hole 0.587 and -0.456 e/Å^3

Table 2. Atomic coordinates (x 10^4) and equivalent isotropic displacement parameters (Å^2 x 10^3) for C65 H88 N20 O14 S4.

U_{eq} is defined as one third of the trace of the orthogonalized Uij tensor.

	Occ.	x	y	z	U_{eq}
C(1)	1	5000	6399(2)	7500	35(1)
C(10)	1	5000(1)	6937(2)	8110(1)	34(1)
N(10)	1	3612(1)	8426(1)	9015(1)	42(1)
C(11)	1	5514(1)	6725(2)	8475(1)	39(1)
N(11)	1	4416(1)	9230(1)	9511(1)	42(1)
C(12)	1	5610(1)	7121(2)	9054(1)	48(1)
N(12)	1	3366(1)	9730(1)	9589(1)	41(1)
C(13)	1	5179(1)	7727(2)	9263(1)	47(1)
N(13)	1	4163(1)	10466(2)	10068(1)	54(1)
C(14)	1	4661(1)	7943(2)	8913(1)	37(1)
N(14)	1	2598(1)	8900(2)	9160(1)	54(1)
C(15)	1	4571(1)	7544(2)	8319(1)	36(1)
C(16)	1	4198(1)	8574(2)	9158(1)	39(1)
C(17)	1	3980(1)	9792(2)	9721(1)	39(1)
C(18)	1	3205(1)	9023(2)	9267(1)	42(1)
C(20)	1	4415(1)	5842(2)	7408(1)	35(1)
N(20)	1	3686(1)	3819(2)	8501(1)	57(1)
C(25)	1	4175(1)	5193(2)	7792(1)	39(1)
N(21)	1	2856(1)	2843(2)	8747(1)	62(1)
C(24)	1	3635(1)	4760(2)	7608(1)	43(1)
N(22)	1	2798(1)	3787(2)	7855(1)	70(1)
C(23)	1	3358(1)	4968(2)	7031(2)	51(1)
N(23)	1	3706(1)	2935(2)	9374(1)	81(1)
C(22)	1	3597(1)	5599(2)	6657(1)	49(1)
N(24)	1	1991(2)	2897(3)	8118(2)	114(1)
C(21)	1	4126(1)	6042(2)	6841(1)	40(1)
C(26)	1	3361(1)	4072(2)	8011(2)	49(1)
C(27)	1	3413(2)	3194(2)	8857(2)	60(1)
C(28)	1	2564(1)	3184(2)	8237(2)	65(1)
S(30)	1	2576(1)	1817(1)	10654(1)	82(1)
O(30)	1	3218(1)	11811(1)	10393(1)	63(1)
C(30)	1	2364(3)	2240(4)	6442(3)	130(2)
C(31)	0.507(7)	2261(5)	2863(9)	10397(5)	147(4)
C(32)	0.493(7)	2510(5)	685(7)	10947(5)	110(3)
S(50)	0.25	3006(3)	4710(3)	5050(3)	112(2)
O(50)	0.25	3296(9)	3794(11)	4674(8)	176(7)
C(50)	1	2500	5000	4431(4)	166(4)
C(51)	1	2500	5000	5598(4)	365(11)
S(51)	0.25	2669(5)	4218(7)	5036(5)	179(3)
C(60)	0.786(6)	4694(6)	5011(8)	9565(6)	201(5)
O(61)	1	4870(4)	4101(6)	9693(5)	284(4)
C(62)	0.786(6)	5497(10)	4412(13)	9992(8)	327(10)
C(60')	0.214(6)	4557(8)	4415(12)	9835(8)	69(5)
C(62')	0.214(6)	4107(13)	5129(17)	10044(12)	112(8)

Table 3. Hydrogen coordinates ($\times 10^4$) and isotropic displacement parameters ($Å^2 \times 10^3$) for C65 H88 N20 O14 S4.

	Occ.	x	y	z	U_{eq}
H(12)	1	5960	6981	9299	57
H(13)	1	5240	7999	9654	56
H(13A)	1	4555	10535	10154	64
H(13B)	1	3890	10838	10208	64
H(14A)	1	2328	9277	9300	65
H(14B)	1	2474	8444	8951	65
H(15)	1	4225	7691	8070	43
H(25)	1	4373	5048	8172	47
H(23)	1	3001	4663	6902	61
H(23A)	1	3534	2553	9622	97
H(23B)	1	4071	3147	9465	97
H(22)	1	3404	5735	6274	58
H(24A)	1	1785	3104	7799	136
H(24B)	1	1823	2502	8358	136
H(30A)	1	2738	2566	6544	196
H(30B)	1	2316	1757	6734	196
H(30C)	1	2006	2623	6471	196
H(31A)	0.507(7)	2178	2841	9950	220
H(31B)	0.507(7)	2559	3323	10483	220
H(31C)	0.507(7)	1877	2982	10621	220
H(50A)	0.50	2702	4887	4032	249
H(50B)	0.50	2398	5617	4462	249
H(50C)	0.50	2122	4656	4460	249
H(51A)	0.50	2679	4899	6010	548
H(51B)	0.50	2124	4655	5554	548
H(51C)	0.50	2400	5616	5552	548
H(60A)	1	5053	5280	9357	242
H(60B)	1	4362	4986	9251	242
H(62A)	1	5722	3921	10182	392
H(62B)	1	5763	4696	9680	392

Table 4. Anisotropic parameters ($Å^2$ x 10^3) for C65 H88 N20 O14 S4.

The anisotropic displacement factor exponent takes the form:

$$-2\pi^2 [h^2 a^{*2} U_{11} + ... + 2 h k a^* b^* U_{12}]$$

	U11	U22	U33	U23	U13	U12
C(1)	29(2)	43(2)	35(2)	0	0(2)	0
C(10)	31(1)	35(1)	35(1)	1(1)	3(1)	-1(1)
N(10)	34(1)	46(1)	47(1)	-10(1)	-1(1)	-1(1)
C(11)	37(1)	39(1)	39(1)	-6(1)	0(1)	0(1)
N(11)	33(1)	45(1)	47(1)	-11(1)	1(1)	4(1)
C(12)	42(2)	58(2)	43(2)	-10(1)	-7(1)	6(1)
N(12)	37(1)	43(1)	44(1)	-9(1)	1(1)	1(1)
C(13)	42(2)	52(2)	46(2)	-18(1)	-8(1)	1(1)
N(13)	38(1)	58(1)	65(2)	-25(1)	-7(1)	4(1)
C(14)	37(1)	37(1)	37(1)	-8(1)	1(1)	0(1)
N(14)	33(1)	54(1)	76(2)	-23(1)	5(1)	-3(1)
C(15)	29(1)	45(1)	33(1)	-5(1)	2(1)	-5(1)
C(16)	38(1)	46(1)	32(1)	-4(1)	0(1)	-3(1)
C(17)	35(1)	43(1)	39(1)	-8(1)	2(1)	1(1)
C(18)	33(1)	43(1)	50(2)	-6(1)	1(1)	-1(1)
C(20)	28(1)	38(1)	39(1)	-2(1)	6(1)	2(1)
N(20)	50(1)	61(1)	59(2)	17(1)	-6(1)	-17(1)
C(25)	36(1)	42(1)	39(1)	2(1)	7(1)	0(1)
N(21)	44(1)	69(2)	75(2)	24(1)	-7(1)	-12(1)
C(24)	37(1)	43(1)	49(2)	-1(1)	6(1)	-1(1)
N(22)	52(1)	75(2)	82(2)	34(2)	-14(2)	-21(1)
C(23)	38(1)	51(2)	63(2)	9(1)	-9(2)	-10(1)
N(23)	64(2)	103(2)	75(2)	42(2)	-20(2)	-30(2)
C(22)	41(1)	58(2)	47(2)	8(1)	-8(1)	-11(1)
N(24)	69(2)	154(3)	117(2)	84(2)	-45(2)	-59(2)
C(21)	35(1)	43(1)	40(1)	2(1)	-2(1)	-1(1)
C(26)	41(2)	48(2)	59(2)	7(1)	1(2)	-4(1)
C(27)	47(2)	62(2)	70(2)	18(2)	-7(2)	-7(2)
C(28)	45(2)	75(2)	75(2)	30(2)	-5(2)	-17(2)
S(30)	69(1)	97(1)	79(1)	3(1)	10(1)	-7(1)
O(30)	53(1)	68(1)	68(1)	-2(1)	1(1)	2(1)
C(30)	150(5)	140(4)	101(3)	-40(3)	-17(4)	31(4)
C(31)	130(7)	213(10)	98(7)	59(7)	37(6)	92(7)
S(50)	119(3)	120(3)	98(3)	-24(3)	4(3)	-60(3)
O(50)	232(17)	147(11)	150(11)	-85(10)	-74(12)	15(13)
C(50)	265(11)	122(6)	112(6)	0	0	-67(7)
C(51)	309(13)	750(30)	42(4)	0	0	292(16)

Table 5. Bond lengths [Å] and angles [°] for C65 H88 N20 O14 S4

C(1)-C(20) 1.533(3)
C(1)-C(20)#1 1.533(3)
C(1)-C(10) 1.537(3)
C(1)-C(10)#1 1.537(3)
C(10)-C(15) 1.382(3)
C(10)-C(11) 1.390(4)
N(10)-C(16) 1.317(3)
N(10)-C(18) 1.373(3)
C(11)-C(12) 1.389(4)
C(11)-C(21)#1 1.463(4)
N(11)-C(16) 1.338(3)
N(11)-C(17) 1.348(3)
C(12)-C(13) 1.383(4)
N(12)-C(18) 1.326(3)
N(12)-C(17) 1.354(3)
C(13)-C(14) 1.380(4)
N(13)-C(17) 1.327(3)
C(14)-C(15) 1.419(4)
C(14)-C(16) 1.481(4)
N(14)-C(18) 1.337(3)
C(20)-C(25) 1.385(3)
C(20)-C(21) 1.392(4)
N(20)-C(26) 1.315(4)
N(20)-C(27) 1.353(4)
C(25)-C(24) 1.393(4)
N(21)-C(27) 1.334(4)
N(21)-C(28) 1.358(4)
C(24)-C(23) 1.402(4)
C(24)-C(26) 1.480(4)
N(22)-C(26) 1.328(4)
N(22)-C(28) 1.329(4)
C(23)-C(22) 1.351(4)
N(23)-C(27) 1.330(4)
C(22)-C(21) 1.382(4)
N(24)-C(28) 1.331(4)
C(21)-C(11)#1 1.463(4)
S(30)-O(30)#2 1.489(2)
S(30)-C(30)#3 1.802(5)
S(30)-C(31) 1.820(12)
O(30)-S(30)#4 1.489(2)
C(30)-S(30)#5 1.802(5)
S(50)-C(51) 1.657(8)
S(50)-O(50) 1.728(17)
S(50)-C(50) 1.766(9)
S(50)-S(50)#6 2.352(12)
S(51)-S(51)#6 2.50(2)
C(60)-C(62)#7 1.36(2)
C(60)-O(61) 1.466(14)
O(61)-C(62) 1.56(2)
C(62)-C(60)#7 1.36(2)
C(60')-C(62') 1.52(3)

C(20)-C(1)-C(20)#1
112.5(3)

C(20)-C(1)-C(10)	113.93(13)
C(20)#1-C(1)-C(10)	100.85(13)
C(20)-C(1)-C(10)#1	100.85(13)
C(20)#1-C(1)-C(10)#1	113.93(13)
C(10)-C(1)-C(10)#1	115.4(3)
C(15)-C(10)-C(11)	120.5(2)
C(15)-C(10)-C(1)	129.1(2)
C(11)-C(10)-C(1)	110.5(2)
C(16)-N(10)-C(18)	114.0(2)
C(12)-C(11)-C(10)	120.9(2)
C(12)-C(11)-C(21)#1	129.9(2)
C(10)-C(11)-C(21)#1	109.1(2)
C(16)-N(11)-C(17)	114.9(2)
C(13)-C(12)-C(11)	118.5(3)
C(18)-N(12)-C(17)	114.8(2)
C(14)-C(13)-C(12)	121.8(3)
C(13)-C(14)-C(15)	119.3(2)
C(13)-C(14)-C(16)	120.5(2)
C(15)-C(14)-C(16)	120.2(2)
C(10)-C(15)-C(14)	119.0(2)
N(10)-C(16)-N(11)	126.4(2)
N(10)-C(16)-C(14)	116.8(2)
N(11)-C(16)-C(14)	116.8(2)
N(13)-C(17)-N(11)	118.3(2)
N(13)-C(17)-N(12)	117.3(2)
N(11)-C(17)-N(12)	124.4(2)
N(12)-C(18)-N(14)	117.2(2)
N(12)-C(18)-N(10)	125.2(2)
N(14)-C(18)-N(10)	117.5(2)
C(25)-C(20)-C(21)	120.3(2)
C(25)-C(20)-C(1)	128.9(2)
C(21)-C(20)-C(1)	110.8(2)
C(26)-N(20)-C(27)	115.0(3)
C(20)-C(25)-C(24)	118.9(2)
C(27)-N(21)-C(28)	113.7(3)

C(25)-C(24)-C(23)
119.6(2)

C(25)-C(24)-C(26)	120.4(2)
C(23)-C(24)-C(26)	120.0(2)
C(26)-N(22)-C(28)	114.8(3)
C(22)-C(23)-C(24)	121.1(3)
C(23)-C(22)-C(21)	119.7(3)
C(22)-C(21)-C(20)	120.3(2)
C(22)-C(21)-C(11)#1	130.9(2)
C(20)-C(21)-C(11)#1	108.8(2)
N(20)-C(26)-N(22)	125.9(3)
N(20)-C(26)-C(24)	117.2(2)
N(22)-C(26)-C(24)	116.8(3)
N(23)-C(27)-N(21)	116.9(3)
N(23)-C(27)-N(20)	118.0(3)
N(21)-C(27)-N(20)	125.0(3)
N(22)-C(28)-N(24)	117.5(3)
N(22)-C(28)-N(21)	125.5(3)

N(24)-C(28)-N(21)
117.0(3)
O(30)#2-S(30)-C(30)#3
106.5(2)
O(30)#2-S(30)-C(31)
103.8(4)
C(30)#3-S(30)-C(31)
89.6(4)
C(51)-S(50)-O(50)
141.2(7)
C(51)-S(50)-C(50)
93.1(4)
O(50)-S(50)-C(50)
94.6(6)

C(51)-S(50)-S(50)#6	44.8(3)
O(50)-S(50)-S(50)#6	129.8(7)
C(50)-S(50)-S(50)#6	48.3(3)
C(62)#7-C(60)-O(61)	124.4(13)
C(60)-O(61)-C(62)	90.6(10)
C(60)#7-C(62)-O(61)	102.7(15)

Symmetry transformations used to generate equivalent atoms:

#1 -x+1,y,-z+3/2 #2 x,y-1,z #3 -x+1/2,y,z+1/2
#4 x,y+1,z #5 -x+1/2,y,z-1/2 #6 -x+1/2,-y+1,z
#7 -x+1,-y+1,-z+2

Table 6. Torsion angles [°] for C65 H88 N20 O14 S4.

C(20)-C(1)-C(10)-C(15) -56.7(4)
C(20)#1-C(1)-C(10)-C(15)-177.4(2)
C(10)#1-C(1)-C(10)-C(15) 59.3(2)
C(20)-C(1)-C(10)-C(11) 122.0(2)
C(20)#1-C(1)-C(10)-C(11) 1.3(3)
C(10)#1-C(1)-C(10)-C(11)-122.0(2)
C(15)-C(10)-C(11)-C(12) -0.4(4)
C(1)-C(10)-C(11)-C(12) -179.2(2)
C(15)-C(10)-C(11)-C(21)#1177.5(2)
C(1)-C(10)-C(11)-C(21)#1 -1.4(3)
C(10)-C(11)-C(12)-C(13) 0.5(4)
C(21)#1-C(11)-C(12)-C(13-176.8(3)
C(11)-C(12)-C(13)-C(14) 0.1(4)
C(12)-C(13)-C(14)-C(15) -1.0(4)
C(12)-C(13)-C(14)-C(16) 178.2(3)
C(11)-C(10)-C(15)-C(14) -0.5(4)
C(1)-C(10)-C(15)-C(14) 178.1(2)
C(13)-C(14)-C(15)-C(10) 1.2(4)
C(16)-C(14)-C(15)-C(10) -178.0(2)
C(18)-N(10)-C(16)-N(11) -0.1(4)
C(18)-N(10)-C(16)-C(14) 178.6(2)
C(17)-N(11)-C(16)-N(10) -1.7(4)
C(17)-N(11)-C(16)-C(14) 179.6(2)
C(13)-C(14)-C(16)-N(10) -144.7(3)
C(15)-C(14)-C(16)-N(10) 34.5(4)
C(13)-C(14)-C(16)-N(11) 34.1(4)
C(15)-C(14)-C(16)-N(11) -146.7(2)
C(16)-N(11)-C(17)-N(13) -179.1(2)
C(16)-N(11)-C(17)-N(12) -0.8(4)
C(18)-N(12)-C(17)-N(13) -176.8(2)
C(18)-N(12)-C(17)-N(11) 4.8(4)
C(17)-N(12)-C(18)-N(14) 175.7(2)
C(17)-N(12)-C(18)-N(10) -7.0(4)
C(16)-N(10)-C(18)-N(12) 4.9(4)
C(16)-N(10)-C(18)-N(14) -177.9(3)
C(20)#1-C(1)-C(20)-C(25) 55.5(2)

C(10)-C(1)-C(20)-C(25) -58.4(4)
C(10)#1-C(1)-C(20)-C(25) 177.3(2)
C(20)#1-C(1)-C(20)-C(21)-122.5(2)
C(10)-C(1)-C(20)-C(21) 123.5(2)
C(10)#1-C(1)-C(20)-C(21) -0.8(3)
C(21)-C(20)-C(25)-C(24) -1.2(4)
C(1)-C(20)-C(25)-C(24) -179.1(2)
C(20)-C(25)-C(24)-C(23) 2.0(4)
C(20)-C(25)-C(24)-C(26) -179.2(2)
C(25)-C(24)-C(23)-C(22) -1.8(4)
C(26)-C(24)-C(23)-C(22) 179.4(3)
C(24)-C(23)-C(22)-C(21) 0.7(5)
C(23)-C(22)-C(21)-C(20) 0.1(4)
C(23)-C(22)-C(21)-C(11)#1178.1(3)
C(25)-C(20)-C(21)-C(22) 0.2(4)
C(1)-C(20)-C(21)-C(22) 178.4(2)
C(25)-C(20)-C(21)-C(11)#-178.2(2)
C(1)-C(20)-C(21)-C(11)#1 0.0(3)
C(27)-N(20)-C(26)-N(22) 2.0(5)
C(27)-N(20)-C(26)-C(24) 179.5(3)
C(28)-N(22)-C(26)-N(20) -1.1(5)
C(28)-N(22)-C(26)-C(24) -178.6(3)
C(25)-C(24)-C(26)-N(20) -8.1(4)
C(23)-C(24)-C(26)-N(20) 170.7(3)
C(25)-C(24)-C(26)-N(22) 169.6(3)
C(23)-C(24)-C(26)-N(22) -11.6(4)
C(28)-N(21)-C(27)-N(23) 175.4(3)
C(28)-N(21)-C(27)-N(20) -1.4(5)
C(26)-N(20)-C(27)-N(23) -177.4(3)
C(26)-N(20)-C(27)-N(21) -0.7(5)
C(26)-N(22)-C(28)-N(24) 177.7(3)
C(26)-N(22)-C(28)-N(21) -1.3(5)
C(27)-N(21)-C(28)-N(22) 2.4(5)
C(27)-N(21)-C(28)-N(24) -176.6(3)
C(62)#7-C(60)-O(61)-C(62)-74.1(18)

C(60)-O(61)-C(62)-C(60)#7 54.4(15)

Symmetry transformations used to generate equivalent atoms:

#1 -x+1,y,-z+3/2	#2 x,y-1,z	#3 -x+1/2,y,z+1/2
#4 x,y+1,z	#5 -x+1/2,y,z-1/2	#6 -x+1/2,-y+1,z
#7 -x+1,-y+1,-z+2		

Table 7. Bond lengths [Å] and angles [°] related to the hydrogen bonding for C65 H88 N20 O14 S4.

D-H	..A	d(D-H)	d(H..A)	d(D..A)	<DHA
N(13)-H(13A)	N(11)#8	0.87	2.35	3.219(3)	174.3
N(13)-H(13B)	O(30)	0.87	2.11	2.971(3)	170.4
N(14)-H(14A)	N(12)#9	0.87	2.22	3.085(3)	176.1
N(14)-H(14B)	N(21)#6	0.87	2.13	2.970(4)	160.9
N(23)-H(23A)	O(30)#2	0.87	2.11	2.960(4)	166.1
N(23)-H(23B)	O(61)	0.87	2.31	3.147(10)	162.6
N(24)-H(24B)	N(10)#6	0.87	2.20	3.069(4)	176.1

Symmetry transformations used to generate equivalent atoms:

#1 -x+1,y,-z+3/2	#2 x,y-1,z	#3 -x+1/2,y,z+1/2
#4 x,y+1,z	#5 -x+1/2,y,z-1/2	#6 -x+1/2,-y+1,z
#7 -x+1,-y+1,-z+2	#8 -x+1,-y+2,-z+2	#9 -x+1/2,-y+2,z

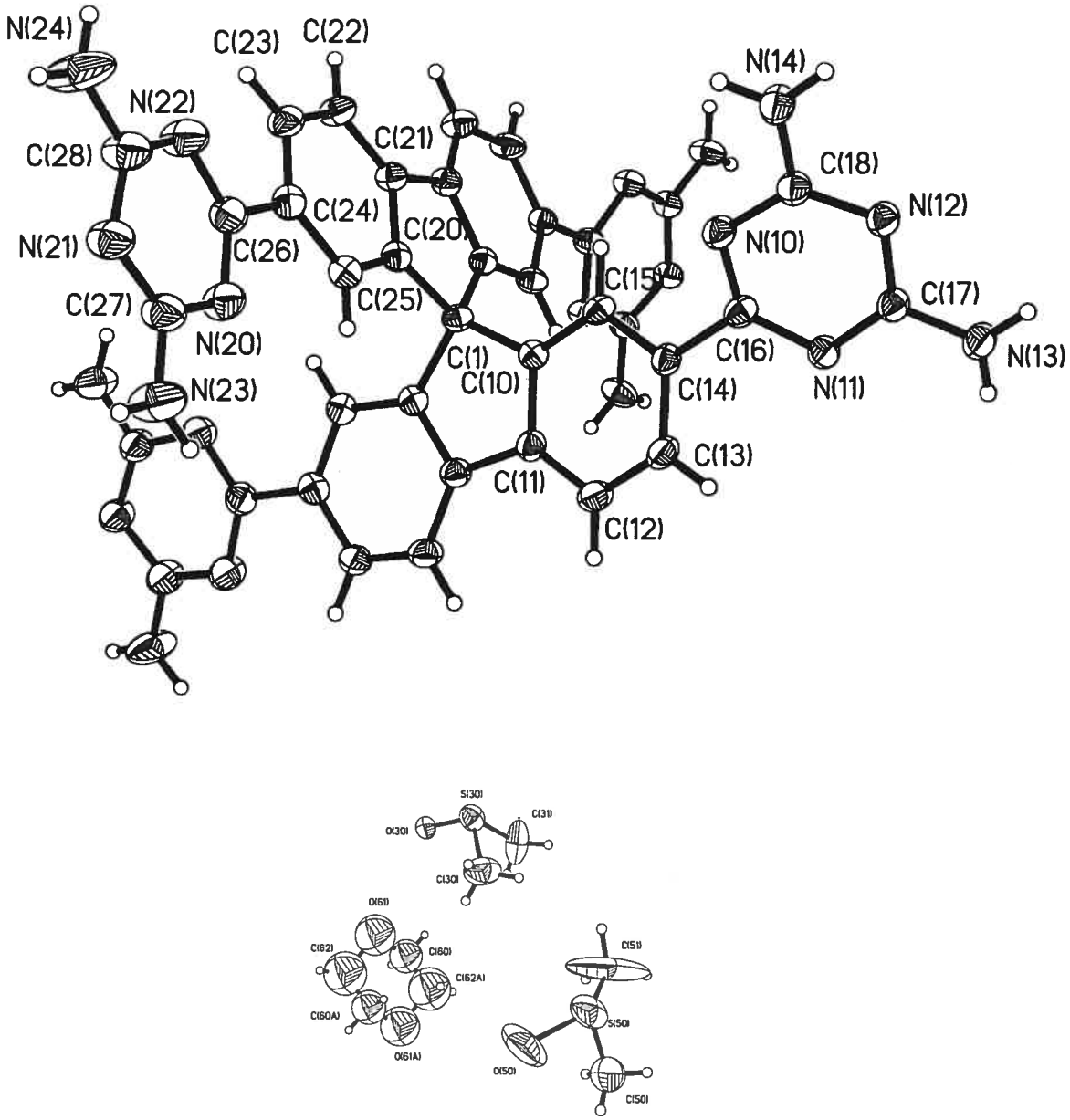

ORTEP view of the C65 H88 N20 O14 S4 compound with the numbering scheme adopted. Ellipsoids drawn at 30% probability level. Hydrogens represented by sphere of arbitrary size.

REFERENCES

International Tables for Crystallography (1992). Vol. C. Tables 4.2.6.8 and
6.1.1.4, Dordrecht: Kluwer Academic Publishers.

SAINT (1999) Release 6.06; Integration Software for Single Crystal Data. Bruker AXS Inc., Madison, WI 53719-1173.

Sheldrick, G.M. (1996). SADABS, Bruker Area Detector Absorption Corrections.
Bruker AXS Inc., Madison, WI 53719-1173.

Sheldrick, G.M. (1997). SHELXS97, Program for the Solution of Crystal Structures. Univ. of Gottingen, Germany.

Sheldrick, G.M. (1997). SHELXL97, Program for the Refinement of Crystal Structures. Univ. of Gottingen, Germany.

SHELXTL (1997) Release 5.10; The Complete Software Package for Single Crystal Structure Determination. Bruker AXS Inc., Madison, WI 53719-1173.

SMART (1999) Release 5.059; Bruker Molecular Analysis Research Tool. Bruker AXS Inc., Madison, WI 53719-1173.

Spek, A.L. (2000). PLATON, Molecular Geometry Program, 2000 version. University of Utrecht, Utrecht, Holland.

XPREP (1997) Release 5.10; X-ray data Preparation and Reciprocal space Exploration Program. Bruker AXS Inc., Madison, WI 53719-1173.

Université de Montréal

CRYSTAL AND MOLECULAR STRUCTURE OF

C85 H144 N24 O24 S8 COMPOUND (JIW538)

Wednesday, January 29, 2003

Equipe WUEST

Département de chimie, Université de Montréal,

C.P. 6128, Succ. Centre-Ville, Montréal, Québec, H3C 3J7 (Canada)

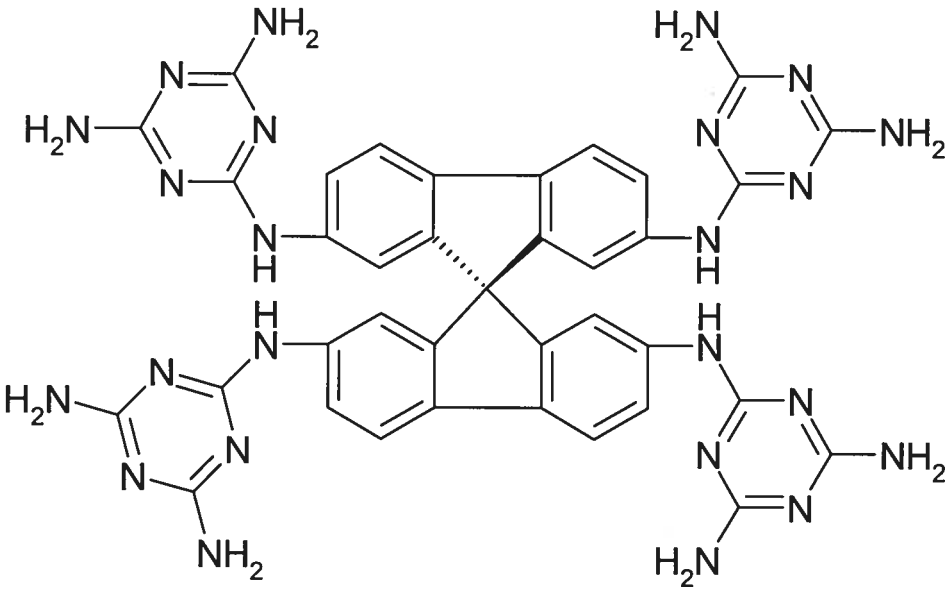

Solvant : DMSO / Dioxane

Structure solved and refined in the laboratory of X-ray diffraction Université de Montréal by Dr. Thierry Maris.

Table 1. Crystal data and structure refinement for C85 H144 N24 O24 S8.

Identification code	JIW538
Empirical formula	C85 H144 N24 O24 S8
Formula weight	2142.72
Temperature	223(2)K
Wavelength	1.54178 Å
Crystal system	Tetragonal
Space group	P-4b2
Unit cell dimensions	a = 23.519(4) Å α = 90° b = 23.519(4) Å β = 90° c = 10.2647(13) Å γ = 90°
Volume	5677.8(14)Å^3
Z	2
Density (calculated)	1.253 Mg/m^3
Absorption coefficient	2.076 mm^{-1}
F(000)	2284
Crystal size	0.60 x 0.20 x 0.20 mm
Theta range for data collection	5.06 to 58.89°
Index ranges	$-26 \leq h \leq 25$, $-25 \leq k \leq 24$, $-10 \leq \ell \leq 11$
Reflections collected	28079
Independent reflections	4057 [R_{int} = 0.056]
Absorption correction	Semi-empirical from equivalents
Max. and min. transmission	1.0000 and 0.6300
Refinement method	Full-matrix least-squares on F^2
Data / restraints / parameters	4057 / 36 / 330
Goodness-of-fit on F^2	1.053
Final R indices [I>2sigma(I)]	R_1 = 0.0743, wR_2 = 0.1838
R indices (all data)	R_1 = 0.0931, wR_2 = 0.1973
Absolute structure parameter	0.00(4)

Largest diff. peak and hole 0.307 and -0.363 e/Å^3

Table 2. Atomic coordinates (x 10^4) and equivalent isotropic displacement parameters (Å^2 x 10^3) for C85 H144 N24 O24 S8.

U_{eq} is defined as one third of the trace of the orthogonalized Uij tensor.

	Occ.	x	y	z	U_{eq}
C(1)	1	10000	0	5000	46(2)
N(1)	1	8665(2)	-1542(2)	6301(3)	70(1)
C(2)	1	9680(2)	-379(2)	5947(3)	48(1)
N(2)	1	8756(2)	-2098(2)	8135(3)	66(1)
C(3)	1	9804(2)	-238(2)	7235(3)	52(1)
N(3)	1	8180(2)	-2940(2)	8273(3)	73(1)
C(4)	1	9543(2)	-539(2)	8226(3)	63(1)
N(4)	1	8133(2)	-2351(2)	6378(3)	68(1)
C(5)	1	9169(2)	-968(2)	7945(3)	70(1)
N(5)	1	8786(2)	-2680(2)	9921(3)	82(1)
C(6)	1	9057(2)	-1112(2)	6644(3)	62(1)
N(6)	1	7610(2)	-3154(2)	6548(3)	91(1)
C(7)	1	9300(2)	-816(2)	5649(3)	53(1)
C(8)	1	8515(2)	-2017(2)	6968(3)	62(1)
C(9)	1	7985(2)	-2803(2)	7072(3)	68(1)
C(10)	1	8575(2)	-2565(2)	8733(4)	76(1)
S(10)	1	6099(1)	-2967(1)	7406(1)	119(1)
O(10)	1	6078(2)	-3216(2)	6096(4)	116(1)
C(10A)	1	5425(4)	-2641(4)	7685(7)	161(3)
C(10B)	1	5982(5)	-3541(4)	8484(8)	183(4)
S(20A)	0.624(4)	8073(1)	222(1)	7128(2)	97(1)
O(20)	1	7787(2)	730(2)	7705(4)	128(2)
C(20A)	1	7837(5)	142(5)	5629(9)	208(5)
C(20B)	1	7724(5)	-380(4)	7760(11)	185(4)
S(20B)	0.376(4)	7482(2)	172(2)	7014(5)	123(2)
O(30)	1	6296(3)	-2139(3)	10130(7)	174(2)
C(31)	1	6859(5)	-2238(5)	10395(14)	207(6)
C(32)	1	6161(5)	-1548(5)	10385(13)	209(5)
C(40)	0.743(12)	6930(6)	-1593(6)	5391(15)	169(5)
C(41)	0.257(12)	6042(10)	-1801(10)	4400(20)	87(7)
C(42)	0.743(12)	6496(13)	-1691(12)	3910(30)	284(12)
C(43A)	0.743(12)	5952(7)	-1195(7)	4319(16)	183(6)
C(43B)	0.257(12)	6234(15)	-794(16)	4660(40)	143(12)
C(60)	0.25	9162(13)	-3971(13)	12390(30)	123(8)
C(61)	0.25	9060(30)	-4630(30)	13120(50)	212(19)
C(62)	0.25	9390(20)	-3900(20)	14160(60)	180(16)
C(63)	0.25	9957(18)	-4541(19)	12000(40)	161(12)
C(64)	0.25	9450(20)	-3920(20)	13290(70)	177(16)
C(65)	0.25	8936(19)	-4920(20)	12250(50)	184(15)

C(66)	0.25	9038(19)	-4250(20)	11220(40)	168(13)
C(67)	0.25	9160(20)	-3660(20)	14940(50)	187(16)
C(68)	0.25	8733(16)	-4379(16)	12410(40)	148(11)
C(69)	0.25	9370(17)	-3920(16)	11470(40)	144(10)
C(70)	0.25	9620(20)	-4220(20)	12520(50)	172(13)
C(71)	0.25	9277(12)	-3373(12)	16380(30)	115(8)
C(72)	0.25	5986(12)	-1835(12)	5150(30)	109(8)
C(73)	0.20	9620(20)	-5160(20)	11690(50)	174(17)
C(74)	0.20	9150(30)	-4740(30)	10870(60)	190(20)

Table 3. Hydrogen coordinates (x 10^4) and isotropic displacement parameters ($Å^2$ x 10^3) for C85 H144 N24 O24 S8.

	Occ.	x	y	z	U_{eq}
H(1)	1	8496	-1496	5554	84
H(4)	1	9623	-448	9098	76
H(5)	1	8988	-1165	8624	83
H(5A)	1	9032	-2451	10275	98
H(5B)	1	8676	-2983	10337	98
H(6A)	1	7472	-3084	5778	109
H(6B)	1	7502	-3456	6973	109
H(7)	1	9214	-904	4777	63
H(10A)	1	5380	-2319	7104	241
H(10B)	1	5403	-2513	8581	241
H(10C)	1	5125	-2915	7520	241
H(10D)	1	6308	-3794	8466	275
H(10E)	1	5645	-3748	8216	275
H(10F)	1	5929	-3397	9360	275
H(20A)	1	7991	441	5082	312
H(20B)	1	7425	163	5626	312
H(20C)	1	7956	-225	5297	312
H(20D)	1	7819	-423	8674	278
H(20E)	1	7844	-715	7286	278
H(20F)	1	7316	-333	7669	278
H(31A)	1	6949	-2637	10204	249
H(31B)	1	6931	-2173	11324	249
H(32A)	1	6204	-1470	11318	251
H(32B)	1	5764	-1474	10146	251

Table 4. Anisotropic parameters ($Å^2$ x 10^3) for C85 H144 N24 O24 S8.

The anisotropic displacement factor exponent takes the form:

$$-2\pi^2 [h^2 a^{*2} U_{11} + ... + 2 h k a^* b^* U_{12}]$$

	U11	U22	U33	U23	U13	U12
C(1)	56(3)	56(3)	27(3)	0	0	0
N(1)	84(2)	86(2)	41(1)	4(2)	-5(1)	-30(2)
C(2)	54(2)	54(2)	35(1)	-2(2)	6(1)	4(2)
N(2)	82(2)	76(2)	40(1)	7(1)	-3(2)	-31(2)
C(3)	58(2)	59(2)	38(1)	1(2)	-9(2)	0(2)
N(3)	96(3)	82(2)	40(2)	5(2)	-6(2)	-38(2)
C(4)	89(3)	72(3)	28(1)	-6(2)	6(2)	-19(2)
N(4)	83(2)	82(2)	39(2)	0(2)	-1(2)	-22(2)
C(5)	91(3)	76(3)	42(2)	-2(2)	10(2)	-30(2)
N(5)	102(3)	89(3)	53(2)	18(2)	-21(2)	-34(2)
C(6)	79(3)	64(3)	43(2)	-1(2)	-5(2)	-15(2)
N(6)	120(3)	103(3)	50(2)	8(2)	-15(2)	-51(3)
C(7)	61(2)	67(2)	31(1)	-4(2)	-1(2)	-1(2)
C(8)	76(3)	74(3)	36(2)	2(2)	2(2)	-17(2)
C(9)	87(3)	76(3)	39(2)	-8(2)	4(2)	-28(2)
C(10)	92(3)	97(3)	38(2)	1(2)	-4(2)	-30(3)
S(10)	135(1)	150(1)	72(1)	-30(1)	7(1)	-28(1)
O(10)	142(3)	128(3)	78(2)	-29(2)	26(2)	-44(2)
C(10A)	171(7)	209(8)	102(5)	-9(5)	16(5)	70(6)
C(10B)	239(10)	199(9)	111(5)	41(6)	34(6)	54(8)
S(20A)	106(2)	90(2)	94(1)	-11(1)	10(1)	19(1)
O(20)	206(4)	94(3)	84(2)	-21(2)	-4(3)	55(3)
C(20A)	263(11)	214(10)	146(6)	-71(7)	87(7)	-76(9)
C(20B)	216(9)	146(6)	194(9)	42(7)	21(8)	24(7)
S(20B)	124(4)	145(4)	101(3)	-8(3)	4(2)	33(3)
O(30)	158(6)	173(6)	191(6)	22(5)	-14(4)	2(5)
C(31)	167(9)	214(11)	240(15)	28(9)	-74(9)	18(8)
C(32)	178(10)	222(13)	227(14)	-2(9)	30(8)	64(10)

Table 5. Selected bond lengths [Å] and angles [°] for C85 H144 N24 O24 S8

C(1)-C(2)#1	
1.519(3)	
C(1)-C(2)#2	
1.519(3)	
C(1)-C(2)#3	
1.519(3)	
C(1)-C(2)	
1.519(3)	
N(1)-C(8)	
1.356(5)	
N(1)-C(6)	
1.413(5)	
C(2)-C(3)	
1.394(4)	
C(2)-C(7)	
1.396(5)	
N(2)-C(10)	
1.328(5)	
N(2)-C(8)	
1.338(5)	
C(3)-C(4)	
1.383(5)	
C(3)-C(3)#3	
1.448(7)	
N(3)-C(9)	
1.355(5)	
N(3)-C(10)	
1.366(5)	
C(4)-C(5)	
1.370(6)	
N(4)-C(9)	
1.326(5)	
N(4)-C(8)	
1.339(5)	
C(5)-C(6)	
1.403(5)	
N(5)-C(10)	
1.344(5)	
C(6)-C(7)	
1.363(5)	
N(6)-C(9)	
1.322(5)	
S(10)-O(10)	
1.468(4)	
S(10)-C(10B)	
1.768(9)	
S(10)-C(10A)	
1.783(7)	
S(20A)-O(20)	
1.492(4)	
S(20A)-C(20A)	
1.646(10)	
S(20A)-C(20B)	
1.760(10)	
O(30)-C(31)	
1.373(11)	
O(30)-C(32)	
1.449(12)	
C(31)-C(31)#4	
1.50(2)	
C(32)-C(32)#4	
1.51(2)	
C(2)#1-C(1)-C(2)#2	
100.4(2)	
C(2)#1-C(1)-C(2)#3	
114.20(13)	
C(2)#2-C(1)-C(2)#3	
114.20(13)	
C(2)#1-C(1)-C(2)	
114.20(13)	
C(2)#2-C(1)-C(2)	114.20(13)
C(2)#3-C(1)-C(2)	100.4(2)
C(8)-N(1)-C(6)	129.3(3)
C(3)-C(2)-C(7)	121.2(3)
C(3)-C(2)-C(1)	111.3(3)
C(7)-C(2)-C(1)	127.5(2)
C(10)-N(2)-C(8)	113.3(3)
C(4)-C(3)-C(2)	118.8(3)
C(4)-C(3)-C(3)#3	132.6(2)
C(2)-C(3)-C(3)#3	108.5(2)
C(9)-N(3)-C(10)	113.1(3)
C(5)-C(4)-C(3)	120.5(3)
C(9)-N(4)-C(8)	113.9(3)
C(4)-C(5)-C(6)	119.9(3)
C(7)-C(6)-C(5)	120.8(4)
C(7)-C(6)-N(1)	116.9(3)
C(5)-C(6)-N(1)	122.2(3)
C(6)-C(7)-C(2)	118.7(3)
N(2)-C(8)-N(4)	127.2(3)
N(2)-C(8)-N(1)	117.3(3)
N(4)-C(8)-N(1)	115.5(3)
N(6)-C(9)-N(4)	117.3(3)
N(6)-C(9)-N(3)	116.6(4)
N(4)-C(9)-N(3)	126.1(4)
N(2)-C(10)-N(5)	117.9(4)
N(2)-C(10)-N(3)	126.3(3)
N(5)-C(10)-N(3)	115.8(4)
O(10)-S(10)-C(10B)	105.2(4)
O(10)-S(10)-C(10A)	106.7(3)
C(10B)-S(10)-C(10A)	95.1(5)
O(20)-S(20A)-C(20A)	108.1(5)
O(20)-S(20A)-C(20B)	106.7(4)
C(20A)-S(20A)-C(20B)	95.5(6)
C(31)-O(30)-C(32)	109.9(9)

O(30)-C(31)-C(31)#4	111.4(9)
O(30)-C(32)-C(32)#4	110.5(8)

Symmetry transformations used to generate equivalent atoms:

#1 y+1,-x+1,-z+1	#2 -y+1,x-1,-z+1
#3 -x+2,-y,z	#4 -y+1/2,-x+1/2,-z+2

Table 6. Selected torsion angles [°] for C85 H144 N24 O24 S8.

C(2)#1-C(1)-C(2)-C(3)	-123.0(2)
C(2)#2-C(1)-C(2)-C(3)	122.2(2)
C(2)#3-C(1)-C(2)-C(3)	-0.41(19)
C(2)#1-C(1)-C(2)-C(7)	56.5(5)
C(2)#2-C(1)-C(2)-C(7)	-58.3(5)
C(2)#3-C(1)-C(2)-C(7)	179.1(4)
C(7)-C(2)-C(3)-C(4)	-0.1(6)
C(1)-C(2)-C(3)-C(4)	179.4(3)
C(7)-C(2)-C(3)-C(3)#3	-178.5(4)
C(1)-C(2)-C(3)-C(3)#3	1.0(5)
C(2)-C(3)-C(4)-C(5)	0.0(6)
C(3)#3-C(3)-C(4)-C(5)	177.9(5)
C(3)-C(4)-C(5)-C(6)	1.3(7)
C(4)-C(5)-C(6)-C(7)	-2.4(7)
C(4)-C(5)-C(6)-N(1)	-178.6(4)
C(8)-N(1)-C(6)-C(7)	154.3(4)
C(8)-N(1)-C(6)-C(5)	-29.4(7)
C(5)-C(6)-C(7)-C(2)	2.2(6)
N(1)-C(6)-C(7)-C(2)	178.6(4)
C(3)-C(2)-C(7)-C(6)	-1.0(6)
C(1)-C(2)-C(7)-C(6)	179.5(3)
C(10)-N(2)-C(8)-N(4)	-0.7(6)
C(10)-N(2)-C(8)-N(1)	178.5(4)
C(9)-N(4)-C(8)-N(2)	0.9(6)
C(9)-N(4)-C(8)-N(1)	-178.3(4)
C(6)-N(1)-C(8)-N(2)	1.4(7)
C(6)-N(1)-C(8)-N(4)	-179.3(4)
C(8)-N(4)-C(9)-N(6)	-179.7(4)
C(8)-N(4)-C(9)-N(3)	0.4(7)
C(10)-N(3)-C(9)-N(6)	178.4(4)
C(10)-N(3)-C(9)-N(4)	-1.7(7)
C(8)-N(2)-C(10)-N(5)	-179.0(4)
C(8)-N(2)-C(10)-N(3)	-0.9(7)
C(9)-N(3)-C(10)-N(2)	2.0(7)
C(9)-N(3)-C(10)-N(5)	-179.8(4)
C(32)-O(30)-C(31)-C(31)#4	-57.9(16)
C(31)-O(30)-C(32)-C(32)#4	55.9(16)

Symmetry transformations used to generate equivalent atoms:

#1 y+1,-x+1,-z+1 #2 -y+1,x-1,-z+1
#3 -x+2,-y,z #4 -y+1/2,-x+1/2,-z+2

Table 7. Bond lengths [Å] and angles [°] related to the hydrogen bonding for C85 H144 N24 O24 S8.

D-H	..A	d(D-H)	d(H..A)	d(D..A)	<DHA
N(1)-H(1)	O(10)#5	0.87	2.07	2.892(5)	157.9
N(5)-H(5A)	O(20)#6	0.87	2.22	2.905(5)	135.5
N(5)-H(5B)	N(3)#4	0.87	2.29	2.963(5)	134.2
N(6)-H(6A)	N(4)#5	0.87	2.23	3.065(4)	159.6
N(6)-H(6B)	O(20)#7	0.87	2.17	3.028(5)	170.2

Symmetry transformations used to generate equivalent atoms:

#1 y+1,-x+1,-z+1 #2 -y+1,x-1,-z+1 #3 -x+2,-y,z
#4 -y+1/2,-x+1/2,-z+2 #5 -y+1/2,-x+1/2,-z+1 #6 -y+1,x-1,-z+2
#7 -x+3/2,y-1/2,z

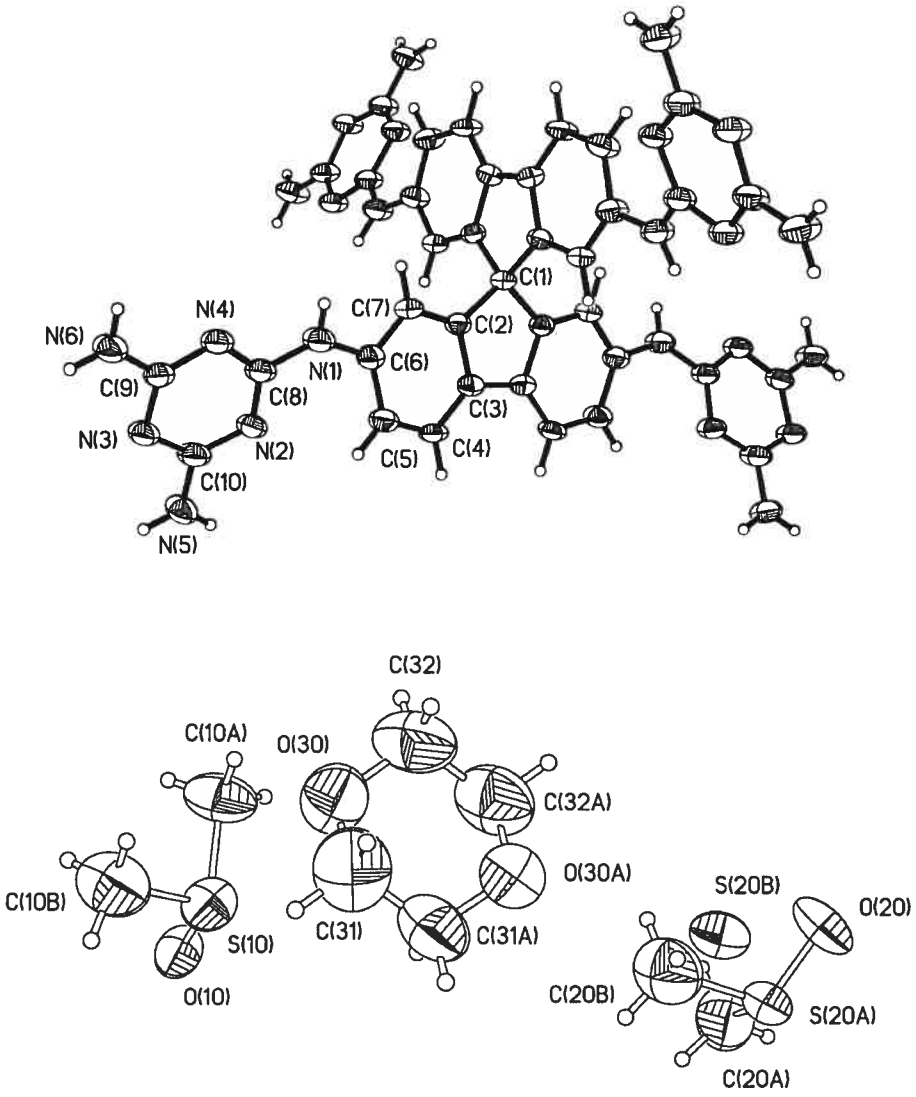

ORTEP view of the C85 H144 N24 O24 S8 compound with the numbering scheme adopted. Ellipsoids drawn at 30% probability level. Hydrogens represented by sphere of arbitrary size.

REFERENCES

Flack, H.D. (1983). Acta Cryst. A39, 876-881.

Flack, H.D. and Schwarzenbach, D. (1988). Acta Cryst. A44, 499-506.

International Tables for Crystallography (1992). Vol. C. Tables 4.2.6.8 and
6.1.1.4, Dordrecht: Kluwer Academic Publishers.

SAINT (1999) Release 6.06; Integration Software for Single Crystal Data. Bruker AXS Inc., Madison, WI 53719-1173.

Sheldrick, G.M. (1996). SADABS, Bruker Area Detector Absorption Corrections.
Bruker AXS Inc., Madison, WI 53719-1173.

Sheldrick, G.M. (1997). SHELXS97, Program for the Solution of Crystal Structures. Univ. of Gottingen, Germany.

Sheldrick, G.M. (1997). SHELXL97, Program for the Refinement of Crystal Structures. Univ. of Gottingen, Germany.

SHELXTL (1997) Release 5.10; The Complete Software Package for Single Crystal Structure Determination. Bruker AXS Inc., Madison, WI 53719-1173.

SMART (1999) Release 5.059; Bruker Molecular Analysis Research Tool. Bruker AXS Inc., Madison, WI 53719-1173.

Spek, A.L. (2000). PLATON, Molecular Geometry Program, 2000 version. University of Utrecht, Utrecht, Holland.

XPREP (1997) Release 5.10; X-ray data Preparation and Reciprocal space Exploration Program. Bruker AXS Inc., Madison, WI 53719-1173.